CONF-900395--1

DE90 008091

7th BES Catalysis and Surface Chemistry Research Conference

Summary of DOE-BES Research Projects

March 26-28, 1990
National Institute of Standards and Technology
Gaithersburg, Maryland

Published: March 1990

U.S. Department of Energy
Office of Energy Research
Office of Basic Energy Sciences
Division of Chemical Sciences
Division of Materials Sciences
Washington, DC 20545

TABLE OF CONTENTS

Seventh BES Catalysis and Surface Chemistry Research Conference

This report summarizes the research programs to be presented at the seventh meeting on basic heterogeneous catalysis and surface chemistry research which is sponsored by the Division of Chemical Sciences, Office of Basic Energy Sciences. Participants in the meeting include researchers from the DOE laboratories, university researchers currently receiving BES support for catalysis research, representatives from DOE Headquarters Divisions, and a few invited guests.

The meeting is being held primarily (1) to acquaint each participant with the research being currently supported, (2) to identify the most recent notable accomplishments, and (3) to focus attention on the needed but unanswered technical and scientific questions. All researchers will present, either orally or in a poster, the current status of their programs.

Special thanks go to Richard Cavanaugh, Patrice Boulanger, and Lori Phillips at the National Institute of Standards and Technology for help in organizing this meeting and to each participant and co-worker for their contributions.

Edwin L. Kugler
Processes and Techniques Branch
Division of Chemical Sciences
Office of Basic Energy Sciences

Seventh BES Catalysis and Surface Chemistry Research Conference

March 26-28, 1990

National Institute of Standards and Technology
Gaithersburg, Maryland

Monday, March 26, 1990

Lecture Room D

8:00 AM Registration (coffee/donuts)

8:30 Welcome -- Donald K. Stevens, Director
Office of Basic Energy Sciences

Opening Remarks -- Edwin L. Kugler (DOE)

9:00 Metal-Support Bonds in Supported Metal Catalysts
Bruce C. Gates (Delaware)

9:45 Structure and Reactivity of Model Thin Film Catalysts
Theodore E. Madey (Rutgers)

10:30 Coffee Break

11:00 Solid State NMR Studies of Heterogeneous Catalysis
Bernard C. Gerstein (Iowa State)

11:45 Support Effects Studied on Model Supported Catalysts
Raymond J. Gorte (Pennsylvania)

12:30 PM Lunch

1:45 Some Fundamental Aspects of Zeolite Catalysis
W. Keith Hall (Pittsburgh)

2:30 -- 4:30 Poster Session A -- Lecture Rooms A & B

Robert L. Augustine
R. Terry K. Baker
Krishnan Balasubramanian
Calvin Bartholomew
Michel Boudart
Alan Brenner
Richard R. Cavanaugh
Sylvia T. Ceyer
Andrew W. Depristo
Charles P. Slichter

Robert P. Eischens
John G. Ekerdt
Richard D. Gonzalez
D. Wayne Goodman
Edward F. Greene
Gary L. Haller
Michael P. Harold
John C. Hemminger
Victor E. Henrich
Jan Hrbek

6:00 No Host Dinner

Tuesday, March 27, 1990

Lecture Room D

8:30 AM	Coffee/donuts
9:00	Dynamics of Non-Dissociative and Dissociative Adsorption on Pt(111) -- Robert J. Madix (Stanford)
9:45	Homogeneous-Heterogeneous Combustion: Thermal and Chemical Coupling -- Lanny D. Schmidt (Minnesota)
10:30	Coffee Break
11:00	Selectivity of the Reactions of Oxygenates on Transition Metal Surfaces -- Mark A. Barteau (Delaware)
11:45	Kinetic and Spectroscopic Characterization of Metal Oxide and Sulfide Catalysts -- Glenn L. Schrader (Iowa State)
12:30 PM	Lunch
1:45	Chemistry and Physics of Transition Metal Clusters Stephen J. Riley (Argonne)
2:30 -- 4:30	Poster Session B -- Lecture Rooms A & B

Deborah R. Huntley
Brett Jackson
Kenneth C. Janda
Terry S. King
Kamil Klier
Thomas F. Koetzle
Harold H. Kung
Dennis L. Lichtenberger
Jack H. Lunsford
Jon G. McCarty
David R. Mullins
Steven H. Overbury
Jerome W. Rathke
Wolfgang M. H. Sachtler
James A. Schwarz
Gabor A. Somorjai
Steven L. Suib
W. Henry Weinberg
Jerry L. Whitten
John T. Yates

Wednesday, March 28, 1990

Lecture Room D

8:30 AM	Coffee/donuts
9:00	Model Heteroatom Removal Reactions on Molybdenum Surfaces Cynthia M. Friend (Harvard)
9:45	Studies of Supported Hydrodesulfurization Catalysts David M. Hercules (Pittsburgh)

Wednesday, March 28, 1990 (continued)

10:30	Coffee Break
11:00	Morphological Aspects of Surface Reactions J. Michael White (Texas)
11:45	Catalytic Hydrogenation of Carbon Monoxide Alexis T. Bell (UC - Berkeley)
12:30 PM	Lunch
1:30	Open Forum Discussion
3:00	Conclusion

SYSTEMATIC PREPARATION OF SELECTIVE HETEROGENEOUS CATALYSTS

Supported by the U.S. Department of Energy, Office of Basic Energy Research
Grant DE-FG02-84ER45120

Dr. Robert L. Augustine
Department of Chemistry, Seton Hall University, South Orange, NJ 07079

As a synthetic organic chemist with experience in the catalytic hydrogenation of organic functional groups I became interested in the idea that synthetically useful heterogeneously catalyzed reactions other than hydrogenation could be developed but to do this would require a detailed understanding of the nature and specific reactivity of the various types of active sites present on the catalyst surface. Research activities were begun with the aim of developing such an understanding and to use the information produced to extend the usefulness of heterogeneous catalysis in synthetic applications.

The key factor in obtaining this information was the Single Turnover (STO) reaction sequence in which the metal surface of a dispersed metal catalyst is treated so that each site reacts stoichiometrically providing a 1:1 correlation between the number of molecules of product formed and the number of active sites producing this material.[1,2] With this technique up to four different types of active sites can be measured on a variety of supported metal catalysts.[2,3] The direct saturation sites having irreversibly adsorbed hydrogen have been named ^3M_I and those having reversibly held hydrogen, ^3M_R. The ^3MH label is given to two-step saturation sites and ^2M to isomerization sites. The ^1M sites are those which adsorb hydrogen but do not take part in the STO reaction sequence.[2,4] Comparison with Pt single crystal catalytic data has shown that these saturation sites are kink or corner atoms on the metal surface and the isomerization sites are probably step or edge atoms while the ^1M sites are thought to be terrace or face atoms.[5]

It was found early in this research that the temperature used for the hydrogen reduction of the supported precursor salts and the mode of heating during the reduction had an effect on the reactive site densities of the resulting catalysts.[6] Thus series of catalysts having identical metal loading but different reactive site densities can be obtained.

STO studies have been used to determine the changes in catalyst activity associated with preheating the catalyst before use[7] and the effect of the competitive adsorption of solvent molecules on the adsorption of hydrogen and alkenes on the various types of active sites present on Pt and Pd catalysts.[8]

STO studies have also led to a more detailed understanding of the processes taking place on dispersed metal catalysts which have been stored in air for various periods of time.[9] With Pt catalysts there are two levels of oxidation. There is an early formation of a "surface oxide" which is easily removed by successive STO reactions or hydrogen treatment at room temperature. Pt catalysts up to a year old are regenerated to their original status by either of these procedures. Longer exposure to air gives more extensively oxidized catalysts. While such catalysts can be reactivated by hydrogen, particularly at 100°-150°C, the resulting materials have STO reaction characteristics different from the original.

Similar effects were found with supported Pd catalysts but the time frame is much shorter than for Pt. Pd catalysts lose their STO activity soon after preparation when exposed to air. The original STO activity can be regenerated by room temperature hydrogen reduction of catalysts up to 2-3 months old. Beyond this time elevated temperature hydrogenation is needed with the resulting Pd catalyst having STO reaction characteristics different from the original. With Rh catalysts extensive oxidation occurs after 2-3 days exposure to air with the resulting species showing non-reproducible STO behavior.

The STO reaction procedure was also used to determine the nature of the metal support interaction between Pt, Pd, and Rh and SiO_2, TiO_2, and Al_2O_3.[10] In almost all cases the site densities decreased on going from $SiO_2 > TiO_2 > Al_2O_3$ providing verification for the proposal that the support influences catalyst activity by changing the morphology of metal crystallite formation.[11] However, with Pt catalysts the ^3M_R site densities increased $SiO_2 > TiO_2 > Al_2O_3$ showing that with Pt the electronic effect of the support influenced the strength by which the hydrogen was adsorbed on the metal. This effect was not observed with Rh or Pd. The significant increase in isomerization observed over Pd/Al_2O_3 as compared to Pd/SiO_2 is also ascribed to electronic interactions. These data show that MSI has both electronic and morphological characteristics which depend not only on the nature of the support but also on the metal, a factor apparently not fully appreciated heretofore.

Most of our recent work has involved the use of series of STO characterized catalysts to study different reactions in order to determine the reaction characteristics of each type of site. In the first of these studies series of STO characterized Pt/CPG catalysts were used for the hydrogenation of cyclohexene in heptane at 10°C[12] and in the vapor phase at ambient temperature[13] as well as for the hydrogenation of neat apopinene at 25°C.[14] From the overall reaction rates turnover frequencies (TOF) for each of the three types of saturation sites were obtained[12] as listed in Table 1.

TABLE 1. SPECIFIC SITE TURNOVER FREQUENCIES

	(Molecules Hydrogenated/Site/Second)		
Hydrogenation	^3M_I	^3M_R	^3MH
Apopinene (neat)	1.1	5.7	1.8
Cyclohexene (heptane)	4.0	19.2	8.2
Cyclohexene (vapor phase)	0.6	0.7	1.2

In the liquid phase reactions the most active site was that on which the hydrogen was weakly held but in the vapor phase hydrogenation the stream of carrier gas presumably removes the hydrogen from the ^3M_R sites before they can react with the alkene thus lowering their activity. A similar study was made of the catalytic oxidation of 2-propanol over Pt/CPG[15] which showed that all three types of corner atoms have essentially the same activity.

There are many synthetically useful C-C bond forming reactions reported to take place over soluble monometallic complexes. Since the surface of dispersed metal particles is composed of a wide variety of atoms having differing coordinative unsaturation,[16] there should be present on a metal surface at least one type of active site which could promote this type of reaction. Initial work in this area involved running the Heck arylation (Equation 1) over a series of STO characterize Pd/Al_2O_3 catalysts to determine the nature of the surface site(s) responsible for C-C bond formation.[17] The amounts of 1 and 2 produced under standard reaction conditions decreased as the number of saturation sites on the catalyst decreased so these species are formed on the more unsaturated corner atoms.

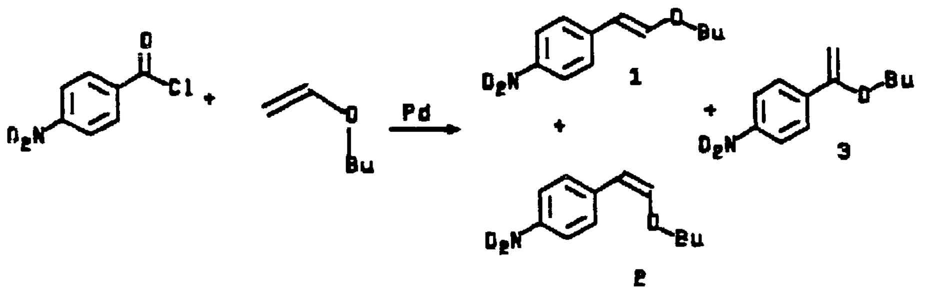

(Eq. 1)

In a small scale liquid phase flow reactor the product composition is influenced by the catalyst:substrate contact time and reaction conditions have been found in which 3 is the only product formed.[17] Early work has also shown that the cyclization of the diene, 4, (Equation 2) takes place over supported Rh catalysts.[18]

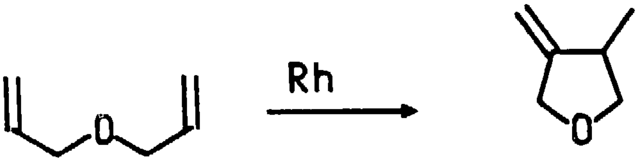

4

(Eq. 2)

Data concerned with the effect of modifiers on specific site activity has shown that "soft" ligands such as phosphines adsorb first on the unreactive face atoms. This indicates that these face atoms are "softer" than the corner atoms so "hard" ligands such as amines would be expected to interact preferentially with the corner atoms.[19]

The most significant aspect of our current research is the development of Frontier Molecular Orbital diagrams for the various reactive sites present on the surface of dispersed metal catalysts. With these diagrams the reactivity of the various types of surface atoms can be rationalized and new catalytic reactions developed. These data will also provide information which will help in understanding the differences between the various types of catalytically active metals. The orbital energies of these various types of surface atoms were calculated using a modified Angular Overlap approach which defined the active site as a single metal atom surrounded by other metal atom 'ligands' making up a 'surface complex'. Calculations for surface atoms on a Ni crystallite show a broad energy range for the 3d orbitals with the 4s level through the middle. The 4s orbital is the LUMO for the "surface complex" on some sites and on others it is the HOMO.[20] From orbital symmetry considerations it is possible to rationalize the specific activity of these different types of sites with respect to the formation of the STO reaction products.

A computer program is presently being debugged which will provide the orbital energy data from the angular overlap calculations for the p and d electrons for all of the different types of sites on any of the fcc catalytically active metals. This information will be compared to published molecular orbital data for verification. It will then be used to rationalize the proposed reactivity of the active sites in various reactions, to predict the types of reactions possible on the different types of sites, and then to utilize these predictions to develop new, synthetically useful, heterogeneously catalyzed reactions.

References

1. Augustine, R.L.; Warner, R.W.; J. Org. Chem., *1981*, **43**, 2614.
2. Augustine, R.L.; Warner, R.W.; J. Catal., *1983*, **80**, 358.
3. Augustine, R.L.; Baum, D.R.; High, K.G.; Szivos, L.S.; Appl. Catal., In Press.
4. Siegel, S.; Outlaw, Jr.,J.; Garti, N.; J. Catal., *1978*, **52**,102.
5. Augustine, R.L.; Thompson, M.M.; J. Org. Chem., *1987*, **52**, 1911.
6. Augustine, R.L.; Kelly, K.P.; Lay, Y.M.; Appl. Catal., *1985*, **19**, 87.
7. Augustine, R.L.; Kelly, K.P.; J. Chem. Soc., Faraday 1, *1986*, **82**, 3025.
8. Augustine, R.L.; Warner, R.W.; Melnick, M.J.; J. Org. Chem., *1984*, **49**, 4853.
9. Augustine, R.L.; Szivos, L.S.; Baum, D.R.; Techasauvapak, P.; Manuscript in preparation.
10. Augustine, R.L.; Szivos, L.S.; High, K.G.; Baum, D.R.; J. Mol. Catal. Submitted for publication.
11. Katzer, J.R.; Sleight, A.W.; Gajardo, P.; Michel, J.B.; Gleason, E.F.; McMillan, S.; Faraday Discuss. Chem. Soc., *1982*, **72**, 121.
12. Augustine, R.L.; Thompson, M.M.; Doran, M.A.; J. Chem. Soc., Chem. Commun., *1987*, 1173.
13. Augustine, R.L.; High, K.G.; Sermon, P.; Georgiades, G.; Manuscript in preparation.
14. Augustine, R.L.; High, K.G.; Smith, G.V.; Manuscript in preparation.
15. Augustine, R.L.; Doyle, L.K.; Manuscript in preparation.
16. Augustine, R.L.; O'Leary, S.; Unpublished results.
17. Augustine, R.L.; Lay, Y.M.; Unpublished results.
18. Augustine, R.L.; Liu, J.; Techasauvapak, P.; Unpublished results.
19. Augustine, R.L.; O'Hagan, P.J.; Catalysis in Organic Synthesis, *1989*, In press.
20. Augustine, R.L.; Lahanas, K.; Unpublished results.

FUTURE PLANS

Future research efforts will be concentrated primarily in three areas:

1. A detailed investigation of the nature of the interaction between the various active sites and different types of modifiers in order to permit the selective blocking of any specific active site in the presence of the others. This will also include the effect of the different modifiers on the reactivity of those sites adjacent to where they are adsorbed and the use of chiral modifiers to produce selective asymmetric heterogeneous catalysts.

2. Development of the Frontier Molecular Orbital applications for the understanding of present catalytic processes and the conception of new, synthetically useful, heterogeneously catalyzed reactions.

3. Providing further examples of the use of metal surfaces in organometallic reactions to expand our knowledge of the potential reactivity of the various types of surface sites.

This information can lead to the developing of specific heterogeneous catalysts for a variety of reactions having practical synthetic interest. This, along with the use of laboratory scale liquid phase flow reactors assembled with familiar apparatus, should provide synthetic chemists with the impetus to investigate more extensively the use of heterogeneously catalyzed reactions for the production of pharmaceuticals and fine chemicals, an area where heterogeneous catalysis is usually only recognized as a means of hydrogenating organic functional groups.

RECENT PUBLICATIONS

Heterogeneous Catalysis in Organic Chemistry. 6. An Experimental Description of the Nature of the Hydrogenation Sites Present on Dispersed Metal Catalysts, Augustine, R.L.; Thompson, M.M.; J. Org. Chem., *1987*, **52**, 1911.

Heterogeneous Catalysis in Organic Chemistry. 7. Stereochemistry of the Hydrogenation of 1,3;5-trimethylcyclohexene, Augustine, R.L.; Yaghmai, F.; J. Org. Chem., *1987*, **52**, 1862.

Determination of Specific Site Turnover Numbers for Cyclohexene Hydrogenation, Augustine, R.L.; Thompson, M.M.; Doran, M.A.; J. Chem. Soc., Chem. Comm., *1987*, 1173.

The Thermal Decomposition of $Rh_6(CO)_{16}$ on Alpha Alumina, Augustine, R.L.; Pierson, C.G.; J. Mol. Catal., *1987*, **43**, 7.

An Inelastic Electron Tunneling Spectral (IETS) Study of $Rh_6(CO)_{16}$ and $Rh_4(CO)_{12}$ adsorbed on Alumina, Augustine, R.L.; D'Addio, A.D.; Ewing, G.W., J. Mol. Catal., *1988*, **43**, 315.

Surface Characterized Dispersed Metal Catalysts, Augustine, R.L.; Warner, R.W.; Kelly, K.P.; Thompson, M.M.; High, K.G.; O'Hagan, P.J.; Catalysis in Organic Synthesis, *1988*, 233.

A Single Turnover (STO) Characterization of Supported Palladium Catalysts, Augustine, R.L.; Baum, D.R.; Materials Research Society, Proceedings, *1988*, **111**, 453.

A Single Turnover Characterization of Pd Metal Catalysts Supported on Phosphinated Inorganic Oxides, Augustine, R.L.; Liu, J.; J. Mol. Catal., *1989*, **53**, 9.

Heterogeneous Catalysis: A Molecular Perspective, Augustine, R.L.; O'Hagan, P.J.; Catalysis in Organic Synthesis, In Press.

A Single Turnover Comparison of Supported Platinum, Palladium and Rhodium Catalysts, Augustine, R.L.; Baum, D.R.; High, K.G.; Szivos, L.S.; Appl. Catal., In Press.

CARBON DEPOSITION AND DEACTIVATION OF METALLIC CATALYSTS

R.Terry K. Baker
Department of Chemical Engineering
Auburn University, Auburn, AL 36849

INTRODUCTION

Carbon deposition on metal surfaces is one of the most common causes of catalyst deactivation in hydrocarbon conversion and CO/H_2 reactions. The structure of the carbon deposit can range from amorphous to highly crystalline. In many cases the metallic component of the catalyst system may promote the formation of the carbonaceous deposit. Carbonaceous species may stay on the particle surface and form a graphitic encapsulating layer or may dissolve in the particle and eventually precipitate at the metal/support interface to form a filamentous structure and as a consequence force the particle off the support surface.

The current program which will focus on the formation of carbonaceous deposits on nickel, cobalt, platinum, and some of their alloys is designed to address the following scientific issues:

a. The effect of crystallographic orientation and size of the catalyst particle on the structure of the carbon deposit.

b. The effect of modifications to the surface and bulk properties of the catalyst particles on the carbon deposition process.

c. The relationship between the structural characteristics of the carbon deposited on a given catalyst system and that of the hydrocarbon source.

d. An examination of the concept of removing deposited carbon from a deactivated catalyst system at low temperature in an atomic oxygen environment, and thereby minimizing the degree of particle sintering.

RESULTS

This program was started in September 1989 and initial efforts have been concentrated on the aspects outlined above in Tasks b and d.

Recent macro-scale studies have revealed some dramatic effects with regard to carbon deposition on cobalt particles which have been preheated in a critical concentration of H_2S prior to exposure to hydrocarbon environment. With trace amounts of H_2S, subsequent yield of catalytically produced carbon were extremely high, whereas effective inhibition of carbon deposition was achieved when cobalt was preheated in significant amounts of H_2S. At present we do not fully understand the enhancement in carbon formation following exposure to low concentration of sulfur, which can be reversed by reaction in hydrogen. Our current thinking is that surface construction of the cobalt crystallites occurs following adsorption of a critical amount of H_2S, resulting in the creation of a new surface which is particularly active towards hydrocarbon decomposition to produce carbon. The validity of this concept is being investigated by controlled atmosphere electron microscopy, where it is possible to not only follow the qualitative changes in specimen appearance as a function of reaction conditions, but also identify structural transformations by the use of in-situ electron diffraction techniques.

Over the past two years we have successfully extended the capabilities of the transmission electron microscope to enable in-situ studies of the interaction of atomic oxygen with various solids to be performed. This has been accomplished by modifying the specimen chamber region of a JEOL 200CX TEM/STEM electron microscope to accommodate a specially designed environmental cell and specimen heating stage. with this arrangement it is possible to continuously observe changes in the appearance of a specimen as it undergoes reaction with abeam of atomic oxygen. In the current experiments atomic oxygen is produced in significant concentrations by passing a mixture of nitrous oxide and nitrogen trough a microwave discharge cavity at a local pressure of 2.0 Torr, and this procedure creates an atomic oxygen environment environment around the specimen which is relatively free of molecular oxygen. Currently the technique is being used to study the interaction of atomic oxygen with a number of carbonaceous materials including graphite and filamentous forms of carbon which are frequently produced on metallic catalyst surfaces.

Attack, of graphite by atomic oxygen was found to take place very readily when the specimen temperature was raised to 50°C. This took the form of the creation of irregular shaped pits over almost the entire basal plane region. This behavior was quite different to the pitting action produced in graphite by certain metal and metal oxide impurities in the presence of molecular oxygen at appreciably higher temperatures. (Pt particles operate by this mode at 650°C in O_2), where attack takes place at isolated imperfections in the basal plane to produce well defined hexagonal shaped pits.

Continuous observation of the reaction revealed some further characteristics of the system. Attack appeared to be restricted to the basal plane region there being no evidence for recession of edges or steps; modes of attack which occur in molecular oxygen. Moreover, atomic oxygen tended to display preferential attack of the basal plane along the twin bands. Although it may be premature to draw any conclusions regarding the kinetics of the reaction it does appear that the extent of pitting is a temperature dependent process.

Filamentous carbon is a type of material which is formed by the catalytic decomposition of certain hydrocarbons on small metal particles. Previous studies have shown that the filaments consist of a unique structure having an amorphous core surrounded by a graphitic skin,as well as a metal component which can be present either as a particle at the tip of the filament.

When carbon filaments were heated in an atomic oxygen environment the first signs of gasification were observed at 50°C. Under these conditions attack took place preferentially at the graphitic skin regions with subsequent oxidation of the disordered inner core structure. This behavior should be contrasted with that found with molecular oxygen, where the inner core gasified at 625°C followed by removal of the graphitic skin at 726°C. These studies indicate that there is a major difference in the mechanism of atomic and molecular oxygen interactions with carbonaceous materials.

The next step in this section of the program will involve reacting a model supported metal catalyst systems which contain a substantial amount of deposited carbon, in an atomic oxygen environment at 50°C. The treated specimens will subsequently be examined in the electron microscope and this procedure should enable us to ascertain whether it has been possible to achieve removal of the carbonaceous deposit without concomitant metal particle sintering.

ELECTRONIC STRUCTURE OF CLUSTERS AND THEIR REACTIVITIES

K. Balasubramanian
Department of Chemistry
Arizona State University
Tempe, AZ 85287-1604

Project Summary

We are investigating electronic structure of very heavy metal clusters such as Rh_3, Pt_3, Au_4, Ag_4, Cu_4, Pd_3, etc. Theoretical investigations of such clusters are made using relativistic ab initio multi-configuration self-consistent field (MCSCF) followed by large-scale configuration interaction (CI) calculations which include up to three million configurations. The geometries, ionization potentials, energy separations of low-lying excited electronic states, binding energies and other properties of such clusters are studied. The reactivity trends of these clusters are investigated through model potential energy surfaces for systems such as Pd_3+H, Ni_3+H, Pt_2+H_2, Pd_2+H_2, etc. Results obtained on both bare metal clusters and their reactivities will be discussed.

Selectivity of the Reactions of Oxygenates on Transition Metal Surfaces

Mark A. Barteau
Department of Chemical Engineering
University of Delaware
Newark, DE 19716

The goal of this research is to understand, by means of surface science studies, the elementary processes involved in the synthesis of methanol and higher oxygenates on transition metals, and the dependence of these processes upon the nature of the surface. Such oxygen-containing molecules may well be the fuels and chemical feedstocks of the future. We have completed a considerable body of work (Ph.D. thesis of J. Lynn Davis, 1988) on the reactions of alcohols, aldehydes, and carboxylic acids on clean and oxygen-containing Pd(111) surfaces. More recent attention has been focussed on the surface chemistry of rhodium. We find both interesting similarities and differences between rhodium and palladium. Comparison of the two sheds light on common reaction networks among the transition metals, and on the differences between them which may permit control of selectivities in catalytic reactions.

On the Pd(111) surface, higher alcohols decompose via the sequence: alcohol → alkoxide → η^2-aldehyde → acyl → CO + H + hydrocarbon. The hydrocarbon in each case is one carbon atom shorter than the parent primary alcohol. η^2-aldehydes and acyls are relatively stable; we have isolated and identified (by High Resolution Electron Energy Loss Spectroscopy) these species starting with the corresponding C_1 to C_4 alcohols and aldehydes (with the exception of the formyl, HCO). While a similar reaction sequence may hold on Rh(111), there are several important differences between rhodium and palladium On Rh(111) the alkoxides are much more stable species, and we have been unable to "stop" the alcohol decomposition reaction at surface aldehyde or acyl intermediates. In effect, the reaction network may be the same on the two metals, but differences in the kinetics of the elementary reactions lead to different species as the most abundant intermediate on each metal. The relative stabilities of adsorbed alcohol, alkoxide, and aldehyde species on Rh(111) are readily apparent in temperature programmed HREELS studies. Below 150 K, molecular methanol can be easily fingerprinted in the vibrational spectrum; between 120 and 180 K this species converts to adsorbed methoxides which decompose to adsorbed hydrogen atoms and carbon monoxide above 200 K. If comparable amounts of formaldehyde are adsorbed, this species dehydrogenates below 130 K. Thus, although dehydrogenation of methoxides must proceed via formaldehyde intermediates, the latter species cannot be isolated, as the activation energy for their dehydrogenation is less than that of the methoxides.

The chemistry of aldehydes on Pd(111) and Rh(111) is very similar, but the two metals provide complementary mechanistic information about carbonylation processes required for synthesis of higher oxygenates. On both metals high coverages of formaldehyde are stabilized by formation of polymeric paraformaldehyde overlayers. There is no evidence in our studies for polymerization of the higher aldehydes on either metal. On Pd(111) decarbonylation of aldehydes bound in an η^2-configuration proceeds via proceed via isolable acyl intermediates. Acyl species were identified by their vibrational spectra (most notably the acyl CO stretch at $1580 \pm 15\ cm^{-1}$). Acetaldehyde reacted through acetyl species which decomposed further to release CO(a), H(a), and C_1 hydrocarbon species to the surface. Likewise, decomposition of propanoyl species produced during the course of propanal conversion resulted in the production of CO(a), H(a), and C_2

hydrocarbon species. Thus, aldehyde decomposition on the Pd(111) surface produced CO, hydrogen, and hydrocarbon species one carbon atom shorter than the parent aldehyde. Similar reaction products were observed for alcohol decomposition on Pd(111). These results provide insights into a variety of reactions involving aldehydes, including their decarbonylation, polymerization, and catalytic synthesis.

Large differences were observed in the onset of CO production from adsorbed aldehydes which illustrate the influence of the substituent upon aldehyde reactivity. The observation of formaldehyde decomposition upon adsorption at 170 K suggests that cleavage of the acyl carbon-hydrogen bond occurred readily at this temperature. However, CO production from the higher aliphatic aldehydes adsorbed on Pd(111) was not detected by HREELS until roughly 300 K. The strengths of the aldehyde carbon-hydrogen bonds for these molecules differ by only ± 1 kcal/mol, which is clearly insufficient to account for the large differences observed in aldehyde decomposition temperatures. This supports the conclusion that it is acyl decomposition rather than acyl formation which is the rate determining step in aldehyde decarbonylation on this surface.

The stability of acyl species was determined via HREELS by monitoring the appearance of the decomposition product CO. Adsorbed acetyl species were the most stable acyl ligands on Pd(111) and decomposed above 310 K to produce CO(a) and C_1 hydrocarbons. Propanoyl species were less stable and decomposed above 280 K to produce CO(a) and C_2 hydrocarbons. Even though the α carbon-carbon bond was stronger for acrolein than for the other aldehydes, propenoyl ($H_2C{=}CHC{=}O$) species produced from acrolein on Pd(111) were the least stable and decomposed at 260 K to produce CO(a) and CCH_3(a). The low stability of propenoyls suggests that factors other than the α carbon-carbon bond strength control the stability of acyl species on the Pd(111) surface.

A kinetic isotope effect was observed for CO elimination from CH_3CO(a) vs CD_3CO(a), clearly demonstrating that C-H bond cleavage is the rate-determining step in decarbonylation of aliphatic acyls, and that this step must precede C-C bond cleavage. This suggests that adsorbed acyls are dehydrogenated to unstable ketene species which deposit CO and the corresponding alkylidene on the surface. This sequence for acyl decomposition is consistent with the interconversion of acetyl and ketene species demonstrated by others on Pt(111) and Ru(0001). It may also explain the apparent inverse relationship between C-C bond strengths and activation energies for decarbonylation of acrolein vs. the aliphatic aldehydes. In the case of the propenoyl species derived from acrolein, C-H bond cleavage is not necessary in order to produce unsaturated sites on the hydrocarbon backbone which can interact strongly with the metal surface. Thus C-C bond cleavage of propenoyls to yield CO plus vinyl species (which presumably isomerize rapidly to ethylidynes) can proceed directly, in effect circumventing the C-H cleavage which is rate determining for aliphatic acyls. One would therefore expect the kinetics of propenoyl decomposition to be representative of those for C-C cleavage; the measurably lower activation energy of this reaction again supports the conclusion that C-H cleavage is rate-determining for decarbonylation of aliphatic acyls.

The decarbonylation of higher aliphatic aldehydes on Pd (111) thus appears to proceed via the following sequence of elementary processes:

$$RCH_2\,CHO(g) \rightarrow \eta 1\text{-}\,RCH_2CHO(a) \qquad (1)$$

$$\eta^1\text{-}RCH_2CHO(a) \rightarrow \eta^2\text{-}RCH_2\,CHO \qquad \text{at } 170\text{ K} \qquad (2)$$

$$\eta^2 - RCH_2CHO(a) \rightarrow \eta^1(C) - RCH_2C = O(a) + H(a) \qquad 170 - 300\text{ K} \qquad (3)$$

$$\eta^1(C) - RCH_2C = O(a) \rightarrow RCH = C = O(a) + H(a) \qquad 260 - 320\ K \qquad (4)$$

$$RCH = C = O \rightarrow RCH(a) + CO(a) \qquad (5)$$

Evidence for this sequence includes the direct observation by HREELS of η^2- acetaldehyde and propanal species and of the corresponding acyls, and the demonstration of a kinetic isotope effect in the decarbonylation of acetyl species. Neither the methylene nor ethylidene species postulated in step 5 were observed directly; the former were hydrogenated to methane and the latter reacted to form stable ethylidynes.

This sequence is in striking accord with the mechanistic information derived by Ponec and co-workers for the synthesis of C_2-oxygenates with supported palladium catalysts. Palladium typically does not catalyze the formation of higher oxygenates from CO and H_2 owing to its lack of activity for dissociation of CO. However, these workers demonstrated that significant yields of acetaldehyde and ethanol could be produced on a Pd/V_2O_3 catalyst when CH_2Cl_2 was added to the feed gas. These products were <u>not</u> observed when CH_3Cl was added to the feed instead. If one assumes that methyl and methylene chlorides supply the corresponding methyl and methylene groups to the surface, respectively, these results indicate that <u>higher oxygenates are synthesized by CO addition to alkylidene</u>, rather than alkyl species. This proposed synthesis reaction is precisely the reverse of reaction (5) in the decomposition of acyls via ketene species above.

Work on Rh(111) sheds light on the characteristics of CO involved in these carbonylation/decarbonylation reactions. On Rh(111) CO can adsorb either in a linear state (atop surface rhodium atoms) or a bridge state (spanning two rhodium atoms). These may be distinguished by a ca. 200 cm^{-1} difference in the carbonyl stretching frequency. If one adsorbs CO on the Rh(111) surface directly, the linear state is filled first and then the bridge state begins to be populated. In contrast decarbonylation of aldehydes on Rh(111) at low temperatures (<240 K) preferentially populates the bridge state; the equilibrium distribution is obtained only when the surface is heated to convert bridging to linear species. This suggests that the decarbonylation of aldehydes occurs at sufficiently low temperature that CO is "frozen" in a non-equilibrium configuration which is related to its bonding configuration in the adsorbed organic molecule. In other words, one decomposes organic carbonyl compounds by replacing bonds to the ligands in them on a one-for-one basis with bonds to surface metal atoms.

Modification of rhodium and palladium surfaces by adsorption of oxygen atoms influences the surface chemistry in a number of ways, most of which are common to both metals. These include alteration of the preferred coordination geometry of aldehydes and ketones from η^2 to η^1, proton abstraction from Brønsted acids, nucleophilic addition to aldehydes (for which Rh is much less active than Pd), and scavenging of adsorbed hydrogen atoms. In addition, oxygen (and presumably other electronegative surface modifiers) interact with adsorbates such as alkoxides and carboxylates, in some cases dramatically altering the kinetics and selectivity of their reactions. Examples include the oxygen induced stabilization of alkoxides on Pd and of formates on Rh. We are in the process of attempting to establish general trends among inorganic surface modifiers, with the goal of applying these directly in the synthesis of higher oxygenates.

Publications:

1. J. L. Davis and M. A. Barteau, "Decarbonylation and Decomposition Pathways of Alcohols on Pd (111)," Surface Science, 187, 387 (1987).
2. J. L. Davis and M. A. Barteau, "The Influence of Oxygen on the Selectivity of Alcohol Conversion on the Pd (111) Surface," Surface Science, 197, 123 (1988).
3. J. L. Davis and M. A. Barteau, "The Influence of Temperature and Surface Composition upon the Coordination of Acetone to the Pd (111) Surface," Surface Science, 208, 383 (1989).
4. J. L. Davis and M. A. Barteau, "Polymerization and Decarbonylation Reactions of Aldehydes on the Pd (111) Surface," Journal of the American Chemical Society, 111, 1782 (1989).
5. J. L. Davis and M. A. Barteau, "Hydrogen Bonding in Carboxylic Acid Adlayers on Pd(111): Evidence for Catemer Formation," Langmuir, 5, 1299 (1989).
6. C. A. Houtman and M. A. Barteau, "Reactions of Methanol on Rh(111) and Rh(111)-(2x2)O Surfaces: Spectroscopic Identification of Adsorbed Methoxide and η^1-Formaldehyde," Langmuir (submitted).

EFFECTS OF DISPERSION AND SUPPORT ON ADSORPTION, CATALYTIC AND ELECTRONIC PROPERTIES OF COBALT/ALUMINA CO HYDROGENATION CATALYSTS

Calvin H. Bartholomew
BYU Catalysis Laboratory
Department of Chemical Engineering
Brigham Young University
Provo, Utah 84602

Research Scope and Objectives

The origin of observed, dramatic variations in CO hydrogenation activity and selectivity of cobalt with variations in preparation, metal loading, and dispersion--whether a result of changes in surface structure or due to support effects--is of fundamental interest. An investigation of the effects of surface structure, dispersion, and support on the adsorption, catalytic, and electronic properties of cobalt/alumina is in progress, the objectives of which are to: (1) determine the effects of surface structure and metal dispersion on the adsorption and catalytic properties of cobalt and (2) determine the effects of support on the adsorption, catalytic and electronic properties of cobalt/alumina.

To accomplish the above-listed objectives the proposed work has been divided into three areas of investigation: (1) study of the effects of surface structure on the adsorption and catalytic properties of cobalt monolayers deposited on W(100) and W(110) using TPD, LEED and AES spectroscopies, and *in situ* CO hydrogenation reaction measurements, (2) study of the effects of dispersion and extent of reduction on the CO adsorption/desorption and catalytic properties of well-dispersed cobalt/alumina using TPD and IR spectroscopies and lab reactor measurements, and (3) Moessbauer study of the effects of metal-support interactions on the electronic properties of metal clusters in well-dispersed cobalt/alumina and iron/alumina.

Description of Recent Results

During the past two years the effects of surface-structure, support and dispersion on the adsorption, activity/selectivity and electronic properties of Co/W surfaces and alumina-supported cobalt and iron were investigated in a surface science investigation [1-3], lab reactor studies [1-3], a TPD/TPR study [4,5], and a Moessbauer spectroscopy study [6,7].

Auger/Surface Science Characterization and Reaction Study of Clean Unsupported Cobalt and Co/W Surfaces. This work, carried out in collaboration with Wayne Goodman (Texas A&M) involved the characterization by various surface spectroscopies and measurement of CO hydrogenation activity and selectivity as a function of temperature and reactant composition for a clean polycrystalline cobalt surface and for cobalt overlayers on tungsten single crystals.

The observed TOF for clean polycrystalline cobalt is comparable to values determined for well-reduced 5-10% Co/alumina and for Co/W surfaces (see Fig. 1). AES data indicate that the active surface in CO hydrogenation is cobalt metal, not cobalt carbide.

The structure, stability, surface electronic properties, and chemisorptive properties of vapor-deposited cobalt overlayers (0-4 ML) on W(110) and W(100) were studied by Auger electron spectroscopy (AES), low energy electron diffraction (LEED), work function changes ($\Delta\phi$), and temperature programmed desorption (TPD) of cobalt, hydrogen, and carbon monoxide [1,2]. The first layer of cobalt grows pseudomorphically with respect to the tungsten substrate, and is thermally stable to 1300 K. Second and subsequent layers grow layer-by-layer at 100 K, but form three-dimensional clusters above 400-500 K. The relative work functions of these surfaces are strongly dependent on temperature, cobalt coverage, and substrate geometry. The annealed pseudomorphic monolayer of Co/W(100) has a positive $\Delta\phi$ value (+155 mV), indicating a net electronic charge transfer from the tungsten to the cobalt. The chemisorptive properties of the cobalt overlayers are quite different from those of bulk cobalt surfaces, the former having new TPD features for hydrogen chemisorption and TPD features consistent with carbon monoxide dissociation. CO apparently dissociates on cobalt-tungsten interfacial sites and on the pseudomorphic monolayer of Co/W(100) around room temperature as it does on stepped cobalt surfaces.

Surface Science and Lab Reactor Studies of the Effects of Surface Structure, Dispersion and Extent of Reduction on CO Hydrogenation Activity/Selectivity Properties of Co/W and Co/alumina. The effects of surface structure on the CO hydrogenation reaction have been investigated by comparing the steady-state activity and selectivity of submonolayer cobalt deposited on W(110) and W(100) with those of carbonyl-derived Co/alumina catalysts of varying dispersion and extent of reduction [3]. The Co/W surfaces have highly strained and very different geometries but have identical activity. The activity matches that of the highly active, highly reduced Co/alumina catalysts, showing that the steady-state activity of cobalt surfaces is apparently independent of surface structure and dispersion (see Fig. 1) AES spectra show the after-reaction Co/W surfaces to have high coverages of both carbon and oxygen, with carbon lineshapes characteristic of carbidic carbon. Activity is apparently not correlated with surface carbon level. Thus, CO hydrogenation on cobalt appears neither primary nor secondary structure sensitive. The high carbon coverages may cause the high olefin selectivities observed for Co/W. Carbonyl-derived Co/dehydroxylated-alumina catalysts have high extents of reduction, high dispersions, and good activity stability. Increasing the dehydroxylation temperature of the alumina support increases the dispersion while decreasing CO_2 and olefin selectivities. The specific activity of carbonyl-derived catalysts appears to be more closely related to the extent of reduction and the support dehydroxylation temperature than to the dispersion. Thus, the chemical nature of the support surface is the controlling factor in determining the specific activity of supported cobalt catalysts.

TPD/TPSR/IR Study of the Effects of Support, Metal Loading, and Extent of Reduction on CO Adsorption Kinetics and Energetics of Cobalt. The adsorption/desorption kinetics and energetics of carbon monoxide on cobalt catalysts supported on alumina, silica, titania, and magnesia (loadings ranging from 1 to 15 wt.% cobalt) were studied by temperature programmed desorption (TPD), while CO hydrogenation on these same catalysts was studied by temperature programmed surface reaction (TPSR) [4].

TPD study of CO desorption from Co/alumina catalysts [4] indicates that CO is more strongly adsorbed and dissociates more readily (forming CO_2) on catalysts of higher loading and of higher reduction temperature. For example, the CO desorption spectrum for 1% Co/alumina consists of one CO peak at 85°C with a heat of adsorption of only 11 kcal/mol (compared to 14 kcal/mole for unsupported Co) consistent with weakened desorption of molecular CO; no CO_2 desorption is observed suggesting that CO does not dissociate on the 1% catalyst. The CO TPD spectrum for 3% Co/alumina is similar with a large peak for molecular desorption at 95°C and small peaks at 250 and 350°C assignable to strongly held molecular and recombinative CO; there is a small CO_2 peak at about 350°C indicating a small amount of CO dissociation on this sample. Larger fractions of CO are desorbed as recombinative CO and as CO_2 on 10% and 15% Co/alumina catalysts, indicating that CO is more strongly adsorbed and dissociates more readily on cobalt catalysts of higher loading.

CO hydrogenation was studied on the same four (1, 3, 10 and 15 wt.%) Co/ Al_2O_3 catalysts using TPSR [4,5]. Two distinct methane peaks (Peaks A and B) are observed for 3, 10 and 15% Co/Al_2O_3 during TPSR of chemisorbed CO at room temperature, indicating the presence of two different reaction states or mechanisms for CO hydrogenation (A and B) (see Fig. 2). No methane peak is observed for 1% Co/Al_2O_3 unless it is reduced at 1023 K. The more active A state, the relative population of which increases with increasing metal loading and increasing extent of reduction, probably corresponds to hydrogenation of atomic carbon on 3D cobalt crystallites while the less active B state is assigned to decomposition on metal crystallites of a methoxy or formate species originally formed on the support from spilled-over hydrogen and carbon monoxide. TPSR spectra of hydrogen with carbon deposited by CO dissociation at 523 K show that the quantity of active α-carbon increases with increasing metal loading and correlates with the relative population of A sites. A linear correlation between logarithm of the steady-state methane turnover frequency and the relative population of A sites suggests that large variations in the steady-state CO hydrogenation with dispersion and metal loading observed for these catalysts may be explained in terms of variations in the distribution of reaction states for CO hydrogenation, i.e., a larger fraction of Reaction A at higher metal loadings and higher extents of reduction. These TPSR data also show a trend of increasing activity with increasing metal loading (and decreasing dispersion). When compared in light of the TPD results there is a correlation of higher activity for the catalysts which bind CO more strongly and on which CO dissociates more readily.

Moessbauer Spectroscopy Study of the Effects of Support, Metal Loading, and Extent of Reduction on the Chemical, Electronic and Magnetic Properties of Iron on Alumina. The reduction and dispersion of small iron crystallites deposited at low loadings (0.5-2 wt.%) on a high-surface area dehydroxylated alumina support using a nonaqueous deposition technique were studied by *in situ* Mössbauer spectroscopy, H_2 chemisorption and O_2 titration [6,7]. After exposure to H_2 at high temperatures (> 673 K) these dilute Fe/alumina catalysts are relatively highly reduced and highly dispersed. Mössbauer spectra reveal that the main iron phases found on the support after reduction at less than 773 K are superparamagnetic metallic Fe^0 (IS = -0.08 mm/s) and Fe^{2+} (IS = 1.08 mm/s, QS = 1.65 mm/s). Ferromagnetic iron is observed in 2% Fe/alumina reduced at 873 K and higher. Small superparamagnetic particles (dia < 6 nm) are not easily detected by zero-magnetic field Mössbauer experiments with the exception of a 2% Fe/alumina sample reduced at 873 K; in this latter case the presence of a singlet for superparamagnetic metallic iron is highly evident [Fig. 3]. These results combined with chemisorption and O_2 titration data suggest a reduction sequence as follows $Fe^{3+} \rightarrow Fe^{2+}$ (octahedral coordination) → Fe^0 (superparamagnetic) → Fe^0 (ferromagnetic). Some of the Fe^{2+}(probably in tetrahedral coordination sites) is irreducible.

Future Plans

Work in the near future will emphasize TPD/TPSR studies of well-dispersed cobalt/alumina prepared from carbonyls to determine the role of preparation, dispersion, and support on CO adsorption and the pathway for CO hydrogenation on cobalt. FTIR studies will be conducted to determine the nature of CO species adsorbed on Co/alumina as a function of dispersion and the nature of reaction intermediates adsorbed on the support during reaction. Moessbauer studies of well-dispersed, highly-reduced Co^{57}/alumina catalysts will be conducted to determine the nature of electronic interactions between metal clusters and the support.

References/ Publications

1. Johnson, B. G., "The Role of Surface Structure in Carbon Monoxide Hydrogenation on Cobalt Catalysts," Ph.D Dissertation, Brigham Young University, July 1989.

2. Johnson, B. G., Berlowitz, P. J., Goodman, D. W., and Bartholomew, C. H., "The Structural and Chemisorptive Properties of Ultrathin Cobalt Overlayers on W(110) and W(100), " Surf. Sci. 217, 13 (1989).

3. Johnson, B. G., Bartholomew, C. H., and Goodman, D. W., "The Role of Surface Structure in CO Hydrogenation on Cobalt," submitted, 1989.

4. Lee, W. H., "Effects of Support, Loading and Pretreatment on the CO Desorption and CO Hydrogenation Kinetics of Cobalt," Ph.D. Dissertation, Brigham Young U., June 1988.

5. Lee, W. H. and Bartholomew, C. H., "Multiple Reaction States in CO Hydrogenation on Alumina-Supported Cobalt Catalysts," J. Catal. 120, 256 (1989).

6. Smith, P. A., "Reduction/Oxidation Behavior of Iron/Alumina Catalysts of Low Loading," M. S. Thesis, Brigham Young University, Summer, 1990.

7. Smith, P. A. and Bartholomew, C. H., "Reduction/Oxidation Behavior of Iron/Alumina Catalysts of Low Loading," Paper submitted, 1990.

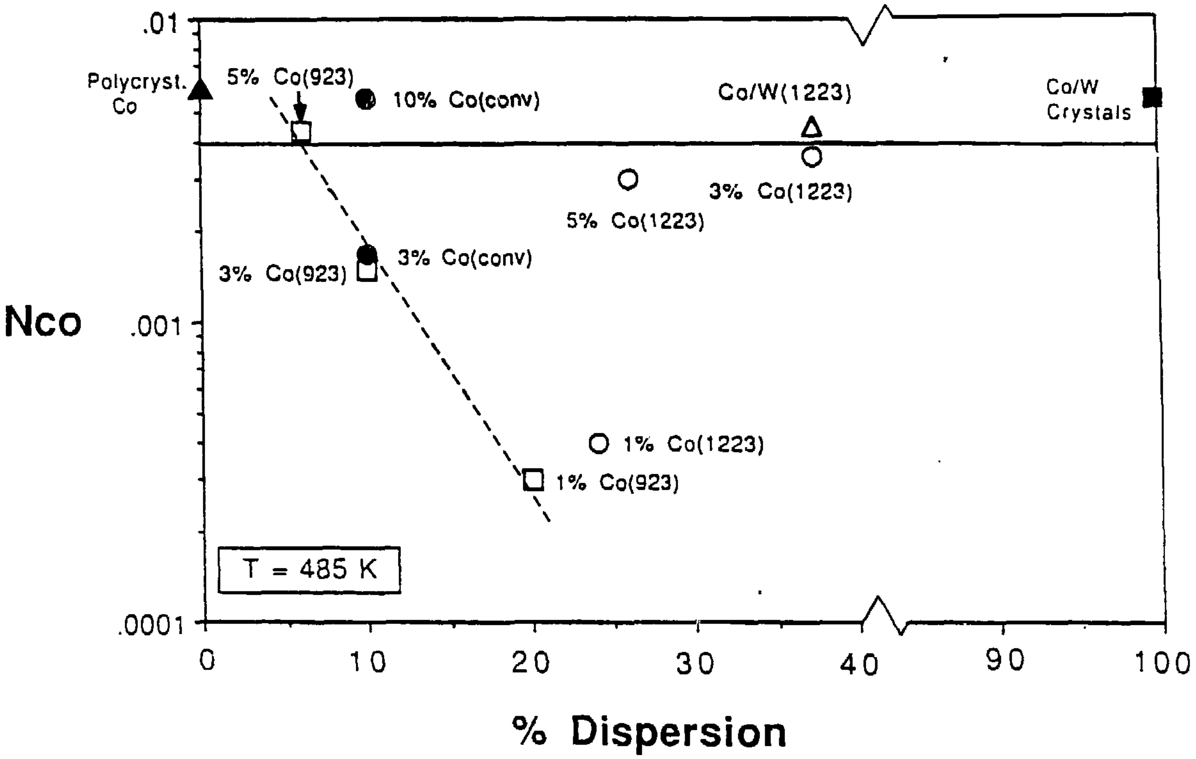

Figure 1. Carbon monoxide turnover frequency (485 K, 1 atm, $H_2/CO = 2$) versus % dispersion of cobalt catalysts (923 or 1223 refers to the temperature of dehydroxylation of support in K).

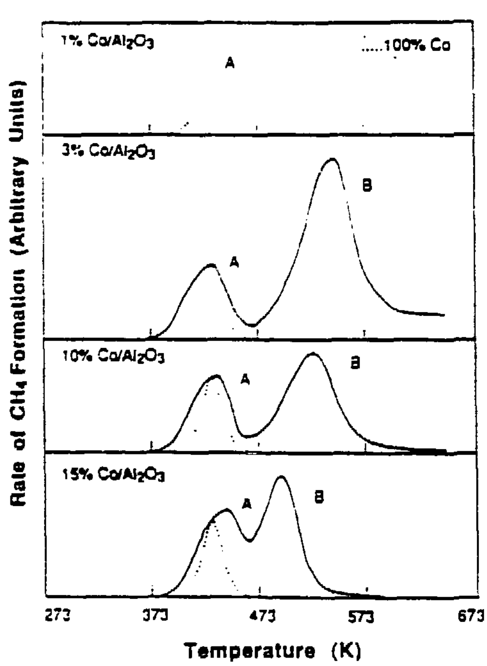

Fig. 2. Methane TPSR spectra for unsupported Co (dotted line) and Co/alumina catalysts (red. at 648 K; CO adsorbed at 298 K)

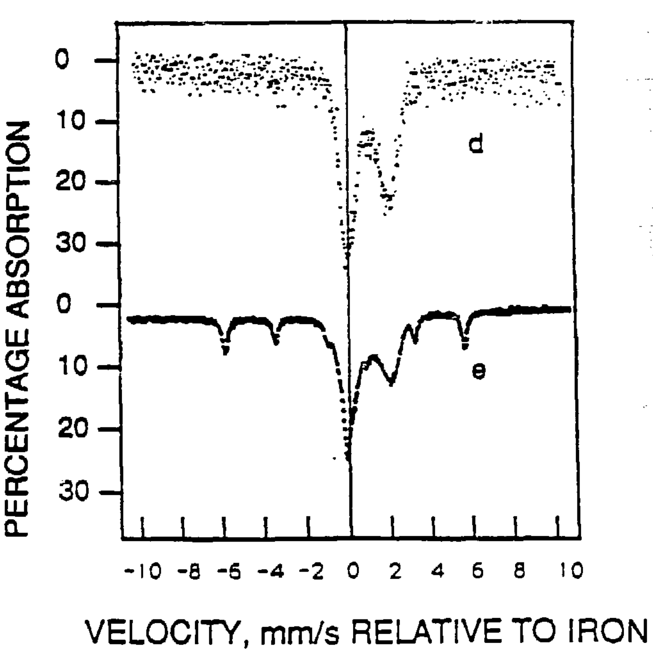

Fig. 3. Moessbauer spectra of 2% Fe/alumina (a) reduced at 773 K, (b) red. at 873 K.

CATALYTIC HYDROGENATION OF
CARBON MONOXIDE

Alexis T. Bell
Center for Advanced Materials
Lawrence Berkeley Laboratory

and

Department of Chemical Engineering
University of California, Berkeley, CA 94720

Research Scope and Objectives

The purpose of this program is to develop an understanding of the fundamental processes involved in catalytic conversion of carbon monoxide and hydrogen to gaseous and liquid fuels. Attention is focused on defining the factors which limit catalyst activity, selectivity, and resistance to poisoning, and the relationship between catalyst composition/structure and performance. To meet these objectives, a variety of surface diagnostic techniques are used to characterize supported and unsupported catalysts before, during, and after reaction. The information thus obtained is combined with detailed studies of reaction kinetics to elucidate reaction mechanisms and the influence of modifications in catalyst composition and/or structure on the elementary reactions involved in carbon monoxide hydrogenation.

Description of Research Effort

1. Isotopic Tracer and NMR Studies of Carbonaceous Species Formed over Ru/TiO_2 (8)

The synthesis of hydrocarbons from CO and H_2 has been carried out over Ru supported on anatase and rutile. The purpose of this work was to establish the effects of Ru dispersion and TiO_2 phase on the catalyst activity and selectivity, the nature and distribution of adsorbed carbonaceous species, and the dynamics of catalyst deactivation. Isotopic tracer experiments, complemented by NMR spectroscopy, revealed the presence of carbidic carbon, C_α, and two pools of alkyl carbon, $C_{\beta'}$ and $C_{\beta''}$. The C_α pool contains monomeric building blocks, whereas the $C_{\beta'}$ pool consists of intermediates to C_{2+} hydrocarbons. The $C_{\beta''}$ pool consists of longer alkyl chains which contribute to progressive catalyst deactivation. The initial activity of all Ru/TiO_2 catalysts was found to depend inversely on D_{Ru}. For the same D_{Ru}, Ru supported on anatase was 2.5 more active than Ru supported on rutile. Product distributions, however, were essentially independent of D_{Ru} or TiO_2 phase, indicating that these variables affect the initial steps of CO hydrogenation, but not the relative rates of chain propagation and termination. The time constant for catalyst deactivation was found to correlate with the turnover frequency for CO consumption, and the loss in activity was directly observed to be proportional to the fraction of surface

Ru not blocked by $C_{\beta''}$.

2. CO and CO_2 Hydrogenation Over $LaMn_{1-x}Cu_xO_{3+\lambda}$ Perovskites and Related Cu-Containing Catalysts (18-20)

CO hydrogenation has been investigated over perovskites with the composition $LaMn_{1-x}Cu_xO_{3+\lambda}$ (x = 0, 0.2, 0.4, 0.5, 0.6, 1.0); Cu supported on SiO_2, unpromoted and promoted with La_2O_3; Cu supported on La_2O_3 and on MnO_2/La_2O_3; and unsupported Cu metal powder containing traces of sodium oxide (NaO/Cu). The x = 0 perovskite ($LaMnO_{3.24}$) is weakly active for CO hydrogenation, and produces only hydrocarbons, whereas all the other perovskites are more active and display > 90% selectivity to alcohols (80% methanol and 20% C_{2+} alcohols). The C_{2+} alcohols follow a distribution characteristic of alkali-promoted copper catalysts. Cu/SiO_2 is > 80% selective to hydrocarbons, and < 5% selective to methanol. Introduction of La_2O_3 or NaO into the copper catalyst increases the CO hydrogenation activity and selectivity to alcohols. The activities and product distributions of the Cu-containing perovskites (x > 0) are similar to those of NaO/Cu and the La_2O_3-containing catalysts, suggesting that the active sites in all of the catalysts are similar. It is proposed that hydrocarbon synthesis occurs at Cu^0 sites, but that Cu^0 and Cu^+ sites are required for the synthesis of methanol and C_{2+} alcohols and that Cu^+ sites are stabilized at the adlineation between metallic copper and lanthana (or soda).

CO_2 hydrogenation has been carried out over Cu/SiO_2, $La_2O_3/Cu/SiO_2$, Cu/La_2O_3, $Cu/MnO_2/La_2O_3$, and NaO/Cu powder. The major products are methanol and methane. Methyl formate was also produced at temperatures below 523 K. In terms of oxygenate yield, the catalysts ranked in the order: $La_2O_3/Cu/SiO_2$ > Cu/SiO_2 > Cu/La_2O_3 > $Cu/MnO_2/La_2O_3$ >> NaO/Cu. Lanthana promotion of Cu/SiO_2 increases the formation of methanol but not of the other products. The selectivity patterns of the lanthana-supported catalysts are similar to that of Cu/SiO_2. Addition of Mn to Cu/La_2O_3 decreases the selectivity to methanol. Hydrogenation of CO_2/CO mixtures was studied over NaO/Cu, Cu/SiO_2, and Cu/La_2O_3. The NaO/Cu powder displayed higher selectivity to methanol in CO/H_2 than in CO_2/H_2. The activity and selectivity to methanol decreased with increasing CO fraction over Cu/SiO_2. Both activity and oxygenate selectivity increased with CO fraction over Cu/La_2O_3. C_{2+} alcohols are produced in CO-rich atmospheres. The observed effects of catalyst composition and feed composition on the activity and selectivity of Cu for methanol synthesis are attributable to the distribution of Cu^0 and Cu^+ sites.

3. Analysis of Reaction Pathways via the BOC-MP Method (3, 6, 14, 15)

The bond-order-conservation-Morse-potential (BOC-MP) approach has been used to calculate the activation energies for methanol synthesis over Cu and Pd. These calculations have revealed that in the absence of H_2O, or other sources of OH groups, CO hydrogenation is initiated by the formation of formyl groups. However, when OH groups are present, formate formation becomes the energetically preferred step, particularly over Cu. Application of the BOC-MP method also reveals that direct hydrogenation of adsorbed CO_2 is energetically unfavorable, relative to hydrogen-assisted CO_2

dissociation to form CO_s and OH_s. This conclusion is critical for understanding the mechanism of CO_2 hydrogenation to methanol.

4. Monte Carlo Simulation of Temperature-Programmed Desorption of Coadsorbed Species (7, 16)

A Monte Carlo model was developed for describing the temperature-programmed desorption of coadsorbed species from single-crystal surfaces. Interactions between the adsorbates and the metal surface, as well as interactions between the adsorbates, are taken into account using the bond-order-conservation-Morse-potential (BOC-MP) approach. The number, shape, and location of the peaks is found to be sensitive to the binding energy, coverage, and coordination of each coadsorbed species. The presence of a strongly bound coadsorbate on a bcc(100) surface is shown to shift the desorption spectrum for associative desorption of adsorbed atoms to lower temperatures. TPD spectra for the concurrent associative desorption of A atoms and the desorption of B molecules from a fcc(100) surface are of two types: in one case, both species exhibit new low-temperature features far removed from their pure component spectra; in the second case, only the species undergoing associative desorption displays new spectral features. The simulated TPD spectra are in qualitative agreement with experimental results for H_2 coadsorbed with strongly bound atomic species on Mo(100) and Fe(100) surfaces, as well as for CO and H_2 coadsorbed on Ni(100) and Rh(100) surfaces.

Future Research

Work on the following projects is now in progress:

1. Transient response studies of chain propagation and termination over Co/SiO_2.
2. BOC-MP calculations of the energetics of chain propagation and termination.
3. Monte Carlo simulation of pressure-assisted desorption of CO.
4. TPD and TPSR studies of the effects of metal oxide promoters on CO and CO_2 hydrogenation.
5. Raman characterization of dispersed metal oxides.

Publications

1. R. P. Underwood and A. T. Bell, J. Catal. 109, 61 (1988).
2. R. P. Underwood and A. T. Bell, J. Catal. 111, 325 (1988).
3. E. Shustorovich and A. T. Bell, J. Catal. 113, 341 (1988).
4. D. S. Jordan and A. T. Bell, J. Catal. 108, [illegible] (1987).

5. M. E. Levin, K. J. Williams, M. Salmeron, A. T. Bell, and G. A. Somorjai, Surf. Sci. 195, 341 (1988).

6. E. Shustorovich and A. T. Bell, Surf. Sci. 205, 492 (1988).

7. S. J. Lombardo, and A. T. Bell, Surf. Sci 206, 101 (1988).

8. G. H. Yokomizo and A.T. Bell, J. Catal. 119, 467 (1989).

9. G. H. Yokomizo, C. Louis, and A. T. Bell, J. Catal. 120, 1 (1989).

10. G. H. Yokomizo, C. Louis, and A. T. Bell, J. Catal. 120, 15 (1989).

11. A. T. Bell, *Proceedings of the 9th International Congress on Catalysis*, M. J. Phillips and M. Terkan, Eds., The Chemical Institute of Canada, Ottawa, Canada, Vol. 5, page 134, 1988.

12. S. T. Oyoma, G. T. Went, K. Lewis, G. A. Somorjai, and A. T. Bell, J. Phys. Chem. 93, 6786 (1989).

13. A. T. Bell, *Structure and Reactivity of Surfaces*, A. Zecchina, G. Costa, and C. Mortena, Eds., Elsevier, Amsterdam, 91 (1989).

14. E. Shustorovich and A. T. Bell, Surface Sci., in press.

15. E. Shustorovich and A. T. Bell, Surface Sci., in press.

16. S. J. Lombardo and A. T. Bell, Surface Sci., in press.

17. G. T. Went, S. T. Oyoma, and A. T. Bell, Surface Sci., in press.

18. M. L. Rojas, J. L. G. Fierro, L. G. Tejuca, and A. T. Bell, J. Catal., in press.

19. J. A. Brown Bourzatschky and A. T. Bell, J. Catal., in press.

20. J. A. Brown Bourzatschky and A. T. Bell, J. Catal., in press.

Catalytic Steam Gasification of Carbon: Research on Tungsten Carbide Catalysts with High Surface Area

M. Boudart
Stanford University

FG03-87ER13762
Progress Report for the Period of 7/15/87 - 8/15/89

Unsupported carbide powders with high specific surface area, namely α-WC (35 m^2g^{-1}, hexagonal), β-$WC_{0.61}$ (100 m^2g^{-1}, cubic face centered) and β-$WC_{0.5}$ (15 m^2g^{-1}, hexagonal) have been prepared. The key element in this preparation is the successful removal of surface polymeric carbon by careful gasification to methane by means of dihydrogen. The following work was carried out by Dr. Gerhard H. Raffeis, a postdoctoral fellow of the Deutsche Forschungsgemeinschaft, following the Stanford Ph.D. work of Fabio Ribeiro and Gerald Guskey reported previously.

Oxidation Reactions

Since many important industrial processes are based on catalytic oxidation reactions, it is interesting to investigate a simple case of an oxidation reaction, namely the oxidation of H_2 with either O_2 or N_2O. The reaction of H_2 and O_2 is interesting both from an application oriented and an academic point of view. Explosive H_2/O_2 mixtures might accidentally build up in closed systems, where both gases are handled, or after an uncontrolled chemical reaction, e.g., after an accident in a nuclear power plant. It is desirable to have a material that catalyzes the reaction of H_2 and O_2 to water in a controlled manner, meaning at a certain constant reaction rate, that allows for sufficient reaction energy dissipation, rather than through a free radical chain mechanism, that results in an explosion.

After preparation in a differential flow reactor and prior to their use in catalytic studies, the unsupported tungsten-carbide powder catalysts have been treated with H_2 at 1000 K to remove polymeric carbon and then passivated by a flow of 1% O_2 in He, so that the otherwise pryophoric material could be transferred through air to a flow recirculation reactor. The oxidation reactions were carried out on the catalysts at atmospheric pressure and in the range of 273 to 650 K in the flow recirculation reactor, with one reactant in large excess, the mixture thereby being beyond the explosion limits.

Studies of the kinetics showed [Guskey, 1989] that the Arrhenius plot for these reactions is not a straight line, as one would expect for a reaction that remains the same within the temperature range. The Arrhenius diagram was constructed by plotting ln k over 1/T, where k is the rate constant and T the reaction temperature in Kelvin. The rate constant is obtained from the areal rate, which is the reaction rate related to the total area of tungsten sites counted by H_2 titration of preadsorbed oxygen at room temperature, assuming that each site covers an area of $9.1 \cdot 10\text{-}16$ cm^2.

In fact in the N_2O/H_2 reaction three different temperatures ranges are observed, in which the slope of the line is different, namely 300-450 K (low), 450-550 K (moderate) and 550-600 K (high temperature). The slope at moderate temperature is four times larger than the slope at low temperature, while the slope at high temperature is about the same or slightly smaller. Whether the difference is significant is still under investigation.

In the O_2/H_2 reaction only two different regions in the range of 300-450 K (low) and 450-600 K (moderate temperature), which were separated by a similar break in the Arrhenius plot line, could be observed. A second break above 600 K similar to the N_2O/H_2 reaction could only be suggested, because in this reaction, at higher temperatures the oxidation of the tungsten carbide surface became substantial.

Although it can be argued that the water produced in the oxidation reaction of H_2 plays an important role for the explanation of the unusual observations in the Arrhenius plot, it remains a challenge to understand this phenomenon more quantitatively. The arguments are based on the fact that the break in the plot occurs at about the same temperature (450 K) as the maximum of the temperature programmed desorption (TPD) curve of water (430-450 K), the only product desorbed in such an experiment. The desorption peak is broad and occurs between 350 and 550 K. This is consistent with the changes in the slope of the Arrhenius line that do not happen abruptly but through a smooth transition. It was also found that the slope in the low temperature regime can be extended to 550 K, when the reaction atmosphere is saturated with water, so that the water desorption is shifted to higher temperature. A possible explanation follows:

In the low temperature region water sticks to the micropores and blocks them, so that the reaction is only taking place in the mesopores which have been shown to account for only 10 to 14% of the total surface area. The areal rate, and therefore the rate constant both in the high temperature and in the low temperature region, is calculated based on the same number of sites counted by the titration method described above, which is at room temperature. If in the high temperature region all water is desorbed, the reaction takes place in both the meso- and the micropores.

Therefore, only one of these regions reflects the "real" reaction, where the reaction takes place only at those sites, that are counted by the titration method. The other region gives only an "apparent" areal rate and therefore an "apparent" reaction rate. The moderate temperature region, where the slope was four times higher, might reflect only a transition regime between those two other regions. Thus a mixture of both the high temperature and the low temperature situation on the catalyst surface may be present in the moderate temperature region. Then the slope and ln k values in the moderate temperature region could have an ambiguous physical meaning and their discussion be misleading.

The question of course is which of the two regions presents the data for the "real" reaction. This depends on whether the titration method at room temperature really counts all active sites that are also available at higher temperature or whether the water produced during the titration blocks the same pores that are also inaccessible for the oxidation of H_2 at low temperatures.

Preliminary Experiments for the Oxidation Reaction

A sample of α-WC has been prepared from 0.575 g WO_3 (Aldrich, 99.9999%) placed on a frit in a quartz cell differential flow reactor by the reaction with a mixture of 27 mole-% H_2 in CH_4 at a flow rate of 0.11 μmol s^{-1} (2.7 cm^3 s^{-1}) for 21.6 ks (6 h) at 1100 K. After cooling down in flowing He to 1000 K the sample was treated with 31.8 μmol s^{-1} (0.77 cm^3 s^{-1}) H_2 for 4.7 ks (1 h 23 min) to remove polymeric carbon and the CH_4 produced was monitored by GC. The reaction was interrupted after a 16% decrease of the CH_4 peak after his maximum by replacing the dihydrogen by He and then cooling down. To passivate the catalyst the cell was then evacuated at room temperature to $6 \cdot 10^{-3}$ Pa, filled with 1% O_2 in He at 295 K up to atmospheric pressure, and then this mixture was allowed to flow through the cell at 0.70 µmol O_2 s^{-1} for 7.2 ks (2 h). The surface area of the passivated sample was determined after evacuation at room temperature 28.8 ks (8 h) by the BET method at 77 K with N_2 in the pressure range between 5 and 30 kPa to 18 m^2 g^{-1}.

To be able to compare the data obtained from the $O_2 + 2H_2$ reaction to other data and to test the reaction sysem, the reaction was carried out on 75.7 mg of a supported Pt catalyst (0.38% Pt/SiO_2, 95% metal exposed). The catalyst was reduced in 0.91 µmol s^{-1} (2.25 ml s^{-1}) H_2 for 3600 s (1 h) at 373 K and then evacuated. The cell was charged with the excess reactant (37.18 kPa O_2) and 53.57 kPa He. After the gas was cycled for 10.8 ks (3 h) a stoichiometric mixture of O_2 and $2H_2$ was added from an electrolytic cell at such a flow rate that the pressure in the system remained constant, so that the reaction rate could be calculated from the electrolysis current (48 mA), and the reaction was carried out for 4.2 ks (70 min). The mixture was recycled for another 13 hours, without addition of the reactant mixture from the electrolysis. The calculation according to a known method [Hanson] yielded 1.10^{-4} cm s^{-1} for the rate constant and 0.18 s^{-1} for the turnover frequency.

Future Work in the Oxidation Reaction

Rates were referred to the number of sites counted by titration of preadsorbed oxygen with H_2 at room temperature. It might be interesting to do the titration either at a temperature above 450 K where all water formed upon the titration is desorbed from the catalyst and readsorbed at a different place, e.g., on zeolite at low temperature so that it can be assumed that no sites are blocked by water and that no water is present in the vapor phase which could disturb the pressure monitoring of the titration process. To get rid of the water produced, the catalyst could be evacuated at the water desorption temperature after no further dihydrogen uptake is observed and continue the titration experiment after all water has been desorbed. If now more dihydrogen would be consumed by oxygen titration it would be clear that not all sites could be measured by titration at room temperature.

Reactions of Alkanes

It is known that tungsten carbide catalysts catalyze the hydrogenolysis reaction of various alkanes such as butane, hexane, and neopentane. After exposure to oxygen they also show some isomerization activity. The role of the oxygen was suggested to create oxycarbides on the surface that provide acidic sites on which a classical isomerization reaction via carbenium ions can occur. Since acidic isomerization sites and metal or metalcarbide sites or ensembles may be different, this mechanism is referred to as "dual function" mechanism, as, e.g., it is known for platinum on acidic alumina supports in the petrochemical reforming process. The other effect proposed is a more subtle one, namely that of a "spectator" oxygen that creates tungsten sites in high oxidation states on which a carbene mechanism can take place as it is known for the metathesis reaction. A better understanding of these mechanisms is of great importance due to their potential impact on the mechanism of important fuel reactions.

Preparation of Unsupported Tungsten Carbide Powders in Three Batches

A total amount of 826 mg of α-WC was produced in three batches from WO_3 (Aldrich, 99.9999%), which were heated up to the reaction temperature in flowing He and then treated with a mixture of 20 mole-% H_2 in CH_4 at a total flow rate of 96 ± 8 µmol s^{-1} (the volume flow is given in Table 2) at 1100 K for 21.6 ks (6 h). The samples were then cooled down in He to 973 K and treated with

0.50 ± 0.02 cm^3 s^{-1} H_2. This surface carbon removal reaction was interrupted after a 15% decrease of the CH_4 development peak maximum the same way as described above. The specific surface area Sg, now of the fresh sample, was determined by the BET method at 77 K with N_2 in the pressure range between 5 and 30 kPa to 18 m^2 g^{-1}, after evacuation at room temperature.

Before passivation of the sample the cell was evacuated to $3 \cdot 10^{-6}$ kPa while heating it up to 800 K within 1.2 ks (20 min) to desorb H_2, closing the cell to the vacuum system and cooling to room temperature. The passivation treatment was carried out by filling a certain dosing volume with O_2 at certain pressure and room temperature, leaking this amount of oxygen as slowly as possible into the cell (ca. 175 Pa s^{-1}) and equilibrating the sample with that mixture over several hours.

Representative Sample of Three Batches of α-W C

All three batches were mixed thoroughly. A sample of 65.2 mg was rectivated by reduction in flowing H_2 at a flow rate of 0.67 cm^3 s^{-1} and 673 K for 7.2 ks (2 h). At the same temperature the H_2 flow was replaced by a He flow of 1.04 $cm^3 s^{-1}$ for 1.2 ks (20 min) to desorb the hydrogen and then cooled down in He.

The specific surface area Sg of this representative sample was 31 $m^2 g^{-1}$, which is higher than the expected value. This was estimated by calculating the mass weighed mean value of Sg of all three samples, which was 23 $m^2 g^{-1}$. Provided this difference is significant, the explanation could be that the reactivation treatment in H_2 removes further polymeric carbon from the surface, which might have blocked pores before and thereby reduced the value of Sg. This would suggest that the carbon removal reaction has not been stopped at the optimum time. It could also be that due to the presence of H_2 and water formed by the reaction with the surface oxygen a combined carbon gasification/hydration process occurs with some kind of polymeric carbon which was presumably left over after the previous carbon removal reaction because it could be of such kind that it is harder to remove under those conditions with H_2 alone.

On this sample 18.75 μmol g^{-1} CO were chemisorbed. The experiment was carried out by measuring a CO chemisorption isotherm at room temperature, evacuating the cell and measuring a CO physisorption isotherm, in the range of 6 to 19 kPa. The isotherms are the plot of the adsorbed volume of CO as a function of pressure. The difference in the isotherms extrapolated to zero pressure is the volume of CO irreversibly adsorbed at room temperature. The amount of CO adsorbed was calculated based on the value of Sg determined and on the assumption that the surface density of tungsten atoms on the surface is $10^{15} cm^{-1}$. The percentage of surface tungsten atoms covered by CO was 4.4%.

The catalyst samples prepared as described below were delivered to Enrique Iglesia at Exxon Corporate Research Laboratories for kinetic studies of alkane hydrogenolysis and isomerization. The work at Exxon is now being written up by Dr. Iglesia, together with the results of Fabio Ribeiro.

Publications

"Molybdenum Carbide Catalysts I. Synthesis of Unsupported Powders", J.S. Lee, S.T. Oyama, and M. Boudart, J. Catal. **106**, 125 (1987).

"Molybdenum Carbide Catalysts II. Topotactic Synthesis of Unsupported Powders", J.S. Lee, L. Volpe, F.H. Ribeiro, and M. Boudart, J. Catal. **112**, 44 (1988).

Accepted for Publication

"Molybdenum Carbide Catalysts 3. Turnover Rates for the Hydrogenolysis of n-Butane", J. S. Lee, S. Locatelli, S. T. Oyama, and M. Boudart, to appear in J. Catal.

Articles In Preparation

"The Reaction Between H_2 and O_2 on Tungsten Carbide Catalysts", G.J. Guskey and M. Boudart, to be submitted to Catal. Lett.

"Preparation and Surface Composition of Tungsten Carbide Powders with High Specific Surface Area", M. Boudart, R.A. Dalla Betta, G. Guskey, and F.H. Ribeiro, to be submitted to Chemistry of Materials.

"Reactions of Neopentane over βW_2C and WC: The Effect of Surface Oxygen", M. Boudart, R.A. Dalla Betta, and F.H. Ribeiro, to be submitted to Catal. Lett.

"Reactions of n-Hexane over βW_2C and WC: The Effect of Surface Oxygen", M. Boudart, R.A. Dalla Betta, and F.H. Ribeiro, to be submitted to J. Catal.

Reactive Characterization as a Probe of the Nature of Catalytic Sites

Alan Brenner

Department of Chemistry
Wayne State University
Detroit, MI 48202

Research Scope and Objectives

This research program is primarily concerned with achieving a better understanding of the nature of active sites on heterogeneous catalysts. It is extremely rare that the identity of an active site is known for a heterogeneous catalyst. At a simpler level, it is even uncommon for the density of active sites to be known. Further, it is often impossible to meaningfully compare the activities of different types of catalysts and this impedes achieving a unified understanding of catalytic action.

For the past two decades the most popular approach to understanding heterogeneous catalysis at the molecular level has been to apply the tools of surface science. A common problem in such studies is that spectroscopic techniques tend to identify the major surface species, whereas active sites often account for a very small fraction of a surface. This research program takes a very different approach. The patterns of activities and product distributions of catalysts are used to gain information on the nature of the active site. Since any reaction product must necessarily channel through the active site, this technique, termed *reactive characterization*, has the advantage that it is only sensitive to the active site. Further, special emphasis is given to determining the concentration of active sites which enables the activities of homogeneous catalysts, metal oxides, and metals to be compared on the same basis (turnover frequency).

This research program has three main objectives:

(1) Prepare and determine the activity of well dispersed and low valent catalysts of base metals.
(2) Determine the activity for H_2-D_2 exchange for a variety of transition metals and metal oxides.
(3) Develop the concept of *reactive characterization* to see if it can be used to assess the morphology of catalysts containing very small metal ensembles.

Substantial data dealing with objective (1) and partial data for the other objectives have been previously reported. This report will describe results of the past year.

Description of Research Effort

Objective 2

Hydrogen activation is an important step in many catalytic reactions and may be conveniently studied by measuring the rate of H_2-D_2 exchange over a catalyst. Although this reaction has been extensively studied by others over metals and moderately studied over metal oxides, in very few cases has the site density for the exchange reaction been determined. This makes it difficult to compare the activities of the two types of catalysts. Also, a wide range of reaction conditions have been employed. This is the first exhaustive study that enables a comparison of the activities of the catalysts.

Earlier work from this project has been expanded and is now almost complete. Table 1 summarizes a large amount of data for metal oxides. An important aspect of the work is that the activity was determined as a function of activation temperature. It is found that the activity varies tremendously with the activation temperature, and thus earlier data in the literature are often incomplete or misleading. In particular, all of the catalysts are inactive when 100% and 0% hydroxylated. The data in Table 1 refer to catalysts activated at the temperature yielding maximum activity. A unique contribution of this study is that both a lower and upper limit to the number of active sites have been determined. Selective poisoning by CO was used to obtain an upper limit to the number of active sites. Since some of the CO can adsorb on inactive sites, it is well known that this technique will yield an upper limit to the number of active sites. The exchange of surface OH groups

Table 1. H_2-D_2 Exchange Over Metal Oxides#

Catalyst	Activity (10^{12} HD/cm^2·s)	(HD/site·s)	CO sites‡ ($10^{12}/cm^2$)	Exch OH ($10^{11}/cm^2$)	$\theta^* x10^2$	(Exch OH/Total OH)$x10^3$
NiO	71	12.9	5.5	0.6	0.8	1.5
Cr_2O_3	38	5.2	7.3	4.6	1	20
Co_3O_4	14	4.5	3.2	0.3	0.4	0.03
MgO	13	3.7	3.5	34	-	7
Fe_2O_3	0.7	1.8	0.4	1.0	0.05	3
ZnO	6.4	1.1	5.8	40	1	6
MoO_2	15	1.1	14	0.8	5	-
TiO_2	0.2	0.7	0.3	1.4	0.004	2
Mn_2O_3	0.2	0.5	0.3	<0.1	0.04	$<4x10^{-5}$
V_2O_3	4.5	0.3	15	0.7	7	-
CuO	0.2	0.3	0.7	< 0.1	0.1	$<4x10^{-5}$

Table 2. H_2-D_2 Exchange Over Metals#

Catalyst	Activity (10^{15} HD/cm^2·s)	(HD/site·s)	CO sites‡ ($10^{14}/cm^2$)	θ^*
Rh	140	200	7	0.25
Mo	5	111	0.5	0.01
Ru	22	47	4.7	0.20
W	1.6	46	0.3	0.02
Ir	6.7	18	3.8	0.12
Fe	1.8	71	2.6	0.06
Os	2.8	4.0	7.1	0.56
Re	0.2	2.2	0.9	0.03
Pd	3.3	2.1	16	0.36
Pt	0.4	2.0	2.2	0.13
Co	0.2	1.3	1.4	0.05
Ni	0.2	0.18	12.2	0.27

#Reaction conditions: 273K, 1 atm total P, flowing gas mixture with 1.33% H_2, 1.33% D_2, and 97.3% He.
‡Active sites determined by CO poisoning.
*Fraction of surface metal atoms which are active.

(σ-OH) with $D_2(g)$ was used to obtain a lower limit to the number of active sites. This is possible because of the very unusual case that any site capable of undergoing this *stoichiometric* reaction must also be a site for the *catalytic* reaction. This is readily seen by the following scheme.

$$\sigma\text{-OH} + D_2(g) \rightleftharpoons HD(g) + \sigma\text{-OD}$$

$$\sigma\text{-OD} + H_2(g) \rightleftharpoons HD(g) + \sigma\text{-OH}$$

$$H_2(g) + D_2(g) \rightleftharpoons 2HD(g)$$

The appearance of HD(g) can be monitored with great sensitivity using a mass spectrometer, so an accurate count of the lower limit of the active sites can be obtained. Table 1 shows that roughly 0.5% of the surface OH are active sites. The ratio of the upper limit to lower limit of active sites varies from about 1000 to 1, and roughly 1% of the surface metal ions are active.

These data lead to a unified picture of reactivity for H_2-D_2 exchange over metal oxides. It appears that a common mechanism may be as follows. Note that the site is an ensemble, consisting of an exposed metal cation, O^{2-} (created by dehydroxylation) and a neighboring σ-OH.

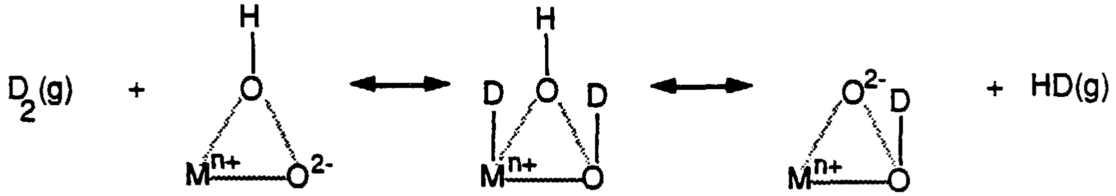

Table 2 summarizes data for H_2-D_2 exchange over metals. It is interesting that the fraction of the surface which is active is usually much higher than for oxides. Also, the specific activity (activity per unit surface area) of the metals is about 10^3 fold higher than for the oxides, but the turnover frequency is only about 10 fold more, reflecting the lower site density on the oxides.

Because of the importance of σ-OH on the activity of metal oxides, it has become necessary to study the temperature dependence of this quantity. This work is still in progress, but at this time some data have been obtained on Fe_2O_3, NiO, Co_3O_4, Cr_2O_3, ZnO, TiO_2, MgO, Mn_2O_3, and CuO using TGA. A major problem with such experiments is being able to differentiate between true σ-OH and adsorbed H_2O. We have adopted an unusual approach to this problem which is simple and accurate. A sample is heated to such a high temperature (about 1000 °C) that there is no further weight loss. This is assigned a hydroxyl content of zero, and additional weight at moderately lower temperatures is then attributed to σ-OH. From knowledge of the crystal structure, it is also possible to determine at what temperature a monolayer of σ-OH is exceeded, so it may be assumed that at lower temperatures adsorbed H_2O is also present. An interesting observation is that the activity of an oxide seems to correlate with its ease of dehydroxylation.

Objective 3

In an earlier report we noted that the isotopic products from the deuteration of ethylene can provide information on the nature of active sites. Homogeneous catalysts and metal oxides usually give a high yield (>80%) of the trivial product, d_2-ethane, but metal surfaces yield considerable scrambled product, $C_2H_nD_{6-n}$, $n = 0 - 6$, so the yield of d_2-ethane is <50%. Strong mechanistic arguments can be made that the scrambling should only readily occur on catalysts which have sites which are both multiatomic and connected (in the sense that a species can migrate from one site to another). Thus, this probe reaction of *reactive characterization* can provide information on the morphology of active sites.

This technique was applied to catalysts of Ni and NiO supported on alumina. The expected result was found that Ni gives a low yield (25%) and NiO gives a high yield (85%) of d_2-ethane. Further, by measuring the activation energy and absolute rates for the formation of d_2-ethane, scrambled ethanes, and for exchange of D into ethylene, it can be shown that the same elementary reaction steps are responsible for the scrambling of ethane and ethylene.

Of particular interest are experiments utilizing Ni catalysts partially poisoned by CO. If islands of Ni are left, then the activity will drop but the isotopic distribution of the ethanes should be the same as the parent catalyst (very scrambled). However, it is observed that as the extent of poisoning increased the yield of d_2-ethane increased, reaching 93%. This result strongly suggests that the CO adsorbs evenly over the Ni and results in small clusters of exposed Ni which are isolated from each other. Thus, the heterogeneous Ni catalyst is now functionally similar to NiO and homogeneous Ni catalysts, which possess discrete sites.

Future Work

During the next year of the project, effort will especially be directed to the following areas.

(1) Additional experiments dealing with *reactive characterization* will be done. Emphasis will be on investigating poisoned catalysts and some work will also be done with alloys (such as Cu-Ni in which one component of the alloy is inactive) and homogeneous catalysts. We will also apply the technique to some immobolized complexes of noble metals. It is expected that the hydrogenation activity of some of these materials will be shown to be due to a small amount of metal which has formed (which would be revealed by a low yield of d_2-ethane). If they have any hydrogenation activity, we will also investigate some of the new high temperature superconductors to see if they have any unusual activity pattern.

(2) The experiments dealing with H_2-D_2 exchange and the hydroxyl content of metal oxides will be completed.

Publications of DOE Sponsored Work From The Last Two Years

1. P. N. Gonzalez and A. Brenner, "Ethylene Deuterogenation as a Probe of Active Sites", "Catalysis: Theory to Practice", M. J. Phillips and M. Ternan, Ed., Chemical Institute Canada, 1988, p. 1020.
2. A. Kadkhodayan and A. Brenner, "Temperature Programmed Reduction and Oxidation of Metals Supported on Alumina", J. Catal., 117, 311 (1989).
3. P. N. Gonzalez, M. A. V. Garcia, and A. Brenner, "Synthesis, Characterization, and Catalytic Activity of Group 6B Metal Carbonyls Supported on Titania", J. Catal., 118, 360 (1989).
4. P. N. Gonzalez and A. Brenner, "Comments on Ethylene Deuterogenation as a Probe of Active Sites", "Catalysis: Theory to Practice", M. J. Phillips and M. Ternan, Ed., Chemical Institute Canada, Volume 5, p. 359, 1989.
5. Y. Gu and A. Brenner, "Hydrogen Activation by Magnesia Catalysts", J. Catal., submitted, 1990.

PROJECT SUMMARY

Title: Model Cu/ZnO Catalysts for Methanol Synthesis: The Role of Surface Structure

Principal Investigator: Charles T. Campbell, Associate Professor of Chemistry, University of Washington

Copper/zinc oxide catalysts are highly active and selective for several reactions of importance in energy technologies: methanol synthesis, water-gas shift, and methanol steam reforming. These reactions are studied here using ultrahigh vacuum surface science combined with reaction kinetics at high pressures 1-10^4 torr). These experiments apply surface analytical techniques to investigate the relationship between catalytic activity and the atomic-level surface structure of model catalysts based on Cu and ZnO single crystals. The structural and electronic properties of adsorbed intermediates are correlated with their kinetics in individual steps, which in turn are compared to the overall reaction rates. In this way, a detailed understanding of the active site involved in each step is developed. The kinetics of the water-gas shift reaction and many elementary steps have been measured on the clean and cesium-doped Cu(110) surface. An ultra low-cast surface vibrational spectrometer was also built. Future work will involve the kinetics of methanol synthesis and its individual steps on clean and Cs-doped Cu crystals and on structurally-characterized Cu and Cs films on ZnO(<0001). These results should improve the fundamental understanding in Cu/ZnO catalysis and also in phenomena generic to catalysis, such as interactions at metal/oxide supports.

I. Water Gas Shift Mechanism over Cu(110) and Cs/Cu(110) [4,10-11,13-14,16-18]

We have recently measured the kinetics of the overall water-gas shift (WGS) reaction and many of its elementary steps over clean and Cs-doped Cu(110), for comparison to our earlier results over Cu(111). Considerable structural sensitivity was seen, with Cu(110) being more active. In addition these results have led to a very complete understanding of the mechanism of the water-gas shift reaction which unifies experimental results from many investigators for the first time [16]. The 1-D potential energy diagram for this reaction mechanism over clean Cu(110) is shown in Fig. 1a (from [16]), where all the energetics are now known with considerable accuracy except for the step: $OH_a \rightarrow O_a + H_a$. This reaction is rapidly achieved via the water-catalyzed route shown in Fig. 1b, or by a single-step process that is even faster. The energetics shown here for Cu(110) are quite similar for Cu(111) except for the barriers for the processes: $H_2O_a \rightleftharpoons H_a + OH_a$, and $CO_2 \rightleftharpoons CO_a + O_a$, which are higher by ~7 and ~2 kcal/mole, respectively, on the (111) plane.

Cesium in submonolayer quantities greatly accelerates the WGS reaction on both Cu(111) and Cu(110) [16,17]. Post-reaction surface analysis has clearly proven that the cesium quickly converts mainly to a surface cesium carbonate ($Cs_n \cdot CO_{3,a}$) under reaction conditions [17]. Adsorption studies in UHV suggest that this carbonate first forms via the process:

$$2CO_2 + nCs_a \rightarrow Cs_nCO_{3,a} + CO, \qquad (1)$$

which occurs very rapidly even at 200 K. The reactions of this carbonate have been studied in detail [17]. Under reaction conditions, the equilibrium

$$Cs_n \cdot CO_{3,a} = Cs_n \cdot O_a + CO_2 \qquad (2)$$

is very rapid, with thermodynamics strongly favoring the left side. Nevertheless, the product $Cs_n \cdot O_a$ is available on the surface in low concentrations at steady-state. This species readily undergoes the following reactions in UHV [10-11]:

$$CO + Cs_n \cdot O_a \rightarrow CO_2 + nCs_a \qquad (3)$$

and

$$H_2O + Cs_n \cdot O_a \rightarrow OH_a + Cs_n \cdot OH_a \, . \qquad (4)$$

These steps are probably important in explaining the promotional influence of Cs in WGS. Particularly important is the facile O-H bond cleavage in step 4. The process:

$$2OH_a \rightarrow H_2O + O_a \qquad (5)$$

has a much higher thermodynamic barrier in the presence of Cs_a [11]. Thus, the surface cesium and hydroxyl groups generated in step 4 are mutually stabilizing, and probably even have some direct bonding. In the presence of Cs, the differentiation between "OH_a" and "$Cs_n \cdot OH_a$" is vague and nearly continuous. At high enough Cs coverages (>1/2 monolayer), a true $CsOH_a$ complex is indeed formed, which decomposes via the evolution of $(CsOH)_2$ gas at ~500K [11]. This Cs-induced stabilization of surface hydroxyls on Cu is probably important in that the hydroxyl groups, while remaining on the surface to higher temperatures, have a better chance for further O-H bond cleavage in a step such as:

$$Cs_n \cdot OH_a \rightarrow Cs_n \cdot O_a + H_a \qquad (6)$$

We have also shown that Cs_a greatly stabilizes both O_a and H_a on Cu(110) [11], which should also favor step (6).

Finally, we have studied the influence of Cs_a and $Cs_n \cdot O_a$ upon the formation (from HCOOH) and decomposition kinetics of surface formate on Cu(110) [18]. Since adsorbed formate is widely accepted as an intermediate in methanol synthesis, these results are also potentially pertinent in understanding the promotional role of Cs there.

II. Future Plans

We have begun to address the role of ZnO in these catalysts by characterizing model catalysts having deposited ZnO_x on the surface of Cu single crystals, and others having Cu vapor-deposited on the ZnO(0001) oxygen-terminated surface. In the future, both these and the Cs/Cu(110) model catalysts will be studied with respect to methanol synthesis kinetics and elementary steps.

III. Subsidiary Research Progress

We have also studied the electronic structure of Cu substituted in the bulk and the surface of ZnO(0001) with semi-empirical quantum chemical (INDO) calculations of $\leq$ 26 atom clusters [2]. We have studied the chemisorption of simple molecules which are important in methanol synthesis such as CO, formate, formaldehyde and methoxy on Cu, ZnO, and Cu/ZnO clusters using INDO calculations [2,3,6]. These results, together with our recent study of ethylene oxide and carbonate on silver clusters [8], have demonstrated the feasibility of this theoretical approach to such problems, highlighting those questions that can and cannot be successfully addressed.

We have also experimentally investigated the interaction of CO with the Al/Ru(0001) surface [1], and the growth of bismuth overlayers on Cu(110) [12]. In the latter case, we have discovered general criteria for predicting submonolayer growth modes of metals on one-dimensionally corrugated surfaces. We have also written a relatively comprehensive review of "Studies of Model Catalysts with Well-Defined Surfaces Combining Ultrahigh Vacuum Surface Characterization with Medium and High Pressure Kinetics" [9].

Accurate quantitative measurements of desorption rates or adsorbate coverages by thermal desorption mass spectroscopy (TDS) are hindered by the fact that some species desorb with much sharper angular distributions than $\cos \phi$ (e.g., frequently up to $\cos_9 \phi$). This can lead to relative errors of >400%. We have shown that such errors can be reduced to less than 7% by placing the mass spectrometer at a "magic angle" of 34° to 42°, depending upon the sample-to-detector distance [15].

Finally, much effort has been devoted during the past year to building a new UHV system with capabilities for high-resolution electron energy loss spectroscopy (HREELS), TDS, AES, and sputter cleaning. This system is almost entirely homemade, and was constructed with no major external funding.

V. Publications Resulting from this Grant Support (Last Two Years)

1. "The Interaction of Aluminum with the Ru(0001) Surface and Its Influence Upon CO Chemisorption," C. T. Campbell and D. W. Goodman, *J. Phys. Chem. 92*(1988), 2569-2573.
2. "A Quantum Chemical Study of ZnO, Cu/ZnO, Cu_2O and CuO Clusters and CO Chemisorption on ZnO(0001), CuZnO(0001) and Cu/ZnO(0001) Surfaces," J. A. Rodriguez and C. T. Campbell,*J. Phys. Chem. 91*(1987), 6648-6658.
3. "A Quantum Chemical Study of the Chemisorption of Ammonia, Pyridine, Formaldehyde, Formate and Methoxy on ZnO(0001)," J. A. Rodriguez and C. T. Campbell, *Surface Sci. 194* (1988), 475-504.
4. "Model Cu/ZnO Catalysts for Water-Gas Shift and Methanol Synthesis Based on Single Crystals," C. T. Campbell, *Stud. Surf. Sci. Catal. 38, "Catalysis 1987"* - Proc. 10th North Am. Catalysis Soc. Meeting, ed. J. H. Ward (Elsevier, Amsterdam, 1988), p. 783-790.
5. "Applications of Surface Analytical Techniques to the Characterization of Catalytic Reactions," C. T. Campbell, *J. Vac. Sci. Technol. A6* (1988), 1108-1112.
6. "A Quantum Chemical Study of the Adsorption of Water, Formaldehyde and Ammonia on Copper Surfaces and Water on ZnO(0001)," J. A. Rodriguez and C. T. Campbell, *Surface Sci. 197* (1988), 567-578.
7. "A Quantum Chemical Study of the Adsorption of CO_2 and OH on Cu and ZnO Surfaces and OH on Pt Surfaces," J. A. Rodriguez, *Langmuir 4* (1988), 1006-1020.
8. "The Chemisorption of Ethylene Epoxide and Carbonate on Silver: A Quantum-Chemical Study," J. A. Rodriguez and C. T. Campbell, *Surface Sci. 206* (1988), 424-450.
9. "Studies of Model Catalysts with Well-Defined Surfaces Combining Ultrahigh Vacuum Surface Characterization with Medium and High Pressure Kinetics," C. T. Campbell, *Advances in Catalysis 36* (2989), 1-54.
10. "Adsorption of CO and CO_2 on Clean and Cesium-Covered Cu(110)," J. A. Rodriguez, W. D. Clendening and C. T. Campbell, *J. Phys. Chem. 93* (1989), 5238-5248.
11. "The Chemisorption and Coadsorption of Water and Oxygen on Cs-Dosed Cu(110)," W. D. Clendening, J. A. Rodriguez, J. M. Campbell and C. T. Campbell, *Surface Sci. 216* (1989), 429-461.
12. "The Growth Modes of Vapor-Deposited Bismuth on a Cu(110) Surface," W. D. Clendening and C. T. Campbell, *J. Chem. Phys. 90* (1989), 6653-6656.
13. "Chemisorption Studies on Cs/Cu(110); Model Studies of Cesium Promoters on Copper-Based Catalysts," J A. Rodriguez, W. D. Clendening, J. M. Campbell, W. Min and C. T. Campbell, *J. Vac. Sci. Technol. A7* (1989), 2118-2120.
14. "Does CO_2 Dissociatively Adsorb on Cu Surfaces?" J. Nakamura, J. A. Rodriguez and C. T. Campbell, *J. Condensed Matter* (in press).
15. "Magic Angle Thermal Desorption Mass Spectroscopy," S. Pauls and C. T. Campbell, *Surface Sci.* (in press).
16. "The Kinetics and Mechanism of the Catalytic Water-Gas Shift Kinetics over Clean and Cesium-Promoted Cu(110); A Comparison with Cu(111)," J. N. Nakamura, J. A. Campbell and C. T. Campbell, Faraday Transactions (invited, submitted).
17. "The Nature of the Cesium Promoter on Copper Catalysts for Water-Gas Shift and Methanol Synthesis," J. N. Nakamura, J. A. Campbell and C. T. Campbell (in preparation).
18. "The Interactions of Formic Acid and Formate with O/Cu(110), Cs/Cu(110) and O/Cs/Cu(110) Surfaces," F. C. Henn and C. T. Campbell (in preparation).

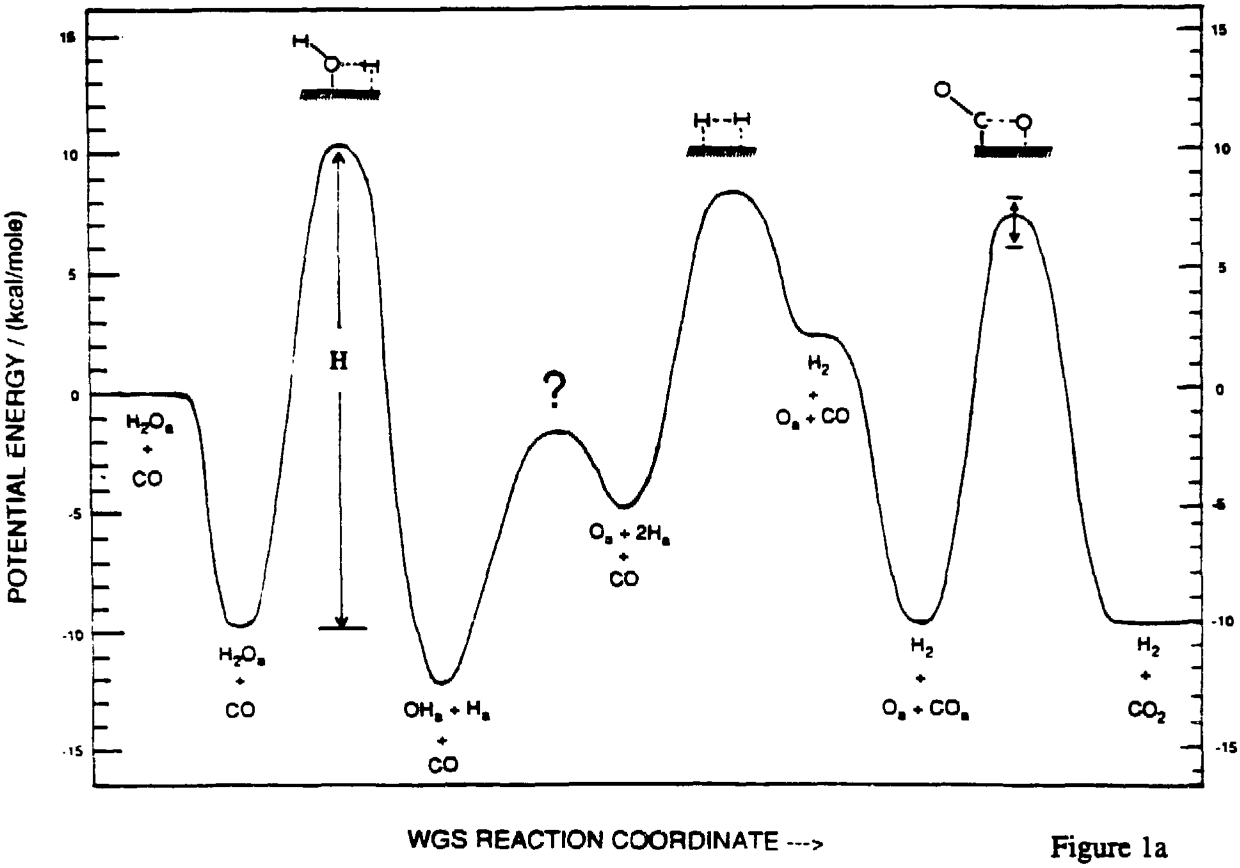

Figure 1a

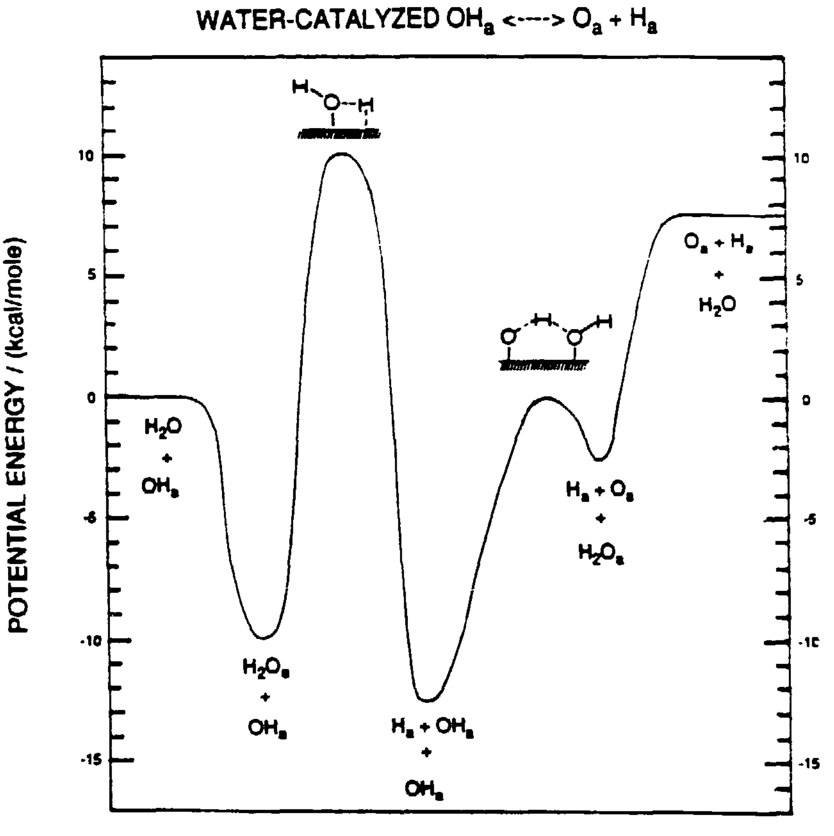

Figure 1b

Laser Studies of Chemical Dynamics at the Gas - Surface Interface

R.R. Cavanagh and D.S. King
Center for Atomic, Molecular and Optical Physics
National Institute of Standards and Technology
Gaithersburg, MD 20899

Dynamics of gas/surface interactions provide the focus for the present experimental program. The primary area of interest involves both the potential and current use of lasers to initiate and control chemical reactions at surfaces. Our studies have been directed towards detailed investigations of molecular desorption induced by pulsed laser radiation. By using quantum-state specific laser diagnostics to examine the energy content of molecules which are released from well characterized surfaces in an ultra high vacuum environment, it is possible to enhance our insight into the nature of the interaction potential involved in the desorption process.[1-3] Based on previous studies, it is clear that laser irradiation of solid surfaces will eventually lead to the thermal heating of the substrate.[4] Consequently, laser driven thermal processes can certainly be involved in the LID process. In addition to thermal effects, however, there has been much speculation regarding adsorbate specific reactions which might be activated given the judicious choice of laser pulse characteristics. Over the past two years, we have performed quantum-state-specific studies that have clarified the role of excited carrier driven desorption processes in the LID of NO from both metallic [Pt(111)][5-8] and semiconductor [Si(111)][9] surfaces.

NO/Pt(111):

Previous work in this program identified the non-thermal nature of LID of NO from platinum foils. By extending these measurements to the LID of NO from Pt(111), it has been possible to clarify the nature of the desorption process. The experimental facilities have been described elsewhere, and are briefly summarized as follows. The Pt(111) crystal is mounted in a UHV chamber equipped with modern surface science diagnostics (Auger, LEED, QMS, and ion sputtering) and ports for the introduction of laser beams. A Q-switched Nd:YAG laser (≈17 nsec fundamental pulse duration) generated the desorption pulses and permitted the wavelength sensitivity (355, 532, 1064, 1907 nm) of the LID process to be investigated. The angle of incidence (0° and 70° with respect to the surface normal), polarization, and fluence of this laser could be varied in order to test different theoretical models of the excitation process. The desorbed NO was detected using single photon laser-induced fluorescence (LIF) of the $A^2\Pi$-$X^2\Sigma^+$ transition. Quantum-state-specific time-of-flight (TOF) spectra were recorded by electronically scanning the time delay between the firing of the desorption and detection lasers. With the time delay held fixed, it was possible to record excitation spectra for desorbed NO within a well defined kinetic energy increment. Subsequent fitting of the observed TOF data to a modified Maxwellian velocity distribution $\{P(v)=v^2\exp[-(a+bv+cv^2)]\}$ leads to an independent determination of the mean kinetic energy <KE> for each internal state.

For the Pt(111) data reported here, the maximum laser induced temperature jump did not exceed 110K, corresponding to a maximum surface temperature of 330K. The surface temperature was typically idled at T_{idle}=220K and an NO saturated surface was prepared which resulted in an NO coverage of 0.25 ML (1 ML = 1.5×10^{15}cm^{-2}) in a p(2x2) ordered overlayer. Even at the extreme laser heating conditions, the desorption yield per incident pulse was less than 10^{-5} ML/shot, corresponding to a quantum yield of 1 NO molecule per 10^8 absorbed photons. The LID channel described in the following exhibited a measurable cross section only for NO in the top-site, and not for NO present in the bridge site at lower surface coverage.

The time-of-flight data revealed two significant aspects of the kinetic energy distributions of the desorbed NO. Figure 1 indicates the observed state-resolved kinetic energy distributions for desorption induced with three different wavelengths derived from the Nd:YAG laser. It is clear that the kinetic energy distributions are sensitive to the desorption-laser wavelength. For each wavelength, it was found that although the absolute yield varied linearly with increasing laser fluence, the mean kinetic energy was independent of fluence. Hence, the discrepancy between the kinetic energies observed using 1064 versus 532 and 355 nm radiation can not be attributed to different heating efficiencies at the three wavelengths, but must be attributed to the different electronic excitations generated at these wavelengths. Similarly, the degree of vibrational excitation was found to be dependent on the desorption-laser wavelength. For both 355 and 532 nm excitation the $v=1$ to $v=0$ population ratio $[N(v=1)/N(v=0)]$ was 0.04, while at 1064 nm the $v=1$ signal was below the detection limit, giving $[N(v=1)/N(v=0)]<0.004$. It should also be noted that desorption was not observed using 1907 nm excitation. Studies evaluating the dependence of the LID signal on the desorption-laser angle of incidence and polarization indicated that the desorption yield scaled with the number of photons absorbed by the substrate. The above results indicate a desorption mechanism which is driven by photogenerated hot carriers produced in the near surface region of the substrate.

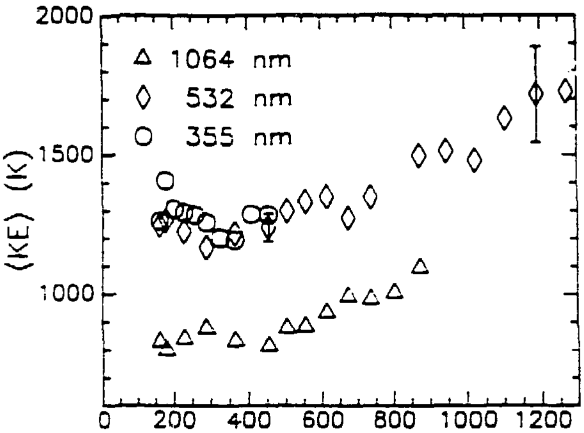

Figure 1: Wavelength dependence of NO desorption from Pt(111) at T_{idle}=220K for wavelengths of 355, 532 and 1064 nm.

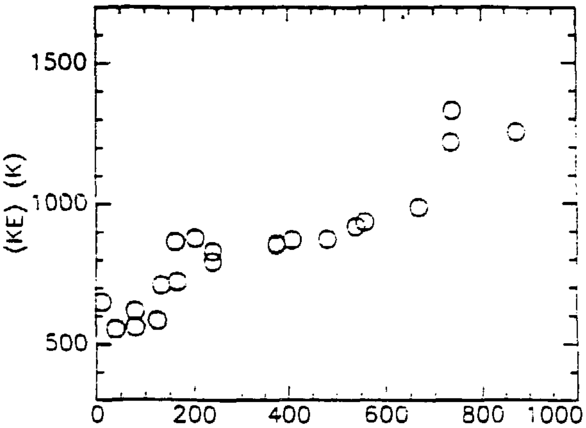

Figure 2: Kinetic energy distribution for LID of NO/Si(111). T_{idle}=95K, $\theta_{NO} \approx 0.02$ ML.

Several physical models have been proposed in order to account for this optically driven desorption process. The model which is best supported can be described as follows: i) Hot electrons are produced by the absorption of photons in the near surface region of the Platinum; ii) These electrons subsequently interact with the unoccupied molecular levels of the adsorbed NO;

iii) The resultant transient NO "negative ion" experiences forces on an excited state potential which displace the adsorbate from its initial equilibrium position; iv) Upon neutralization, the NO is found on a repulsive region of the ground state potential, and has energy sufficient to desorb. Consequences of this model have been pursued using wavepacket techniques by invoking reasonable approximations to the ground and excited state potential energy curves.[8] It has been found that this simple model qualitatively accounts for several aspects of the data, indicating that excited state lifetimes on the order of 10^{-15} sec are sufficient to yield the observed dynamics. There remain inconsistencies between the predictions of the model and the observed trends in the experimental data in that the degree of vibrational excitation and the desorption yield can not be reproduced given a single set of model parameters. The source of this quantitative disagreement remains to be established; it may either be due to inadequacies in the simple potential energy functions which were employed, or it may be more fundamental limitations inherent to the model.

NO/Si(111):

Since the role of optically generated carriers in driving chemical processes at metallic surfaces was clearly controversial, a series of measurements was initiated to characterize the desorption of NO from a surface where carrier chemistry was established. A semiconductor substrate was sought, since carrier lifetimes are known to be significantly longer in these systems, such that their associated chemistry should be more pronounced. NO adsorbed on Si(111) at 95K was pursued based on published reports of the optically induced desorption of NO under these conditions. Initial experiments revealed two significant aspects the LID process; 1) significant NO desorption occurred even with the laser fluence adjusted to achieve a surface temperature jump of only 0.05K and 2) there is a marked coverage dependence in the NO/LID signal. With an NO coverage of approximately 0.02 ML and a desorption-laser wavelength of 355 nm, the desorbed NO is seen to emerge with a state-specific kinetic energy near 1000K which increases with increasing internal energy, and a vibrational state population [N(v=1)/N(v=0)] of 0.2. As the coverage approaches saturation, the kinetic energy distributions remain approximately the same, however, the internal state population is dramatically altered, and the vibrational population ratio is observed to be 0.6.

Additional experiments examining the wavelength dependence of the desorption process suggest that the high coverage signal and the low coverage processes reflect interactions with different types of excited carriers. Since the yield and internal state populations of the low coverage state are essentially independent of desorption laser wavelength, it appears that thermallized carriers are responsible for this desorption channel. The high coverage system exhibits a strong wavelength dependence. There is a three order of magnitude decrease in yield as the desorption laser is tuned from 355 to 1064 nm, and the internal state populations are radically altered. Hence, it appears that hot carriers are important for this channel.

For either coverage state and for all wavelengths examined, the enhanced population of excited vibrational states is consistent with expectations based on the model of transient-ion assisted desorption and the hypothesis that the transient-ion has a longer lifetime on the semiconductor surface. The nature of the carriers which create the transient ion appear to be substantially different as manifest in the yields and internal state populations. Additional experiments are underway to test these models by using substrates of different doping, where excited electrons can be selectively swept away or towards the interface.

CO Detection:

The ability to characterize the dynamics of chemical transients by probing the population distributions following laser excitation of surfaces is well demonstrated by the recent experiments which probe desorbed NO. There are a variety of reasons to want to extend these measurements to other types of molecules. For instance, the open shell character of NO complicates the theoretical modelling of both its ground and excited state interactions. In addition, a broader range of surface processes can be addressed if a greater variety of molecules were accessible. With these motivations at heart, we have begun the implementation of the state-specific detection of CO, which would be both sufficiently linear to permit the determination of relative state populations, and have adequate sensitivity to probe desorbed densities on the order of 10^9 per cc - similar to the sensitivity which is presently enjoyed in the LIF detection of NO.

The detection method of choice is single-photon LIF. The optimal method for generating the probe wavelength is two-photon resonance enhanced four-wave sum frequency generation in Mg vapor. In this nonlinear frequency conversion process, three photons from two dye lasers are combined to generate a single VUV photon ($\omega_{VUV} = 2\omega_1 + \omega_2$). A VUV test apparatus has been constructed and detector optimization (for both VUV signal and CO LIF) is currently underway for frequency tripling in Xe. It is anticipated that the first tests using Mg vapor for VUV generation will take place in the spring of 1990, with desorption studies commencing shortly thereafter. In these experiments, the dynamics of laser heating and carrier-driven desorption for metal based systems such as CO/Pt(111) and CO/K/Pt(111) will clarify the influence of adsorbate properties (eg. electronic structure, binding energies, etc.) on LID. In addition, studies of the photofragmentation/photodesorption of CO from $Mo(CO)_6$/Si(111) will provide insight into adsorbate moderated energy relaxation at surfaces.

References:

1) D.S. King and R.R. Cavanagh in "Advances in Chemical Physics, Molecule Surface Interactions", Vol. LXXVI K.P. Lawley, ed. (Wiley, New York, 1989) pg 45.
2) D. Burgess, Jr., D.S. King, and R.R. Cavanagh, J. Vac. Sci. Tech. A5, 2959 (1987).
3) D. Burgess, Jr., R.R. Cavanagh, and D.S. King, Surf. Science 214, 358 (1989).
4) D. Burgess, Jr., R.R. Cavanagh, and D.S. King, J. Chem. Phys. 88, 6556 (1988).
5) L.J. Richter, S.A. Buntin, R.R. Cavanagh and D.S. King, J. Chem. Phys. 89, 5344 (1988).
6) S.A. Buntin, L.J. Richter, R.R. Cavanagh and D.S. King, Phys. Rev. Lett. 61, 1321 (1988).
7) S.A. Buntin, L.J. Richter, D.S. King and R.R. Cavanagh, J. Chem. Phys. 91, 6429 (1989).
8) J.W. Gadzuk, L.J. Richter, S.A. Buntin, D.S. King and R.R. Cavanagh, "Laser-Excited Hot-Electron Induced Desorption: A Theoretical Model for NO/Pt(111)" (submitted to Surface Science).
9) L.J. Richter, S.A. Buntin, D.A. King and R.R. Cavanagh, "Laser Induced Desorption of NO/Si(111)" (to be published).

High Pressure Heterogeneous Catalysis in a Low Pressure, Ultrahigh Vacuum Environment

Sylvia T. Ceyer
Department of Chemistry
Massachusetts Institute of Technology
Cambridge, MA 02139

The major thrust of our proposed research is to carry out for the first time a heterogeneous catalytic reaction that normally is observed only at high pressures (>1 atm) of reactant gas at low pressures (<10^{-4} Torr) in an ultrahigh vacuum environment on a Ni(111) crystal surface. This is possible using a scheme which couples molecular beam techniques with high resolution electron energy loss spectroscopy. Two molecular beams provide a means to activate each of the two reactants and the HREELS is a sensitive and chemically specific detector of the reaction progress. These studies will verify the principles behind the lack of reactivity at low pressures. The ability to carry out a "high pressure" reaction, such as the steam reforming of CH_4, in a UHV environment enables the use of surface sensitive electron spectroscopies such as HREELS to identify unambiguously the reaction intermediates, thereby testing the mechanisms proposed from high pressure kinetics measurements. With the receipt six months ago of funding for this new project, work has begun on the design of the apparatus.

Publications relevant to proposed research

Effect of Translational and Vibrational Energy on Adsorption: The Dynamics of Molecular and Dissociative Chemisorption
S. T. Ceyer, J. D. Beckerle, M. B. Lee, S. L. Tang, Q. Y. Yang and M. A. Hines
J. Vac. Sci. Tech. **A5**, 501 (1987)

Collision-Induced Dissociative Chemisorption of Adsorbates: Chemistry with a Hammer
J. D. Beckerle, Q. Y. Yang, A. D. Johnson and S. T. Ceyer
J. Chem. Phys. **86**, 7236 (1987)

Lack of Translational Energy Activation of the Dissociative Chemisorption of CO on Ni(111)
M. B. Lee, J. D. Beckerle, S. L. Tang and S. T. Ceyer
J. Chem. Phys. **87**, 723 (1987)

Dynamics of the Activated Dissociative Chemisorption of CH_4 and Implication for the Pressure Gap in Catalysis: A Molecular Beam-High Resolution Electron Energy Loss Study
M. B. Lee, Q. Y. Yang and S. T. Ceyer
J. Chem. Phys. **87**, 2724 (1987)

The Mechanism for the Dissociation of Methane on a Nickel Catalyst
S. T. Ceyer, M. B. Lee, Q. Y. Yang, J. D. Beckerle and A. D. Johnson,
Methane Conversion, D. Bibby, C. Chang, R. Howe, S. Yurchak, eds.
(Amsterdam: Elsevier Science, 1988), p. 51

The Stability and Chemistry of Adsorbed Methyl Radicals--Summary Abstract
Q. Y. Yang and S. T. Ceyer
J. Vac. Sci. Tech. **A6**, 851 (1988)

Collision Induced Dissociation and Desorption: CH_4 and CO on Ni(111)--Summary Abstract
J. D. Beckerle, A. D. Johnson, Q. Y. Yang and S. T. Ceyer
J. Vac. Sci. Tech. **A6**, 903 (1988)

Dissociative Chemisorption: Dynamics and Mechanisms
S. T. Ceyer
Ann. Rev. Phys. Chem. **39**, 479 (1988)

Collision Induced Dissociation and Desorption: CH_4 on Ni(111)
J. D. Beckerle, A. D. Johnson, Q. Y. Yang and S. T. Ceyer
Solvay Conference on Surface Science, F.W. deWette, ed.,
(Berlin: Springer-Verlag, 1988), p.109

Observation and Mechanism of Collision Induced Desorption: CH_4 on Ni(111)
J. D. Beckerle, A. D. Johnson and S. T. Ceyer
Phys. Rev. Lett. **62**, 685 (1989)

Collision Induced Dissociative Chemisorption of CH_4 on Ni(111) by Inert Gas Atoms: The Mechanism for Chemistry with a Hammer
J. D. Beckerle, A. D. Johnson, Q. Y. Yang and S. T. Ceyer
J. Chem. Phys. **91**, 5756 (1989)

Synthesis of Benzene from Methane over a Ni(111) Catalyst
Q. Y. Yang, A. D. Johnson, K. J. Maynard and S. T. Ceyer
J. Am. Chem. Soc. **111**, 8748 (1989)

Translational and Collision Induced Activation of CH_4 on Ni(111): Phenomena Connecting UHV Surface Science to High Pressure Heterogeneous Catalysis, Langmuir Lecture
S. T. Ceyer
Langmuir, in press

Molecular Beams: Probes of the Dynamics of Reactions on Surfaces
S. T. Ceyer, D. J. Gladstone, M. McGonigal and M. T. Schulberg
Physical Methods of Chemistry , 2nd ed., B. W. Rossiter, J. F. Hamilton, and
R. C. Baetzold, eds., (New York: Wiley, 1990), in press

SURFACE STUDIES OF CERAMICS USING MICROBEAM METHODS

Work supported by Grant no. DE-FG02-90ER45228

J.M. Cowley
Department of Physics, Arizona State University
Tempe, Arizona 85287-1504

The dedicated scanning transmission electron microscopy (STEM) instruments provide a range of powerful techniques for the study of surfaces including scanning reflection electron microscopy (SREM), microdiffraction from surface features as small as 1nm in diameter, electron energy loss spectroscopy in the reflection mode (REELS) [1] and high-resolution secondary electron microscopy (HRSEM) [2] with 1nm resolution , with or without energy analysis [8,11]. Especially when used in an ultra-high vacuum environment with properly prepared specimens, these techniques may be applied to clean surfaces and to surfaces treated under well-controlled conditions, as in the MIDAS system (a Microscopy for Imaging Diffraction and Analysis of Surfaces) which is based on an HB501S instrument from VG Microscopes. These techniques may profitably be applied in parallel with observations of surfaces using related techniques in conventional transmission electron microscopy (TEM) instruments, including reflection electron microscopy (REM) and REELS from large surface areas, up to 1μm in diameter.

Our earlier studies of the surfaces of MgO crystals and their interactions with thin metal films have served as a means for exploring and demonstrating these techniques for the study of surface structure and at the same time have provided a considerable amount of information on metal-oxide interactions. Evidence was found for several rather surprising surface reactions, including the reaction of Au with MgO at high temperatures and the reaction of Ag and Pd with MgO at room temperature under electron irradiation to form the metal oxides [8]. It has been suspected that surface layers of oxygen or hydroxyl ions, remaining on the oxide surface in a vacuum of 10^{-8} torr may play a role in such reaction. A program is now under way to study such surface reactions under ultra-high vacuum conditions in the MIDAS system. Evidence from microdiffraction patterns, obtained with a 1nm diameter electron beam running parallel to a crystal surface [7] suggests that atomically clean surfaces of MgO may be produced by the electron irradiation of surfaces under UHV conditions.

The techniques have been developed for the preparation of clean surfaces of α-alumina suitable for use in electron-optical surface studies. REM and SREM observations have been made of the equilibrium forms of monatomic and multi-layer steps on vicinal (0001) faces and of the interaction of thin Ag and Cu layers with the oxide at the steps and on the step-free terraces.

Under particular diffraction conditions in the RHEED geometry, a surface-resonance channelling condition is established [6,11]. It has been shown by experiment and by calculations that this condition involves the confinement of the electron beam in the crystal to the first one or two layers of atoms on the surface so that the diffraction intensities, image contrast and REELS spectra become highly sensitive to the structure and composition of the surface layers. We have recently defined in more detail the conditions under which the surface channelling phenomenon occurs [15].

It would seem reasonable to suppose that a similar phenomenon should occur for solid-solid interfaces when there is an appreciable difference in mean inner potential between the two components, provided that the material having the larger value of inner potential is a sharply-terminated single crystal [14]. Detection of the interface-channelled electrons would then provide a sensitive probe of interface structure and composition. We have initiated a program to investigate this possibility.

The use of microdiffraction to investigate the structures of small crystals, using an electron beam of diameter 1nm or less, has been established as a convenient and power tool for the study of catalyst samples, particularly when used in conjunction with high resolution bright-field or annular dark-field STEM and high resolution SEM. Investigations of several supported metal catalyst systems have been made in this way [16].

By using computer simulations, involving many-beam dynamical diffraction calculations and the method of periodic continuation, some account has been given of the origins of the distortions and splitting of diffraction spots that have often been observed. It has been shown that such distortions and splittings of spots may be related in a reasonably direct manner with the shapes and edges of the crystal regions illuminated by the electron beam. It follows that the possibility exists for making use of the microdiffraction patterns to determine not only the crystal structure but also the sizes and shapes of the individual metal particles having sizes in the range of 1-3nm. In this size range, which is of great interest for the study of catalysts, the use of direct imaging by high resolution electron microscopy to determine shape and size is usually very difficult because of the perturbations of the image by the support. The microdiffraction method should be much less sensitive to these perturbations.

Publications based on the grant program 1987-1989

1. "Reflection electron energy-loss spectroscopy (REELS)--a technique for the study of surfaces" Z.L. Wang and J.M. Cowley, Surface Science 193 (1988) 501-512.
2. "High resolution SEM in a STEM instrument" J. Liu and J.M. Cowley in Scanning Microscopy 2 (1988) 65-81.
3. "Errors arising from numerical use of the Mott formula in electron image simulation" L.M. Peng and J.M. Cowley, Acta Cryst. A44 (1988) 1-5.
4. "Assessing the information content of HREM images" G.Y. Fan and J.M. Cowley, Ultramicroscopy 24 (1988) 49-60.
5. "Atomic inner shell excitations for EELS in the reflection mode" Z.L. Wang and J.M. Cowley, J. Micros. Spectros. Electroniques 13 (1988) 189-204.
6. "REELS and RHEED characterizations of electron resonance channelling in crystal surfaces" Z.L. Wang and J.M. Cowley, Ultramicroscopy 26 (1988) 233-238.
7. "Computer-simulated electron microdiffraction patterns from MgO crystal surfaces" M. Pan and J.M. Cowley, Ultramicroscopy 26 (1988) 205-216.
8. "The surface reaction of Pd/MgO studied by the scanning reflection electron microscopy" H.J. Ou and J.M. Cowley, Phys. Status Solidi (a) 107 (1988) 1719-729.
9. "High resolution STEM imaging $YBa_2Cu_3O_{7-x}$" H.J. Ou and J.M. Cowley in Proc. 46th Annual Meeting EMSA, G.W. Bailey, Ed., San Francisco Press, San Francisco (1988) 882-3.
10. "The effects of surface-absorbed monolayer on electron microdiffraction patterns" M. Pan and J.M. Cowley, Proc. 46th Annual Meeting EMSA, G.W. Bailey, Ed., San Francisco Press, San Francisco (1988) 680-681.
11. "Reflection electron microscopy" J.M. Cowley in Surface Interface Characterization by Electron Optical Methods, A. Howie and U. Valdre, Eds., Plenum Publ. Co. (1988) 127-158.
12. "Determination of the local Al concentration in $Al_xGa_{1-x}As$-GaAs quantum well structures using the (200) diffraction intensity obtained with a 10Å electron beam, H.J. Ou, S.C.Y. Tsen, K.T. Tsen, J.M. Cowley, J.I. Chyi, A. Salvador and H. Morkoc, Appl. Physics Letters 54 (15) (19889) 1454-6.
13. "Geometric explanation of parabolas and resonance in electron diffraction", M. Gajdardziska-Josifovska and J.M. Cowley Proc. 46th Annual Meeting EMSA, G.W. Bailey, Ed., San Francisco Press, San Francisco (1989) 498-9.
14. "Novel technique for studying interface abruptness in a STEM" M. Gajdardziska-Josifovskaka and J.M. Cowley in Proc. 46th Annual Meeting EMSA, G.W. Bailey, Ed., San Francisco Press, San Francisco (1989) 524-5.
15. "High spatial resolution microanalysis on the (200) nanodiffraction of AlGaAs-GaAs MQWS" H.J. Ou, A.A. Higgs, P.R. Perkes and J.M. Cowley in Proc. 46th Annual Meeting EMSA, G.W. Bailey, Ed., San Francisco Press, San Francisco (1989) 232-3.
16. "Characterization of ceria-supported rhodium catalyst by HRTEM', M. Pan, J.M. Cowley and R. Garcia, J. Catalysis (1989) in press.
17. "Using the (200) thickness contour to measure the Al concentration in $Al_xGa_{1-x}As$-GaAs MQWS Structures" H.J. Ou, R.W. Glaisher, J.M. Cowley

and H. Morkoc, in Microbeam Analysis-1989, P.E. Russell, Ed., San Francisco Press, San Francisco (1989) 480-482

RESEARCH SUMMARY

Andrew E. DePristo
Ames Laboratory of the USDOE
and
Department of Chemistry
Iowa State University
December 1989

The general focus of this research is the theoretical description of the structure and dynamics of chemically reactive systems in terms of their fundamental atomic (and electronic) constituents. Research is designed to describe, calculate, predict and understand the properties of unusual chemical systems. One particular focus is the area of metal cluster chemistry. The goal is to determine the structure and energy of various metal clusters, and to investigate the relationship between these properties and the reactivity of clusters with different gas phase molecules.

We have carried out the first detailed theoretical and computational investigation of the structures and reactivity of various isomers of small metal clusters. This was accomplished for Ni clusters in the size range from 4 to 13 atoms reacting with D_2. The geometries of the clusters were optimized within a particular point group symmetry by minimization of the binding energy calculated by the corrected effective medium (CEM) theory, a near-first-principle density functional based method capable of quantitative and near-quantitative accuracy for a wide variety of metallic and non-metallic systems.

All clusters were found to have significantly contracted nearest neighbor distances compared to the bulk value of 2.49 Å as well as substantially lower binding energy per atom compared to the bulk cohesive energy of 4.5 eV. In addition, the variation in binding energy per atom with isomer was found to be ≈0.1 eV which is quite significant.

We also determined the influence of cluster size and geometry on the reactivity with respect to the dissociative adsorption of D_2. This was the first (and only) such theoretical investigation of reactions on metal clusters, to our knowledge. Chemically realistic potential energy surfaces were used to describe the interaction between D_2 and the Ni clusters. Our major findings were:

- for clusters smaller than Ni_9, the rate constants varied strongly with cluster size;

- for all size clusters, the rate constants were sensitive to different isomers, varying from one to two orders of magnitude in some cases.

This behavior was discussed in terms of various structural features in different isomers, paying particular attention to a detailed comparison between the reactions on metal clusters and metal surfaces. We were able to characterize the reactivity of Ni clusters in terms of the structural aspects in the cluster:

(i) Clusters with close packed structures increased in reactivity as the number of 4-fold faces increased in comparison to that number of 3-fold faces. This was due to the increased binding energy of the D atom on a 4-fold vs. 3-fold face.

(ii) Clusters with open structures also showed high reactivity. This was favorable since, when the molecule approached the open face, each atom attained a high coordination leading to dissociation.

(iii) Extended planar surfaces on the cluster were also found to increase the reactivity as noticed in the clusters which are fragments of FCC unit cell.

Point "i" is the cluster analog of the known increased reactivity of D_2 dissociative chemisorption on Ni(100) vs. Ni(111) surfaces. Point "ii" was thought to be the analog of increased dissociative chemisorption at steps and kinks. Point "iii" did not appear to have any direct surface analogy and illustrated the novel information which was provided by studies on small metal clusters.

Recently, we have developed a more approximate CEM based theory, termed MD/MC-CEM, which is still capable of quantitative accuracy for large metallic systems, but not generally for diatomics, triatomics and other small covalently bonded systems. Evaluation of the energy and forces within this theory is extremely rapid due to a number of developments including:

- the use of neighbor lists to restrict the number of atoms needed for the evaluation of forces; this ensures a nearly linear increase of computer time with the number of atoms;

- the evaluation of all energies, forces and electron densities by cubic polynomial interpolation in conjunction with Chebyshev smoothing techniques; this is fast when used in conjunction with a direct interval location method.

This new theory has been successfully integrated in a number of dynamics programs including Monte-Carlo, simulated annealing and molecular dynamics.

In the future, a closer connection with experimental results on the reactivity of nickel clusters with D_2 will be made. These are available as a function of cluster size from two different research groups (Morse at the University of Utah, and Riley at Argonne National Lab). There are several factors which have prevented a rigorous comparison of our theoretical results with experiment. First, the structures of the Ni clusters in these experiments are unknown. Second, the optimization used to obtain the structures of the Ni clusters was geometry restricted. With the new MD/MC-CEM based techniques we intend to remove these roadblocks by forming the clusters with a thermal distribution of isomers and by explicitly allowing for the Ni atoms to move during the collision.

In another project, work on the structure and dynamics of bimetallic RhPt and CuNi clusters is being pursued. Such bimetallic clusters play a significant role in catalysis. Segregation of the constituent atom types leads to marked effects upon the catalytic selectivity of these clusters. The figure below shows a Cu_6Ni_{13} cluster that was obtained from the a melting-annealing process using the MD/MC-CEM forces.

3

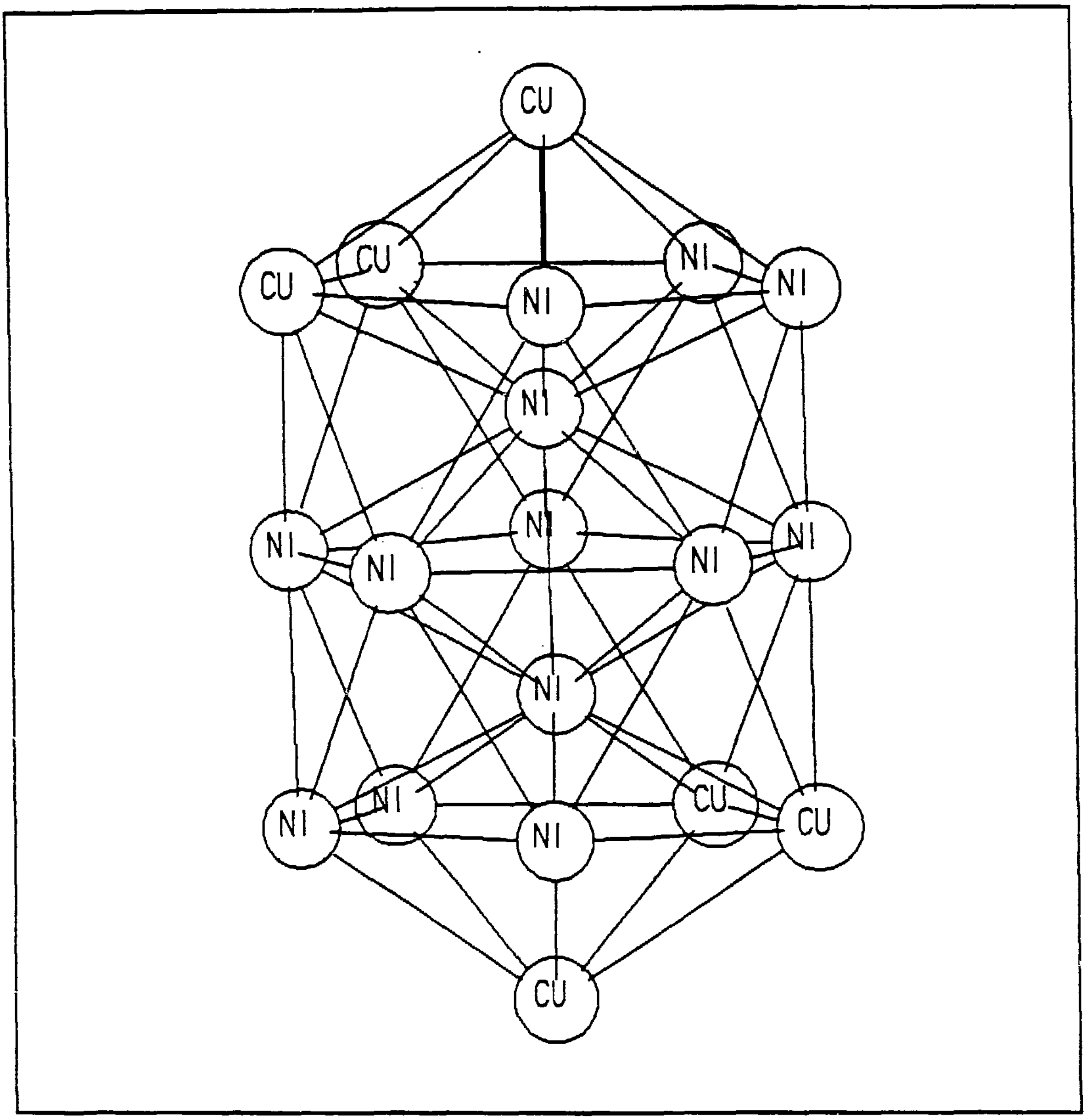

The overall structure of the cluster is a double icosahedron, as might be expected. The top and bottom axial atoms and those atoms in the top and bottom pentagonal planes have a coordination of 6; those in the middle pentagonal plane have a coordination of 8; and, the two inner Ni atoms have a coordination of 12. The average coordination is 6.00 for Cu and 7.69 for Ni. The separation of the Cu atoms into two groups has little significance upon the energy of the cluster. In fact, a similar structure with all the Cu atoms grouped together in the lower sixfold coordinated sites is 0.05 eV more stable than the cluster shown above. In contrast, a structure with one interior Cu atom is 0.54 eV less stable. Thus, segregation to the "surface" is exhibited even by this small bimetallic cluster.

It would be difficult to predict such segregation based upon the dimer binding energies of D_0=2.08±.25, 2.01±.08 and 2.068±.01 eV for NiCu, Cu_2 and Ni_2, respectively. The surface free energies of 1.79 and 2.38 J/m^2 for Cu and Ni would allow such a prediction, but one could not be sure that such a quantity is applicable to a 19 atom cluster. MD/MC-CEM calculations provide the theoretical basis for determining the effects at any cluster size.

PUBLICATIONS

J.D. Kress, M. S. Stave and A. E. DePristo, Corrected Effective Medium Method: III. applications to clusters of Mg and Cu, J. Phys. Chem. 93, 1556-1565 (1989).

A. E. DePristo, K. Haug and H. Metiu, A New Method for Calculating Time Dependent Quantum Correlation Functions for Systems of Many Degrees of Freedom, Chem. Phys. Lett. 155, 376-80 (1989).

K. Raghavan, M. S. Stave and A. E. DePristo, Dissociation Dynamics of D_2 on Ni_{13} Clusters: structural dependence, Chem. Phys. Lett. 149, 89-94 (1988).

K. Raghavan, M. S. Stave and A. E. DePristo, Ni Clusters: Structures and Reactivity with D_2, J. Chem. Phys. 91, 1904-17 (1989).

M.S. Stave, D.E. Sanders, T.J. Raeker and A.E. DePristo, Corrected Effective Medium Method: V. simplifications for molecular dynamics and monte-carlo simulations, J. Chem. Phys. (submitted 9/89).

T.J. Raeker and A.E. DePristo, Theory of Chemical Bonding based upon the Atom-Homogeneous Electron Gas System, Int. Rev. Phys. Chem. (in press, 12/89).

ACID/BASE AND REDOX REACTIONS OVER OXIDE CATALYSTS
Seventh DOE Catalysis and Surface Chemistry Research Conference

J.A. Dumesic
Department of Chemical Engineering
University of Wisconsin, Madison

ABSTRACT

During the past two years our research funded by the Department of Energy has focused in the following two areas: (i) calorimetric measurements of surface acidity for silica-supported oxides and H-Y zeolites and (ii) temperature programmed reaction studies of the selective reduction of nitric oxide over thin-film vanadia/titania model catalysts. Various aspects of these studies are outlined in the following paragraphs.

MICROCALORIMETRIC STUDIES OF SURFACE ACIDITY

The use of microcalorimetry in the measurement of surface acidity has been an area of active research in our laboratories for the past three years. One of the important considerations in this research is whether the basic probe molecule employed to titrate the acid sites attains thermodynamic equilibrium with the surface under the calorimetric experimental conditions. In our particular case, micromolar quantities of pyridine are dosed successively onto the surface at 473 K and equilibration times of typically 1-2 h are allowed between doses.

It can be shown that adsorption/desorption equilibrium can be attained by the basic probe molecule at 473 K only if the heat of adsorption is less than about 140 kJ/mol. This would limit the use of microcalorimetry to the study of rather weak acidity. However, surface diffusion of the adsorbed basic molecule could provide a pathway for equilibration of the adsorbate between acid sites of different strength without the need to desorb into the gas phase. This possibility was studied by determining the absolute entropy of pyridine adsorbed on silica.

By measuring the heat of adsorption calorimetrically and the adsorption isotherm volumetrically, the entropy change of adsorption can be calculated through Gibbs free energy and enthalpy relationships. Using the calculated entropy for the adsorbate and assumptions of its degrees of freedom, we have found that the activation energy for surface diffusion is about 20 kJ/mol, compared to the heat of adsorption determined to be 95 kJ/mol. This corresponds to an adsorbed pyridine molecule sampling about 10^6 sites per second on the surface of silica. Therefore, surface diffusion is a fast process on the time scale of the calorimetric experiment, and this process provides an effective equilibration pathway for adsorbed basic molecules. We estimate that acid sites with heats of adsorption as high as 220 kJ/mol at 473 K can be titrated calorimetrically in an equilibrium manner due to surface diffusion. We have recently completed a manuscript detailing the above results and calculations for pyridine adsorbed on silica and silica/alumina (1).

We have employed our calorimetric approach to the measurement of surface acidity for a series of silica-supported metal oxides. In particular, oxides of zinc, aluminum, gallium, iron, magnesium, and scandium were deposited onto silica at low loadings (e.g., 0.5 wt.%) and calcined. All samples showed a region of constant differential heat of pyridine adsorption at low adsorbate coverages, followed by a region of decreasing heat of adsorption with coverage, with the differential heat finally approaching the value characteristic of pyridine on silica.

The experimental curves of differential heat versus pyridine coverage, as well as the adsorption isotherm of coverage versus pyridine pressure could be described well by the combination of three Langmuir isotherms for each sample. Adsorption on the strongest sites was characterized by differential heats in the range of 180-250 kJ/mol and low absolute entropies, indicative of immobile adsorbed species. Pyridine adsorption on the sites of intermediate strength gave differential heats in the of 120-170 kJ/mol and absolute entropies consistent with appreciable rates of surface diffusion. Adsorption on the weakest sites was due to pyridine hydrogen-bonded on the silica surface, and the thermodynamic quantities for these sites were the same as determined for pyridine adsorbed on the support alone.

Infrared spectra were collected as a function of pyridine coverage for the silica/alumina sample to identify which types of sites are associated with adsorption sites of a particular strength. Only those peaks characteristic of pyridine adsorbed on Lewis acid sites were detected at low pyridine coverages. Infrared bands due to pyridine on Bronsted acid sites were observed at higher pyridine coverages. Hydrogen-bonded pyridine on the silica surface was observed after the Lewis and Bronsted acid sites had become saturated with pyridine. These infrared results indicate that the strongest sites on all of the silica-supported samples studied are Lewis acid sites. For those samples that showed both Lewis and Bronsted acid sites (i.e., oxides of aluminum, gallium and scandium on silica), the Bronsted acid sites contribute to the calorimetric curve of differential heat versus pyridine coverage in the intermediate region of 120-170 kJ/mol.

Given that the strongest acid sites on all of the silica-supported oxides studied were Lewis centers, we attempted to correlate the initial heat of pyridine adsorption with the electronegativity of the oxides, since both Lewis acidity and electro-negativity are related to the electron accepting properties of the oxide. An excellent correlation was obtained. A paper is being submitted for publication that reports and discusses these aforementioned studies of silica-supported oxides (2).

In addition to our microcalorimetric studies of pyridine adsorption on a series of silica-supported oxides, we have investigated the adsorption of a series of different basic probe molecules (i.e., ammonia, trimethylamine, triethylamine, and pyridine) on silica and silica/alumina. The first conclusion from this work is that the heats of adsorption of these molecules can not be correlated with the corresponding pKa values characteristic of aqueous basicity. Instead, the heats of adsorption are related to the gas phase proton affinities or vertical ionization energies of the basic probe molecules. Thus, surface acid-base interactions appear to be related more to gas phase acid/base properties than to aqueous acid/base chemistry.

Another approach to interpreting the variation in heat of adsorption with gas phase basicity of the probe molecule utilizes the two-parameter acid/base scale of Drago and Wayland. Specifically, each gaseous acid or base is characterized by a pair of parameters (i.e., electrostatic and covalent contributions), and the heat of acid-base adduct formation is given by the product of electrostatic parameters for the two molecules plus an analogous product of the covalent terms. Using tabulated Drago-Wayland parameters, we found that this theory was successful in describing surface acidity for silica and silica-alumina; more data will be required to assess the wider applicability of the theory. Our early results in this direction suggest, however, that electrostatic interactions are important in determining the heat of adsorption, since the ratio of the electrostatic parameter to the covalent parameter determined for silica/alumina is significantly greater than for gas phase acids. This may be due to the Madelung field generated by the oxide. Our studies of a series of basic molecule adsorptions on silica and silica/alumina are described in a manuscript that is being submitted for publication (3).

Our more recent microcalorimetric studies of surface acidity have involved H-Y zeolites used for catalytic cracking. These samples were kindly provided to us by Dr.

R. Madon at Engelhard Corporation. One of these samples, denoted as HY-2, showed high gas oil cracking activity and high gasoline selectivity, whereas an extensively steamed sample, denoted as HY-60, showed low activity and low gasoline selectivity. For comparison, an amorphous silica/alumina catalyst, denoted as S/A, showed high activity for gas oil conversion but low gasoline selectivity. Microcalorimetric measurements of pyridine adsorption at 473 K showed high acid site concentrations for HY-2 and S/A, while HY-60 contained a lower acid site concentration. These total acidity measurements are consistent with the overall catalytic activities observed for these three materials. More importantly,the HY-2 sample showed a significant number of acid sites with intermediate heats of pyridine adsorption near 150 kJ/mol. The HY-60 and S/A catalysts had fewer acid sites of intermediate strength, and these sites were characterized by pyridine heats of adsorption near 130 kJ/mol. Thus, the gasoline selectivity can be correlated directly with the presence of acid sites of intermediate strength, with sites near 150 kJ/mol apparently being more effective than sites near 130 kJ/mol. In view of our earlier infrared studies of pyridine adsorbed on silica/alumina, sites with heats of pyridine adsorption in the range of 130-150 kJ/mol appear to be Bronsted acid sites. The S/A catalyst showed high overall catalyst activity but low gasoline selectivity. This sample contained a large number of strong acid sites with heats of pyridine adsorption near 220 kJ/mol. This suggests that these strong sites lead to excessive cracking and coke formation. These strong sites appear to be Lewis acid sites. We recently reported the above correlations between microcalorimetric acidity determinations and catalyst activity/selectivity at the annual AIChE meeting in San Francisco (4).

SELECTIVE CATALYTIC REDUCTION OF NITRIC OXIDE

Another direction of our research during the past two years has been the study of the selective catalytic reduction of nitric oxide over model vanadia/titania surfaces. Temperature programmed reaction spectroscopy has been employed under ultra-high vacuum conditions over surfaces prepared by first depositing titania onto tungsten foils and subsequently depositing monolayer amounts of vanadia on titania.

Ammonia adsorption measurements indicated that the sticking coefficient was high (i.e., greater than 0.1). Three peaks were observed in the ammonia TPD spectra. The lowest temperature peak corresponded to hydrogen-bonded ammonia, while the two higher temperature peaks were due to chemisorbed species with heats of desorption in the range of 70-100 kJ/mol. The addition of water to the surface diminishes the intensity of the strongest ammonia adsorption site, suggesting that this site is due to Lewis acid sites. Furthermore, the ammonia adsorption site of intermediate strength leads to extensive H-D exchange with ammonia, as evidenced by treatment of the surface with H_2O and subsequent adsorption of ND_3. These sites can thus be identified as Bronsted acid sites. As for the case of pyridine adsorption on silica/alumina outlined above, ammonia adsorption on vanadia/titania is stronger on Lewis sites than on Bronsted sites.

Nitric oxide desorbed from the vanadia/titania surface with an activation energy near 80 kJ/mol. The preadsorption of water, however, blocked nitric oxide adsorption sites, suggesting that the amount of nitric oxide on a working catalyst is small under reaction conditions (since the water concentration in typical flue gases is several percent).

Temperature programmed reaction studies employing co-adsorbed ammonia and nitric oxide showed the formation of dinitrogen. When $^{15}NH_3$ and ^{14}NO were used, the cross-labeled species $^{14}N^{15}N$ was formed, indicating chemical reaction between these two reactants. Evidence was also found in these studies that the presence of ammonia facilitated the adsorption of nitric oxide, perhaps due to reduction of the surface by the former reactant. In short, these studies provide good estimates of the rate constants for several of the key steps in the reduction of nitric oxide by ammonia, namely (i) the adsorption of ammonia, (ii) the adsorption of nitric oxide, (iii) the reaction between ammonia and nitric oxide surface species to form dinitrogen, and (iv) the desorption of water. These rate constants allow us to predict the performance of a working vanadia/titania catalyst.

The first conclusion of this extrapolation of kinetic data obtained under ultra-high vacuum conditions to high pressure reaction conditions is that the adsorption of ammonia is a fast process and can be assumed to be in equilibrium. In fact, the equilibrium constant, estimated by the ratio of the adsorption and desorption rate constants from our studies, is in excellent agreement with the equilibrium constant determined from TPD spectra of porous vanadia/titania catalysts, obtained under conditions where readsorption of ammonia is fast (5). Furthermore, our estimates of the surface coverages by ammonia under reaction conditions are in agreement with the ammonia coverages determined by in situ infrared spectroscopy on working vanadia/titania catalysts (6). These infrared experiments also confirm our result that ammonia is adsorbed more strongly on Lewis acid sites than an Bronsted centers. Finally, the predicted turnover frequencies for the catalytic reduction of nitric oxide are in good agreement with the reaction rates measured on porous vanadia/titania catalysts. The above results of our temperature programmed reaction studies on model vanadia/titania surfaces are currently being prepared for publication (7).

REFERENCES

1. Cardona-Martinez, N., and Dumesic, J.A., Microcalorimetric Studies of Surface Acidity for Silica and Silica/Alumina, submitted for publication.
2. Cardona-Martinez, N., and Dumesic, J.A., Acid Strength of Silica-Supported Oxide Catalysts Studied by Microcalorimetric Measurements of Pyridine Adsorption, submitted for publication.
3. Cardona-Martinez, N., and Dumesic, J.A., Correlations of Surface Acidity for Silica and Silica/Alumina via Microcalorimetric Measurements of Basic Molecule Adsorption, submitted for publication.
4. Cardona-Martinez, N., Madon, R.J., Bell, V., and Dumesic, J.A., Effect of Acid Strength of HY Zeolites on Catalytic Cracking Activity and Selectivity, paper presented at 1989 Annual Meeting of the AIChE in San Francisco.
5. Clausen, B.S., Tornqvist, E., Steffensen, G., and Dumesic, J.A., Mass Spectrometry Studies of Vanadia-Titania DeNOx Catalysts, paper presented at Second Nordic Symposium on Catalysis, Lyngby, Denmark, 1989.
6. Topsoe, N., Clausen, B.S., and Dumesic, J.A., In Situ Infrared Spectroscopic Studies of Vanadia-Titania DeNOx Catalysts, submitted for publication.
7. Srnak, T., and Dumesic, J.A., Temperature Programmed Reaction Studies of the Selective Catalytic Reduction of Nitric over Model Vanadia/Titania Catalysts, paper in preparation.

INFRARED STUDY OF CARBON DEPOSITS ON BIMETALLIC CATALYSTS

R. P. Eischens
Zettlemoyer Center for Surface Studies
Lehigh University, Bethlehem, PA 18015

Early infrared studies of carbon deposited on Al_2O_3, Pt/Al_2O_3, and $Pt\text{-}Re/Al_2O_3$, by exposure to acetylene at 250°C, indicated that the deposit includes an oxidized species [1]. This species was detected by infrared bands near 1580 and 1470 cm^{-1}. These bands were assigned to a carboxylate because they were identical to those observed after chemisorption of acetic acid. Bands attributable to surface carboxylates had been observed after heating olefins chemisorbed on alumina [2]. Similar bands had also been detected in coke deposition studies but had been assigned to carbon-carbon stretchings in aromatic rings and to carbon-hydrogen bendings [3]. The latter assignment is reasonable because coke deposition occurs under reducing conditions. One of the first objectives of the work at Lehigh was to unambiguously determine whether the bands can be assigned to an oxidized species. This was accomplished by depositing coke on alumina in which the oxygens had been replaced with oxygen-18 [4]. The 1580 and 1470 cm^{-1} bands were each lowered by about 20 cm^{-1} as expected from substitution of oxygen-18 into a carboxylate.

The infrared study of carbon deposition is conveniently conducted in an apparatus in which the catalyst sample is suspended from a Cahn balance. This facilitates an *in situ* measure of the total weight of coke deposited while the infrared spectra are being observed. Commercial experience indicates that the coke deposited on a $Pt\text{-}Re/Al_2O_3$ bimetallic reforming catalyst is less deleterious to catalyst performance than is an equivalent amount of coke on Pt/Al_2O_3. This suggests that there are differences in the nature of the coke deposits. In the early studies it was found that rhenium does not affect the total coke deposition but does lower the fraction of carboxylate in the coke [1].

When the study of coke deposition was resumed at Lehigh, this observation of the effect of rhenium was confirmed using a variety of aluminas as supports. Differences between aluminas could not be detected except those related to differences in surface area. The current work utilizes Degussa Al_2O_3-C as the support because it is convenient to use in infrared experiments.

Iridium and tin, which are often used in commercial bimetallic catalysts, also lowered the fraction of carboxylate in coke deposits. This indicates that the rhenium results are not an isolated observation. However, an important difference was observed between $Pt\text{-}Re/Al_2O_3$ and $Pt\text{-}Sn/Al_2O_3$. In the case of $Pt\text{-}Re/Al_2O_3$ the total coke deposition is about the same as for Pt/Al_2O_3 and the carboxylate is lowered as it is for Re/Al_2O_3. A catalyst containing 3% Pt and 3% Sn produces a strong increase in total coke and a moderate increase in carboxylate. This result is shown in Figure 1 where the wt% of coke on the catalyst is plotted as a function of time of exposure to 10 Torr of acetylene at 250°C. The catalyst used for Figure 1 was prepared by the incipient wetness impregnation method with a solution containing chloroplatinic acid and tin chloride. After drying at 280°C for 10 hours, the catalysts were reduced in the infrared cell in static hydrogen at a pressure of one atmosphere for 24 hours with three changes of hydrogen. The 3% Pt/Al_2O_3

and 3% Sn/Al_2O_3 samples were prepared by the same procedure using solutions containing either chloroplatinic acid or tin chloride.

The strong increase in coke deposition for $Pt-Sn/Al_2O_3$ does not appear to be consistent with the use of this bimetallic pair in commercial catalysts. One the basis of hydrogen chemisorption data, Burch concluded that tin enhances the dispersion of Pt in $Pt-Sn/Al_2O_3$ catalysts [5]. Since it might be expected that coke deposition would be enhanced by increasing the number of exposed platinum atoms, an effort was made to test the dispersion concept by chemisorption of carbon monoxide. The chemisorption was determined at 100°C with a CO pressure of 10 Torr.

Spectrum A of Figure 2 was observed after chemisorption of CO on 3% Pt/Al_2O_3. The strongest band is found at 2060 cm^{-1} with a shoulder at 2085 cm^{-1}. There is also a small bridged CO band (not shown) near 1850 cm^{-1}. Spectrum B was observed at 3% Pt-3% Sn/Al_2O_3. From Spectrum B it is seen that the 2060 cm^{-1} band has almost been eliminated while the shoulder at 2085 cm^{-1} remains unaffected. The bridged CO band also is markedly decreased. In Spectrum B there may be a band at 2070 cm^{-1}. It is not clear whether the 2070 cm^{-1} band was present, but unobserved, in Spectrum A or whether it represents a shift of the remnant of the 2060 cm^{-1} band. The weight of the chemisorbed CO in Spectrum A indicates a platinum dispersion of 0.25 assuming a coverage of one CO per platinum. The weight of the adsorbed CO in B is 40% that of A and the integrated intensity of B is 35% as large as A. This indicates that there are no large differences in specific intensities so band intensities are a reasonable measure of exposed platinum capable of adsorbing CO.

Figure 2 makes it evident that the enhanced carbon deposition of $Pt-Sn/Al_2O_3$ is not simply due to enhanced platinum dispersion. On the basis of ESCA measurements, Adkins and Davis concluded that tin forms a tin aluminate layer and platinum is deposited on this layer [6]. They attribute an enhanced activity for alcohol dehydration to this platinum. It might be that enhanced activity for coke deposition is related to the activity for alcohol dehydration. However, it is not clear how this can be reconciled with the decrease in CO chemisorption.

Because the enhanced carbon deposition for the 3% $Pt-Sn/Al_2O_3$ is not easily reconciled with the commercial catalysts, samples with Pt and Sn contents closer to those of the commercial catalysts were studied for carbon deposition and carbon monoxide chemisorption. Figure 3 is from metal contents 1.0% and Figure 4 is from 0.3%. Figure 3 shows that the tin decreases the 2060 cm^{-1} but to a smaller extent than observed for the 3% samples. The remaining band is at 2070 cm^{-1}. The 2085 cm^{-1} shoulder is not evident in Spectrum B but it may be hidden by the 2070 cm^{-1} band. Figure 4, for the 0.3% sample, which is close to the commercial loadings, does not show any decrease in the major band but again there appears to be a shift towards higher frequency. Catalysts containing metal loadings of 0.6% give results intermediate between those of the 0.3% and 1.0% catalysts.

Total carbon deposition and carboxylate formation mirror the results of the decreases in CO chemisorption. The 0.3% $Pt-Sn/Al_2O_3$ produces coke and carboxylate equivalent to that of pure Al_2O_3. Thus, the 3.0% Pt-Sn results cannot be extrapolated to the commercial catalysts. It may indicate that the type of tin-platinum interaction which causes the decrease in CO chemisorption is to be avoided. It is also evident that the nature of this interaction is not evident and attempts to clarify it would be worthwhile.

Tin, by itself, on alumina decreases both coke deposition and carboxylate formation. These results might be due to a decrease in acidity of the alumina since it is known that both total coke and carboxylate are decreased by prior chemisorption of ammonia [7]. Use of pyridine as an absorbent showed that the Lewis acidity, as indicated by the 1455 cm^{-1} band was about the same for Al_2O_3, 3% Pt/Al_2O_3, 3% Sn/Al_2O_3 and 3% $Pt\text{-}Sn/Al_2O_3$. There was no evidence of Bronsted acidity. Therefore, the enhanced coke deposition for Pt-Sn cannot be attributed to a higher acidity. However, a 3% Sn/Al_2O_3 which was heated, but not reduced with hydrogen, showed an acidity which was almost double that of the reduced samples. This enhanced acidity produced coke and carboxylate which was equivalent to that of alumina, i.e., tin's ability to lower these factors is lost when the tin is not subjected to a prior treatment in hydrogen.

Future efforts will involve attempts to better understand the Sn-Pt interaction. Lehigh's new high resolution ESCA will be used in this effort. Work will be continued to determine the mechanism of the carboxylate formation. The most simple mechanism involves a hydration of the acetylene by surface hydroxyls after which the reaction proceeds by the mechanism which Greenler postulates for the production of surface carboxylates from alcohols [8]. The alumina has hydroxyl bands at 3765, 3715, 3670 and 3587 cm^{-1}. Preliminary results show that about 10% of the total hydroxyl intensity is lost during carboxylate formation. This loss is confined to the higher frequency 3765 and 3715 cm^{-1} bands. A loss of OH supports the hydration mechanism but does not prove it. The two high frequency bands also decrease when carboxylates are formed by adsorption of acetic acid. In this latter case, there is no need to utilize oxygens provided by surface hydroxyls.

REFERENCES

[1] K.H. Ludlum and R.P. Eischens, Petroleum Division Preprints, ACS Meeting, New York (1976)

[2] A. Corodo, A. Kiss, H. Knotzinger, and H.D. Muller, J. Catalysis <u>37</u>, 68 (1975).

[3] D. Eisenbach and E. Gallei, J. Catalysis <u>56</u>, 377 (1979).

[4] J. Najbar and R.P. Eischens, 9th International Congress on Catalysis, Calgary, 1984, Paper 184.

[5] R. Burch, J. Catalysis <u>71</u>, 348 (1981).

[6] S.R. Adkins and B.H. Davis, J. Catlysis <u>89</u>, 371 (1984).

[7] R.P. Eischens, Stud. Surf. Sci. Catal. <u>44</u>, 51 (1989).

[8] R.G. Greenler, J. Chem. Phys. <u>37</u>, 2094 (1962).

References 4 and 7 were published with support from the DOE Division of Chemical Sciences.

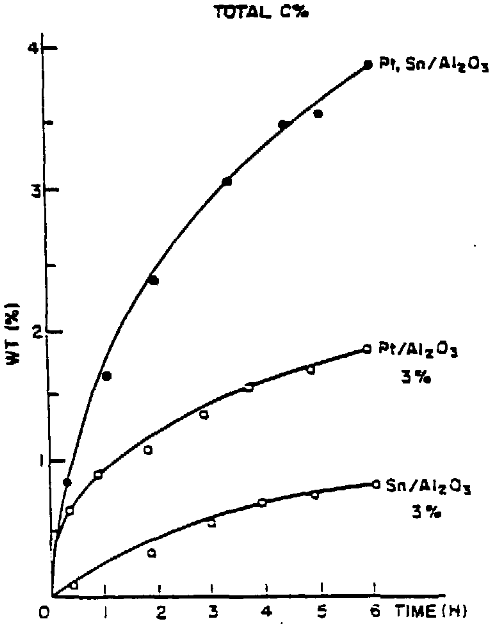

Fig. 1. Coke deposition from acetylene on Pt/Al_2O_3, Sn/Al_2O_3 and $Pt\text{-}Sn/Al_2O_3$ at 3 wt% metal loadings.

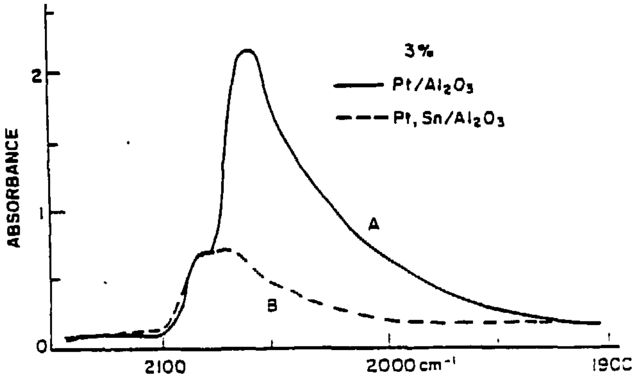

Fig. 2. Comparison of CO on Pt/Al_2O_3 and $Pt\text{-}Sn/Al_2O_3$ at 3 wt% metal loadings.

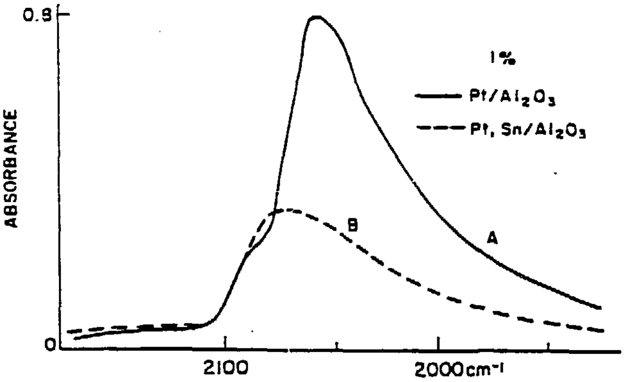

Fig. 3. Comparison of CO on Pt/Al_2O_3 and $Pt\text{-}Sn/Al_2O_3$ at 1 wt% metal loadings.

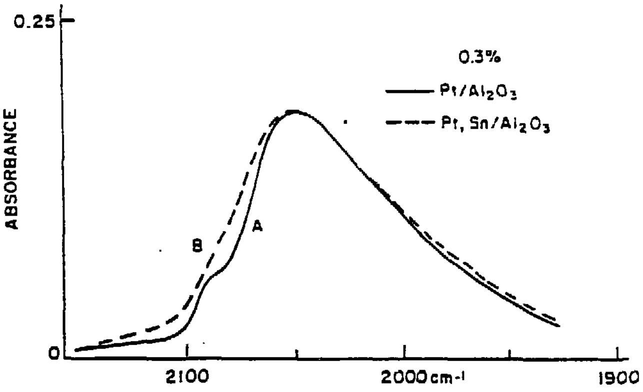

Fig. 4. Comparison of CO on Pt/Al_2O_3 and $Pt\text{-}Sn/Al_2O_3$ at 0.3 wt% metal loadings.

MODEL CATALYTIC OXIDATION STUDIES USING SUPPORTED MONOMETALLIC AND HETEROBIMETALLIC OXIDES

John G. Ekerdt

Department of Chemical Engineering
University of Texas at Austin
Austin, Texas 78712

Research Scope and Objectives

This research program is directed toward a more fundamental understanding of the effects of catalyst composition and structure on the catalytic properties of metal oxides. A key limitation to developing insight into how oxides function in catalytic reactions is in not having precise information of the surface composition under reaction conditions. To address this problem we propose to develop oxide systems which can be used to model oxide catalysis in a systematic fashion. Since many oxide catalyst systems involve mixtures of oxides, we have selected a model system which will permit us to examine the role of each cation separately and in pairwise combinations. Organometallic complexes containing η^3-C_3H_5 or cyclopentadienyl ligands will be bound to silica, alumina, and magnesia supports by exchange of these ligands with surface hydroxyl groups. The anchored complex will be subsequently oxidized to generate an oxide supported on the surface of silica, alumina, or magnesia. We will attempt to support molybdenum and tungsten as isolated monomeric cations, isolated monometallic MoMo and WW dimers or cation pairs, isolated bimetallic MoW dimers or cation pairs, and polymolybdate or polytungstate clusters. These model systems will be used to investigate C-H abstraction from alkanes and olefins, hydrogenolysis of cyclopropane, and the oxidation of methanol and hydrocarbons. The research will involve characterization of the organometallic deposition process, characterization of the resulting oxides using spectroscopic and structure sensitive molecular probes, and use of these oxides in catalytic studies.

Description of the Research Effort

Organometallic molybdenum and tungsten complexes will be used in attempts to prepare model systems having various cation combinations on silica, alumina, and magnesia. The monometallic and bimetallic dimers or cation pairs will be used as models of more complex mixed oxide catalysts, and should permit us to explore the synergism which exists between cations in mixed oxide catalysts. The oxidation state of the cations can be changed and, in principle, we will have a system in which all the cations have the same structure and oxidation state. Raman, UV-diffuse reflectance, and photoluminescence spectroscopies are used to characterize the coordination and structure of the supported cations. Thermal oxidation/reduction, photochemical reduction in CO, and IR of adsorbed CO are used to study the adsorptive and reductive characteristics of the cations.

Simple reactions will be used to probe the catalytic properties. These reactions include methanol oxidation, oxidative dehydrogenation of alkanes, oxidation of olefins, and hydrogenolysis of cyclopropane. We will attempt to determine how cation ensemble size rather than crystallographic orientation influences the selectivity and activity of these oxide catalyzed reactions.

Progress to Date

Catalytic research over oxides had concentrated on the CO hydrogenation reaction to branched hydrocarbons and alcohols over zirconium dioxide and cation doped zirconium dioxides. This work relied on changes in the bulk composition and phases of the oxides to probe various aspects of the catalytic chemistry. The key findings of the CO hydrogenation studies are listed below.

Through the use of IR spectroscopy, temperature programmed desorption, gravimetric titration, steady state reaction rate studies, isotope incorporation studies, and composition modification we were able to determine how CO was activated, what the reaction intermediates were, and how the oxide influenced the synthesis selectivity. In particular we determined that CO adsorbed at oxygen anion vacancy sites as a formate and was reduced sequentially to adsorbed formaldehyde and then methoxide. The reactions of these C_1 intermediates and CO to higher weight hydrocarbons were found to involve two chain growth steps, CO insertion into aldehyde/ketone C-Zr bonds and condensation between enolates and methoxide. The condensation reaction was found responsible for the unique product distributions that are characteristic of isosynthesis (the formation of branched hydrocarbons over oxides). Lewis acid sites and oxygen vacancies were found to enhance the condensation reaction and CO insertion was enhanced by basic sites. The Lewis acid sites stabilized the enolates and increased the probability of the condensation reaction. The selectivity of the isosynthesis reaction is caused by a balance between the strength and quantity of acid and base sites on zirconium dioxide.

The research with supported cations is now the central focus of our work. We were motivated by papers in the literature which claimed Mo could be selectively deposited on the surfaces of silica and alumina by exchange of a surface hydroxyl hydrogen with a Mo precursor ligand, such as η^3-C_3H_5 or Cl. Raman spectroscopy and molecular probe studies we performed suggested that the formation of isolated Mo, Mo dimers, and Mo cation pairs over silica and alumina was not possible in many of the situations discussed in the literature. As a check on our techniques and on the purity of our supports we prepared samples by a variety of alternate methods, obtained the same supports that have been used by previous workers in this field, and even obtained some of their supported samples. We also used magnesia as a third support because of its basic properties.

Molybdenum was supported on silica, alumina, and magnesia surfaces using $(NH_4)_6Mo_7O_{24}\cdot 4H_2O$, $H_2(MoO_3C_2O_4)\cdot 2H_2O$, $MoCl_5$, $Mo(\eta^3\text{-}C_3H_5)_4$, and $Mo_2(\eta^3\text{-}C_3H_5)_4$. Raman and UV-diffuse reflectance spectroscopy and CO photoreduction were used to characterize the Mo. Methanol oxidation was used to probe the catalytic properties of silica-supported Mo. The Raman spectra were recorded for the fully oxidized cations in ambient air. On silica, aqueous preparation steps, not necessarily the use of $MoCl_5$, led to the formation of some tetrahedrally coordinated and isolated Mo cations. In general however, Mo tended to form octahedrally coordinated polymolybdate clusters and MoO_3 crystallites on silica. The structure over alumina was dependent on weight loading with isolated and paired tetrahedra observed at low loading and aggregation into octahedral polymolybdate observed at higher loadings. Tetrahedrally coordinated Mo was found on magnesia at all loadings provided a monolayer loading was not exceeded. The resulting molybdena overlayer structure was dependent on the interaction between the fully oxidized Mo cation and the support and was not dependent on the precursor structure or method of preparation. Other structures are likely formed during precursor deposition/exchange and before total oxidation; however, once oxidized the structure appears to be influenced by the acid-base interactions between Mo and the support. The tabulation below summarizes the results.

Support	Coordination	Structure	Loading (Mo/nm^2)
MgO	T_d	Bidentate monomer	< 6
Al_2O_3	T_d	Bidentate monomer	< 1
Al_2O_3	T_d	Bidentate monomer, dimer, cation pair	$\sim 1-2$
Al_2O_3	O_h	Polymolybdate	$\sim 2-5$
Al_2O_3	O_h	MoO_3 crystallites	> 5
SiO_2	T_d	Undefined monomer	< 0.2
SiO_2	O_h	Polymolybdate	> 0.1
SiO_2	O_h	MoO_3 crystallites	> 0.2

These results suggest that MgO may be the best support to employ for the stabilization of isolated sites and paired sites. We have not determined the proximity of cations on MgO merely that they are tetrahedral and equivalent to Raman standards for monomer models. We expect that cation pairs formed from $Mo_2(\eta^3\text{-}C_3H_5)_4$ precursors and are currently exploring this possibility with CO adsorption. We have also prepared a number of other allylic precursors from W, Cr, and Zr which were supported on MgO to determine how MgO interacts with other cations but have not yet completed the Raman characterization of these systems.

Additional work has included an examination of CO photoreduction of Mo(VI). Carbon monoxide appears to be a molecular probe for determining the structure of the supported Mo, because different sets of carbonyl bands are observed depending on the coordination and cluster size. Work in progress suggests that polymolybdate cluster size, isolated monomers, and dimers versus cation pairs may be distinguishable by controlled photoreduction.

We have also synthesized the following precursors for use in the W and WMo systems, $Cp_2Mo_2(CO)_4$, $Cp_2MoW(CO)_4$, and $Cp_2W_2(CO)_4$. Attempts to synthesize WW dimers with either $\eta^3\text{-}C_3H_5$ or $\eta^3\text{-}C_5H_9$ and thereby avoid the use of CO ligands were unsuccessful.

Future Research

The work with Mo will continue. We have a detailed picture of the structure of Mo(VI) and are interested in determining if dehydrogenation, hydrogenation or hydrogenolysis reactions can be used to discriminate the structure of noncrystalline metal oxides. If reactions can be found over less than fully oxidized Mo we should be able to investigate the evolution of the structures following deposition of the precursors. We will also begin to employ the $Cp_2Mo_2(CO)_4$ precursor and follow the CO IR bands during exchange and subsequent ligand loss. One of the central questions is at what stage the cations form clusters over SiO_2.

Tungsten complexes will be supported on the three supports to determine how similar the interactions of W and Mo with the supports is. We anticipate that low loadings of W on alumina and less than monolayer loadings on magnesia will lead to tetrahedrally coordinated W cations that are structurally similar to those of Mo. Once the W system is understood, we will begin to employ heterobimetallic MoW complexes with the intention of forming cation pairs or dimers. Following characterization of the supported cations, they will be subjected to identical reaction conditions to determine how the oxidizing ability of the cations, alone and in pairwise combinations, affect selectivity and activity.

<u>Publications</u>

Isosynthesis Reactions of CO/H_2 over Zirconium Dioxide (S. C. Tseng, N. B. Jackson, and J. G. Ekerdt), Journal of Catalysis <u>109</u>, 284 (1988).

The Role of Lattice Anion Vacancies in the Activation of CO and as the Catalytic Site for Methanol Synthesis over Zirconium Dioxide and Yttria-Doped Zirconium Dioxide (R. G. Silver, C. H. Hou, and J. G. Ekerdt), Journal of Catalysis <u>118</u>, 400 (1989).

The Surface Characteristics Required for Isosynthesis Over Zirconium Dioxide and Modified Zirconium Dioxide (N. B. Jackson and J. G. Ekerdt), Journal of Catalysis (submitted).

Isotope Studies of the Effect of Acid Sites on the Reactions of C_3 Intermediates During Isosynthesis Over Zirconium Dioxide and Modified Zirconium Dioxide (N. B. Jackson and J. G. Ekerdt), Journal of Catalysis (submitted).

A Laser Raman and UV Diffuse Reflectance Spectroscopic Investigation of Silica-Supported Molybdenum Oxide (C. C. Williams, J. G. Ekerdt, I. E. Wachs, J-M. Jehng, and F. D. Hardcastle), manuscript in preparation.

A Laser Raman and UV Diffuse Reflectance Spectroscopic Investigation of Alumina- and Magnesia-Supported Molybdenum Oxide (C. C. Williams, J. G. Ekerdt, I. E. Wachs, J-M. Jehng, F. D. Hardcastle, and C-K. Chen), manuscript in preparation.

A Molecular Probe Study of Silica-Supported Molybdenum Oxide: CO, H_2 and O_2 Adsorption, and Methanol Oxidation (C. C. Williams and J. G. Ekerdt), manuscript in preparation.

An FTIR and Temperature Programmed Desorption Study of Thermally and Photochemically Activated CO on Silica-, Alumina- and Magnesia-Supported Molybdenum (C. C. Williams and J. G. Ekerdt), manuscript in preparation.

A Novel Oscillating Reaction: Methanol Oxidation Over Silica-Supported Molybdenum (C. C. Williams and J. G. Ekerdt), manuscript in preparation.

MODEL HETEROATOM REMOVAL REACTIONS ON MOLYBDENUM SURFACES, DOE Grant No. DE-FGO2-84ER13289

Cynthia M. Friend, Department of Chemistry
Harvard University; Cambridge, MA 02138

The mechanism for heteroatom-removal reactions induced by clean and chemically modified Mo(110) have been studied under idealized conditions in an effort to understand factors that control the reaction kinetics and selectivity in the related catalytic hydrodesulfurization and hydrodeoxygenation processes. The focus of recent work has been the investigation of Mo-induced deoxygenation of alcohols and cyclic oxides and the desulfurization of thiols and cyclic sulfides. The studies of alcohols[10,11,14] and cyclic oxides[12] serve as models for catalytic deoxygenation of synthetic fuels while the studies of the S-analogs [1-7, 13], thiols and cyclic sulfides, are models for desulfurization catalysis. The effect of surface modification by oxygen and sulfur overlayers has also been investigated in order to better understand the effect of sulfides and oxides on the catalytic process. Experimentally, the comparison of the reactivity for related molecules, such as thiols and alcohols, allows for a general understanding of important factors controlling heteroatom removal reactions. The methods used to investigate these processes are X-ray photoemission, temperature programmed reaction, near edge X-ray absorption fine structure, and Auger electron spectroscopies in conjunction with isotopic labelling.

Our recent work suggests that adsorbed alkoxide and thiolate intermediates decompose via a transition state in which there is a substantial amount of C-X (X=O,S) bond cleavage. As a result, the reaction selectivity and kinetics depend upon the nature of the alkyl group in the alcohol due to the different stability of the corresponding alkyl radicals formed from C-O bond cleavage. All alcohols studied to date, phenol, methanol, and 1- and 2-propanol, form surface alkoxides below 300 K on both clean and oxygen precovered surfaces. Similarly, all thiols studied from the respective thiolates: ethanethiol, 1-propanethiol, *t*-butanethiol, *n*-butanethiol, and benzenethiol. The kinetics for alkoxide decomposition correlate with the stability of the corresponding radicals formed via C-O bond cleavage: 2-propoxide reacts most rapidly and phenoxide most slowly with 1-propoxide and methoxide exhibiting intermediate reactivity. Similar trends in relative reactivity are observed on the oxygen-precovered surface. The corresponding thiolates rapidly than the alkoxides but the alkoxides but kinetics likewise parallel alkyl stabilities.

Surface oxygen is found to generally inhibit nonselective decomposition compared to initially clean Mo(110). While a surface alkoxide has been shown to readily form in all cases, based on X-ray photoemission and isotopic labelling studies, a range of reaction products are observed. Of particular interest is the observed formation of gaseous methyl radicals from the decomposition of adsorbed methoxide on oxygen-pretreated (θ_O=0.25-0.33) Mo(110) but not on initially clean Mo(110). (See Figure 1.) Previously, gas phase methyl radicals have been observed from the activation of methane over metal oxide catalysts, but were attributed to direct activation of C-H bonds whereas methoxide was thought to only lead to oxidation products. Our work suggests that methoxide may also be a source of methyl radicals. 1- and 2-propoxide produce propene with relatively high selectivity (~70%) with minor amounts of accompanying propane formation (hydrogenolysis) and nonselective decomposition. A radical-like transition state is also proposed for both propoxides but facile C-H bond activation is possible due to the stability of the propene relative to the propyl radical. In contrast, phenoxide, the most kinetically stable intermediate, disproportionates to reform gaseous phenol with competing nonselective decomposition. The differences in reactivity are, in part, attributed to the differences in stability of the adsorbed alkoxides but the altered reactivity of surface hydrogen by coadsorbed oxygen and alkoxides is also important. Related studies of the adsorption structure of phenoxide and methoxide suggest that molecular geometry may also play a role in determining reactivity: methoxide is oriented perpendicular to the surface whereas the phenyl ring of phenoxide is tilted 30° with respect to the surface normal.

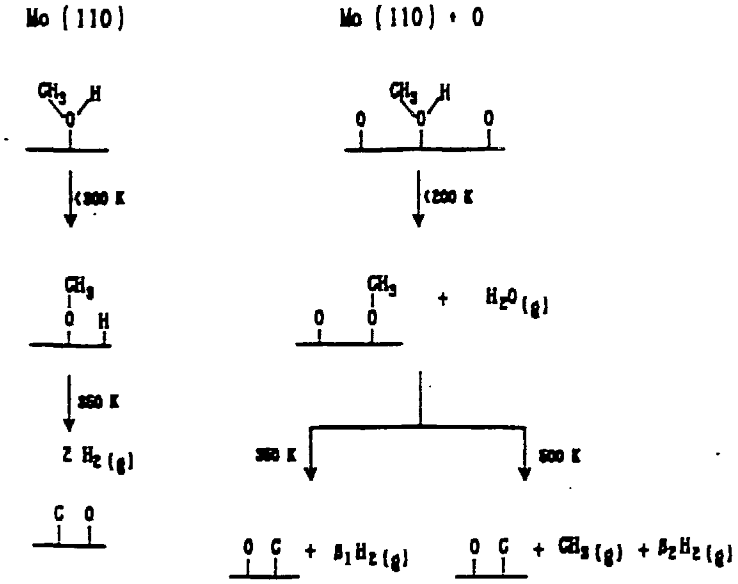

Figure 1: Reaction schemes for methanol adsorbed on clean and oxygen-precovered (θ_O=0.33) Mo(110).

Surface oxygen also increases the selectivity for ethylene oxide deoxygenation on Mo(110) by inhibiting nonselective decomposition processes. Ethylene oxide is an important component of metal adhesives and is structurally analogous to ethylene sulfide, one of a series of cyclic sulfides studied previously. Both ethylene oxide and ethylene sulfide eliminate gaseous ethylene in an intramolecular process induced by Mo(110). The stronger C-O bond in ethylene sulfide makes the ethylene formation reaction considerably less favorable both kinetically and thermodynamically than the corresponding desulfurization of ethylene sulfide. The correlation between the kinetics for heteroatom removal and C-X (X=O or S) bond strength is strong evidence that C-X bond breaking largely determines the barrier for heteroatom removal, as suggested earlier by us for a range of cyclic sulfides. Our experimental studies of cyclic sulfide and oxide reactions on Mo(110) have also fostered collaborative theoretical work in the group of Roald Hoffmann at Cornell.

Studies of sulfur-containing reactants have also been extended to cyclic molecules with varying degrees of C-C bond unsaturation and to secondary and tertiary thiols as model substrates for desulfurization processes. In this aspect of our work, the reactivity of tetrahydrothiophene, 1,5-dihydrothiophene and thiophene have been compared and contrasted to the reactivity of organometallic complexes reported in the literature. The effects of surface sulfur and oxygen are specifically being contrasted in these studies to determine the relative importance of blocking of coordination sites and changes in surface electronic structure induced by these overlayers. This work is still in the preliminary stages and will be continued during the next year.

DOE-supported Publications, Cynthia M. Friend, 1987-present

1. J.T. Roberts and C.M. Friend, Desulfurization of Saturated C_3S Molecules on Mo(110): The Effect of Ring Strain, J. Am. Chem. Soc., 109, 3872, **1987**.

2. J.T. Roberts and C.M. Friend, The Reactions of Thiophene on Mo(110) and Mo(110)-p(2x2)-S, Surface Sci., 186, **1987**.

3. J.T. Roberts, C.M. Friend, "Ring Strain and Size as a Control of Reaction Selectivity: Ethylene Sulfide on Mo(110)." **J. Am. Chem. Soc.**, 109, **1987**, 7899.

4. J.T. Roberts, C.M. Friend, "Vibrational Studies of 1-Propanethiol on Mo(110)." **Surf. Sci.**, 198, **1988**, L321.

5. J.T. Roberts and C.M. Friend, "Desulfurization of Ethylene Sulfide on Mo(110): The Roles of Ring Size and Strain in Adsorbate Reaction Selectivity". **Surf. Sci.**, 202, 405-432, **1988**.

6. J.T. Roberts and C.M. Friend, "Spectroscopic Identification of Surface Phenyl Thiolate and Benzyne on Mo(110)". **J. Chem. Phys.**, 88, 7172-7180, **1988**.

7. J.T. Roberts and C.M. Friend, "The Reactions of Ethanethiol on Mo(110): Formation and Decomposition of a Surface Alkyl Thiolate." **J. Phys. Chem.**, 92, 5205-5213, **1988**.

8. C.M. Friend and J.T. Roberts, "Deduction of Reaction Mechanisms for Surface Processes: Desulfurization of Organic Sulfides and Thiols on Mo(110)." **Accts. Chem. Res.**, 21, 394-400, **1988**.

9. J.G. Serafin and C.M. Friend, "Reactivity of Pyridine on Mo(110): C-H and C-N Bond Activation." **J. Phys. Chem.**, 93, 1998-2004, **1989**.

10. Serafin, J.G. and C.M. Friend, "Carbon-Oxygen Bond Strength as a Control of Reaction Kinetics: Phenol on Mo(110)." **Surf. Sci.**, 209, L163-L175, **1989**.

11. J.G. Serafin and C.M. Friend "Inhibition of C-H and C-O Bond Activation by Surface Oxygen: Stabilization of Phenoxide in the Reaction of Phenol on Oxygen Precovered Mo(110)". **J. Am. Chem. Soc.**, 111, 4233-4239, **1989**.

12. J.G. Serafin and C.M. Friend, "Controlling Factors in Deoxygenation Kinetics and Selectivity: The Reactions of Ethylene Oxide on Mo(110)." **J. Am. Chem. Soc.**, 111, 6019-6026, **1989**.

13. J.T. Roberts, B.C. Wiegand, C.M. Friend, "Adsorbate Thermodynamics as a Determinant of Reaction Mechanism: Pentamethylene Sulfide on Mo(110)." **Langmuir**, *In Press*, **1989.**

14. J.G. Serafin, C.M. Friend, "Evidence for Formation of Gaseous Methyl Radical in the Decomposition of Methoxide on Oxygen-Precovered Mo(110)" **J.Am.** Chem. Soc., *In Press*, **1989.**

METAL-SUPPORT BONDS IN SUPPORTED METAL CATALYSTS

Bruce C. Gates
Center for Catalytic Science and Technology
Department of Chemical Engineering
University of Delaware
Newark, DE 19716

SUMMARY

This research is an investigation of the synthesis, structure, and bonding of a family of metal complexes and metal aggregates on the surfaces of metal oxide supports. The primary focus is the metal-support interface and the interactions between the metals and the supports. Surface structures have been prepared by the reactions of organometallic precursors with the support surfaces. The precursors are complexes of W, Re, Os, Ir, and Pt, including $W(CO)_6$, $HRe(CO)_5$, $Re_2(CO)_{10}$, $H_3Re_3(CO)_{12}$, $H_2Os(CO)_4$, $Ir(\eta-C_3H_5)_3$, $Pt(\eta-C_3H_5)_2$, and $Pt(CH_3)_2(COD)$. The supports are primarily MgO and $\gamma-Al_2O_3$.

The major results have been obtained for complexes of Re and W; this report emphasizes the results for the former. When the hydridorhenium precursors react with the MgO surface from organic solutions, they are chemisorbed as a result of acid-base interactions, with the hydrido trirhenium cluster being deprotonated to give surface ion pairs involving $[H_2Re_3(CO)_{12}]^-$ and the mononuclear rhenium complex giving an undissociated species. When either of these is heated under vacuum, it is oxidized, with the formation of a rhenium subcarbonyl, formulated as $Re(CO)_3\{OMg\}\{HOMg\}_2$, on the basis of infrared and EXAFS spectra, among other data. (Here the braces denote groups terminating the MgO surface.) The exact identities of the oxygen-containing ligands in the surface structures are still uncertain.

Other rhenium carbonyls, e.g., $Re_2(CO)_{10}$, also form the subcarbonyl, but the chemistry can be manipulated to give other intermediate surface structures, including the dianion $[Re_2(CO)_9]^-$, which is formed easily from $Re_2(CO)_{10}$ at -40°C; the surface chemistry mimics that occurring in basic solutions. The dianions are inferred to be ion-paired to the surface; oxidation gives the subcarbonyl.

When $H_3Re_3(CO)_{12}$ is adsorbed on $\gamma-Al_2O_3$ and then treated in H_2 at 400°C, a unique new surface species is

formed, which has been characterized in detail by infrared spectroscopy, XANES, and EXAFS spectroscopy. The surface species is trinuclear, and the average Re-Re distance is less than that in bulk Re. The results suggest that the surface species has multiple Re-Re bonds.

RESULTS AND DISCUSSION

Samples formed from $HRe(CO)_5$ on MgO

The reaction of $HRe(CO)_5$ with the surface of MgO powder takes place as a solution of this precursor in an organic solvent is allowed to come in contact with the solid. The resulting surface species has been characterized by infrared spectroscopy; the exact structure is unknown, but the results show that the organometallic species is not dissociated on the surface. It is, however, strongly chemisorbed and cannot be washed off the surface by neutral solvents.

When the surface species is oxidized, by treatment in oxygen or even in helium or under vacuum, a rhenium subcarbonyl is formed on the surface. This has been characterized by infrared spectroscopy, EXAFS spectroscopy (the latter data are not yet analyzed), and temperature programmed decomposition. The data are consistent with a structure formulated as $Re(CO)_3\{OMg\}\{HOMg\}_2$. However, the exact nature of the ligands provided by the support surface (which are inferred to incorporate oxygen) is not yet established. There are two kinds of these ligands, as demonstrated by the symmetry indicated by the infrared spectra.

To clarify this issue, experiments are being done with MgO supports having controlled degrees of (de)hydroxylation in attempts to allow inference of the identities of the ligands provided by the support. Infrared spectra are being measured to identify a family of surface subcarbonyls on the systematically varied support surfaces. Evaluation of the EXAFS data is expected to give quantitative measures of the average metal-oxygen, metal-carbon, and metal-O* distances, where O* refers to the carbonyl oxygen.

Samples formed from $Re_2(CO)_{10}$ on MgO

When a solution of $Re_2(CO)_{10}$ in an organic solvent is brought in contact with MgO powder, the organometallic is chemisorbed. The surface species can be extracted into solution by ion exchange, e.g., with a solution of [PPN]Cl. The extracted species has been identified by its infrared spectrum as $[Re_2(CO)_9]^{2-}$. A series of salts of this dianion has been investigated and their uv-visible and infrared spectra compared with those of the surface species. The carbonyl stretching frequencies are sensitive to electrostatic interactions of cations with the dianion, and the band locations of the surface species give evidence that it is strongly ion-paired to the MgO surface.

In contrast, when the $Re_2(CO)_{10}$ is brought in contact with the MgO surface after it has been hydrated--and the contacting is carried out at very low temperatures (roughly -50°C), the organometallic is weakly adsorbed. Infrared spectra measured at low temperature suggest that the surface species is $Re_2(CO)_9(H_2O)$ and that this is hydrogen-bonded to the surface.

When the surface-bound dianion is oxidized, it is converted to a covalently bonded rhenium subcarbonyl, as indicated by infrared spectra.

In summary, the rhenium carbonyls evidence a wide range of surface interactions, ranging from weakly hydrogen-bonded structures to strongly ion-paired structures to covalently bonded structures.

To complete the picture, some samples incorporating the rhenium subcarbonyls were treated in H_2 to give metallic aggregates on the MgO surface. The subcarbonyl is highly resistant to oxidation, and temperatures well in excess of 400°C are required for substantial metal crystallite formation. Some samples incorporating mixtures of metal particles and cationic Re species have been characterized by EXAFS spectroscopy.

Samples formed from $H_3Re_3(CO)_{12}$ on γ-Al_2O_3

When $H_3Re_3(CO)_{12}$ is adsorbed from organic solution onto alumina, a chemisorbed species is formed. When this sample is treated in H_2 at 400°C, a new structure is formed, which has been characterized in depth by infrared and, especially, EXAFS spectroscopies, as well as XANES. The structure is remarkably simple, as indicated by the EXAFS data: the Re-Re coordination number is 2, indicating that the surface structure is still a trirhenium structure, even after the high-temperature treatment in H_2. Further, the average Re-Re distance is 0.267 nm, which is substantially less that the Re-Re distance in the bulk metal, 0.274 nm.

These results have been used to formulate a model of the surface structure, shown in Fig. 1. The short Re-Re distance suggests that the surface species has Re-Re multiple bonds; in this sense, it is roughly comparable to some molecular structures with multiple metal-metal bonds, such as that shown in Fig. 2.

PUBLICATIONS

1. "Catalyst Design: Multicenter Surface Sites," Y. Iwasawa and B. C. Gates, CHEMTECH, **19**, 173 (1989).

2. "Supported Metals and Supported Organometallics," B. C. Gates and H. H. Lamb, *J. Mol. Catal.*, **52**, 1 (1989).

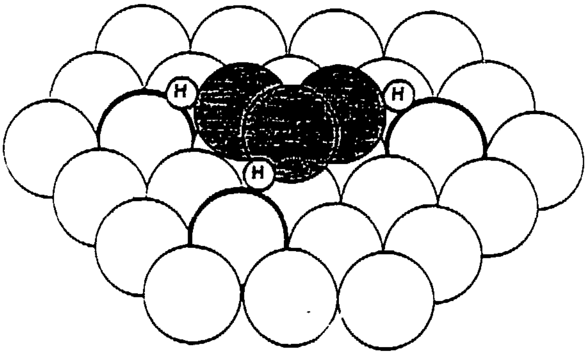

Fig. 1. Model of a trirhenium structure on the alumina surface. The structure is formulated on the basis of EXAFS data.

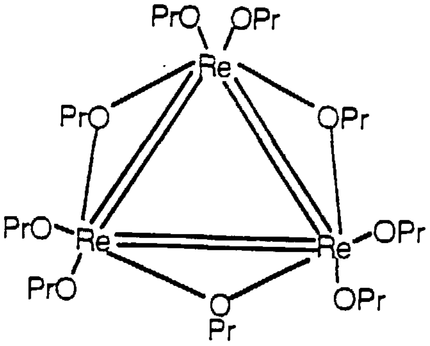

Fig. 2. A metal cluster with multiple metal-metal bonds.

Project Summary

B.C. Gerstein

SCOPE

Our work in heterogeneous catalysis uses nuclear spin dynamics to study catalytically active surfaces, and deposited molecules and molecular fragments on these surfaces.

Catalysts include zeolites, vanadium phosphorous oxides, used in the conversion of C_4 hydrocarbons to maleic anhydride, supported bimetallic catalysts such as Cu-Ru/SiO_2 which model catalysts used in petroleum reforming, and alkali metal doped copper oxides, which have been found to convert $CO + H_2$ to higher alcohols.

We study the NMR of appropriate tags, such as ^{51}V, ^{31}P, ^{17}O, ^{13}C, ^{1}H, ^{63}Cu, ^{65}Cu, and ^{133}Cs, in broad-banded, home-built NMR spectrometers operating in pulse mode at frequencies ranging from 56 MHz for ^{1}H to 300 MHz for ^{1}H.

RECENT RESULTS

1) We have developed a single quantum propagator for use in counting the numbers of protons in isolated clusters, such as that found in the possible intermediate $(-CH_2CH_3)^{ads}$. Detection of numbers of coupled spins rather than chemical shifts as an identifying fingerprint is useful when susceptibility dispersion of the surface results in linebroadening of the NMR signal even under conditions of high resolution. Figure 1 shows the multiple quantum spectrum of coupled protons in K_2PtH_4, counted using a single quantum propagator, such that multiple quantum coherences are counted in increments of single quanta (note the increment in k on the abscissa).

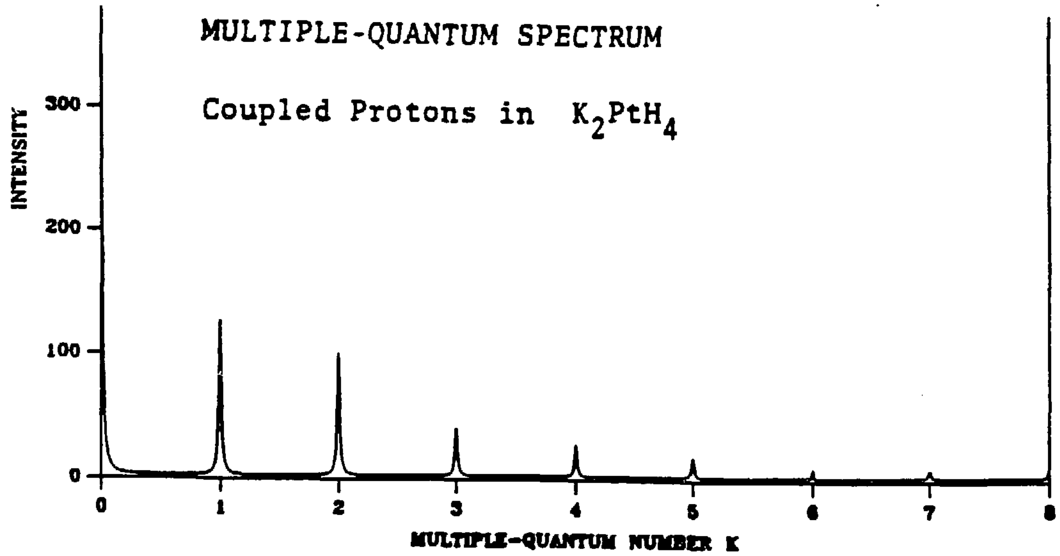

2) We have investigated the utility of the quadrupolar nucleus ^{133}Cs *as an NMR tag, and used this nucleus to detail the process of dehydration in a mordenite.*

3) NMR of ^{133}Cs *and* ^{63}Cu *has been used to provide information on local chemical structures present in alkali metal doped copper catalysts used to convert CO and* H_2 *into higher alcohols.*

4) We have determined that dissociated hydrogen exists on the surface of Cu/SiO_2*, and have found at least four species of hydrogen on* $Cu\text{-}Ru/SiO_2$ *at room temperature.*

5) We have observed for the first time the NMR of ^{13}C **during the reaction of singly doped ethylene to form ethane, 2-butene, and butane on** Ru/SiO_2, *and detected immobile, strongly chemisorbed species on the surface which yield susceptibility dispersion broadened NMR chemical shifts, but which lie in the chemical shift range allowed by* $(-C\equiv CH)^{ads}$, $(-CH_2CH_3)^{ads}$, *and* $(-CH_2CH_2CH_2CH_2-)^{ads}$. *These experiments involved the use of a sealed NMR tube spinning at 5 KHz in variable temperature operation.*

6) NMR has been used for the first time to determine the presence of V^{+3} *in vanadium phosphorous oxides used for conversion of butane and butene to maleic anhydride.*

7) NMR of ^{63}Cu *has been used to determine dispersion of supported copper,* Cu/SiO_2.

FUTURE PLANS

Identification of sites for hydrogen adsorption on supported metal catalysts, and possible chemical identities of hydrogen in V-P-O catalysts will be extended to low (100K) temperatures in an NMR probe constructed to have a minimal hydrogen background, and capable of high resolution NMR of hydrogen in solids contained in sealed ampules spun at 5 KHz.

Double resonance NMR involving $^{195}Pt\text{-}^{13}C$, *and* $^{195}Pt\text{-}^{1}H$, *and multiple quantum spin counting will be used to identify intermediates involved in reforming of* *hydrocarbons by supported bimetallic, M-Pt/SiO$_2$, catalysts. The role of the "non-active" metal in the catalytic process will be investigated by correlating these experiments with kinetic studies over catalysts with varying ratios of the two supported metals (collaboration with Terry King).*

High resolution solid state proton NMR will be applied to molybdenum sulfide desulfurization catalysts in the beginnings of an effort to determine the nature of hydrogen involved in these systems, and to probe the role of hydrogen in the desulfurization process. The possibility of identifying ^{33}S in natural abundance in sulfur poisoned catalysts as one means of determining the nature of the of sulfur in these materials will be investigated (Collaboration with Glen Schrader).

PUBLICATIONS

"A Study by Solid State NMR of ^{133}Cs and ^{1}H of a Hydrated and a Dehydrated Cesium Mordenite"
P_J Chu, B.C. Gerstein, John Nunan, and Kamil Klier
*J. Phys. Chem. **91**, 3588 (1987)*

"Nuclear Magnetic Resonance"
B.C. Gerstein
Encyclopedia of Science and Technology, Academic >Press (1987)

"Dispersion of Silica Supported Copper Catalysts Determined by NMR of ^{63}Cu"
T.S. King, W.J. Goretzke, and B.C. Gerstein
*J. Catalysis, **107**, 583 (1987)*

"NMR Studies of ^{65}Cu and ^{133}Cs in Alkali-Metal-Promoted Copper Catalysts"
P-J Chu, B.C. Gerstein, R.G. Scheffer, and T.S. King,
*J. Catalysis, **115**, 194 (1989)*

"Quaternary Cation Effects on the Crystallization of Zeolites of the Offretite-Erionite Family: Part III: ^{29}Si NMR, ^{27}Al NMR, and Mid IR Characterization"
M.L. Occelli, G.P. Ritz, P.S. Iyer, R.D. Walker, and B.C. Gerstein
*Zeolites, **9**, 104 (1989)*

The Formation of Supported Bimetallic Clusters: The Effect of Support - Metal Precursor Interactions.

By
Richard D. Gonzalez
Department of Chemical Engineering, University of Illinois at Chicago
Box 4348, Chicago, Illinois 60680

Progress Report

In previous studies, Pt-Ru bimetallic clusters were prepared by coimpregnation using $H_2PtCl_6.6H_2O$ and $RuCl_3$ (1). In that study, the surface composition was found to be enriched in Pt. After careful consideration of the preparative variables, it was concluded that surface enrichment in Pt occurred as a result of the higher surface mobility of the Pt metal precursor. In the case of $H_2Pt\ Cl_6$, a repulsive anionic interaction between the negatively charge silica surface and $PtCl_6^{2-}$ resulted in a very weak metal-precursor-support interaction. Because the aqueous speciation of $RuCl_3$ is predominantly cationic, it is strongly bound to the negatively charged silica support. When thse precursors are contacted with flowing hydrogen, Ru centers capable of adsorbing hydrogen are formed first. Surface diffusion of the mobile precursor ($PtCl_6^{2-}$ or $PtCl_4$) to these centers results in nucleation of Pt atop the Ru surface atoms which form a metallic core. The reduction is therefore assisted by the presence of hydrogen chemisorbed atop the Ru centers.

Studies completed during the current funding year were aimed at reversing this process (2-3). Because it is possible to control the surface charge by adjusting the pH of the impregnating solution, the relative strength of the metal precursor interactions can be controlled through a careful choice of metal precursors. After consideration of several possible choices, two different sets of metal precursors were selected. These were as follows:

I Strong metal precursor-support interactions. At a pH in excess of 7, the negative surface charge on silica is observed to increase sharply (4). However, the pH must be kept below 10 in order to prevent disolution of the silica. When either $Pt(NH_4)_4\ (NO_3)_2$ or $Ru(NH_3)_6.Cl_3$ are dissolved in an aqueous solution, the pH was observed to be between 8 and 9. Because of these considerations, it was concluded that coimpregnation of a solution containing these precursors at a pH of 9 would lead to strong adsorption of both metal precursors.

A series of catalysts prepared by coimpregnation using these precursors were characterized using several chemical and spectroscopic techniques. The results of this study are summarized as follows:

(1) Effect of pretreatment. Pretreatment of the pure supported precursors in O_2 at 300C followed by reduction in H_2 at 400C resulted in poorly dispersed Ru (10%) and highly dispersed Pt(80%). Direct reduction in H_2, on the other hand, resulted in highly dispersed Ru (70%) and poorly dispersed Pt (20-30%). Pretreatment of a mixed adlayer of Pt and Ru precursors in O_2 at 300C followed by H_2 at 400C resulted in Pt and Ru phase segregation. Pretreatment in H_2 at 400C resulted in the formation of Pt-Ru bimetallic clusters.

(2) Elemental analysis. Elemental analysis of all of the catalysts prepared by coimpregnation was performed following washing in deionized water to eliminate weakly adsorbed species. The preferred method of analysis was ICP (induced coupled plasma). An elemental analysis of the 5 catalysts is summarized in Table 1.

Table 1.

Metal loadings of Pt-Ru/SiO_2 Catalysts

ID	Pt wt%	Ru wt%	mmoles Pt per g support	mmoles Ru per g support	mmoles metal per g support
IV1	2.68	0.00	0.14	0.00	0.14
IV2	1.16	0.61	0.06	0.06	0.12
IV3	0.98	1.03	0.05	0.10	0.15
IV4	0.19	1.12	0.01	0.11	0.12
IV5	0.00	1.00	0.00	0.10	0.10

The data in the above Table shows that when the Pt and Ru precursors are coadsorbed, the Ru precursor appears to be more tightly bound to the support, i.e., it is more difficult to elute by washing than the Pt precursor.

(3). Diffuse U.V. reflectance experiments. The U.V. spectra of the pure precursors dissolved in solution were compared to those obtained for the supported materials. Because the spectra were identical, these experiments showed that the structure of the precursor was preserved following adsorption.

(4). Surface composition experiments. The surface composition of the resulting bimetallic clusters was measured using a selective O_2-CO pulse titration experiment to a CO_2 end point (5). Advantage was taken of the fact that the CO-O_2 titration ratio was four for Pt and one for Ru. This difference was used to backcalculate the surface composition of the bimetallic clusters. The results of this study show that the surface composition is enriched in Pt. This surface enrichment in Pt is considerably lower than that observed when the bimetallic clusters were prepared from a solution containing H_2PtCl_6 and $RuCl_3$.

Surface enrichment in Pt was explained by considering the higher surface mobility of the Pt precursor during H_2 reduction. According to Dalla Beta and Boudart (6) this mobile Pt surface species may have the structure $[Pt(NH_3)_2(H)_2]^{0}$.

(5). The elemental analysis of individual bimetallic particles. The elemental analysis of individual bimetallic particles was performed using energy dispersive x-ray spectroscopy (EDXS). This study was performed in the microscope facility at the University of Wisconsin, Madison using a VG-501 electron microscope equipped with a field emission gun. Using this instrument, it was possible to focus the electron beam down to a diameter of 2.0 nm. The results of this study showed that for all of the catalysts prepared by coimpregnation the particles analyzed contained both Pt and Ru. Small particles were enriched in Ru, while large particles were Pt rich. When the catalysts were prepared by the sequential impregnation of Pt/SiO_2 with Ru $(NH_3)_6Cl_3$, a bimodal distribution consisting of only large Pt and small Ru particles was obtained. Treatment of a bimetallic catalyst with O_2 at 30C resulted in phase segregation.

II Strong Pt metal precursor-support interaction and weak Ru metal precursor-support interaction.

In an attempt to prepare supported Pt-Ru bimetallic clusters which were surface enriched in Ru, a volatile Ru precursor was used. Several methods of preparation are described as follows:

(1). Direct deposition of Ru atop a Pt gauze. The vapor phase deposition of ruthenocene (bis-cyclopentadienyl Ru) atop the Pt gauze was studied at 450K in flowing H_2. The deposition temperature of 450X was found to be optimum. At temperatures in excess of 450K, the deposition of ruthenocene occured non-selectively on the quartz wool, the pyrex tube and on the Pt wire gauze. At temperatures below 450K, reduction of the ruthenocene precursor did not occur on the Pt surface and the ruthenocene was preferentially deposited downstream of the Pt gauze. The results of the Ru deposition in a H_2 flow for periods of one and six hours at 450K were followed using electron microprobe analysis (EPMA). Subsequent analysis of the surface layer using x-ray photoelectric spectroscopy (XPS) showed strong surface enrichment in Ru. A subsequent heat treatment at 600 and 900K for three (3) hours showed the reappearance of the Pt(4f) band together with a concomittant decrease in the intensity of the Ru(3p) band. The corresponding EPMA spectra, confirmed that the Ru was not lost by evaporation. It is apparent that this heat treatment results in the diffusion of surface Ru atoms into the bulk according to the reaction,

$$Ru_{(s)} + Pt_{(b)} \rightarrow Ru_{(b)} + Pt_{(s)}$$

(2) The stepwise impregnaiton of Pt/SiO_2. An attempt was made to prepare Pt-Ru/SiO_2 bimetalic particles by the deposition of ruthenocene atop a Pt/SiO_2 catalyst by a procedure which was identical to that used in the preparation of the Ru/Pt gauze. Unfortunately, this method did not result in the formation of Pt-Ru bimetallic particles. Only Pt and very large Ru particles were formed.

The formation of supported Pt-Ru/SiO_2 particles was easily accomplished using a stepwise impregnation technique. In this method, a Pt/SiO_2 catalyst was prepared by the impregnation of SiO_2 with $H_2PtCl_6 \cdot 6H_2O$ followed by drying at room temperature and reduction in H_2 at 600K. The Pt metal loading of this catalyst was 0.3 mmoles/g (5.8% by wt.). The resulting Pt/SiO_2 catalyst was then impregnated with either a benzene solution of ruthenocene or an aqueous solution of $RuCl_3.3H_2O$. Following drying at room temperature, the ruthenocene was slowly decomposed in flowing H_2. In this procedure, the temperature was increased in flowing H_2 from room temperature to 453K (x 2k/min.). It was subsequently reduced at 600K for three (3) hours followed by evacuation at 600K for 0.5 hour. When the catalysts were prepared by the sequential impregnation of Pt/SiO_2 with ruthenocene, more than 90% of the Ru was retained on the surface of the Pt/SiO_2.

The results of the surface composition measurements performed using the O_2-CO titration method are shown in Table 2 as a function of Ru metal loading.

Table 2.

Structure of $Ru-Pt/SiO_2$ catalysts prepared by the sequential impregnation of Pt/SiO_2 with $Ru(cp)_2$

Amount of $Ru(cp)_2$ (m.mole/g)	Dispersion (%)	Surface Comp.(1) Ru/Pt (% / %)	Number of Surface Atoms Ru/Pt (μ mol/g)	Number of Metal Particles $10^{16}/g-SiO_2$
0.00[illegible]	30.3	0/100	0/58.8	9.59
0.115	27.3	7.8/92.2	13.9/[illegible]	9.42
0.174	26.1	31.6/68.4	34.9/75.6	9.56
0.227	26.7	39.6/60.4	77.6/52.3	9.75
0.227 (750K)	26.4	19.4/80.6	27.0/112	11.9
0.227 (900K)	26.7	23.6/76.4	33.2/107	23.3

(1) Measured using the O_2-CO titration method as in ref. (2).

The total metal dispersion, the number of surface atoms in mmoles.g and the total number of metal particles are also show in Table 2. As the metal loading was increased, the total number of Pt surface atoms was observed to decrease (column 4, Table 2). However, the total number of metal particles remained constant to within the experimental error of the measurements. This observation suggested that the Ru did not form separate particles but that the bimetallic particles were formed as the result of surface migration of the ruthenocene to a Pt particle where its ligand was rapidly reduced by the presence of H_2 chemisorbed on the surface of Pt. This is, therefore, consistent with a proposed bimetallic assisted reduction process.

The bimetallic catalyst, which had a Ru metal loading corresponding to 0.227 mmoles of Ru/g of catalyst (2.3 wt % Ru), was heat treated in flowing H_2 at 750K and 900K for three (3) hours. The total number of surface Pt atoms decreased (column 4, Table 1). However, the total number of metal particles remained roughly constant (column 5, Table 1). The corresponding surface composition showed a sharp drop in Ru (column 3, Table 1). The observation that the total number of particles remains constant, as a result of this heat treatment, strongly suggests that the surface-bulk phase compositional changes are occuring within each particle and not as the result of the formation of separate Ru and Pt particles.

The structures of the bimetallic catalysts prepared by the sequential impregnation of Pt/SiO_2 with an aqueous solution of $RuCl_3.3H_2O$ are shown in Table 3.

Table 3

Structure of $Ru-Pt/SiO_2$ catalysts prepared by the sequential impregnation of Pt/SiO_2 with $RuCl_3$

Amount of $RuCl_3$ (m.mol/g)	Dispersion (%)	Surface Comp.(1) Ru/Pt (% / %)	Number of Surface Atoms Ru/Pt (μ mol/g)
0	30.0	0/100	0/90.0
0.0[illegible]	24.5	2.9/97.1	2.9/97.3
0.135	24.0	4.0/96.0	4.2/101
0.240	18.9	11.2/88.8	12.1/[illegible]

(1) Measured using the O_2-CO titration method as in ref. (2).

The number of Pt surface atoms remained roughly constant (column 4, Table 3) while the number of Ru surface atoms increased. Additionally, there was a sharp drop in metal dispersion as the Ru metal loading was increased. These results strongly suggest the simultaneous formation of large monometallic particles coupled with a smaller number of bimetallic particles. In order to verify these observations, the hydrogenolysis of propane and the hydrogenation of benzene were studied over both series of catalysts. The respective rates were compared to those obtained for a series of Pt-Ru/SiO_2 bimetallic catalysts prepared by standard coimpregnation methods and the rates obtained over a mechanical mixture consisting of Pt/SiO_2 and Ru/SiO_2.

The hydrogenation of benzene. A substantial synergistic effect in the turnover frequency for the hydrogenation of benzene was observed on both the bimetallic catalysts prepared by coimpregnation and those prepared by the sequential impregnation of Pt/SiO_2 with Ru $(cp)_2$ (Fig. 1). The maximum TOF occured over both series of bimetallic catalysts at a surface composition which corresponded to between 60 and 80% Pt. The TOF exceeded that observed over the monometallic Pt/SiO_2 and Ru/SiO_2 catalysts by nearly an order of magnitude. This synergistic effect for the hydrogenation of benzene has been observed before and has been attributed to the formation of strongly bound, dehydrogenated C_6H_x intermediates on the surface of Pt. These strongly adsorbed C_6H_x intermediates result in the poisoning of surface sites responsible for the hydrogenation of benzene. The presence of adjacent dual metal sites apparently results in a decrease in the number of strongly bound dehydrogenated C_6H_x intermediates. This leads to an increase in the reaction rate by nearly an order of magnitude. A much smaller synergistic effect was observed over the bimetallic catalysts prepared by the sequential impregnation of Pt/SiO_2 with $RuCl_3.3H_2O$ suggesting the presence of a large number or monometallic Ru/SiO_2 particles. Synergism was not observed when the hydrogenation of benzene was studied over the physical mixture.

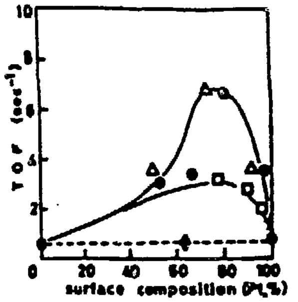

Change in the TOF of benzene hydrogenation as a function of Ru-Pt surface composition corresponding to catalysts prepared by the following methods: △, stepwise impregnation of Pt/SiO_2 using $Ru(cp)_2$; ●, co-impregnation using $H_2PtCl_6.6H_2O$ and $RuCl_3.H_2O$; □, stepwise impregnation of Pt/SiO_2 using $RuCl_3.H_2O$; ◆, mechanical mixture of Ru/SiO_2 and Pt/SiO_2. H_2/C_6H_6 = 10/1, T = 350K. Flow rate 110 ml/min.

(Fig. 1.)

Propane hydrogenolysis. The hydrogenolysis of propane was studied over the bimetallic catalysts prepared by coimpregnation using $H_2PtCl_6.6H_2O$ and $RuCl_3.3H_2O$ and those prepared by the sequential impregnation of Pt/SiO_2 with a solution of Ru $(Cp)_2$ in benzene. The results show that the TOF's as a function of surface composition are comparable over both series of catalysts (Fig. 2). The curve shows a $y=x^3$ dependence suggesting a Ru surface ensemble requirement of about 3. This is in good agreement with a previous study on propane hydrogenolysis in which the poisoning of Ru surface by chlorine was studied (7).

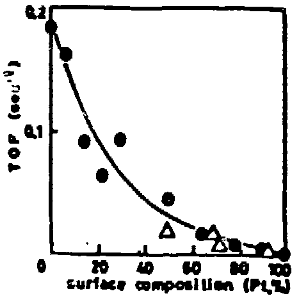

Change in the TOF of propane hydrogenolysis as a function of Ru-Pt surface composition corresponding to catalysts prepared by the following methods: △, stepwise impregnation using $Ru(cp)_2$; ●, co-impregnation using $RuCl_3.H_2O$ and $H_2PtCl_6.6H_2O$. H_2/C_3H_8 = 4/1, T = 400K, Flow rate = 50 ml/min.

Fig. 2

References

(1) Alerasool, S., Boecker, D., Rejai, B., Gonzalez, R. D., Del Angel G., Asomoza, M., and Gomez, R., Langmuir, 4, 5, 1083 (1988).

(2) Alerasool, S. E., Bradley, S., and Gonzalez, R. D., Submitted to J. Catalysis.

(3) Miura, H., Tagushi, H., Sugiyama, K., Matsuda, T., and Gonzalez, R. D., Submitted to J. Catalysis.

(4) Brunalla, J. P., Pure and Appl. Chem. 50, 1211 (1978).

(5) Miura, H., Suzubi, T., Ushikubo, Y., Sugiyama, K., Matsuda, T., and Gonzalez, R. D., J. Catal. 331 (1984).

(6) Dalla Beta, R. A., and Boudart, M., "Proceedings of 5th International Congress on Catalysis" (J. W. Hightower, Ed.), North-Holland, Amsterdam, p. 1329, (1973).

(7) Miura, H., Hondou, N., Sugiyama, K., Matsuda, T., and Gonzalez, R. D., "Proceedings of 9th International Congress on Catalysis, Calgary, 1988," Vol. 3, p. 1307, The Chemical Institute of Canada, Ottawa, 1988.

CORRELATIONS BETWEEN SURFACE STRUCTURE AND CATALYTIC ACTIVITY/SELECTIVITY

D. W. Goodman
Department of Chemistry
Texas A&M University
College Station, TX 77843

The project objective is to address those issues which are keys to understanding the relationship between surface structure and catalytic activity/selectivity. This objective also includes the understanding of the origins of the enhanced catalytic properties of mixed-metal catalysts. The experimental approach utilizes a microcatalytic reactor contiguous to a surface analysis system, an arrangement which allows in vacuo transfer of the catalyst from one chamber to the other. Surface techniques being used include Auger (AES), UV and X-ray photoemission spectroscopy (UPS and XPS), temperature programmed desorption (TPD), low energy electron diffraction (LEED), high resolution electron energy loss spectroscopy (HREELS) and fourier transform infrared spectroscopy (FTIR).

Selected examples of recent research activities are summarized below:

ETHANE HYDROGENOLYSIS AND DISSOCIATIVE ADSORPTION ON Pt-Ni BIMETALLIC SURFACES

The hydrogenolysis of ethane has been investigated as a function of nickel (a relatively active metal) coverage on a Pt(111) (a relatively inactive metal) surface. The reaction rate, as expected, increases as Ni is added to the Pt surface. The catalytic activity of a Pt(111) surface with the equivalent of a monolayer of Ni is higher than that observed on Pt(111), but lower than those reported for Ni(100) and Ni(111). An analysis of the increase in the rate of hydrogenolysis with Ni coverage suggests an ensemble requirement of two or three nickel atoms for this reaction. The dependence of the rate of ethane hydrogenolysis with respect to the partial pressures of the reactants has been analyzed using a kinetic model which involves a rate-limiting, irreversible C-C bond cleavage step. The results indicate that the hydrocarbon fragments preceding C-C bond breaking are C_2H_4 or C_2H_3 (perhaps ethylidyne) on clean Pt(111), and C_2H_2 on Pt(111) surfaces with Ni coverages of 1 monolayers.

The kinetics of the ethane decomposition reaction on Pt(111) and Ni/Pt(111) surfaces has also been measured. The dissociative sticking probabilities of ethane on a Pt(111) surface covered with a monolayer of Ni are ~20 times larger than those seen on clean Pt(111). These results show that Ni/Pt(111) surfaces are able to hydrogenate hydrocarbon fragments faster than Pt(111).

THE EFFECT OF SULFUR ON THE DISSOCIATIVE ADSORPTION SULFUR ON NICKEL

The dissociative adsorption of methane was carried out on a Ni(100) surface covered with various amounts of sulfur under the high incident flux conditions of 1 Torr methane. Auger electron spectroscopy was used to measure the rate of carbon buildup and thus to determine the initial methane decomposition rates on the surface. It was shown that the sulfur atoms poison this reaction by a simple site-blocking process. These results are consistent with the activated dissociative adsorption of methane on Ni(100) occurring via a direct adsorption process.

THE STRUCTURAL, CHEMISORPTIVE, AND CATALYTIC PROPERTIES OF ULTRA-THIN METAL OVERLAYERS ON W, Mo, Re AND Ta SINGLE CRYSTAL SURFACES

The adsorption and reaction of hydrogen, carbon monoxide and nitrogen with a number of metal overlayers on W(110), W(100), Re(0001), Ta(110) and Mo(110) surfaces has been investigated. In general only the first monolayer grows pseudomorphically, though more than one monolayer may be stable before three dimensional islands are formed. The binding strength of CO is always altered from the bulk metal, though the magnitude of the effect is seemingly more dependent on the metal overlayer than on the degree of strain induced by the substrate. The systems investigated and the change in the CO desorption peak maximum on the monolayer metal compared to the bulk metal are shown in fig. 1. The effect on CO binding energy extends primarily to only the first monolayer; subsequent layers exhibit behavior close to the bulk metal.

A noteworthy example of the dramatic altered properties of the thin overlayer material compared to the bulk metal is shown in fig. 2. The chemisorptive properties of thin-film Pd is observed to depend markedly on the environment with the CO peak desorption temperature changing from ~450K on bulk Pd to ~230K on Pd/Ta. Intermediate temperatures of CO desorption are observed for Pd on other substrates and/or other thicknesses. Thus by carefully selecting substrates and thicknesses, the possibility exists for "tuning" the properties of Pd for CO desorption and reaction.

Current and future work is being directed toward exploring the relationship among the structural, electronic and catalytic properties of these exciting thin metal film materials.

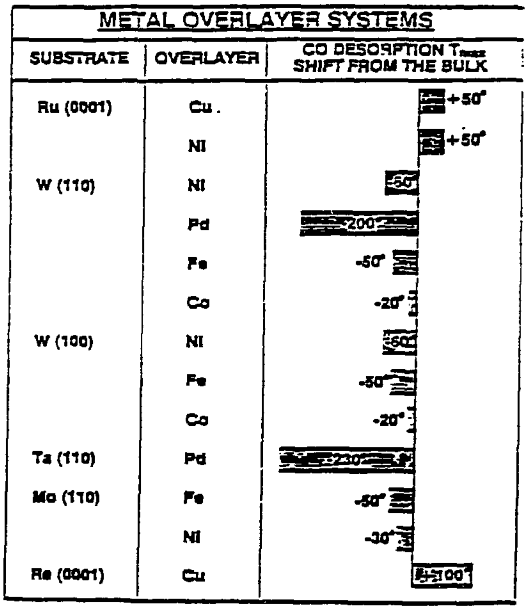

METAL OVERLAYER SYSTEMS

SUBSTRATE	OVERLAYER	CO DESORPTION T_{max} SHIFT FROM THE BULK
Ru (0001)	Cu	+50°
	Ni	+50°
W (110)	Ni	-50°
	Pd	-200°
	Fe	-50°
	Co	-20°
W (100)	Ni	-50°
	Fe	-50°
	Co	-20°
Ta (110)	Pd	-230°
Mo (110)	Fe	-50°
	Ni	-30°
Re (0001)	Cu	+100°

Fig. 1 Metal overlayer/substrate combinations and the observed temperature shift in the CO desorption peak maximum from that measured for the bulk overlayer metal.

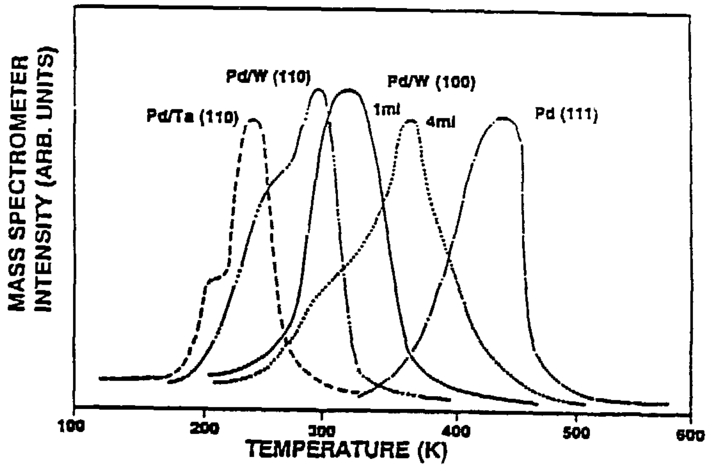

Figure 2. TPD results for CO adsorbed to saturation levels on clean Pd(111), on a 1ML Pd covered Ta(110) and W(110) surfaces, and on a 4ML Pd covered W(100) surface.

PUBLICATIONS ACKNOWLEDGING DOE-BES SUPPORT 1988-1989

"Kinetics of CO Oxidation by O_2 or NO on Rh(111) and Rh(100) Single Crystals," C. H. F. Peden, D. W. Goodman, D. S. Blair, P. J. Berlowitz, G. B. Fisher, and S. H. Oh, J. Phys. Chem., 92, 1563, (1988).

"Subsurface Hydrogen on Ru(0001): Quantification by Cu Titration," C. H. F. Peden, D. W. Goodman, J. E. Houston, and J. T. Yates, Jr., Surf. Sci., 194, 92 (1988).

"The Hydrogenolysis of Ethane, Propane, n-Butane, and Neopentane over the (111) and (110)-(1X2) Surfaces of Iridium," J. R. Engstrom, D. W. Goodman, and W. H. Weinberg, J. Amer. Chem. Soc., 110, 8305 (1988).

"The Kinetics of CO Oxidation on Single Crystal Pd, Pt, and Ir," P. J. Berlowitz, C. H. F. Peden, and D. W. Goodman, J. Phys. Chem., 92, 5213 (1988).

"The Interaction of Aluminum with the Ru(0001) Surface and Its Influence upon CO Chemisorption," C. T. Campbell and D. W. Goodman, J. Phys. Chem. 92, 2569 (1988).

"Dissociative Adsorption of Alkanes on Ni(100): Comparison with Molecular Beam Results," A. G. Sault and D. W. Goodman, J. Chem. Phys., 88, 7232 (1988).

"Subsurface Hydrogen on Ru(0001): Quantification by Cu Titration," C. H. F. Peden, D. W. Goodman, J. E. Houston, and J. T. Yates, Jr., J. Vac. Sci. Technol. A, 6, 822 (1988).

"Auger Spectra of C_2-Hydrocarbons on Ni(100)," R. R. Rye, C. M. Greenlief, D. W. Goodman, E. L. Hardegree, and J. M. White, Surface Sci., 203, 101 (1988).

"Structural and Electronic Modification of Ni, Pd, and Fe Strained Metal Overlayers on W(110) and W(100)," P. J. Berlowitz and D. W. Goodman, J. Vac. Sci. Technol. A, 634 (1988).

"Contrast between the Chemical, Structural and Electronic Properties of Thin Films of Cu and Ni on the Ru(0001) Surface," J. E. Houston, P. J. Berlowitz, J. M. White, and D. W. Goodman, J. Vac. Sci. Technol. A6, 887 (1988).

"Properties of Monolayer and Multilayer Ni Films on the Ru(0001) Surface," P. J. Berlowitz, J. W. Houston, J. M. White, and D. W. Goodman, Surface Sci., 205, 1 (1988).

"Chemisorption on Ultra-Thin Pd Layers on W(110) and W(100): Adsorption of H_2 and CO," P. J. Berlowitz and D. W. Goodman, Langmuir, 4. 1091 (1988).

"The Structural, Catalytic, Electronic, and Electrochemical Properties of Strained-Metal Overlayers," D. W. Goodman, Chapter in ACS Symposium Series, "Molecular Phenomena at Electrode Surfaces," 1988.

"Ultrahigh Vacuum and Electrochemical CO-Characterization Studies of Cu Deposition on Ru(0001)," E. M. Stuve, J. W. Rogers, Jr., D. Ingersoll, D. W. Goodman, and M. L. Thomas, Chem. Phys. Lett., 149, 557 (1988).

"Model Studies of Surface Catalyzed Reactions," A. G. Sault and D. W. Goodman, in "Molecule-Surface Interactions," Vol. LXXVI, K. Lawley, ed., Advances in Chemical Physics, (John Wiley & Sons, England, 1989).

"Adsorption and Catalysis on Silicon Modified W(110) Surfaces," A. G. Sault and D. W. Goodman, J. Phys. Chem. ***, 153 (1989).

"Nitrogen Adsorption on Re(0001) Studied by LEED, TPD, AES and ELS," J.-W. He and D. W. Goodman, Surface Sci. 218, 211 (1989)

"Butane Hydrogenolysis on Rhodium Single Crystals," B. Hegarty, A. Datye, and D. W. Goodman, J. Chem. Soc., Faraday Discuss. Chem. Soc., 87 (1989) paper 216.

"Surface Properties of Mixed-metal Catalysts," D. W. Goodman, Chapter in ACS Symposium Series, "Role of Characterization in Catalyst Development," 1989.

"The Role of Potassium Promoters in Nickel Catalysts for CO Hydrogenation," D. W. Goodman, Chapter in Alkali Adsorption on Metals and Semiconductors, Edited by H. P. Bonzel, A. M. Bradshaw, and G. Ertl, Elsevier, 1989.

"Surface Chemistry of Mixed-metal Systems," D. W. Goodman, in Metal-Metal Bonds and Clusters in Chemistry and Catalysis," Proc. IUCCP Conf., Texas A&M University, Ed. J. Fackler (Texas A&M Press, Austin, TX), 1989.

"Borazine Adsorption and Reaction on a Re(0001) Surface", J.-W. He and D.W. Goodman, Proceedings of the MRS Symposium on the Chemical Vapor Deposition of Refractory Metals and Ceramics, Eds. T. E. Besmann and B. M. Ballois, MRS Publication, Pittsburgh, PA, 1990.

"Copper Overlayers on Re(0001)," J.-W. He and D. W. Goodman, J. Phys. Chem., in press.

"The Structural and Chemisorptive Properties of Ultrathin Cobalt Overlayers on W(110) and W(100)," B. G. Johnson, P. J. Berlowitz, C. H. Bartholomew, and D. W. Goodman, Surface Sci., in press.

"The Adsorption of Hydrogen, Carbon Monoxide and Nitrogen on Cu Overlayers on Re(0001)," J. -W. He and D. W. Goodman, J. Phys. Chem., in press.

"Overlayer Growth and Chemisorptive Properties of Ultra- Thin Fe Films on W(110) and W(100)," J. -W. He, P. J. Berlowitz, and D. W. Goodman, Surface Sci., in press.

"Interaction of Borazine with a Re(0001) Surface, Studied by LEED, TDS, AES and ELS, J.-W. He and D. W. Goodman, Surface Sci., in press.

"The Effect of Sulfur on the Dissociative Adsorption of Methane on Nickel," Xudong Jiang and D. W. Goodman, Catal. Lett., in press.

"Surface Chemistry of Monolayer Metallic Films on Re(0001) and Mo(110)," J.-W. He, Wei-Lu Shea, Xudong Jiang, and D. W. Goodman, J. Vac. Sci. Technol., in press.

"Dissociative Adsorption of Alkanes on Clean and Sulfur-Modified Nickel Surfaces," Xudong Jiang and D.W. Goodman, chapter in Springer Series in Surface Science, in press.

"Surface Chemistry of Monolayer Metallic Films", D. W. Goodman, J. Ultramicroscopy, in press.

"The Reaction of Cyclopropane, Methycyclopropane and Propylene with Hydrogen over the (111) and (110)-(1x2) Surfaces of Iridium," J. R. Engstrom, D. W. Goodman, and W. H. Weinberg, J. Amer. Chem. Soc., submitted for publication.

"Reactions of Silane with W(110)," A. G. Sault and D. W. Goodman, Surface Sci., submitted for publication.

"In-Situ FT-IRAS Study of the CO Oxidation Reaction over Ru(001)," C. H. F. Peden, D. W. Goodman, and F. M. Hoffman, J. Phys. Chem., submitted for publication.

"The Role of Surface Structure in CO Hydrogenation on Cobalt," B. G. Johnson, C. H. Bartholomew, and D. W. Goodman, J. Catal., submitted for publication.

"CO Hydrogenation Kinetics on Clean Cobalt," C. H. Bartholomew, C. M. Greenlief, P. J. Berlowitz, B. G. Johnson, and D. W. Goodman, Catal. Letters, submitted for publication.

"Adsorption of CO and H_2 on Ultra-thin Films of Fe and Ni on Mo(110)," J.-W. He and D. W. Goodman, Surface Sci., submitted for publication.

"Dissociative Adsorption and Hydrogenolysis of Ethane over Clean and Ni Covered Pt(111)," Jose Rodriguez and D.W. Goodman, J. Phys. Chem., submitted for publication.

SUPPORT EFFECTS STUDIED ON MODEL SUPPORTED CATALYSTS

Raymond J. Gorte
Department of Chemical Engineering
University of Pennsylvania
Philadelphia, PA 19104

Research Objectives:

The aim of this research is to understand how an oxide support can modify the catalytic and adsorption properties of a metal or oxide catalyst.

Description of Research:

Most of our past work on how a support can modify catalytic properties has been for supported, group VIII metals. Our approach to studying this question has been to use low-surface-area, model catalysts, which allow us to use surface sensitive characterization techniques, such as Auger electron spectroscopy (AES) and x-ray photoelectron spectroscopy (XPS), to obtain the surface composition and chemical state of the catalyst. The use of model catalysts also simplifies the interpretation of temperature programmed desorption (TPD) for the characterization of adsorption properties by eliminating diffusion and readsorption effects.

The model catalysts we have used in our studies were prepared by vapor deposition of metals onto flat oxide supports. The metal coverages were measured using a quartz-crystal, film thickness monitor. By monitoring AES peak heights as a function of metal coverage, the growth modes for the metal overlayers can be obtained, which in turn gives information on how well the metal "wets" the oxide. TPD was used to measure adsorption properties and to determine saturation adsorption coverages. Metal particle sizes were calculated from dispersion as determined from saturation adsorption uptakes and metal coverages, and are checked using transmission electron microscopy (TEM) of selected samples.

CO on Pt/Al_2O_3 and Rh/Al_2O_3

Our first studies were for Pt on alumina.[1] We examined the adsorption properties and growth modes for Pt on both oxidized Al and on an α-Al_2O_3(0001) crystal. On the α-Al_2O_3 crystal, Pt formed 3-D particles during deposition, even at 150K, indicating very weak interactions between Pt and the support. While deposition at room temperature on the oxidized Al did result in 2-D overlayers, these overlayers aglomerated into particles upon heating to ~500K. For a given metal coverage, the particle size and CO adsorption properties of those particles were identical on both alumina supports, suggesting that the 2-D growth on oxidized Al was due to kinetic limitations and not to stronger interactions with the Pt.

The CO adsorption properties were found to change with particle size, but the changes appear to be due to changes in site geometry and not to electronic effects or interactions with the support. For very small particles (<2.0 nm), we observed a single desorption state in TPD at 510K, a similar desorption temperature to that reported for CO from stepped Pt crystals. As particle size increased, a second desorption state appeared at ~400K, which increased in relation to the 510-K state in a regular manner with particle size. Since the main desorption feature on Pt(111) and other crystal planes with high surface coordination also occurs at this temperature, we assign the changes in the TPD curves with particle size as being due to changes in site geometry. However, while TPD curves for H_2 from these model catalysts exhibited similar desorption features to those found with bulk metals, one cannot match the desorption peaks to any particular single crystal, suggesting that one does not have extended single crystal planes on the small particles.

To further examine our assignment of changes in TPD with particle size as being due to changes in site geometry, we examined TPD curves for CO from Rh particles on α-Al_2O_3.[2] Unlike CO desorption from Pt, CO from Rh is not strongly dependent on crystallographic orientation on single crystals. As for Pt, Rh formed 3-D particles on α-Al_2O_3 following room temperature deposition, indicating a weak interaction with the support. In agreement with the geometrical interpretation of desorption changes with particle size, TPD curves for Rh particles on α-Al_2O_3 were found to be only weakly dependent on particle size.

XPS and UPS measurements were also made of the Pt/α-Al_2O_3 samples, before and after CO adsorption.[5] Unlike previous studies, we observed no changes in either the CO features or Pt_{4f} features with particle size down to ~17Å. We concluded that observed shifts are frequently due to final-state effects and depend on the techniques used to neutralize the samples.

NO on Pt/Al_2O_3 and Rh/Al_2O_3

A more sensitive probe of crystallographic effects on both Pt and Rh is NO adsorption. For Pt in particular, the desorption temperature and fraction dissociation in TPD are strongly dependent on crystal plane. For Pt particles on α-Al_2O_3, we also observe changes in NO TPD with particle size; however, the TPD results cannot be interpreted by viewing the particles as a collection of simple single crystals.[3] On large particles (>4 nm), for which CO desorption looked similar to Pt(111), the TPD curves look similar to NO from Pt foils and stepped crystals, with more than 80% of the NO dissociating, even though NO does not dissociate on Pt(111). For very small particles (<2 nm), desorption shifted upward in temperature by ~100K and dissociation was reduced. Coadsorption of labelled ^{15}NO with CO to determine the temperatures at which dissociation occurs show that NO dissociation requires higher temperatures (~100K) on small particles. Also, unlike the results for CO adsorption, the changes in NO adsorption properties do not occur gradually with particle size, but change dramatically as the particle size decreases from 2.5 to 1.7 nm. The results of our studies imply that the sites on Pt are probably more complex than would be indicated by CO TPD and that other factors besides crystallographic effects must be important for NO adsorption.

NO adsorption on Rh was also affected by particle size and again the results could not be explained by considering the Rh particles to be a simple combination of single crystals.[4] On small particles, desorption of N_2 from NO occurred at considerably higher temperatures than are observed on any simple single crystals. A most interesting result of our studies is that we were able to use the desorption and dissociation rates to explain the observed structure sensitivity in the reduction of NO by CO, which is important in automotive catalysis. Using CO titration of the adsorbed oxygen formed by NO dissociation, we were able to show that the dissociation reaction is not strongly affected by Rh particle size. The large upward shift in the desorption temperature for N_2 formed from NO appears to be due to an increase in the desorption activation energy for N_2. Using a model of the NO-CO reaction developed for Rh(111) (S.H. Oh, G.B. Fisher, J.E. Carpenter, and D.W. Goodman, J.Catal., 100 (1986) 360.), we showed that these results satisfactorily explained the differences in the reactivity of Rh(111) and supported Rh catalysts.

Pt on ZnO and ZrO_2

More recently, we have examined Pt on oxides other than alumina to determine the effect of oxide composition.[6] On ZnO, we have examined the growth and adsorption properties of Pt on the ZnO(0001)Zn and ZnO(0001)O surfaces. These two ZnO surfaces differ by the fact that Zn^{+2} cations are present in the outermost layer on the ZnO(0001)Zn face, while only oxygen anions are present in the ZnO(0001)O surface. On both surfaces, AES showed that Pt grew in layer-by-layer manner. TEM micrographs, shown in the attached figure, agree with this. The micrographs, which were obtained on a surface with 2 monolayers of Pt, show Moire' fringes over the entire surface in the diffraction contrast images and ordered reflections in the diffraction pattern arising from the Pt overlayer and double diffraction of the Pt reflections through ZnO, implying that the Pt layers grow epitaxially. This is in contrast to the Pt/α-Al_2O_3 micrographs which indicate only 3-D particles and additional rings due to Pt in the diffraction pattern, indicating that Pt is randomly oriented.

The adsorption results for CO are significantly different on the two polar surfaces for Pt coverages below one monolayer. On the Zn-polar surface, the desorption temperature is shifted downward by ~100K from the peak temperatures on the O-polar surface. We believe our results indicate an interaction between the Pt and the Zn^{+2} ions. Also of interest in the Pt/ZnO system is that Pt migrates into the ZnO when the sample is heated above ~600K in vacuum.

For $ZrO_2(001)$, the Pt again grows in a layer-by-layer manner. Peak temperatures for CO are also shifted downward for Pt coverages below one monolayer, perhaps indicating interactions between Pt atoms and Zr^{+4} cations in surface. As we observed with ZnO, Pt migrates into the ZrO_2 surface when the layers are heated above ~600K.

Publications:

1. "A Study of Small Pt Particles on Amorphous Al_2O_3 and α-$Al_2O_3\{0001\}$ Substrates Using TPD of CO and H_2", E.I. Altman and R.J. Gorte, Journal of Catalysis 110 (1988) 191.
2. "A Comparison of the Desorption of CO from Pt and Rh Particles on α-$Al_2O_3\{0001\}$", E.I. Altman and R.J. Gorte, Surface Science 195 (1988) 392.
3. "The Adsorption of NO on Small Rh Particles on α-$Al_2O_3\{0001\}$", E.I. Altman and R.J. Gorte, Journal of Catalysis 113 (1988) 185.
4. "The Adsorption of NO on Small Pt Particles on α-$Al_2O_3\{0001\}$", E.I. Altman and R.J. Gorte, Journal of Physical Chemistry 93 (1989) 1993.
5. "A Photoelectron Spectroscopy Study of Pt Particles on α-$Al_2O_3\{0001\}$", E.I. Altman and R.J. Gorte, Surface Science 216 (1989) 386.
6. "A Comparison of Pt Overlayers on α-$Al_2O_3\{0001\}$ and $ZnO\{0001\}$ ", S. Roberts and R.J. Gorte, in preparation.

Future Research:

While we are continuing reaction studies of Pt particles on α-$Al_2O_3(0001)$ to address questions of how the changes in adsorption properties which we observe with particle size are related to reactivities, the primary emphasis in our future work will be studies of supported oxides. We have chosen to study Nb_2O_5 and WO_3 on alumina since the interaction between these oxides leads to acidic properties which can be probed by adsorption of simple bases. Initial TEM, AES, and TPD studies of niobia on α-Al_2O_3 and oxidized Al agree with literature reports that the structure of the alumina surface is important in determining the properties of the supported oxide and have demonstrated that these techniques will provide important information. On α-Al_2O_3, niobia grows layer-by-layer but transmission electron diffraction indicates that the niobia is T-Nb_2O_5, implying that interactions with the α-Al_2O_3 are weak. The niobia film is unaffected by high temperatures. TPD of 2-propanamine on either the clean or niobia-covered α-Al_2O_3 gives only a physically adsorbed feature at ~160K. On oxidized Al, the niobia layers are unstable upon heating and appear to form an aluminate at the surface. Strongly adsorbed features are observed for TPD of 2-propanamine and the desorption temperatures depend on whether the Al is oxidized by O_2 or water. Future work will be directed at determining the conditions which lead to acidic properties and at characterizing the samples prepared under those conditions.

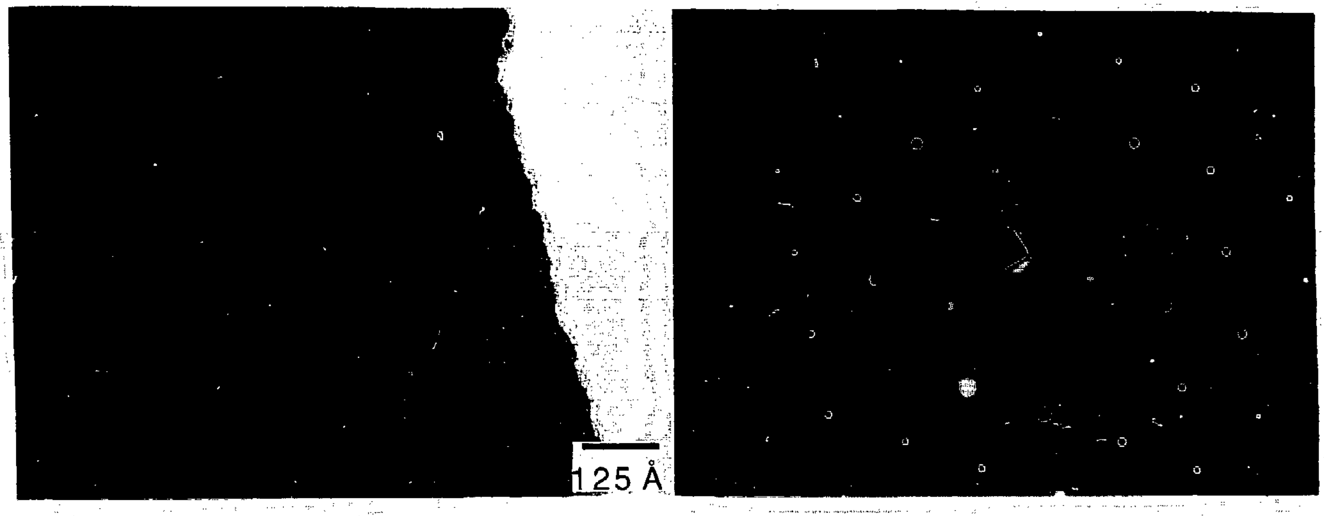

TEM results for 2×10^{15} Pt/cm^2 on α-Al_2O_3(0001). Moire' fringes, oriented randomly, can be seen on some of the particles. Diffraction shows only rings due to randomly orientied Pt particles.

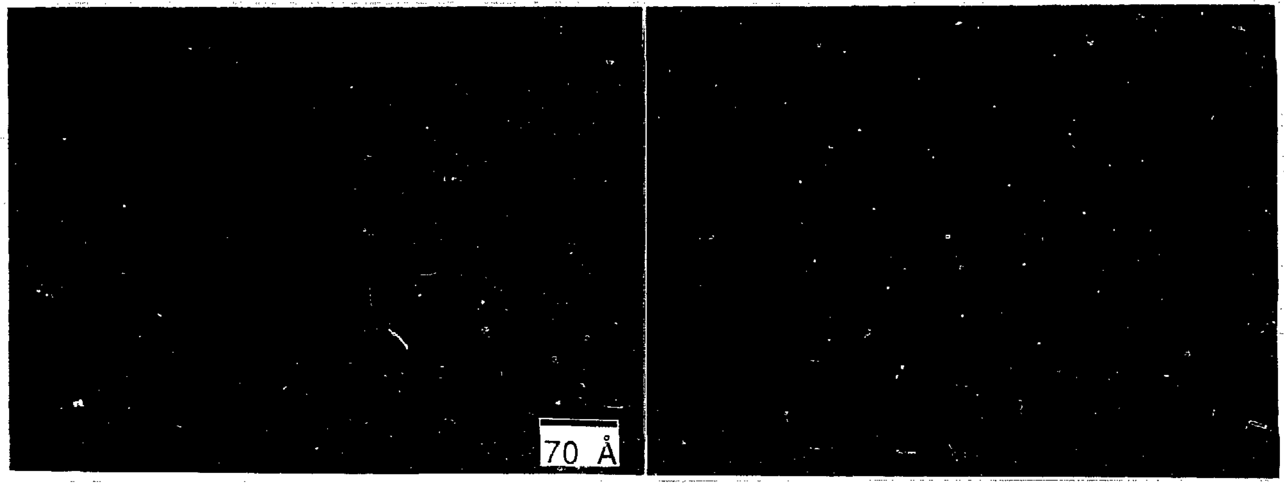

TEM results for the clean Zn(0001)Zn surface.

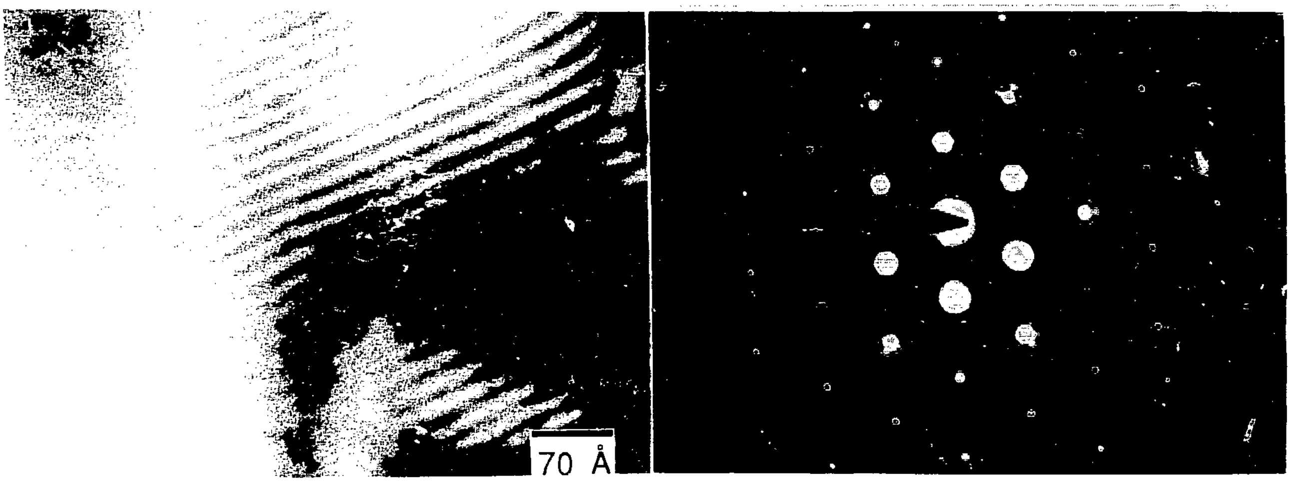

TEM for 2×10^{15} Pt/cm^2 on Zn(0001)Zn. The Moire' fringes on the contrast diffraction image and the diffraction pattern show that Pt forms an epitaxial film.

INTERACTION OF MOLECULES WITH SURFACES

E. F. Greene

Chemistry Department
Brown University
Providence, Rhode Island 02912

Scope of the Research

We use beams of atoms and molecules striking surfaces to study: the rate of transfer of electrons between a gas and a solid; the transfer of energy between gases and solids; and the rearrangements of the atoms on surfaces of crystals that occur when the temperature changes, when atoms are adsorbed, or when forces parallel to the surfaces change, e. g. as a result of bending the crystal.

Results and Plans

The rate of electron transfer is studied with the technique of surface ionization. Measurement of the energy dependence of the yields of Na^+, K^+, and Cs^+ ions formed when beams of the corresponding alkali atoms M hit a Si(111) surface and of Na^+ for Na striking a Pt surface at a temperature T are those expected for equilibrium for thermal kinetic energies of the incident atoms. Above a threshold energy of 0.5-1.0 eV the yields rise abruptly to maxima greater than 0.1 and then remain approximately constant as the energy increases to 100 eV. In this range they are nearly independent of T from 300 to 1100 K. The results are represented well by a classical model having: 1) a rate of electron transfer that varies exponentially with the distance z of M from the surface; 2) potentials that slow the incoming atom down as it nears the surface; and 3) energy transfer by elastic two-body collisions with the surface represented as hard cubes each having the mass of an integral number n of surface atoms. At z = 5 Å the rate for Na and K near a Si surface is 10 E 12.5±0.2 s^{-1} with n equal to 3 and 5 respectively while for Cs it is three times less with n equal to 20. For Na on Pt it is 10 E 12.9±0.1s^{-1} with n equal to 1. This project is being continued by trying to do the corresponding experiments with negative ions produced when atoms of high electronegativity pick up electrons on collision with surfaces having low work functions. Our first experiments are directed to I atoms and I containing molecules striking Hf and LaB_6 surfaces. Preliminary indications are that the analogous ionization does proceed as expected to form I^-.

Energy transfer to surfaces is being studied by measuring the temperature rises of thermocouple surfaces exposed to molecular beams. For example a platinum surface initially at room temperature is exposed to intense molecular beams of He, Ar, H_2, N_2, and SF_6 emerging from a nozzle also at room temperature. If the mass of the Pt is small, after a few minutes it reaches a steady temperature uniform throughout the sample. Because the rate of heat loss to the surroundings is low, a thermocouple records temperature rises that for pure gases are as much as 30 K and that for mixtures of He with Ar can exceed 100 K. Interpretation of the results shows that these rises can be understood quantitatively and thus provide information about energy transfer occurring when gaseous molecules collide with surfaces. In particular the method gives (1) a way of measuring the temperature T_s a surface attains at steady state due to interaction with gas molecules in the absence of heat conduction or radiation, (2) a simple determination of the average kinetic energy $E_i = 2k_BT_s$ of an incoming atomic beam without the need for measurement of the velocity distribution or the flux in the beam, and (3) a quantity γ that, like an energy accomodation coefficient, is a measure of the effect of the temperature of the surface on the scattering.

He diffraction is used to study structural phase transitions on the (111) and (100) surfaces of Si and Ge. The seventh-order peaks of the Si(111)-7x7 reconstructed surface observed at room temperature first decrease with increasing temperature and then disappear near 1140 K where there are also a sharp decrease in the specular intensity and an increase in the diffuse scattering. This confirms earlier evidence that the 7x7 to "1x1" phase transition at 1138 ± 7 K on Si(111) is an order-disorder one. The specular scattering of He from the Si(100)-2x1 reconstructed surface stable at room temperature shows a change in the Debye-Waller slope at 930 ± 20 K which is evidence for the existence of a surface phase transition previously deduced in this laboratory from kinetic measurements of the desorption of alkali atoms. The work is continuing with similar studies of Ge surfaces, in particular the surface phase transition near 550 K between a c(2x8) reconstruction stable at room temperature and phase for which the superlattice peaks disappear while the half-order peaks are broadened and shifted toward the specular direction.

Work is in progress to measure the effect of adsorbed atoms on the forces parallel to the surface of a crystal as they are revealed by changes in the curvature of the surface. The first experiments are being done with alkali atoms adsorbed on a Si(111) surface. As others have shown, the opposite process of producing changes in the surface by bending the crystal can be observed. There is the expectation that control of the surface forces will provide another degree of freedom in experiments on the interaction of molecules with surfaces.

Publications in 1988 and 1989 resulting from this work

1. Observations of phase transitions on the (111) and (100) surface of Si near 1000 K with He atom diffraction. J. S. Ha and E. F. Greene, J. Chem. Phys. **91**, 571 (1989).

2. Temperature rises produced by a molecular beam striking a Pt surface. E. F. Greene, T. Tao, and N. Thantu, J. Phys. Chem. **93**, 6778 (1989).

3. He diffraction study of the structural phase transition on the Ge(111) surface at 550 K. J. S. Ha and E. F. Greene, J. Chem. Phys. **91**, 000 (1989) (in press).

4. The ionization of thermal and hyperthermal beams of Na, K, and Cs on Si(111) surfaces. J. Chem. Phys. (submitted).

5. Temperature rises produced by a molecular beam striking a Pt surface. II. T. Tao and E. F. Greene (in preparation).

PROJECT SUMMARY

SOME FUNDAMENTAL ASPECTS OF ZEOLITE CATALYSIS

by

W. Keith Hall, Department of Chemistry
Chevron Science Center, University of Pittsburgh
Pittsburgh, Pennsylvania 15260

This research has been directed toward the development of understanding of catalyst acidity and its influence on activity and selectivity in acid catalyzed reactions. Two approaches have been used. The first involved spectroscopic measurements of chemisorbed species to test the ability of various preparations to form carbenium ions and other protonated bases. The second was through studies of the reactions of model compounds. The motivation was to determine whether or not any of the preparations (mainly zeolites) qualified as superacids. It had been suggested that simple aliphatic carbenium ions such as the isopropyl and the t-butyl ions could be stabilized on HY or HZSM-5 zeolites on reaction of the corresponding alcohols and/or olefins with catalyst protons. ^{13}C-MASNMR experiments (ours and others) have now shown that this was a false alarm. Such simple ions are formed as metastable intermediates and they may isomerize or desorb as olefins, making oligomerization possible. In this way surface residues containing conjugated unsaturation are formed and these may in turn form stable cations which are observable by this technique. They may also form stable alkoxides by reaction with the conjugate base of the Brönsted site. These solid state resonance techniques have also proved useful for studies of the neutral surface polymers themselves, and for the characterization of the zeolite in terms of the lattice Si/Al ratios, the coordination of the various aluminum species and the composition and nature of the "extra-lattice aluminum".

Spectroscopic studies of adsorbed H^0 and H_R indicators have led to important findings. First it was demonstrated that existing assessments of acid strength based on observations of color of the adsorbed base can be very misleading, e.g., the H_2SO_4/ZrO_2 system has been said to form superacids with $H^0 < -16$; spectroscopically we have determined it to be $H^0 \approx -12$, i.e., the value for 100% H_2SO_4. Second, H-mordenites were found to be mild superacids ($H^0 < -12.4$) whereas H-Y preparations had acidities equivalent to 95%-100% H_2SO_4, and amorphous silica-aluminas fell in the range of 75-80% H_2SO_4. Third, the catalytic activities for isobutane cracking correlated nicely with these measurements. Finally, insight was gained into how H^0 should be interpreted. This is a thermodynamic parameter defined by Hammett in a way analogous to pH. At first sight, therefore, the concepts of hydrogen ion concentration and mass action suggest themselves, i.e., that the extensive factor of the acidity is being assessed. However, this is clearly not the case. A relatively small number of indicator molecules is used to probe a much higher concentration of Brönsted sites. These search for sites with sufficient "strength" (intensive factor) to protonate them. Thus HM catalysts having smaller extensive factors nevertheless show higher acidities (intensive factors) than HY preparations. Having clarified this point, the question still remained, how should these catalyst properties affect the kinetic properties of the catalytic reaction, vide infra.

A second approach used in this work was through studies of the catalytic reactions of light paraffins. Isobutane and neopentane served as model compounds. The reaction networks of these are greatly simplified by the fact that they cannot crack by ß-scission. As in liquid superacids, C-C or the tertiary C-H bonds of isobutane were attacked by catalyst protons forming transient pentacoordinated carbonium ions which decomposed yielding CH_4, H_2 and the corresponding carbenium ions. Interestingly, superacids were not required for this chemistry over solid acids, just higher temperatures (activation energies) the weaker the acid.

The resulting carbenium ions had several options. They could decompose releasing the corresponding olefins (some of which could oligomerize with existing carbenium ions when the latter were present in sufficient concentration) or, if the lifetime was sufficient, they could be transformed into the corresponding paraffins by H^- transfer of the labile tertiary hydrogen from the parent isobutane reactant. This reaction of the primary t-butyl ions which were formed together with H_2 in the monomolecular initiation step is degenerate. However, when the t-butyl cation underwent isomerization to the sec-butyl carbenium ion, the degeneracy was removed and in many cases this was demonstrated to be the major reaction pathway because now a carbenium ion chain reaction was established.

A simple method was developed to separate the rates of the primary monomolecular initiation steps from the rates of the secondary carbenium ion reactions (mainly H^- transfer) and it was determined that the former followed first order and the latter second order kinetics in isobutane pressure. In this way comparisons could be made among catalysts of varying "acidity", and, in particular, catalysts which had been partially poisoned by NH_3 (NH_4^+) or by Na^+. These poisoning effects were found to be nonlinear, e.g., poisoning equivalent to 5% of the Brönsted sites lowered the conversion by an order of magnitude (when the reaction was run at constant temperature and flow rate) or reduced the TOF by a factor of 50 (when the conversion was maintained constant at 2.33% at constant temperature by changing the flow rate.) These results showed that either the Brönsted sites of these zeolites were not all equally active (as has been frequently postulated) or else the addition of increasing amounts of poison adversely affected (the intensive factor of) all the remaining sites in a nearly exponential manner. A theory was formulated to explain this phenomenon which stressed the importance of the conjugate anion (which is formed when a proton has been transferred from the site to a substrate molecule.) This factor has not been taken into account explicitly in establishing the H^0 function, but its importance in dealing with strong acid systems is quite evident in the superacid literature.

Neopentane may be attacked by a proton at a C-C bond to form CH_4 and the t-butylcarbenium ion, in a way analogous to isobutane. Nevertheless, these two molecules differ from each other in a very fundamental way. Neopentane has only primary C-H bonds which are not labile for H^- transfer like the tertiary hydrogen of isobutane. Consequently carbenium ion chain reactions are quenched; olefin desorption with concomitant oligomerization would appear unavoidable. Stoichiometric desorption of butenes occurred with weaker acids, but with the stronger ones the olefins were unable to escape the surface. Consequently these catalysts poisoned rapidly as a result of the formation of coke deposits which furnished the hydrogen required for release of the paraffin products. Both substrates yielded similar results in microcatalytic pulse experiments. These two model compounds, neither of which can crack by β-scission, have been found particularly valuable for defining catalytic characteristics and their relationship to properties of the surface.

A SPECTROSCOPIC AND CATALYTIC INVESTIGATION OF ACTIVE PHASE-SUPPORT INTERACTIONS

Gary L. Haller
Department of Chemical Engineering
Yale University
New Haven, Connecticut 06520

Research Scope and Objectives

Active catalytic phases (metal, mixed metals, oxide or mixed oxides) interacting with oxide support on which the active phase is dispersed can affect the percentage exposed, the morphology of metal or bimetallic particles, the degree of reducibility of cations, etc., in a variety of ways. Our objective is to characterize the physical chemistry of the active phase-oxide interaction by spectroscopic methods (primarily using the element specific spectroscopies X-ray absorption-XANES/EXAFS-and NMR) and to correlate this structure with catalytic function. An important corollary to this objective is an understanding of the interaction chemistry between the active phase precursors and the oxide supports using the same spectrscopies used to characterize the final active phase.

Description of Research Effort

In the last two years, five papers which recognize DoE support have been published. In addition, an **Adv. Catal.** review of earlier work, and research not yet published in the open literature, is summarized in one dissertation. These are listed, respectively, below. A brief description of Pt interaction with L-zeolite, an improved EXAFS analysis and Ag interaction with TiO_2 follow.

'XANES Evidence for Direct Metal-Metal Bonding and Electron Transfer in Reduced Rh/TiO_2 Catalysts', D. E. Resasco, R. S. Weber, S. Sakellson, M. McMillan and G. L. Haller, **J. Phys. Chem.**, 92, 189 (1988).

'Characterization of $RuCu/SiO_2$ Catalysts by Chemisorption, Catalysis and Spectroscopy', A. J. Hong, B. J. McHugh, L. Bonneviot, D. E. Resasco, R. S. Weber and G. L. Haller, **Proc. 9th Intern. Congr. Catalysis**, (Eds., M. J. Phillips and M. Ternan), Vol. 3, p. 1198, Chemical Instit. of Canada, 1988.

'EPR Characterization of Ti^{+3} Ions at the Metal-Support Interface in Pt/TiO_2 Catalysts', L. Bonneviot and G. L. Haller, **J. Catal.**, 113 96 (1988).

'Metal-Support Effects in Pt/L-Zeolite Catalysts', G. Larsen and G. L. Haller, **Catalysis Letters**, 3, 103 (1989).

'A ^{29}Si NMR Investigation of the Structure of Amorphous Silica-Alumina Supports', M. McMillan, J. S. Brinen, J. D. Carruthers and G. L. Haller, **Colloids and Surfaces**, 38, 133 (1989).

'Metal-Support Interaction: Group VIII Metals and Reducible Oxides', **Advances in Catalysis**, 36, 173 (1989).

'Metal-support Interaction in Silver/Titania Catalysts', Yuejin Li, Ph. D. Thesis, Yale University, 1989.

Pt Interaction with L-Zeolite

A series of Pt/L-zeolites with different cations (varying acidity) were prepared and characterized by H_2 and CO chemisorption and competitive toluene/benzene hydrogenation. The ratio of adsorption equilibrium constants for toluene/benzene was extracted from rates of competitive hydrogenation. The ratio of adsorption equilibrium constants extracted from the competitive toluene/benzene hydrogenation are consistent with a charge transfer from the alkaline earth exchanged zeolite support to the Pt particle, i.e., to the extent that this occurs, toluene is expected to compete less effectively and $K_{t/b}$ would be expected to be smaller. As we have reported [1], all of the alkaline earth exchanged L-zeolites result in smaller $K_{t/b}$ than Pt/SiO_2 (and very much smaller than on acidic Pt/Y-zeolites), where little metal-support interaction would be expected, and the Mg, Ca and Ba exchanged zeolites are ordered as might be predicted if increased ionic radius-to-charge (softer Lewis acid) implied less charge withdrawal.

An Improved EXAFS Analysis

It is essential that the selected region of the EXAFS magnitude spectrum be isolated in the sense that it contains all, or most, of the spectral intensity of the coordination region under investigation and nothing else. Because the X-ray absorption spectrum is collected discretely over finite data lengths and the fast Fourier transform algorithm is used to characterize the frequencies of the discrete signal, there is necessarily uncertainty in the spectral estimate. That is, spectral intensity at frequencies in the true continuous spectrum cannot be expressed at their corresponding frequencies in the spectral estimate, because of its descrete nature, and are dispersed among several 'false' frequencies. To introduce more frequencies in the spectral estimate at which to express spectral intensity, it is common to extend the data length, in data-space with zerosµ this practice of 'zero padding' or using the 'boxcar window' is equivalent to interpolating in transform-space, but it results in 'spectral leakage', i.e., aliased spectral intensities due to the false frequencies that have been introduced. The extent of this problem can be seen by a forward and backward Fourier transform to determine the reversibily of the operations. Because of the discontinuities between the EXAFS and the padded zeros, the boxcar window will result in only 36% of the total transform intensity under the isolated peak of the magnitude spectrum (the remaining intensity it distributed in the sidelobes of the Gibbs oscillations).

The spectral estimate can be improved by windowing the data with non-trivial functions which decrease the abruptness of the transition between data and zero padding. The essential property of the spectral window is that its effect on the data set be reversible. The effects of some spectral windows, e.g., Bartlett, Hamming, Hann, Parzen, Welch, etc., have been reported [2,3] We believe that discrete prolate spheroidal (DPS) wave functions result in more accurate spectral estimates and a fundamental improvement in the Fourier analysis of EXAFS. We have described the use of DPS wave functions as tapering windows and demonstrated their superiority on a trival example of Rh foil in a recent submission to the **J. Phys. Chem.** [4].

Ag Interaction with TiO_2

The disperson of Ag/TiO_2 was measured by hydrogen-oxygen titration at 170°C following either an oxidation pretreatment at 400°C or a reduction pretreatment at 500°C. Two Ag loadings of 1 and 10 wt% on TiO_2 were studied and these were compared to comparable catalysts using a SiO_2 support. The dispersion is always substantially greater on TiO_2 than on SiO_2 for a given pretreatment (see Table below for results on the 1 wt% catalysts), but the effect of pretreatment has the opposite effect with the two supports. Oxidation results in a pronounced increase in dispersion on SiO_2 but a very modest effect on TiO_2. Eventhough TiO_2 gives higher dispersion of Ag, this material is not very active catalytically. All catalysts supported on SiO_2 have turnover frequencies that are equivalent to unsupported Ag but the rates of CO oxidation are suppressed when Ag is supported on TiO_2 and the degree of suppression is more pronounced on the catalyst of lower loading which has a higher dispersion.

Table

Catalyst	1%Ag/TiO_2		1%Ag/SiO_2	
Pretreatment	Red*	Ox*	Red*	Ox*
Dispersion	0.41	0.35	0.051	0.22

* Ref = 500°C in situ reduction; Ox = 400°C oxidation in situ.

Using a pulsed chemisorption technique, we have been able to measure the steady-state oxygen and CO coverage at reaction temperatures. On Ag/SiO_2, oxygen coverages are high in the temperature range 60 – 140°C and they increase with temperature. On Ag/TiO_2, oxygen coverages are very low and, where they can be measured, they decrease with increasing temperature. These results can be used to rationalize both the suppression of CO oxidation activity on Ag/TiO_2 and the fact that there is a maximum in the Arrhenius plot. We attribute this oxygen adsorption suppression to the formation of a surface compound between Ag and TiO_2. The evidence for this conclusion comes from XANES and EXAFS analysis. The EXAFS of Ag/SiO_2 is essentially that of Ag metal independent of pretreatment, but the EXAFS of oxidized 1%Ag/TiO_2 is not that of Ag metal or of silver oxide. (The reduced 1%Ag/TiO_2 is a mixture of Ag metal and the new phase.) We have tenatively identified this new phase as $AgTiO_2$. This is not a known bulk phase compound and, indeed, we observe no phases other than TiO_2 (rutile) in the X-ray diffraction of oxidized 1%Ag/TiO_2, i.e., this is the reason that we refer to this as a surface compound.

Future Research

We believe that we have evidence that there is evidence for electronic interaction between Pt particles and L-zeolite support. It has been suggested by Foger [5] that such electron transfer from TiO_2 support to Pt is the origin of the greater rate of CO hydrogenation on Pt/TiO_2 as opposed to the direct interaction of CO with Ti^{3+} as postulated by Vannice [6]. We plan experiments in the future to test if Pt particles in L-zeolite also have a greater rate of CO hydrogenation relative to Pt/SiO_2. At the same time we will use XANES of Rh/TiO_2 under CO hydrogenation reaction to demonstate that the high temperature induced interaction detected by XANES [7] does not survive under reaction conditions. These experiments are intended to draw together the common properties of L-zeolite and TiO_2 interaction with noble metals and to demonstrate that the migration of reduced TiO_x is not the source of the increased activity of noble metals supported on TiO_2, i.e., that there are two kinds of interactions of noble metals with TiO_2, an electronic interaction that promotes CO hydrogenation and a geometric one which blocks the surface for all reactions.

References

[1] G. Larsen and G. L. Haller, **Catalysis Letters**, 3, 103 (1989).

[2] J. H. A. Martens, R. Prins, H. Zandbergen and D. C. Koningsberger, **J. Phys. Chem.**, 92, 1903 (1988).

[3] W. H. Press, B. P. Flannery, S. A. Teukolsky and W. T. Vetterling, 'Numerical Recipes', Press Syndicate of the University of Cambridge, New York, 1987.

[4] B. J. McHugh and G. L. Haller, 'A Method of Fourier Analysis that Results in Improved Spectral Estimates of EXAFS', **J. Phys. Chem.**, submitted.

[5] K. Foger, in 'Catalysis: Science and Technology', J. R. Anderson and M. Boudart, eds., Springer-Verlag, Berlin, 1984, vol. 6 p. 227.

[6] M. A. Vannice and C. C. Twu, **J. Catal.**, 82, 213 (1983).

[7] D. E. Resasco, R. S. Weber, S. Sakellson, M. McMillan and G. L. Haller, **J. Phys. Chem.**, 92, 189 (1988).

Surface Analyses and Modelling of Rate Multiplicity and Instabilities

Michael P. Harold and W. Curtis Conner
University of Massachusetts
Department of Chemical Engineering
Amherst, Massachusetts 01003

Overview of the Research

This research is an integrated experimental and modelling study of catalytic reactions which exhibit multiple rate phenomena and oscillatory behavior. The occurrence of a multivalued or time-dependent rate implies the existence of nonlinear interactions between the reaction sequence steps and transport processes. Most previous observations of these phenomena were carried out under conditions with external transport limitations and nonisothermalities. Confirmation that such phenomena occur in the absence of transport effects demands the development of kinetic models capable of predicting the multiplicity and oscillation features. Determining the origin(s) of an oscillatory rate requires knowledge of the degree of spatial uniformity along the catalyst surface. The ability to spatially resolve the surface composition during an oscillation and under uniform temperature conditions would help to identify the isothermal communication mechanisms.

This research confronts these issues with two different studies:

The first study couples nonlinear mathematical tools with careful kinetics experiments involving the oxidations of CO and formaldehyde on an electrically heated platinum wire. Operating regimes in which rate multiplicity exists are determined by locating the bifurcation (ignition and extinction) points. A wide range of total pressures (760 to 0.1 torr) are spanned to assess the impact of transport limitations, and to compare the kinetics over a wide range of pressure. We exploit the multiplicity in the discrimination between rival models based on the relative ability of the models to predict the kinetic trends (e.g., reaction orders, activation energies) and the multiplicity features (e.g., bifurcation map shape). Singularity theory is used as a tool in the analysis of the qualitative multiplicity features and in the estimation of kinetic parameters based on a fit of bifurcation points.

The second study involves the development of Fourier transform infrared emission spectroscopy as a new *in situ* surface probe of catalysts. Our first objective is to assess the capabilities of the emission technique by studying the infrared emission spectra of adsorbed species on different catalysts types. Our second objective is to use the emission technique under reaction conditions. A translatable flow-through cell and parabolic sampling optics permit the scanning of a catalyst surface with excellent spatial resolution (< 1 mm). The ultimate goal is to use scanning FTIR emission spectroscopy to assess the spatial features associated with kinetic instabilities.

Accomplishments

In the first study we have completed our atmospheric pressure studies of CO oxidation on an electrically heated Pt wire. The rate was determined to be a multivalued function of the CO-oxygen pressure ratio (p_{CO}/p_{O_2}) over a wide range of average wire temperatures (T_w). The T_w - p_{CO}/p_{O_2} multiplicity region (bifurcation map) is shaped as a cusp opening upwards for low p_{CO}/p_{O_2}.

We have studied the question whether the isothermal multiplicity is of an intrinsic kinetic origin, or whether it is a result of coupling between a single-valued rate and external mass transport limitations. This was accomplished by comparing the rate behavior obtained using nitrogen and helium as the diluent. Figure 1 compares the T_w - p_{CO}/p_{O_2} bifurcation maps obtained for each. The cusp-shaped region persists with He as the diluent. The existence of multiplicity with helium is evidence for intrinsically multivalued reaction kinetics since the transport rates are higher using helium. This conclusion was further strengthened as the multiplicity is also present at lower total pressures (down to 190 torr), conditions for which transport limitations are reduced. The experiment has been recently modified to study the kinetics at lower pressures (0.1 - 10 torr).

We have carried out detailed modelling and analysis of the kinetics and rate multiplicity features of Pt catalyzed CO oxidation. A few studies have demonstrated the existence of multiplicity at UHV ([1], [2]). The first step is to construct the kinetic model(s) that can predict the multiplicity features and the basic kinetic trends. Our aim is to link the UHV and atmospheric pressure kinetics of CO oxidation. One need is to explain the change in shape of the temperature - CO pressure bifurcation map (inverted to upright cusp) as the pressure is increased from UHV levels to near atmospheric.

Four different models have been investigated. The first is the three-step model (I):

(1): $CO + X \longleftrightarrow CO\text{-}X$
(2): $O_2 + 2X \longleftrightarrow 2O\text{-}X$
(3): $CO\text{-}X + O\text{-}X \longrightarrow CO_2 + 2X$

Model II consists of steps (1) - (3) in model I and includes the additional steps ((4) - (6)) involving molecularly adsorbed oxygen and Eley-Rideal reaction steps ((7) - (8)):

(4): $O_2 + X \longrightarrow O_2\text{-}X$
(5): $O_2\text{-}X + X \longrightarrow 2O\text{-}X$
(6): $2CO\text{-}X + O_2\text{-}X \longrightarrow 2CO_2 + 3X$
(7): $CO + O\text{-}X \longrightarrow CO_2 + X$
(8): $CO + O_2\text{-}X \longrightarrow CO_2 + O\text{-}X$

Model III consists of steps (1) - (6) but assumes that the adsorbed oxygen (atomic and molecular) excludes a fraction of the remaining vacant sites for additional oxygen adsorption. Model IV consists of steps (1)-(3) and has both an oxygen and CO exclusion feature.

Discrimination between models I, II, III and IV is based on the ability to predict the following experimentally determined kinetics and multiplicity features of Pt catalyzed CO oxidation:

(i) Reaction order w/r CO of 1 to 4 for the oxygen covered surface (low p_{CO}/p_{O_2}).
(ii) Reaction order w/r CO of (-1) for the CO covered surface (higher p_{CO}/p_{O_2}).
(iii) Reaction order w/r O_2 of 0 to 1 for the CO covered surface
(iv) Activation energy of about 30 kcal/mole (equal to CO binding energy) for high p_{CO}/p_{O_2}.
(v) Catalyst temperature - CO pressure bifurcation map in the form of an inverted cusp.
(vi) Oxygen pressure - CO pressure bifurcation map in the form of an upright cusp.

Our analytical and computational work resulted in the following four key conclusions:

(a) Model I cannot satisfy (ii) and (iv). It predicts a (-2) order w/r CO and activation energy twice the CO desorption activation energy in the CO inhibition regime.
(b) A reaction step involving molecular oxygen must occur in the CO inhibition regime in order to satisfy (ii) and (iv), if CO site exclusion (model IV) does not occur. Molecular oxygen adsorption (step (4)), followed by dissociation (step (5)) or reaction with adsorbed CO (step (6)) is a likely pathway.
(c) The Eley-Rideal steps (7) and (8) (model II) or the oxygen site exclusion feature (model III) are necessary to predict the first-order dependence on CO for low p_{CO}/p_{O_2}.
(d) The basic three steps (1)-(3) are necessary for multiplicity to be predicted.

Ignition-extinction phenomena that is of an intrinsic kinetic origin may be exploited for kinetic model discrimination and parameter estimation. Discrimination between models II and III was conducted by carrying out simulations of the UHV data of Sung [2]. A parameter estimation scheme was developed in which the four projections of the folds in two different three-dimensional surfaces ((T, p_{CO}, rate) and (p_{CO}, p_{O_2}, rate)), and nonsingular data points are fit simultaneously. Models II and III predict well the shape and location of the singular point projections and the basic kinetic trends.

Models II and III were then used to predict higher pressure CO oxidation behavior using the parameters estimated from the UHV data simulation. Our analyses indicate that both model II and III adequately predict the kinetics and multiplicity features of CO oxidation for all pressures between and UHV and atmospheric. For example, Figure 2 shows a plot of turnover number versus reciprocal temperature for a stoichiometric mixture of CO and oxygen at intermediate pressures. A comparison is made between the model predictions and data from experiments using a Pt(100) crystal (Berlowitz et al. [4]) and a Pt wire (Garske and Harold [5]). Very good agreement is evident. Mass transport rate processes were incorporated into the models to assess their interaction with the intrinsic rate processes. The predicted multiplicity features are consistent with atmospheric pressure data [6].

Singularity theory concepts were used to carry out a detailed analysis of the multiplicity features of a model. A scheme was developed in which parameter space is divided into different regions in which different shapes of temperature - CO pressure maps are obtained. The boundaries between the regions are loci of higher codimension singular points. This scheme enables one to bound values of kinetic parameters based on the shape of an experimental temperature - CO pressure map.

The second study involves the development of IR emission spectroscopy to monitor adsorbed species. Initially we have concentrated on evaluating the capabilities of IR emission spectroscopy using a Mattson Cygnus 100 FTIR spectrometer. The catalyst is mounted within a flowthrough IR cell on a heated block which serves to minimize temperature nonuniformities. The transmission spectroscopy capabilities of the FTIR enable us to compare the two techniques for certain samples.

The emission spectra of several different solids have been obtained, such as Mylar, ZSM-5, SiO_2, and Al_2O_3. Spectra for the latter two agree well with their absorption spectra.

We have determined that two factors are crucial for detecting adsorbed species by IR emission spectroscopy. These are the sample thickness and the background emission intensity (signal-to-noise). The former factor involves optimizing the loading of the catalyst deposited onto the heated stage. The latter factor requires that the reference system be properly designed to minimize background emission. An example emission spectra obtained for a flowing mixture of CO in nitrogen (9% CO) over a Pt/Al_2O_3 powder heated to 200 ^oC is shown in Figure 3. Bands corresponding to linear-bonded CO (2060 cm^{-1}), bridge-bonded CO (1810 cm^{-1}), and gas phase CO (2100-2300 cm^{-1}) are detected. The spectra was obtained by averaging 1000 scans at 2 cm^{-1} resolution. The catalyst loading is 2 mg/cm^2, and the spectra was obtained using pure nitrogen as the reference. Lower loadings give a poorer signal, and higher loadings result in distorted spectra due to reabsorption of radiation by the cooler surface layer not in direct contact with the heated block. The emission spectra agree very well with absorption spectra obtained using IR transmission through a 1 mm thick Pt/Al_2O_3 wafer.

Future Plans

In the first study we plan to complete our study of CO oxidation kinetics for total pressures at or below 100 torr. Three-dimensional bifurcation maps will be constructed in the space of total pressure, average wire temperature, and CO/O_2 ratio. The data over a wide pressure range should help to link the kinetics of CO oxidation at atmospheric and intermediate total pressures. We will then move on the oxidation of formaldehyde and carry out a similar set of experiments. We also plan to construct kinetic model for formaldehyde oxidation using CO oxidation models II and III as the starting point.

Since emission spectroscopy is a new technique and it has considerable potential as a tool for the study of the adsorbed state on opaque samples, our immediate goal for the second study is to obtain the emission spectra of CO and NO adsorbed on Pt/Al_2O_3 to further optimize the technique. The next step is to demonstrate the use of IR emission as an *in situ* surface probe of a catalytic reaction. CO oxidation and CO + NO on Pt/Al_2O_3 will be the probe reactions. Two key questions are (i) whether emission spectroscopy is fast enough to monitor time-dependent phenomena, and (ii) if the surface temperature can be estimated from the spectra. The excellent spatial resolution of the emission technique should enable us to address the issue of spatial uniformity during an oscillatory state.

References

1. Golchet, A., and White, J. M., J. Catal., 53, 266 (1978).
2. Sung, B. P., Sc. Dissertation, MIT (1981).
3. Herz, R., and Marin, S.P., J. Catal., 65, 281 (1980).
4. Berlowitz, P. J., Peden, C. H. F., and Goodman, D. W., J. Phys. Chem., 92, 5213 (1988).
5. Garske, M. E., and Harold, M. P., paper presented at N. A. Catalysis Meeting, Dearborn, MI (1989); ibid, Annual AIChE Meeting, San Francisco, CA (1989).
6. Kaul, D. J., Sant, R., and Wolf, E. E., Chem. Eng. Sci., 42, 1399 (1987).

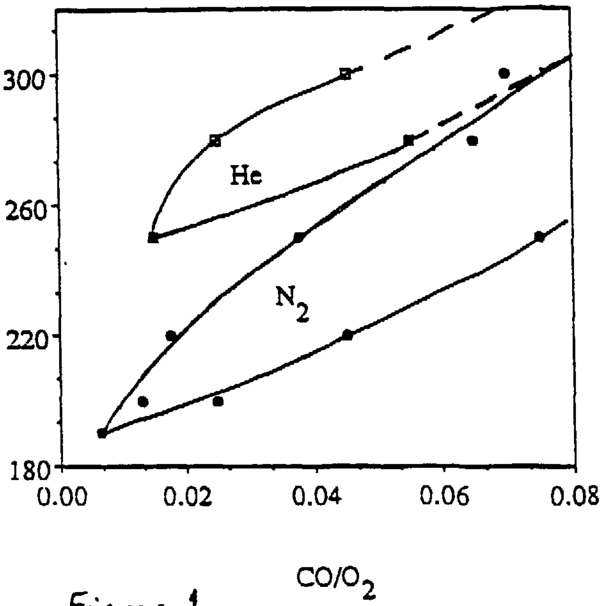

Figure 1.

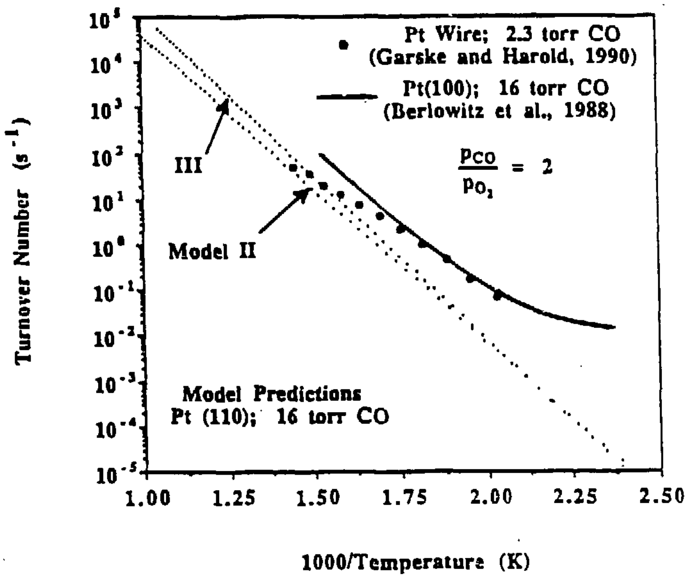

Figure 2.

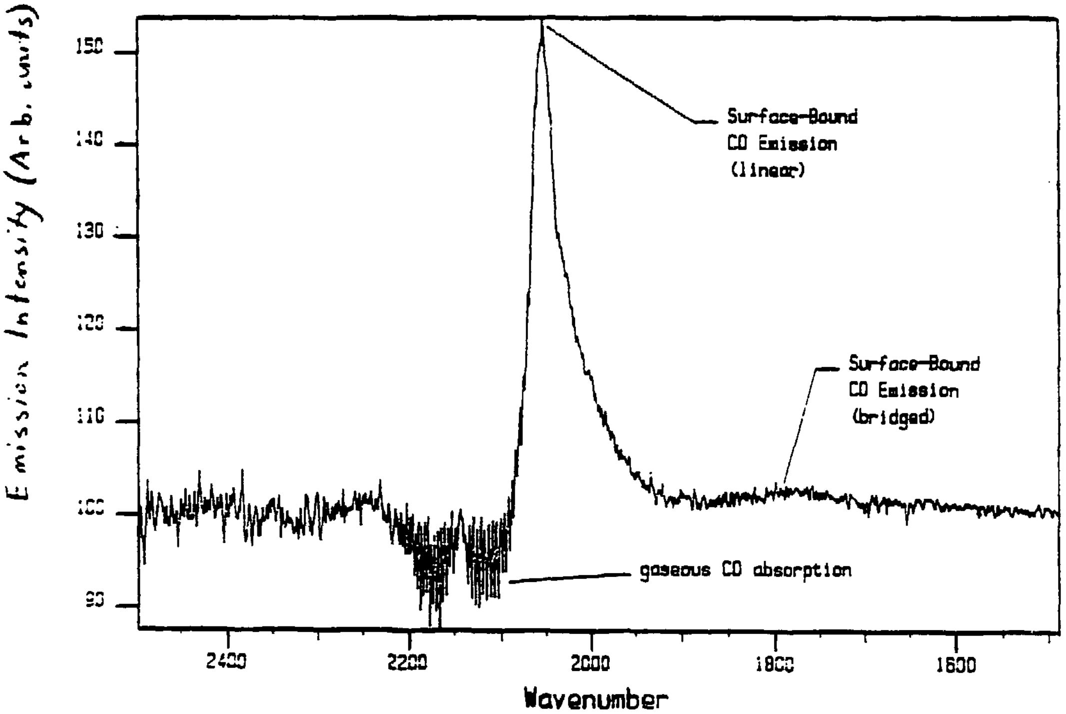

Figure 3.

Manuscripts from Research

Harold, M. P., and Garske, M. E., '*Multiple Rate States and Kinetics of CO Oxidation on Platinum: Kinetic Model Development and Multiplicity Analysis*', submitted to J. Catalysis (1989)

Harold, M. P., and Garske, M. E., '*Multiple Rate States and Kinetics of CO Oxidation on Platinum: Analysis of Experimental Data*,' submitted to J. Catalysis (1989).

OPTICAL STUDIES OF MOLECULAR ADSORBATES

JOHN C. HEMMINGER

INSTITUTE FOR SURFACE AND INTERFACE SCIENCE
AND
DEPARTMENT OF CHEMISTRY
UNIVERSITY OF CALIFORNIA
IRVINE, CALIFORNIA 92717

INTRODUCTION

This research program utilizes optical probes to study the chemistry of molecular adsorbates in monolayers and few layer thick thin films on single crystal metal substrates. While many advances have been made in the development of methods to study surfaces and surface phenomena, the determination of the molecular composition of a complex monolayer reaction mixture, or a few layer thick film on a low surface area material is still extremely difficult. It is with the development of such molecular probes of surfaces in mind that we are carrying out optical studies of molecular adsorbates. The chemistry which is of particular interest to our DOE program at present is the chemistry of strong organic oxidizing agents such as tetracyanoquinodimethane and thiophene which can be polymerized in ultra-thin films. However, the methods which we have developed are also being used to study a wide range of chemical phenomena at surfaces. The optical probes which we use fall into two broad categories: laser Raman scattering spectroscopy, and laser induced desorption coupled with Fourier transform mass spectrometry (FTMS). The optical experiments are supplemented, when necessary by electron spectroscopic probes which we have available .

RAMAN SPECTROSCOPY

The Raman spectroscopy studies involve both conventional laser Raman spectroscopy from few layer thick films as well as Raman spectroscopy enhanced by the excitation of surface plasmon polaritons (SPP) of the metal substrate. The use of Raman spectroscopy is often limited by the very low cross sections for the Raman process. Typically, this limits the applicability of Raman spectroscopy to multilayer films, high surface area solids or surfaces which exhibit unique large cross sections for Raman scattering. We have implemented an optical method which allows us to generate very large electromagnetic fields at the surface of a metal film. The generation of large electromagnetic fields at the metal/vacuum interface results in significant enhancement in the Raman scattering from molecular adsorbates. A Kretschmann geometry prism configuration which will be described in the presentation is used to couple the incident laser radiation to the surface plasmons of the metal film. If the sample (metal film plus adsorbates) can safely absorb all available incident power an enhancement factor of 1000 compared to conventional Raman scattering can be expected when SPP excitations are utilized. This is the expected situation if the sample of interest is at a metal/liquid interface. However, in the case of a metal/vacuum interface the dissipation of the incident power in the metal film may result in film damage or even evaporation. We have carried out an experimental evaluation of this situation and established a "figure of merit" for the experiments which is the ratio of the square of the electric field at the vacuum-metal interface to the power dissipated in the metal film. Under conditions which are limited by power dissipation in the metal film an enhancement in the Raman scattering intensity of a factor of 50 is still realized.

We are also utilizing conventional Raman scattering to study the electron beam induced polymerization of ultra-thin films of tetracyanoquinodimethane(TCNQ) and thiophene on Ni and Cu single crystal substrates. These films are of great materials interests as passivation films with very interesting electrical (conductivity) and optical properties. Details of the monolayer chemistry of TCNQ on Ni(111) have been determined by thermal desorption spectroscopy and x-ray photoelectron spectroscopy. Few layer thick films of TCNQ can be polymerized by electron bombardment. The polymerized films are thermally very stable and provide substantial protection against strong oxidizing environments.

LASER INDUCED DESORPTION WITH FTMS DETECTION

A pulsed laser can be used to rapidly heat the surface of a sample. Under typical conditions heating rates in excess of 10^{10} per second can be easily achieved. We have demonstrated that such high heating rates result in the direct desorption of intact molecular adsorbates. This is true even for molecular adsorbates which would completely decompose on the surface if slower heating rates are used (as in the case of conventional thermal desorption). This phenomena can be understood as a competition between competing kinetic channels (direct desorption versus surface reaction) in which the pre-exponential of the direct desorption kinetics dominates for high heating rates. If the desorbed neutral molecules can be detected and identified this method can provide a powerful way to obtain a snapshot of the molecular composition of a surface (e.g. during a reaction). We have implemented Fourier transform mass spectrometry (FTMS) to detect and identify the desorbed species in our experiments. FTMS provides many advantages in these experiments over other methods of mass spectrometry. In particular, with each laser shot a complete mass spectrum is obtained, the mass resolution is routinely high ($M/\partial M > 50,000$), and high sensitivity is easily achieved (sensitivity to less than .0001 of a monolayer has been experimentally demonstrated with high signal to noise). Since the pulsed laser used to cause molecular desorption can have a small spot size (50 micron is our routine experimental conditions) the laser spot can be moved on the sample to study either spatial variations in the **molecular** composition of a heterogeneous surface or the time dependence of a surface reaction on a homogeneous surface. This technique has been used in our lab to study the kinetics of reactions on single crystal metal surfaces. We have used this new combined technique to study the TCNQ polymers discussed above. The resulting mass spectrometry evidence provides conclusive proof of polymerization of the TCNQ by electron beam or low energy ion beam irradiation.

FUTURE DIRECTIONS

In addition to carrying forward our use of Raman scattering and laser desorption to study the particle beam induced modification of ultra-thin organic films on metal surfaces, we are planning two major new directions of work. In the Raman scattering area we are designing a new prism coupling method which will allow us to utilize SPP excitations on metal single crystals in ultra high vacuum to obtain Raman spectra of adsorbates on single crystal surfaces as opposed to evaporated films. These experiments are based on the implementation of a coupling geometry referred to in the literature as the Otto geometry in which a metal surface is held at a very well defined spacing away from a coupling prism. In the area of laser induced desorption we hope to construct a new apparatus which will utilize a superconducting magnet for the FTMS experiments. The higher magnetic field of the superconducting magnet will allow us to observe higher molecular weight species. Our present instrument is limited to the detection of species with molecular weights up to ~ 1200 amu. The superconducting magnet FTMS should allow us to detect and identify species with molecular weights above 30,000 amu while still retaining high sensitivity and high mass resolution. This will provide us with a substantial advance in our ultra-thin film polymerization studies.

REPRESENTATIVE RECENT PUBLICATIONS

1. Dipole Radiation in a Multilayer Geometry, C.E. Reed, J. Giergiel, S. Ushioda, J.C. Hemminger, Physical Review B, 36,4990(1987)
2. Surface Plasmon Polariton Enhancement of Raman Scattering in Kretschmann Geometry, J. Giergiel, C.E. Reed, S. Ushioda, J.C. Hemminger, Journal of Physical Chemistry, 92, 5357 (1988).
3. Monolayer Chemistry of Tetracyanoquinodimethane on Ni(111), J. Giergiel, J. Lindquist, S. Wells, J.C. Hemminger, Submitted to Surface Science.
4. Particle Beam Induced Modification of Tetracyanoquinodimethane Thin Films on Ni(111), S. Wells, J. Giergiel, J. Lindquist, J.C. Hemminger, Submitted to Surface Science.
5. Laser Induced Desorption/FTMS Studies of Electron Beam Polymerized Films of Tetracyanoquinodimethane on Ni(111), J. Giergiel, J.C. Hemminger. Submitted to Surface Science.

Model Catalyst Studies of Active Sites and Metal/Support Interactions on Vanadia and Vanadia-Supported Catalysts

Progress Report, December 1989

Victor E. Henrich

Applied Physics, Yale University
New Haven, Ct 06520

This program utilizes single-crystal model catalysts and a variety of surface sensitive electron spectroscopic techniques to study the nature of active sites on the surfaces of vanadias and titanias and the properties of metal catalyst atoms supported on vanadias and titania. Although problems with the installation of our new HREELS spectrometer have prevented us from pursuing one of the main experimental directions proposed in the grant, we have expanded our research program in several directions; these will be described in more detail below. Working with Dr. Tony Cox of the Inorganic Chemistry Laboratory, Oxford University, we have considered ways to adapt Dr. Cox's Fourier transform method of removing surface phonon overtones from HREELS spectra to the cases of oxides that are supporting small metal particles and of very thin oxide layers on a different oxide. The electronic structure of model TiO_2 catalyst support surfaces has been studied by means of a series of photoemission experiments conducted at the National Synchrotron Light Source, Brookhaven National Laboratory. Using tunable energy photons from the VUV storage ring, we performed resonant photoemission experiments on both stoichiometric and reduced TiO_2 (110) surfaces in order to obtain information about the hybridization of cation and anion electronic states on the surface. Initial studies of the interaction of water with both stoichiometric and defect TiO_2 surfaces using resonant photoemission were also conducted. Work on the electronic properties of vanadia surfaces concentrated on single-crystal V_2O_5, since we were recently able to obtain a sample from Bell Laboratories, and on the deposition of V atoms onto single-crystal TiO_2 supports. The V_2O_5 model catalyst work is necessary in order to understand what types of sites are the active ones in real V_2O_5 catalysts. The model supported V experiments will try to determine the interactions that take place between V, Ti and O ions in titania-supported vanadia catalysts.

1. High Resolution Electronic Energy Loss Spectroscopy (HREELS) studies of adsorption on titania and vanadia

Although HREELS experiments have not yet been performed, we have made major progress in understanding how to analyze and interpret HREELS data on oxides and the concepts involved in vibrational loss spectra. For two months this past spring, Dr. Tony Cox from the Inorganic Chemistry Laboratory, Oxford University, visited Yale. Dr. Cox is the developer of a Fourier transform deconvolution technique for removal of Fuchs-Kliewer surface phonon modes from the HREELS spectra of oxides. The presence of these strong surface phonon loss features in HREELS can severely complicate the interpretation of the vibrational spectra of adsorbed molecules on oxide surfaces, since phonon overtones (i.e., loss peaks resulting from the excitation of more than one surface phonon by the incident electron) of large amplitude appear in regions of the spectrum where vibrational frequencies such as C-C and O-H stretching modes occur. The deconvolution technique has been used successfully by several groups on spectra taken from homogeneous oxide surfaces, but it has not yet been tested on the more complex problems of interest to us: oxides that are supporting small metal particles or very thin (a few monolayers) oxide layers on a different oxide [e.g., the thin vanadia layers that are present on TiO_2 during operation of TiO_2-supported vanadium (or vanadia) catalysts]. Dr. Cox worked with us on ways to modify the basic Fourier transform procedure to treat the cases of interest. The procedures will be tested as soon as the HREELS spectrometer is yielding data.

II. Electronic interactions in Rh/TiO_2 model supported catalysts

One of the goals of this DoE grant is to better understand the surface electronic structure of model supported catalysts and its effect on chemisorption and catalysis. To this end we initiated a series of experiments during April-June, 1989, on beam line U14 of VUV storage ring at the National Synchrotron Light Source, Brookhaven National Laboratory. The tunable radiation from the storage ring was used to perform resonant photoemission experiments on both stoichiometric (i.e., fully oxidized) and reduced TiO_2 (110) surfaces. As the photon energy is increased through the 3p→3d optical transition energy for transition-metal atoms, resonances (and anti-resonances) occur in the intensity of photoemission features due to the interference between the direct photoemission process and the super-Coster-Kronig decay of the 3d state produced by excitation from the 3p level. Since no resonant optical transitions occur on the oxygen ions in this photon energy range (30-100 eV), it is possible to separate cation and anion contributions to photoemission spectra and hence obtain information about the hybridization of electronic states.

Figures 1 presents a series of UPS spectra as a function of photon energy for nearly perfect, fully oxidized TiO_2 (110); similar experiments have been performed on partially reduced TiO_2 (110) having a measurable density of O vacancy defects and associated reduced surface Ti cations. The spectra, all of which are normalized to the incident photon flux, exhibit both an overall change in intensity and relative changes in the shape of the O 2p band. The intensity of the O 2p valence band of stoichiometic TiO_2 (110), integrated above background, is plotted in Fig. 2. Similar intensity profiles are found for both the O 2p and Ti 3d bands in reduced TiO_2, and the results are similar to those that have been measured for nearly perfect Ti_2O_3 (1012) surfaces [K.E. Smith and V.E. Henrich, Solid State Commun. 68, 29 (1988)], where all of the Ti cations have a Ti^{3+} $3d^1$ electronic configuration. However, the smaller amplitude of the resonance behavior for the O 2p band seen in reduced TiO_2 suggests that there is less hybridization between the Ti 3d and O 2p orbitals on the surface of TiO_2 than there is in Ti_2O_3.

Since The O 2p - Ti 3d hybridization in titanias is predicted to involve primarily the σ O 2p orbitals, which are the ones lying at the bottom of the O 2p valence band (i.e., farthest from E_F). Therefore the intensity of emission from the σ bands should resonate more than does emission from the higher lying, non-bonding O 2p π orbitals. That this is so can be seen by plotting the ratio of the O 2p σ to π emission versus photon energy. This has been done in Fig. 3 for both the fully oxidized and the reduced TiO_2 (110) surfaces. The two curves exhibit maxima at the same photon energy (about 47 eV), but the resonance is significantly narrower for the reduced sample than for fully oxidized TiO_2 (110). The origin of this difference is not understood at the present time.

When Rh or other catalyst atoms are deposited onto oxide supports, bonding interactions should lead to changes in the hybridization between both the support cation and the catalyst atoms with the O 2p band, as well as direct cation-atom bonding. In future runs at NSLS we propose to study this effect by performing resonant photoemission experiments on Rh/TiO_2 model catalysts similar to those reported here . Such measurements provide information that is complementary to that obtained from conventional UPS and XPS measurements.

We have also used resonant photoemission in an attempt to study the interaction of water with single crystal titania supports. The sticking coefficient of water on TiO_2 is fairly low, however, and vacuum requirements placed upon the experimental chambers at NSLS limited us to a water exposure of about 10 L. Spectra for both the atomically clean and the water-exposed TiO_2 surfaces, both oxidized and reduced, were taken at photon energies just below and above resonance. Slight differences were observed in the spectra before and after water exposure, but the small amount of water that adsorbs at 10 L exposure gave changes that were too small to interpret unambiguously. The experiments will be repeated once a doser can be installed on the experimental chamber so that water exposures up to at least 10^3 L can be achieved.

III. Active sites on vanadias

One major hurdle in our program to study the properties of different V ion valence states on well characterized vanadia surfaces has been overcome with the acquisition from Bell Labs of a large single crystal of V_2O_5. V_2O_5 is one of the most important oxides for us to study since commercial vanadia catalysts often begin as V_2O_5 before being exposed to a reaction environment, where their surface V cations are reduced to lower oxidation states. The layered structure of V_2O_5 results in easy cleavage along the basal plane. Although stoichiometric V_2O_5 is fairly insulating, we have been able to obtain good Auger spectra that exhibit only slight charging. We are currently developing techniques for cleaning the V_2O_5 surface in UHV without damaging it. We will then reduce the surface by controlled amounts using ion or electron bombardment in order to produce lower valence V ions. These model surfaces will then be used in UPS, HREELS and other measurements of the interaction of various molecules with the surface V cations (and associated defect states).

We are also beginning to pursue a more complicated aspect of the properties of vanadia catalysts. Practical vanadia catalysts are often supported on a different oxide, and the strength of the V-O bond means that the V atoms will compete with the support cations for lattice oxygen. Thus complicated bonding effects can occur at vanadia-oxide interfaces in supported catalysts. We are studying the vanadia - TiO_2 interaction on model single crystals by depositing small (sub-monolayer to a few monolayers) amounts of V on $TiO_2(110)$ in UHV and following the resulting reactions using all of the spectroscopies that we have at our disposal. The experiments are straightforward, but the V-oxide interactions are expected to be much more complicated than those that occur in the Rh/TiO_2 system that we have previously studied.

Papers Presented

"Catalyst Supports and Metal/Support Interactions Studied by Electron Spectroscopies", V.E. Henrich, W.R. Grace and Co., Washington Research Center, Columbia, MD (November, 1988).

"Single Crystal Studies of Adsorption on Prefect and Defect Transition Metal Oxide Surfaces", V.E. Henrich, Symposium on Surface Science of Catalysis: Adsorption and Reaction on Oxide Surfaces, American Chemical Society, Miami Beach, FL (September, 1989).

"Resonant Photoemission in TiO_2 (110)", Z. Zhang, S.-P. Jeng and V.E. Henrich, Thirty-Sixth National Symposium, American Vacuum Society, Boston, MA (October, 1989).

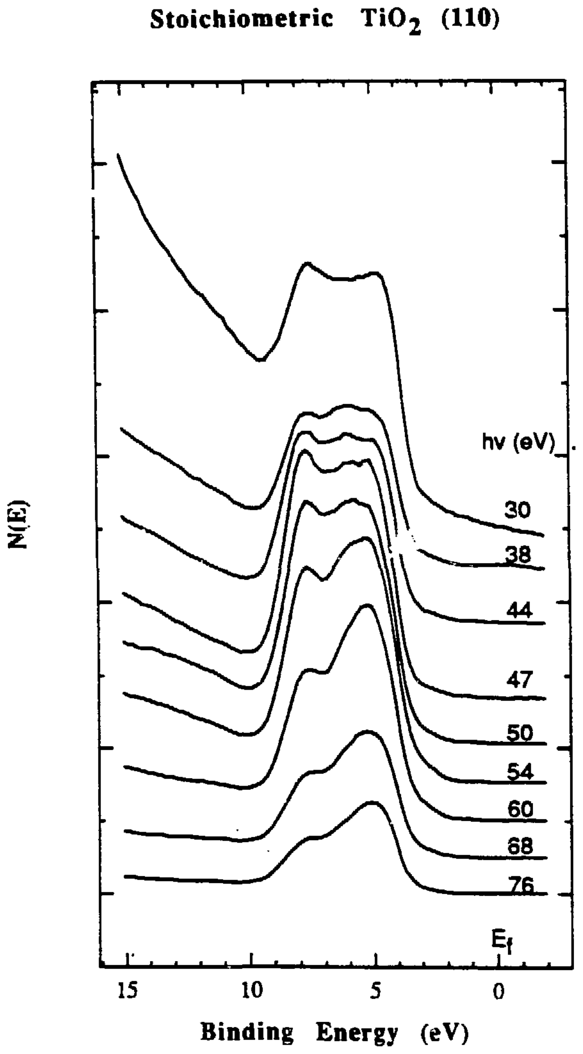

Stoichiometric TiO_2 (110)

Figure 1. UPS spectra as a function of photon energy for stoichiometric, nearly perfect $TiO_2(110)$.

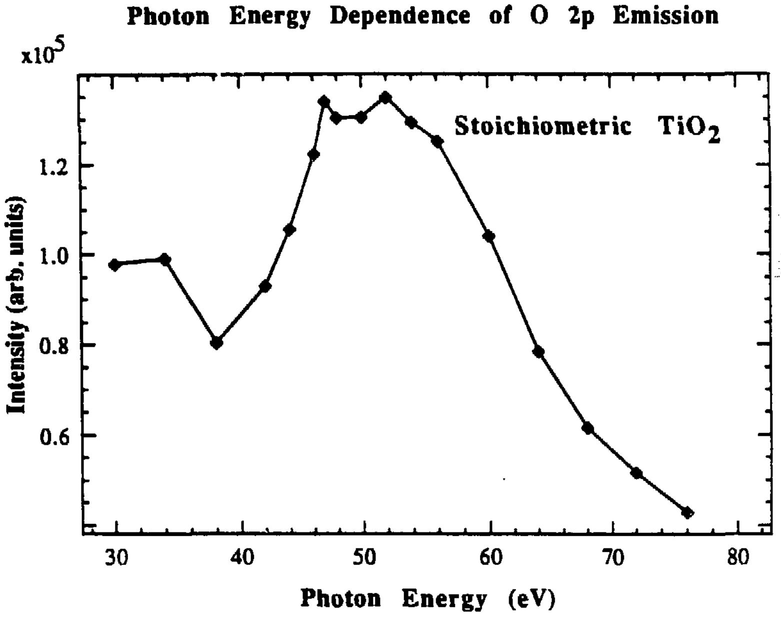

Photon Energy Dependence of O 2p Emission

Figure 2. Integrated area of the O 2p valence band emission (above background) as a function of photon energy for stoichiometric $TiO_2(110)$.

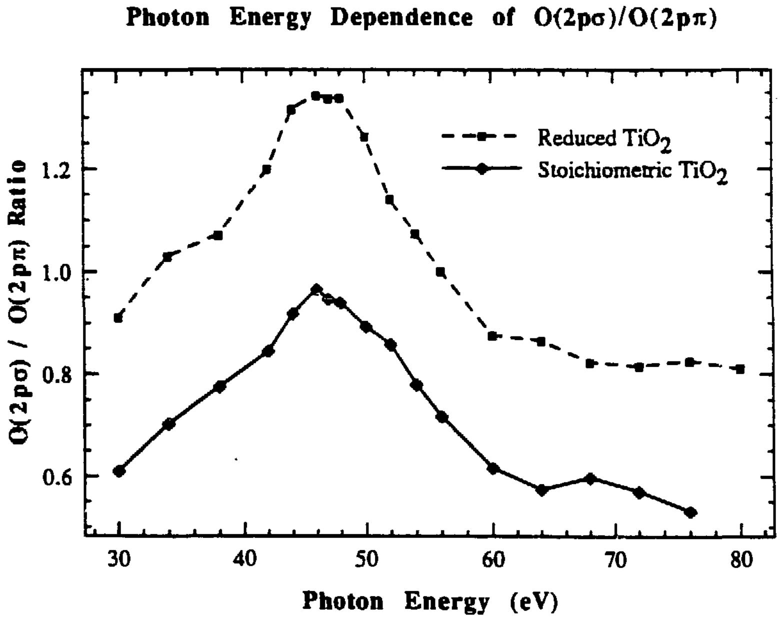

Photon Energy Dependence of O(2pσ)/O(2pπ)

Figure 3. Ratio of the amplitude of the O 2p σ to π emission as a function of photon energy for both stoichiometric and reduced $TiO_2(110)$.

Studies of Supported Hydrodesulfurization Catalysts

by

Professor David M. Hercules
Department of Chemistry
University of Pittsburgh
Pittsburgh, PA 15260

The overall objective of the proposal is to investigate the structure/activity relationship for Mo or W based hydrodesulfurization catalysts promoted by Ni or Co and supported on undoped or modified Al_2O_3 and TiO_2 surfaces. Specifically the proposed research focused on the following areas: (1) the study of the mechanism of adsorption of Mo and W oxyanions on Al_2O_3 and TiO_2, (2) Quantitative analysis of the distribution of supported Mo and W species present in the catalysts oxidic precursors, (3) the determination of the distribution of Mo (or W) oxidation states in reduced Mo (or W)/TiO_2 (or Al_2O_3) catalysts and correlation of the results with ~~the catalytic activity for various~~ probe reactions and (4) characterization of the sulfided catalysts and correlation of the Mo and W speciation with HDS activity.

Adsorption of Molybdate and Tungstate on Modified Alumina Surfaces

The nature of the interaction between Mo (or W) oxyanions and the alumina surface has been investigated by examining the effect of rinsing the catalysts (following Mo or W adsorption) with biphtalate solution. The results show that only part of the molybdate or tungstate can be removed by washing. This suggests that Mo and W adsorb on two types of surface sites producing loosely and tightly bound surface species. From the amounts of molybdate and tungstate adsorbed and from EXAFS study of the washed and unwashed Mo/Al_2O_3 catalysts, it appears that both loosely and tightly bound molybdate and tungstate are polymeric in nature.

The effect of F and Mg addition to alumina on the adsorption of Molybdate and Tungstate has been previously investigated. The ability of alumina to adsorb Mo and W from solution decreases with F addition and increases with Mg doping. This can be explained by the effects of F and Mg addition on the basic hydroxyl groups of the alumina surface believed to be the adsorption sites for molybdate and tungstate. Fluoride replaces the basic hydroxyl groups, thus decreasing the capacity of the alumina surface for Mo or W adsorption. The opposite effect is expected from Mg addition. The results derived from adsorption studies were used to interpret the effect of F and Mg on the dispersion of Mo and W catalysts prepared by incipient wetness impregnation.

Quantitative analysis of the distribution of supported species in calcined W/TiO_2 catalysts.

The distribution of W species in a series of W/TiO_2 catalysts (1.6 - 28 wt% WO_3) was determined by Raman and ESCA. The results show that three tungsten species are present on oxidic W/TiO_2 catalysts. A tungsten interaction species of uniform dispersion is formed almost exclusively for catalysts with W loadings below 10 wt% WO_3. For catalysts with W loadings above 10 wt% WO_3/TiO_2, a disordered W species and WO_3 are also present. The disordered W species and WO_3 are the only W species which increase with tungsten loading above ca. 10 wt% WO_3. The particle size of the disordered W species increases from ca. 12 Å for catalysts below 16 wt% WO_3 to ~25 Å for catalysts ≥22 wt% WO_3.

ESCA studies of the distribution of Mo oxidation states in reduced Mo/Al_2O_3 catalysts.

A systematic study of the reduction of a Mo/Al_2O_3 catalysts (8% Mo) has been conducted. The reduction conditions were varied to obtain Mo oxidation states ranging from Mo^{+6} to Mo metal. The distribution of Mo oxidation states in the reduced catalysts was determined by ESCA. The following Mo oxidation states Mo^{+6}, Mo^{+5}, Mo^{+4}, Mo^{+3}, Mo^{+2} and Mo metal were detected. The distributions of Mo oxidation states were correlated with the catalytic activity for propene and benzene hydrogenation. The results show that Mo^{+5} is not relevant for propene hydrogenation. The onset of the catalyst activity for this reaction appears to coincide Mo^{+4} formation. Benzene hydrogenation requires deeper reduction of the Mo phase (Mo^{+2}, Mo metal). This is consistent with a previous study of Mo/TiO_2 system.

Surface structure and hydrodesulfurization activity of Ti-modified Mo/Al_2O_3 catalysts.

The influence of Ti (1-14 wt%) addition on the surface structure of Mo/Al_2O_3 catalyst (8 wt% Mo) following sulfidation with thiophene/H_2 mixture has been investigated by ESCA. The results were correlated with the catalysts activity for thiophene hydrodesulfurization. Molybdenum remains highly dispersed following sulfidation in thiophene. An increase in sulfidability with increasing additive loading was observed by ESCA. The increased sulfidability can be attributed to formation of octahedral Mo-O-Ti species. The HDS activity of the titania modified Mo/Al_2O_3 catalysts increased with increasing Ti loading. The increase in HDS activity of the titania modified catalysts was correlated with formation of octahedral Mo-O-Ti species on the oxidic precursor.

FUTURE WORK

Distribution of Mo oxidation states in reduced Mo/Al_2O_3 and Mo/TiO_2 catalysts.

We have previously determined the distribution of Mo oxidation states in reduced Mo/TiO_2 catalysts. The results were compared with the catalysts activity for benzene hydrogenation. A good correlation between the catalytic activity and the abundance of Mo^{+2} was obtained. We will extend this study to other probe reactions (e.g. cyclopropane isomerization, propene metathesis, propene hydrogenation, propane hydrogenolysis). The variation of catalytic activity for a given reaction with the reduction treatment will be compared with the distribution of Mo oxidation states derived from ESCA. This will provide insight into the oxidation state of active Mo for each reaction. Similar study will be conducted on the Mo/Al_2O_3 system.

The methodology for determination of the distribution of Mo Mo oxidation states by ESCA evolved from the study of Mo catalysts supported on a "Degussa P25" TiO_2. This particular variety consists of ca. 80:20 mixture of two crystallographically different phases (Anatase (A) and Rutile (R)). One might reasonably argue that the type of the interaction of the active phase with the support will be a function of the composition of the TiO_2 carrier (Anatase/Rutile). Thus, it is of interest to determine the Mo speciation on pure Anatase or Rutile. We will also assess the effect of the type of TiO_2 used (i.e. A vs. R) on the degree of interaction of the Mo phase with the support. This study will primarily involve a comparison of the distribution of Mo oxidation states in Mo/(A) and Mo/(R) catalysts for a given reduction treatment. The comparison will be made between catalysts of equal Mo coverage (Mo atom/m^2). A special emphasis will be given to the reactivity of catalysts containing the same type of species (i.e. polymolybdate or monomer). Any difference in the reactivity of these catalysts will give insight into the effect of the type of TiO_2 support (A vs. R) on the nature of the interaction of the Mo phase with the carrier.

Study of the reduction of model catalysts.

Reduction of Mo allyl based catalysts formed by reaction of $Mo(\eta^3\text{-}C_3H_5)_4$ with Al_2O_3 or SiO_2 reportedly leads to the formation of a discrete oxidation state of Mo^{+2}. It was equally proposed in the literature that controlled oxidation of the reduced catalyst yields only Mo^{+4}. We propose to verify by ESCA the presence of discrete Mo oxidation state in the allyl based Mo/SiO_2 and Mo/Al_2O_3 catalysts. If this is confirmed the results will be compared with those obtained from conventionally prepared Mo/Al_2O_3 catalysts.

Study of the reduction of W/TiO_2 catalysts.

As stated in the Progress report we have determined from ESCA and Raman studies, the distribution of W species in a series of calcined W/TiO_2 catalysts. Additional information concerning W speciation is currently sought from EXAFS measurements. Based on the detailed structural characterization of the calcined W/TiO_2 series, we will select a catalyst containing a single W species (ex: tetrahedral W) for reduction studies. The distribution of W oxidation states will be determined according to the methodology adopted for the study of Mo/Al_2O_3 and Mo/TiO_2 systems. The results will be correlated with catalytic activity for various probe reactions.

Molecular Structure and Chemical Reactivity On Surfaces

Jan Hrbek

Department of Chemistry
Brookhaven National Laboratory
Upton, New York 11973

Research Scope. The main objective of this research program is to improve the understanding of molecular processes at the gas-solid interface. The characterization of adsorbate bonding, identification of surface intermediates and their molecular structure, and the effects of surface modifiers on the bond activation and dissociation is of fundamental importance to surface chemistry. The ultimate goal of these research activities is to control molecular interactions at surfaces with the aim of altering the activity, selectivity and poison resistance of catalysts.

Recent Results. During the past two years, our experimental work has concentrated on the interaction of alkali metals with a ruthenium surface; on their interaction with oxygen; on the reactivity of a potassium-dioxygen surface complex; on the sulfur adsorption on a Ru surface and its effect on hydrogen coadsorption; and on the adsorption of manganese on Ru and carbon monoxide coadsorption on Mn/Ru system.

As a part of our effort to understand the chemisorptive properties of bimetallic catalysts, we have studied the CO adsorption on Mn overlayers on a ruthenium single crystal surface. Based on photoemission, infrared and isotopic exchange experiments the following mechanism of CO adsorption was proposed: CO is adsorbed in molecular form and probably incorporated in the Mn lattice. Weakened C-O bond breaks in the course of heating and recombinates before the onset of desorption. The desorbing CO molecules are scrambled with an unusually high mole fraction of 0.5.

Sulfur adsorbs on a Ru(001) surface in a sequence of ordered structures depending on coverage and temperature. Hydrogen and sulfur are competing for the same surface sites and hydrogen adsorbs only on surfaces with S coverage lower than 1/3. Two weakly bound hydrogen states were observed on the S covered Ru(001) surface and we proposed that their origin is hydrogen adsorbed on three-fold hollows within the p(2x2)-S unit cell. Each S adatoms blocks four hydrogen adsorption sites in this surface structure. At higher S coverages, where the islands of $(\sqrt{3}\times\sqrt{3})$-R30° structure are formed, the H adsorption is completely blocked. The low binding energy of hydrogen is caused by the long-range electronic effect of S adatoms and possibly by the repulsive interaction among coadsorbates.

In a layer-resolved spectroscopic study of potassium adsorbed on Ru(001) we have demonstrated the application of the equivalent core level approximation to the experimental results of photoemission and thermal desorption spectroscopies. The first three layers of potassium adsorbed on Ru(001) surface have distinct spectroscopic properties that can be observed in both thermal desorption and photoemission results. Three doublets of the $K_{3/2,1/2}$ core level arising from the interface, bulk and surface layers have been correlated with the measured adsorption heats.

The interpretation of binding energy shifts of adsorbed potassium based on a Born-Haber cycle has yielded reasonable agreement between measured and calculated data. Similar conclusions have been drawn for Li, Na and Cs ovelayers.

Oxygen reacts with the K multilayer to form a potassium-dioxygen complex in which both peroxide and superoxide ions were indentified. The comparison of valence band photoemission spectra of condensed and chemisorbed molecular oxygen with our results shows that the triply-peaked valence feature at intermediate oxygen exposure can be attributed to the $[\pi_u(2p)]$, $[\pi_g(2p)]$ and $[\sigma_g(2p)]$ molecular orbitals of the peroxide ion. At saturation oxygen exposure the binding energy shifts and the $[\sigma_g(2p)]$ splitting show the formation of the superoxide ion. The assignment of the O 2p-derived valence band peaks was confirmed by a near edge x-ray-absorption fine-structure study.

It is known that one of the active forms of the potassium promoter in catalytic reactions is potassium-oxygen compound. We have therefore studied the interaction of CO with the K-O surface complex. Although CO adsorbs readily on the K-O modified surface, only subtle changes are seen in the photoemission spectra. Thermal desorption spectra from CO coadsorbed on K-O modified surface show the quantitative conversion of CO into CO_2, which desorbs from the surface simultaneously with K at rather high temperature (>800 K). Isotopic exchange experiments proved that there is a new reaction mechanism responsible for CO oxidation. Carbon monoxide is either dissociatively chemisorbed and CO_2 is formed by the recombination of dioxygen and carbon, or alternatively, a carbonate intermediate can be formed by interaction between coadsorbed CO and dioxygen. Further work is planned to resolve this question.

Publications

J. Hrbek,J. Vac Sci. & Technol. A5, 864-865 (1987)

J. Hrbek, T. K. Sham and M.-L. Shek, Surface Sci. 191, L772-L778 (1987)

T. K. Sham and J. Hrbek, J. Chem. Phys. 89, 1188-1194 (1988)

J. Hrbek, Surface Sci. 205, 408-418 (1988)

G.-Q. Xu and J. A. Hrbek, Catalysis Lett. 2, 35-42 (1989)

J. Hrbek, G.-Q. Xu, T. K. Sham and M.-L. Shek, J. Vac. Sci. Technol. A7, 2013-2015 (1989)

T. K. Sham, M.-L. Shek, G. Q. Xu, and J. Hrbek, J. Vac. Sci. Technol. A7, 2191-2193 (1989)

T. K. Sham, G.-Q. Xu, J. Hrbek and M.-L. Shek, Surface Sci. 210, 185-192 (1989)

J. Hrbek, M.-L. Shek, T. K. Sham and G.-Q. Xu, J. Chem. Phys. 91, 5786-5792 (1989)

J. Hrbek, J. Phys. Chem., accepted

M.-L. Shek, J. Hrbek, T. K. Sham and G.-Q. Xu, Phys. Rev. B, accepted

Future Plans

Our plans for the near future include the extension of the studies of modification of transition metal surfaces by eletropositive and electronegative adsorbates. These experiments will involve the alkaline earth metals. We will also investigate the properties of bimetallic catalysts and transition metal clusters prepared by chemical vapor deposition on metal and oxide surfaces under UHV conditions.

Heterogenous Catalysis Related to Energy Systems

D.R.Huntley, M.O.Krause, D.R.Mullins and S.H.Overbury
Chemistry Division
Oak Ridge National Laboratory
Oak Ridge, TN 37831-6201

Research Scope and Objectives

The general objective of this project is to study fundamentals of surface reactivity by examining atomic and molecular interactions at well characterized surfaces. The emphasis is on elucidation of mechanistic details of reactions, especially hydrodesulfurization, at metal and modified metal surfaces. The adsorption, decomposition, reaction and desorption of organosulfur compounds are studied on single crystal surfaces by a variety of surface analytical techniques, including various electron spectroscopies, isotope incorporation, and temperature programmed reactions. Structure is probed through the use of low energy alkali ion scattering to analyze atomic structure of clean surfaces, the effects of adsorbates on substrate structure and the bonding sites of adatoms. A long term goal is understanding the relation between structure and reactivity.

Description of Research Effort

An ultra-high vacuum system with capabilities for Auger electron spectroscopy, x-ray photoelectron spectroscopy (XPS), temperature programmed desorption (TPD) and high resolution electron energy loss spectroscopy (HREELS) has been used to study the reactions of H_2S and CH_3SH on clean and modified Ni(110). It has been found that adsorbed hydrogen sulfide decomposes on Ni(110) at 110 K to form primarily surface S and H for coverages of less than 0.5 monolayers (ML). The hydrogen evolves in two separate TPD peaks, characteristic of hydrogen recombination and desorption from the clean surface and from regions perturbed by chemisorbed sulfur. XPS and HREELS indicate the presence of intact S-H bonds at 110 K for high coverages. However, all of the molecular species decompose prior to hydrogen desorption. Physisorbed H_2S is observed on the surface for coverages greater than about 0.5 ML. The sulfur Auger lineshape was found to be a sensitive indicator of perturbations in local bonding interactions between the S and the Ni surface; perhaps involving some change in either bonding sites or distances but not involving S-H bond scission.

The presence of oxygen on Ni(110) was found to alter the decomposition pathways of H_2S. For high coverages of oxygen predosed on Ni(110) it was found that H_2S reacts by direct transfer of sulfhydryl H to O to form H_2O at 110 K. Formation by this mechanism is indicated by XPS and HREELS at 110 K, the desorption of H_2O, and by isotope labeling experiments in which the surface is pre-covered with D before adsorbing H_2S. Although at high coverages of oxygen and H_2S the reaction by this mechanism to form water is quantitative, the mechanism of the reaction differs at lower oxygen and H_2S coverages.

A similar approach was used to study the reaction of methanethiol on Ni(110). The major products of the reaction are is methane and hydrogen. The coverage dependence of the methane yield indicates a competition between decomposition and methane formation with decomposition dominating at low coverage and methane formation dominating at high coverages. Evidence from HREELS, XPS, and deuterium incorporation indicate that methyl thiolate is a stable surface species below 200 K which presumably is hydrogenolyzed to form methane. The presence of surface oxygen results in water formation, and the presence of either atomic O or S enhances the formation of methane relative to decomposition.

Recently a project has been initiated using synchrotron based techniques as an additional means of studying molecular adsorption. An experimental apparatus has been recently completed which will be transportable between ORNL and synchrotron light sources. The ultra-high vacuum chamber contains an electron energy analyzer to allow photoelectron spectroscopy either using a synchrotron source or laboratory UV and x-ray sources. AES and TPD will allow further characterization. A separate electron detection system is positioned to measure near edge x-ray adsorption fine structure (NEXAFS) when resident at a synchrotron.

Experiments with this equipment are in progress to further study the reaction of organosulfur compounds on Ru(0001). Initially the adsorption and decomposition of hydrogen sulfide, methanethiol, benzenethiol and thiophene on Ru(0001) and clean and modified Ni(110) will be studied at temperatures from 100 K to above the temperature required for complete desorption or decomposition. At an upcoming synchrotron run it is planned to use NEXAFS at the S 2p edge, as well as photoemission to study the stages of decomposition of the organosulfur molecules and to identify intermediates. In collaboration with Fred Grimm of the University of Tennessee, MSX-α calculations of molecules on small metal clusters are in progress for use as a theoretical model to aid in interpretation of NEXAFS results.

Within this group there has been an ongoing program to use synchrotron radiation to study the atomic spectroscopy of open shell atoms. A specialized chamber and electron spectrometer has allowed measurements of photoionization cross sections and asymmetry parameters (the β parameter) as a function of photon energy. The technique has been applied to free metal atoms such as Mn, Ga, Cd and Be. In both Mn and Be it was demonstrated that prominent features in the spectra of metals, alloys and compounds, are due to atomic type resonances. Recently a microwave discharge source for producing atomic oxygen atoms has been developed and used to study the electron spectroscopy of this reactive open shell atom. The technique will be extended to study free halogen atoms.

A continuing effort within this group has been the application of low energy alkali ion scattering as a technique to analyze surface structure. Recently, the emphasis has been the study of ultra-thin metal overlayers on single crystal metal surfaces and on single crystal alloy surfaces. For example, initial stages of growth of Cu on W(100) have been studied. Incident polar and azimuthal angular scans of the Cu and W single-scattering intensity were obtained as a function of Cu coverage and annealing temperature, and were used to evaluate various models for the surface structure. Dosing submonolayer amounts of Cu near room temperature results in two-dimensional islands of Cu bonded in fourfold hollows and some dispersed Cu atoms. Annealing at 1000 K causes irreversible displacement of first-layer W atoms and Cu incorporation. This result is interesting in view of the immiscibility of Cu and W. Analysis of contour plots of the Li^+/Cu single scattering support a growth of up to two pseudomorphic layers of Cu on W(001), although there is Cu and W mixing at the interface. Deposition of Ni overlayers has also been studied and found to behave identically to Cu in nearly every respect.

Beside metal overlayers on the open W(001) surface, recent work has included metal overlayers on close packed surfaces, in particular Sn/Pt(111) and Cu/Ru(0001). These systems were chosen for study because of recent interest in the chemisorption and catalytic reactivity of these surfaces. Although complete analysis of the results is not yet complete, it is found in the case of Sn/Pt(111), that the incident angle dependence of the ion scattering intensity from the substrate is largely unaffected by the presence of the Sn except for a uniform decrease in intensity at all angles. This result is indicative of overlayer growth in a pseudomorphic manner with adatoms at three-fold hollow sites. Differences in the Sn single scattering brought about by annealing indicate rearrangements in which Sn overlayer atoms either form islands or incorporate into the Pt surface.

In addition to studies of these bimetallic interfaces, surfaces of bulk NiAl alloy have been studied to determine the relation between surface structure and composition in a strongly ordered alloy system. To this end, the (110) and (100) faces and a stepped (111) surface of this alloy have been examined. It is found that the surface composition of the (111) and (110) surfaces are determined by the bulk termination, suggesting that the strong tendency for ordering prevails in the surface region. By contrast, the (100) surface preferentially terminated on Al planes but with high concentration of Ni anti-site defects and vacancies in the first layer. In agreement with previous LEED results, relaxation of the first-second layer spacing occurs for (111) and (110) surfaces but the magnitude depends upon whether the first layer atom is Ni or Al.

Future Research

Our major thrust will continue to be the study of molecular adsorption and reactions on various metal surfaces. One approach will be to study the reaction of molecules with dual functionality such as benzenethiol and $HO-(CH_2)_n-SH$ to examine intra-molecular competition for surface bonding sites. It is expected that adsorption of such molecules will be dependent not only upon temperature and coverage but also upon surface structure. Therefore, it is planned to study adsorption on other crystal faces of Ni and also on Ni overlayers deposited upon W substrates. The effect of adsorbate molecules on the structure of the substrate, especially for metal overlayer systems will be studied. Other metals of interest for their ability to catalyze hydrodesulfurization reactions will also be studied, in particular Ru. A detailed understanding will be sought by applying a combination of structural analysis by ion scattering of substrate and bonding site geometry and by analysis of reaction stages and identification of intermediates by HREELS, NEXAFS, photoemission and TPD.

Publications

D. R. Mullins and S. H. Overbury, "The structure of the carburized W(001) surface," Surface Sci., 193, (1988), 455.

D. R. Mullins and S. H. Overbury, "The structure and composition of the NiAl(110) and NiAl(100) surfaces," Surface Science 199, (1988), 141.

D. R. Mullins and S. H. Overbury, "The structure of oxygen on W(001) by low energy ion scattering," Surf. Sci. 210, (1989), 481.

D. R. Mullins and S. H. Overbury, "Adsorption of oxygen on carbon-covered W(001)," Surf. Sci. 210, (1989), 501.

S. H. Overbury and D. R. Mullins, "Interaction of Cu overlayers with W(001) studies on low energy alkali ion scattering," J. Vac. Sci. Technol. A7, (1989), 1942.

D. R. Huntley, "Adsorption and reactions of methanethiol on clean and modified Ni(110)," J. Phys. Chem. 93, (1989), 6156.

J. Jimenez-Mier, C. D. Caldwell and M. O. Krause, "Autoionizing resonances 4d→nl in cadmium," Phys. Rev. B 39, (1989), 95.

C. D. Caldwell, M. O. Krause, and J. Jimenez-Mier, "Photoionization of gallium at 3d→4p and 4s→np ($n=5,6$) resonances," , Phys. Rev. B 37, (1988), 2408.

M. O. Krause and C. D. Caldwell, "Strong correlation and alignment near the Be 1s photoionization threshold" Phys. Rev. Lett. 59, (1987), 2736

B. Hermsmeier, C. S. Fadley, M. O. Krause, J. Jimenez-Mier, P. Gerard and S. T. Manson, "Direct evidence from gas-phase atomic spectra for an unscreened intra-atomic origin of outer-core multiplet splittings in solid manganese compounds," Phys. Rev. Lett. 61, (1988), 2592.

Theory of the Dissociation Dynamics of Small Molecules on Metal Surfaces: Finite Temperature Studies

Bret E. Jackson
Department of Chemistry
University of Massachusetts
Amherst, MA 01003

Research Scope and Objectives

Our goal is to understand the detailed dynamics of molecule-metal interactions, particularly dissociative adsorption. The work is theoretical and makes use of recently developed time dependent quantum scattering techniques. Much of our effort has focused on introducing the effects of finite surface temperature into these calculations. Specific problems to be addressed are:

1. How does the dissociative sticking probability of a diatomic on a metal surface depend upon the translational and internal energy of the molecule, as well as the angle and site of impact? How is the dissociation rate influenced by various aspects of the molecule-metal interaction potential?

2. Nearly all quantum mechanical calculations of gas-surface scattering ignore surface temperature. That is, the lattice atoms are fixed and the colliding molecule is not allowed to exchange energy with the vibrations of the metal. We wish to develop ways of introducing lattice motion and energy exchange into these theories, while keeping the calculations tractable. It is preferable to treat the lattice vibrations (phonons) quantum mechanically.

3. Given the developments in 2 above, what are the effects of surface temperature on dissociative adsorption ? We wish to know how dissociative sticking probabilities vary with the gas-phonon coupling and the properties of the metal's surface and bulk vibrations.

4. We are also interested in non-reactive systems. They tell us a great deal about gas-metal interactions, and a vast amount of data is available. In particular we want to understand how the sticking probability of atoms and diatoms depends upon particle mass, temperature, beam energy, and the form of the interaction potential. The temperature dependence of rotationally and translationally inelastic scattering is also of interest.

Recent Results

1. In our initial project we implemented the first quantum mechanical study of H_2 dissociation on a metal surface[1]. The atop-to-bridge-site dissociation of H_2 and D_2 on Ni(100) was examined using a simple two-dimensional model. The two degrees of freedom were z, the translation of the molecule perpendicular to the surface, and r, the vibrational/dissociative coordinate. The molecular wave function $\Psi(r,z;t)$ was represented by its values at a fixed set of points on a 2D grid in r and z. The wave function was then evolved in time using the Schrödinger Equation and allowed to both scatter from and dissociate on the metal surface. The dissociation probability was computed as a function of beam kinetic energy. The influence of barriers to adsorption, dissociation, and surface mobility were examined. The molecular mass was varied, and recently observed isotope effects were explained in terms of the mass dependence of the vibrational zero point energy. Classical trajectories were also run on these potentials, in order to compare with the quantum results, and to identify sources of error in the classical calculations.

2. Methods have been devised for extending these time dependent scattering theories to finite temperature. That is, the surface and bulk vibrations of the solid are coupled to, and allowed to exchange energy with, the scattering molecule. Both the molecule and the solid vibrations are treated quantum mechanically, using a variational approach. The result is that the molecular wave function evolves on a gas-surface potential that is both time and temperature dependent. Such a potential is easily dealt with using our time dependent methods.

Our first formulation was a single-phonon theory, adequate for light molecules such as He and H_2. Probabilities for energy transfer were computed for He and Ne beams scattered from Cu and Ni[2,3]. Excellent agreement with experiment was found for the thermal attenuation of the elastic peak of He scattered from Cu(100)[3]. The rotationally inelastic diffraction of H_2, HD, and D_2 was also studied[4]. Rotational excitation, energy transfer, and diffraction peak heights were examined as a function of surface temperature.

A multiphonon theory capable of describing the strong gas-phonon interactions experienced by heavier particles was developed and tested. The method uses a trial wave function containing n-phonon states to all orders. Probabilities for energy transfer were computed for He, Ne, and Ar scattered from a Cu(100) surface[5]. A semiclassical form of this theory was also derived, using a Gaussian wave packet as the molecular part of the wave function[6]. The same He, Ne, and Ar systems were examined. Reasonable agreement with experiment was found for the temperature dependence of Ar trapping on Ir(110), and the scattered beam energy of Ar on Ni(115).

3. Recent efforts have been spent developing better models for dissociative adsorption. Like our earlier 2D model, the quantum variables are represented by a wave function defined on a fixed set of grid points. Various ways of including rotations and translational motion parallel to the surface are being examined. A full cartesian representation of ro-vibrational motion was used to describe H_2-metal scattering[7]. The effect of bond length distortion (due to chemisorption effects near the surface) on rotational excitation was computed. We have had success with a mixed quantum-classical approach to dissociative adsorption. The bond length (r), the center of mass distance above the surface (z), and the polar orientation angle (θ) are treated in a fully quantum fashion. These "strong" degrees of freedom dominate the energetics of the problem and are fully coupled together. The azimuthal orientation (ϕ) and the molecular position over the unit cell (x,y) are treated semiclassically. Early results for H_2 and D_2 on Cu(100) indicate that inclusion of rotational motion lowers the dissociation probability and modifies its dependence upon beam kinetic energy. One reason is that many molecules are unfavorably oriented for dissociation. Also, rotational degrees of freedom compete with the vibration/dissociation coordinate for energy from the translational coordinates.

Future Plans

1. Our plans for the immediate future are to further develop the mixed quantum-classical model described above. Ideally we would like to treat r, z, θ, and ϕ quantum mechanically. This allows us to properly quantize the rotational motion. Various grid methods which use spherical and/or cartesian coordinate systems will be explored. The variables x and y will probably remain semiclassical.

2. We will then use our single or multiphonon techniques to include temperature in these studies. At this point we will finally be able to make a full and proper comparison with experiment. Experimental systems of interest include H_2 and D_2 on Ni and Cu, N_2 on W, and O_2 on Pt. The dissociation probability, as well as the interaction between translational, rotational, vibrational/dissociative, and phonon degrees of freedom will be studied as a function of beam energy, surface temperature, and angle and site of impact. Various model potentials will be examined.

3. An improved description of trapping has recently been formulated. We hope to implement and test this some time soon, and examine the sticking of atoms and diatoms on metals as a function of beam energy and temperature. This study should help us to understand the competition which often exists between precursor trapping and direct dissociation on surfaces.

References

1. Chao-Ming Chiang and Bret Jackson, "Quantum and Classical Studies of the Dissociation Dynamics of H_2 and its Isotopes on Ni," J. Chem. Phys. 87, 5497 (1987).

2. Bret Jackson, "Time Dependent Quantum Mechanical Theory of Gas-Surface Energy Transfer," J. Chem. Phys. 88, 1383 (1988).

3. Bret Jackson, "Mean Field Approach to Molecule-Surface Scattering at Finite Temperature: One-Phonon Theory," J. Chem. Phys. 89, 2473 (1988).

4. Astrid J. Cruz and Bret Jackson, "A Finite Temperature Theory of Rotationally Inelastic Diffraction: H_2, HD, and D_2 on Cu(100)," J. Chem. Phys. 91, 4985 (1989).

5. Bret Jackson, "Mean Field Approach to Molecule-Surface Scattering at Finite Temperature: Multiphonon Theory," J. Chem. Phys. 90, 140 (1989).

6. Bret Jackson, "A Semiclassical Study of Gas-Solid Energy Transfer: He, Ne and Ar on Metal Surfaces," J. Chem Phys. (accepted; to appear Jan 15, 1990).

7. Bret Jackson, "A Spectral Grid Study of Ro-vibrational Coupling in H_2- Metal Scattering," J. Phys. Chem. 93, 7699 (1989).

Dynamics of Desorption from Surfaces

Kenneth C. Janda

Department of Chemistry
University of Pittsburgh
Pittsburgh, PA 15260

The goal of our DOE sponsored research is to apply the types of laser techniques that have been very effective for characterizing gas phase chemical dynamics to problems associated with molecules interacting with surfaces. Although the dynamics of molecules interacting with surfaces are obviously much more complicated than those of small molecules interacting in the gas phase, we try to choose systems for which the degrees of freedom are separable enough that the concept of motion on a potential energy surface is useful. By measuring product state distributions of the desorption reactions, we will try to specify effective potentials that govern the molecular dynamics. In this respect our goals are quite similar to those of the Zare group at Stanford, the Auerbach group at IBM, the Cavanagh group at NIST and the Cowin group at the University of California at Santa Barbara (among others).

One specific example of the fruitation of this line of research is provided by a collaboration between the IBM group and Andrew DePristo at Iowa State University. Auerbach and colleagues found that the probability of sticking of N_2 on a tungsten(110) surface scales with the total kinetic energy of the incident N_2 rather than with the projection of the incident momentum perpendicular to the surface.[1] Using molecular dynamics modeling DePristo was able to show that this effect is due to a fairly specific coupling of the rotational and translational degrees of freedom as the molecules approach the surface.[2] A second example is from the NIST group which has shown that the mechanism for photodesorption of NO from Pt surfaces involves hot electron quenching at the surface.[3] These, and other projects, have shown that the study of dynamics at surfaces is going to be a very rich field with many interesting effects to be understood. Still, the amount of data available for gas-surface dynamics is much less than for gas phase dynamics, and many more systems need to be studied before the process of obtaining a general picture of gas-surface dynamics can be seriously discussed. Although our work is still in the preliminary stages, we feel that we have identified two dynamical problems that will significantly enhance the scope of this field. Each of the two problems which we have chosen to study was chosen because it seemed to offer a relatively simple example of a gas surface interaction that might be useful as a model problem. In each case, it appears that the dynamics will be more complex than might have originally been apparent. Specifically, we have studied the recombinative desorption of H_2 from the Si(100) surface, and the desorption of CO from a potassium promoted Ni(111) surface.

A. Recombination Desorption of H_2 from Si(100)

H_2 bonding to Si surfaces was chosen as a likely candidate for study because the bonding would be expected to be highly directional in comparison to that of many admolecules on metal surfaces. It seems likely that the anisotropy in the potential for desorbing molecules would have a pronounced effect on the desorption dynamics. Before studying the dynamics of recombinative desorption, we decided to study the overall kinetics of the reaction. The laser induced thermal desorption technique, LITD, developed by George and Hall,[5] was employed. To our surprise, the rate was found to scale with the first power of the hydrogen atom coverage on the surface. Another surprise was that the activation energy for the reaction is only 45 kcal/mole, less than the expected reaction enthalpy. Figures 1 and 2 show some of the kinetic data and an Arrhenius plot for these studies.

In an attempt to explain these results, we have proposed that the rate limiting step for the reaction is excitation of an H atom from a bonding site to a delocalized state at 45 kcal/mol excitation energy. The desorption reaction takes place when an atom in the delocalized state reacts with a second atom still in a bonding site. For the kinetics to agree with the data, it must also be assumed that relaxation from the delocalized excitation state into a bonding site is extremely slow.

In support of this new mechanism, the following experiments were performed. The surface was first exposed to D atoms, some of which became attached to bonding sites. Next, the surface was exposed to H atoms while the surface temperature was maintained below that necessary to desorb D_2 molecules. It was found that while some H atoms settled into bonding sites, others reacted with D atoms and removed them from the surface. This phenomenology, which can be described as a generalized Eley-Rideal mechanism, is consistent with our proposed mechanism.

A complete description of these results has been submitted for publication.[5] The new mechanism suggests many follow up experiments. Dynamics studies of H_2 desorption and H atom sticking would be especially interesting because our results show that the kinetics is governed by nonequilibrium processes. This suggests that desorption product state distributions will be quite different from those expected of "statistical" phenomena.

B. CO Isotope Mixing on K promoted Ni(111)

It is well known that carbon monoxide bonds molecularly to Ni(111) so that when a surface is exposed to a mixture of isotopes at low temperature and then heated, the CO desorbes at ~ 420 K with no isotope mixing. A partial overlayer of potassium, however, has dramatic effects on the surface chemistry. If a potassium "promoted" (>0.2 K coverage) Ni surface is exposed to a mixture of CO isotopes, desorption proceeds at 620 K with complete isotope mixing. There have been a variety of mechanisms proposed to explain these phenomena. They range from complete decomposition of the CO to the formation of a $K_x(CO)_y$ complex[6] to molecular adsorption with isotope mixing occurring via a concerted desorption mechanism at high temperature.[7] Traditional methods for looking at isotope mixing cannot clearly reveal the surface temperature dependence of the process because the spectra of the isotopes are not resolvable under the relevant conditions. We are studying this problem by monitoring the desoprtion kinetics and dynamics as a function of surface coverage and temperature.

So far, we have applied the LITD technique to study the degree of isotope mixing on the surface as a function of surface temperature during a linear heating ramp. We know that the laser desorption process itself does not lead to isotope mixing because when $^{13}C^{16}O$ and $^{12}C^{18}O$ are dosed onto a K promoted Ni surface, the surface is heated to 400 K and a laser pulse is used to desorb the CO, the desorption takes place with no production of $^{13}C^{18}O$. Starting at 450 K, $^{13}C^{18}O$ is observed. This shows that LITD can be used to monitor the onset of isotopic mixing. Figure 3 shows an example of our results on the extent of $^{13}C^{18}O$ production as a function of surface temperature. Work is in progress to measure the kinetics of isotope mixing as a function of surface temperature. Upon completion of that work, laser multiphoton ionization spectroscopy will be used to study the desorption dynamics of CO from this and other surfaces.

References

1. H. E. Pfnur, C. T. Rettner, J. Lee, R. J. Madix and D. J. Auerbach, J. Chem. Phys. 85, 7452 (1986).
2. A. Kara and A. E. DePristo, J. Chem. Phys. 88, 2033 (1988).
3. S. A. Buntin, L. J. Richter, D. S. King and R. R. Cavanagh, J. Chem. Phys. 91, 6429 (1989).
4. S. M. George, A. M. DeSantolo and R. B. Hall, Surface Science 159, L425 (1985).
5. K. Sinniah, M. G. Sherman, L. Lewis, W. H. Weinberg, J. T. Yates, Jr. and K. C. Janda, J. Chem. Phys. Submitted for publication.
6. K. J. Uram, L. Ng and J. T. Yates, Jr., Surface Science 177, 253 (1986).
7. D. Lackey, M. Surman, S. Jacobs, D. Grider and D. A. King, Surface Science 152/153, 513 (1985).
8. J. Arias, J. Lee, J. Dunaway, R. M. Martin and H. Metiu, Surface Science 159, L433 (1985).

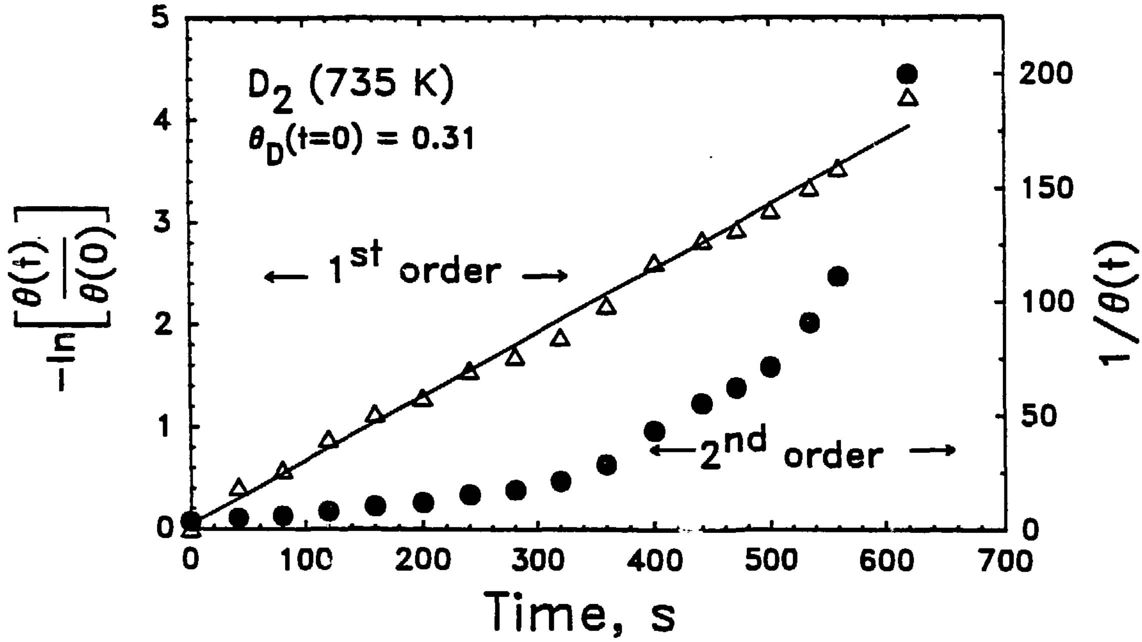

Figure 1. Comparison of first- and second-order kinetics of D_2 desorption from Si(100) using the LITD method at 735 K. The linear fit demonstrates that the desorption reaction is first-order in θ_D.

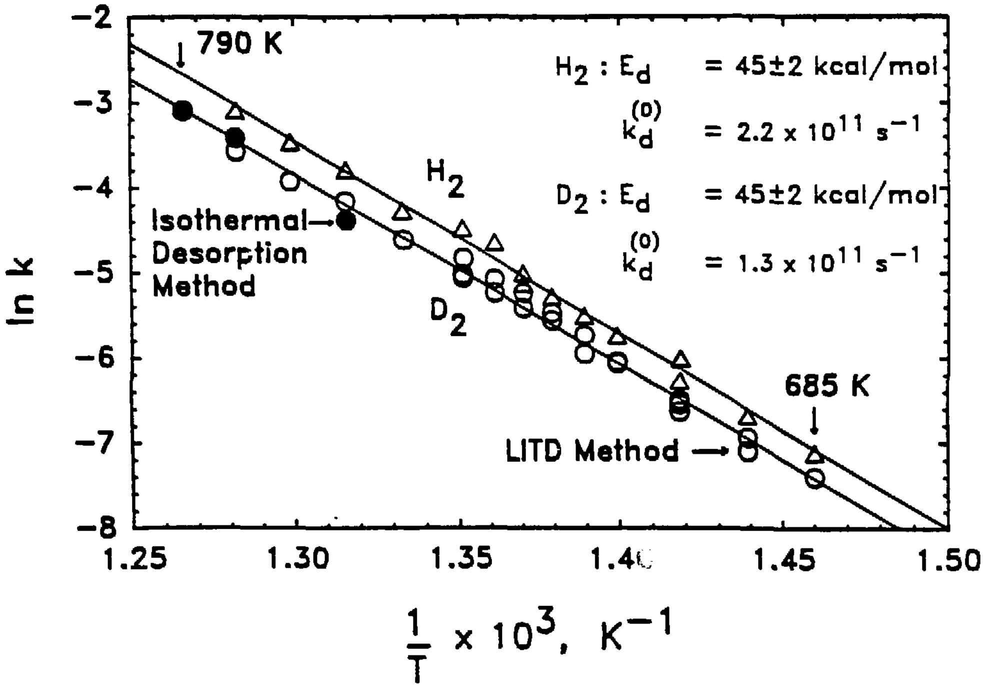

Figure 2. Arrhenius plots for the desorption of H_2 (open triangles) and D_2 (open circles for LITD data, closed circles for isothermal desorption data) from Si(100). The implied activation energies and pre-exponential factors of the desorption rate coefficients are 45±2 kcal/mol and 1.3 x 10^{11} s^{-1} for D_2.

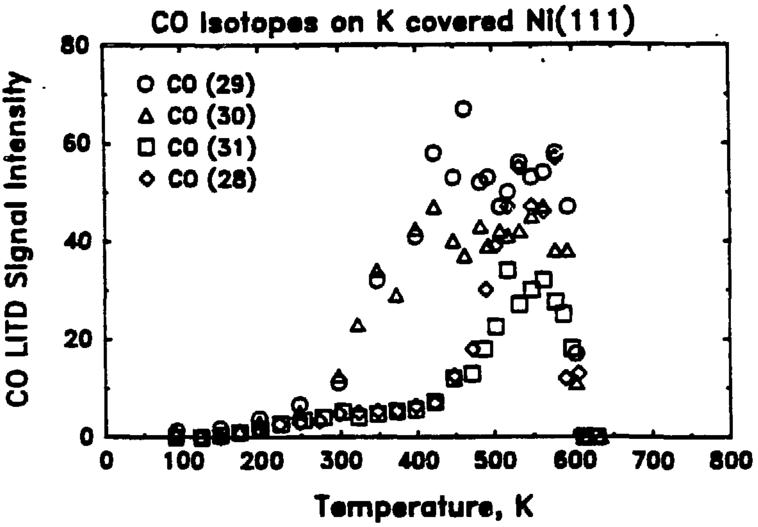

Figure 3. LITD signals for $^{13}C^{16}O$, $^{12}C^{18}O$ and $^{13}C^{18}O$ as a function of surface temperature during a linear heating ramp. At the start of the experiment, the K promoted Ni(111) surface had been dosed with equal amounts of $^{13}C^{16}O$ and $^{12}C^{18}O$. Below 450 K, all observed $^{13}C^{18}O$ is due to isotopic impurities in the initial sample. From 450 K to 800 K the fraction of $^{13}C^{18}O$ increases dramatically, indicating the onset of isotopic mixing. (The $^{12}C^{16}O$ signals are also shown for completeness.)

Terry S. King
Ames Laboratory
Iowa State University

Scope

The focus of this investigation is on the relationship between the chemical and structural properties of highly dispersed, supported transition metal catalysts and their catalytic behavior. The goal of these investigations into the nature and behavior of supported bimetallic catalysts is to answer a number of specific, fundamental questions regarding the interactions between constituent metals and how these interactions give rise to catalytic behavior quite different from that of pure metal catalysts. For example, for a given bimetallic catalyst is the catalytic behavior for a specific reaction dominated by geometric (ensemble size) or electronic effects? To what extent is the metal crystallite morphology a factor in the catalytic processes and how is this modified by combining metals? What is the mode of interaction of molecules adsorbed on these catalysts and how does it change with relative composition of metals? What role does the "metallic character" of the catalyst particle play and how does it vary with metal composition and particle size? The key to answering these questions is determining the properties of the catalyst surface and nature of species adsorbed on the surface. The combination of solid state NMR investigations and catalytic activity/selectivity studies is central to the method of approach to the above questions.

Recent Results

We have pursued three experimental projects over the past two years that are directed toward fulfilling the research objectives outlined above. These experimental projects are: ^{1}H NMR of hydrogen adsorbed on supported metal catalysts, ^{13}C NMR of hydrocarbon molecules (mostly ethylene) adsorbed on the same catalysts, and model reaction studies over series of bimetallic catalysts. In addition to investigating hydrogen chemisorption, proton NMR is used in combination with volumetric selective chemisorption procedures to characterize the catalyst's surface properties, particularly the bimetallic surface composition.

^{1}H NMR of Hydrogen Chemisorbed on Silica-Supported Ru, Ru Bimetallic, and Cu Catalysts [1-3]

On Ru/SiO_2 catalysts strongly and weakly (reversible at room temperature) chemisorbed hydrogen is clearly observed by NMR. The weakly adsorbed hydrogen is composed of hydrogen atoms on the metal and hydrogen atoms that spill over to the silica support interacting with bridging oxygens atoms (Si ^{O} Si). The ratio of weakly to strongly chemisorbed hydrogen increases with increasing metal dispersion. The weakly adsorbed hydrogen also exchanges slowly with silanol hydrogen atoms (Si-OH). The standard volumetric technique (selective hydrogen chemisorption) accurately measures only the strongly adsorbed hydrogen. When using selective hydrogen chemisorption to measure the weakly adsorbed species, errors occur due to the inability to distinguish hydrogen adsorbed on metals from hydrogen adsorbed on supports. Co-adsorption of chlorine inhibits hydrogen adsorption and reduces the ratio of strongly to weakly adsorbed hydrogen. Also, we see hydrogen chemisorption on pure Cu/SiO_2 catalysts which is somewhat surprising considering the reported 5 kcal/mol activation energy for dissociative adsorption on copper surfaces. When atomic hydrogen is directly available to the copper, such as when ruthenium is present in the Ru-Cu/SiO_2 bimetallic catalyst, the copper surface quickly becomes saturated with weakly and strongly adsorbed atomic hydrogen. The hydrogen exchanges quickly between copper sites and ruthenium sites. It is this exchange that allows us to determine the relative surface composition for the metal particles in this particular catalyst. The spillover of hydrogen from ruthenium to the second metal does not occur when silver or gold is combined with ruthenium. However, the ratio of weakly-to-strongly adsorbed hydrogen is reduced.

^{13}C NMR of Ethylene Adsorbed on Silica-Supported Ru, Ru-Cu, Cu, and Pt Catalysts [4-7]

A variety of experimental nuclear spin dynamics on ^{13}C, including standard cross-polarization (CP), CP with magic angle spinning (CP/MAS), CP/MAS with dipolar dephasing, and single pulse experiments with and without proton decoupling have been applied to the study of adsorption and reaction of ethylene at relatively high pressures on silica-supported ruthenium (37% dispersion). The amount of ethylene introduced to the samples was about 3 molecules for every surface ruthenium atom. NMR of ^{13}C using CP/MAS allowed us to simultaneously observe the transformations of chemisorbed and weakly adsorbed molecules during reaction of ethylene to form products. Direct ^{13}C excitation allowed quantitative measurements of the various species present. From these experiments it was determined that the decomposition of ethylene at room temperature formed strongly adsorbed acetylide and alkyl species. Recombination of adsorbed species and hydrogenation of ethylene occurred rapidly at room temperature, forming weakly adsorbed ethane and cis- and trans-2-butene that subsequently hydrogenated to butane. Strongly adsorbed acetylide was not appreciably consumed in the formation of products, although it most likely served as a source of hydrogen for other reactions. Spin counting revealed that there was one carbon in the strongly adsorbed layer for each surface ruthenium atom.

In Cu-Ru bimetallic catalysts copper strongly segregates to defect-like edge and corner lattice positions. When ethylene is adsorbed on these catalysts, butadiene is observed along with butane and 2-butenes. Very little ethane is produced. The butadiene and butenes are hydrogenated to butane much more slowly than on the pure Ru catalysts. The ethylene does not react and only weakly adsorbs on copper. Hence it is concluded that edge and corner Ru atoms facilitate hydrogenation reactions.

Similar experiments were performed on silica supported Pt catalysts. Ethylene was adsorbed to an amount corresponding to 10 to 15 molecules per surface Pt atom (dispersion was about 60%). At temperatures up to 413K only weakly adsorbed ethylene was observed. When the sample was treated at 513K for 24 hours a significant amount of strongly adsorbed alkyl and aromatic species were detected but no resonance attributed to ethylidyne was noted. Exposing the samples to a temperature of 673K for 24 hours produced weakly adsorbed ethane, methane and a benzene-like aromatic. In addition, a large amount of coke with a stoichiometry of $C_{2.4}H$ was found.

Model Reaction Studies [8-10]

We have studied the effect of adding copper and silver to a silica-supported ruthenium catalyst for the ethane hydrogenolysis reaction. Specific activities were determined as a function of the fraction of group Ib metal at a number of temperatures. In addition, the effect of changing the ratio of hydrogen to ethane in the feed gas was used to measure apparent orders of reaction as a function of temperature and group Ib metal added. No evidence for ensemble effects was observed for either series of catalysts consistent with earlier work with the Fischer-Tropsch reaction on the same catalysts. However, variations in turnover frequency were observed as the Ib metal populated defect-like edge and corner sites. This suggests a structure sensitivity effect. At lower temperatures studied we found that the effect of adding copper or silver to the catalyst was virtually the same, the differences being attributed to the greater affinity of copper for defect-like sites on the ruthenium crystallites. At higher temperatures, copper and silver acted differently; copper seemed to be active for the removal of site-blocking hydrogen from the active ruthenium surface, while silver merely blocked the ruthenium sites most active for the removal of hydrogen from the surface. We postulate that the defect-like sites of supported ruthenium crystallites are most active for the desorption of hydrogen and the basal planes are active for the breaking of carbon-carbon bonds. The increase in specific activity observed as the dispersion of the pure Ru catalyst decreased was attributed to the increase in relative number of carbon-carbon bond breaking sites. This effect overcame the decrease in the proportion of sites active for the removal of site-blocking hydrogen.

A simple kinetic analysis of the bimetallic data assumed that hydrogen gas was in adsorption/desorption quasi-equilibrium with dissociated hydrogen atoms and ethane was in adsorption/desorption quasi-equilibrium with a deeply dehydrogenated C_2 species. The rate limiting step was taken to be the C-C bond cleavage. The fit of the data to the model suggested that the deeply dehydrogenated species has a stoichiometry of C_2H_3 (perhaps ethylidyne). The model also suggested that the order with respect to hydrogen should shift from -2.5 to -1.5 as the coverage of hydrogen decreases. These numbers compare favorably with the experimentally observed orders of -2.4 for the Ag-Ru bimetallic and -1.4 for the pure ruthenium catalyst.

Future Plans

It is our plan to continue three general approaches to the studies of supported metal catalysts: (1) model reaction studies and traditional chemisorption experiments; (2) solid state NMR of molecules adsorbed on catalyst surfaces; and (3) solid state NMR of catalytic metals.

The choice of model reaction is somewhat guided by the results of the NMR work. For example, the change in selectivity associated with the addition of copper to ruthenium for ethylene adsorption and reaction noted by ^{13}C NMR suggests that C_4 hydrocarbons may be selectively cracked to form C_2 products over this bimetallic catalyst. The change in the relative abundance of weakly and strongly adsorbed hydrogen can play a role in a variety of other reactions as well.

Another approach to the studies we plan to explore is the use of ^1H NMR of adsorbed hydrogen to probe surface electronic states of the metal and the bonding states of adsorbed species. Preliminary studies of chlorine adsorbed on ruthenium revealed a large shift of the adsorbed hydrogen resonance. Because the hydrogen-ruthenium system has a bonding state (or states) near the fermi level the knight shift dominates the lineshift. This large shift is very sensitive to the density of states near the metal fermi level at the surface.

Presumably other poisons (e.g.. sulfur) and promoters will have an analogous effect. It is our intention to investigate these effects by NMR of adsorbed species (hydrogen and hydrocarbons) and, in certain cases, the metal or promoter itself [11,12]. Model reaction studies of the same catalysts can also be performed.

References (last two years)

1. Wu, X., B. C. Gerstein, and T. S. King, "Characterization of Silica Supported Ruthenium Catalysts by Hydrogen Chemisorption and Nuclear Magnetic Resonance of Adsorbed Hydrogen," J. Catal. 118 (1989) 238.

2. Wu, X., B. C. Gerstein, and T. S. King, "Characterization of Silica Supported Ru-Cu and Cu Catalysts by Hydrogen Chemisorption and NMR of Adsorbed Hydrogen," J. Catal. (in press).

3. Wu, X., B. C. Gerstein, and T. S. King, "Characterization of Silica Supported Ru-Ag and Ru-Au Catalysts by Hydrogen Chemisorption and NMR of Adsorbed Hydrogen," J. Catal. (accepted).

4. Pruski, M., J. C. Kelzenberg, M. Sprock, B. C. Gerstein, and T. S. King, "13C High Resolution NMR Studies of Adsorption and Reaction of Ethylene on Silica-Supported Ru and Ru-Cu Catalysts," Colloids and Surfaces (in press).

5. Pruski, M., J. C. Kelzenberg, B. C. Gerstein, and T. S. King, "Solid State NMR of 13C in Ethylene Adsorbed on Silica-Supported Ruthenium," J. Am. Chem. Soc. (accepted).

6. Sprock, M., M. Pruski, B. C. Gerstein, and T. S. King, "The Effect of Copper on the Hydrogenation of Ethylene on Silica-supported Ru-Cu Catalysts as Studied by ^{13}C NMR," Catalysis Letters (submitted).

7. Smale, M. W., M. Pruski, V. Rutar, B. C. Gerstein, and T. S. King, "NMR Studies of High Coverages of Ethylene Adsorbed on Silica-Supported Platinum Catalysts," J. Catal. (submitted).

8. Smale, M. W. and T. S. King, "Ethane Hydrogenolysis over Well-Defined Ru-Cu/SiO2 Catalysts," J. Catal. 119 (1989) 441.

9. Smale, M. W. and T. S. King, "Kinetics of Ethane Hydrogenolysis over Silica-Supported Ruthenium-Group Ib Metal Catalysts," J. Catal. (accepted).

10. Kelzenberg, J. C. and T. S. King, "Fischer-Tropsch Synthesis Over Silica Supported Ru-Group Ib Catalysts," J. Catal. (submitted).

11. King, T. S., W. J. Goretzke, and B. C. Gerstein, "Dispersion of Silica Supported Copper Catalyst Determined by NMR of 63Cu," J. Catal. 107 (1987) 583.

12. Chu, P.-J., B. C. Gerstein, G. R. Sheffer, and T. S. King, "NMR Studies of 65Cu and 133Cs in Alkali-Metal Promoted Copper Catalysts," 115 (1989) 194.

MECHANISMS AND CONTROLLING CHARACTERISTICS OF THE CATALYTIC OXIDATION OF METHANE

Kamil Klier, Gary W. Simmons, and Richard G. Herman
Department of Chemistry and Zettlemoyer Center of Surface Studies
Lehigh University, Bethlehem, PA 18015

Research Scope and Objectives

The objective of this research is to develop an understanding of the fundamental processes involved in the catalytic conversion of methane to oxygenates and C_2^+ hydrocarbons over noble metal surfaces, i.e. Pd, based on the earlier discovery that Pd may be a potential catalyst for selective methane oxidation under mild reaction temperatures. The novel aspect of the study is the identification of the physical and chemical states of the catalyst surface that activate C-H bonds and enhance the formation of C-O and C-C bonds. In addition, the modification of catalytic properties of the metal catalysts through dissociative adsorption of chlorinated hydrocarbons is of particular interest. Successful achievement of our research goals will provide knowledge of the limiting factors in partial oxidation of methane and will lead to new catalysts for these processes.

Description of Research Effort

The oxidation of methane on the Pd(100) surface was studied by AES, LEED, TPD, and HREELS techniques. With oxygen adsorbed on the surface, the previously observed disproportionation of the c(2x2)-O structure into a mixture of a dense phase, $(\sqrt{5}x\sqrt{5})R27^\circ$-O, and a rare phase, "(2x2)", is accounted for by a reconstruction-relaxation process of the Pd(100) surface that arises as a response to a critical coverage at a critical temperature. Proposed lateral shifts of palladium atoms in the top layer gives rise to distorted four-fold sites that are stabilized by an increase in the palladium-oxygen bond strength. Direct evidence for oxygen adsorbed in distorted four-fold sites is afforded by the appearance of an energy loss peak in the HREELS spectrum that can be attributed to one of the "silent" in-plane, oxygen-palladium modes of vibration. Modeling studies of vibrational frequencies for Pd_4O and $Pd_{16}O_8$ clusters, using the GF-Wilson method via QCPE #342 code, have been carried out and led to a better understanding of the HREELS spectra for oxygen adsorbed on the reconstructed Pd(100) surface. Activation energies for initial rates of desorption from coverages of 0.80 monolayer (ML), 0.68 ML and 0.50 ML were similar, 45 kcal/mol, while a value of 30 kcal/mol was obtained for coverages less than 0.25 ML. A positive activation entropy of desorption from the $(\sqrt{5}x\sqrt{5})R27^\circ$-O phase suggests that desorption occurs via an mobile activated molecular complex formed from immobile adsorbed atoms. For desorption from the "(2x2)" phase a negative activation entropy indicates that desorption occurs by the formation of a mobile molecular complex from a two dimensional lattice gas of oxygen atoms. The O/Pd(100) study suggests that the rare adsorbed oxygen phase with a surface coverage $\theta_O \leq 0.25$ ML, achievable at 650K and low partial pressure of oxygen, is the most reactive state for oxidation reactions. This rare phase features adsorbed oxygen with a suitable chemisorption strength while leaving part of the Pd surface uncovered for breaking the C-H bond in methane, which subsequently reacts with the active surface oxygen from the part of surface containing chemisorbed oxygen atoms.

Dichloromethane, CH_2Cl_2, which is a compound used to control oxidation of methane to formaldehyde supported real palladium catalysts, adsorbed dissociatively on Pd(100) surface at room temperature, as revealed by HREELS spectra. Loss peaks were observed with characteristic vibrational modes corresponding to Pd_4C, Pd_4Cl and Pd_4H surface species but not to C-Cl or C-H fragments. The CH_2Cl_2 adsorption proceeds with a near unity initial sticking coefficient and reaches saturation with Cl coverage of 0.22 ML. Carbon fragments could be removed through reaction with oxygen at ≤900K while leaving the atomic chlorine in a disordered state. The surface structures formed from CH_2Cl_2 adsorption, as well as the residual Cl layers and their interactions with oxygen, have been modeled as a random arrangement of CCl_2 units and oxygen atoms. Of the structures studied for fitting the CH_2Cl_2 adsorption data, the best features are obtained with surface Cl-C-Cl ensembles, having 90° Cl-C-Cl angles, that exclude nearest-neighbor adsorption and Cl-Cl next-nearest-neighbor adsorption. Upon oxidation of the carbon fragment, CO was increasingly selectively produced compared to CO_2 with CH_2Cl_2 preexposures, i.e. Cl-C-Cl coverages. A Monte-Carlo simulation of the oxidation of surface carbon by surface oxygen atoms, for a range of partial coverages of the palladium surface by chlorine, resulted in semi-quantitative agreement with the observed rates of production of CO and CO_2 as a function of chlorine coverage, as shown in Figure 1. The model explains selective oxidation to CO_2 on chlorine-free palladium and to CO on palladium covered by some 20% chlorine atoms in terms of a restricted supply of oxygen on partially chlorine-covered surfaces. The controlling characteristic of carbon oxidation by chlorine is believed to be an ensemble size effect and the *ensemble-controlled* reaction pattern is therefore expected to be of catalytic significance in the partial oxidation process for hydrocarbons.

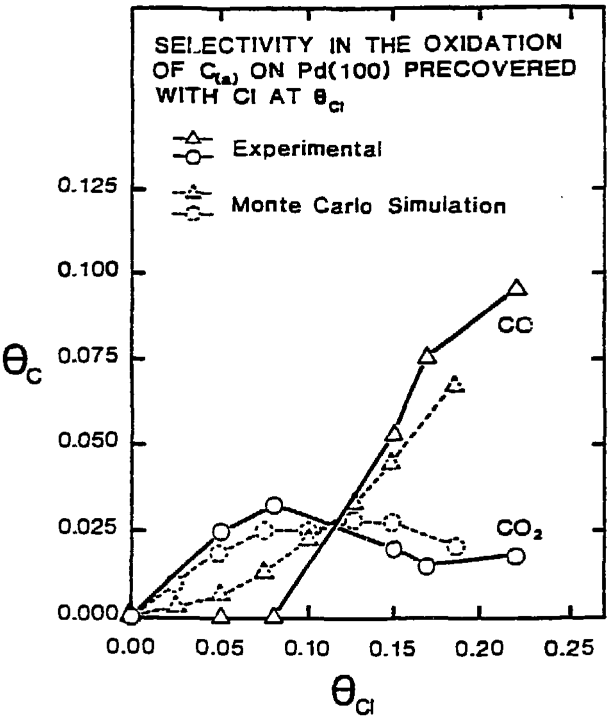

Figure 1. The experimental and simulated CO and CO_2 selectivities over Pd(100) in terms of carbon and chlorine coverages. The experimental distributions were derived from thermal desorption yields obtained after the first oxygen dose on the dichloromethane precovered surface. The simulated distributions were obtained via the Monte Carlo method by statistically counting the oxygen atoms that reside adjacent to each carbon atom.

The exposures of clean, pre-oxidized and/or pre-chlorinated Pd(100) to methane at pressures of $\leq 10^{-5}$ torr and temperatures of 300-1000K had been carried out with no indication of reactions despite the high reactivity of methane achieved over high surface area Pd catalysts that were tested above atmospheric pressure. The difference of the reaction rates in studies conducted between these two cases may be attributed to the *pressure gap* or the *surface structure gap* that often occurs in heterogeneous catalysis. It is the goal of future research to explore the dependence of each of these effects, or the interplay of the two, upon the activation of methane.

References

1. "Oxygen Adsorption on Pd(100) Surface: A study of Phase Transformations, Surface Reconstruction, and Oxygen Activation," G. W. Simmons, Y.-N. Wang, J. A. Marcos, and K. Klier (submitted to Surface Science).

2. "The Adsorption of Dichloromethane and its Interactions with Oxygen on Pd(100): The Effect of Surface Cl on Oxygen Chemisorption and Oxidation of C Residues," Y.-N. Wang, J. A. Marcos, G. W. Simmons, and K. Klier (to be submitted).

Future Research

The current contract is terminating but a new research proposal to continue this research has been submitted. To determine directly the specific states of the palladium surface that activate methane for selective oxidation and to identify reaction intermediates, modifications for the experiments are necessary. A novel UHV-compatible high-pressure cell that is mounted on a 6" flange and can be readily attached to the original chamber has been constructed. To model the surface morphology of the high-surface-area supported metallic catalysts and to study the effect of structure of catalyst surfaces upon the methane activation, high-index-plane single crystals of palladium have been obtained and will be used for future studies.

CHEMISTRY OF BIMETALLIC AND ALLOY SURFACES

Bruce E. Koel

Department of Chemistry,
University of Southern California,
Los Angeles, CA 90089-0482.

Careful design of experiments can isolate the several factors that control surface chemistry and catalysis on bimetallic and alloy surfaces [1]. We use well-characterized surfaces formed by vapor deposition of metal adatoms on single crystal metal substrates. The span of systems investigated allows us to carry out for the first time a separation of geometric and electronic effects on bimetallic platinum surface chemistry. For example, K and Sn adatoms on Pt clearly have both important electronic and geometric effects, and these effects are distinguished. Importantly, this work considers at the atomic scale the influence of bimetallic surfaces on hydrocarbon reactions.

We report here on results of chemisorption studies of H_2, CO, C_2H_4, and C_2H_2 on these model bimetallic catalysts. Potassium adatoms strongly affect the chemisorption and reaction of ethylene on Pt surfaces [2-4]. The heat of adsorption of ethylene is reduced in half, and the activation barrier to dehydrogenation is doubled. These particular changes are due to the alteration of the electronic structure of the Pt surface. Bismuth is a fairly good model site-blocking agent, with only small electronic effects on Pt surface chemistry, and thus Bi coadsorption provides benchmark data on ensemble sizes required for chemical reactions on the Pt(111) surface [5,6]. Ordered surface alloys of Sn and Pt can be used for detailed probing of ensemble sizes and also reactive site requirements. Ethylene is strongly adsorbed on two Sn/Pt(111) alloy surfaces [7], and UPS and HREELS data indicate that molecular ethylene is di-σ-bonded to both alloy surfaces as on Pt(111). However, in stark contrast to Pt(111), no ethylene decomposition occurs upon heating the alloy surfaces. These observations are interpreted in terms of a critical ensemble effect for ethylene adsorption and decomposition on these surfaces, but electronic effects are also present since there is a decrease in the ethylene heat of adsorption as the Sn concentration in the surface alloy is increased and no dissociative H_2 adsorption is observed on either alloy surface at 150 K.

Understanding the influence of electronegative adatoms on metal surface chemistry can also be helpful in laying the foundation for describing the chemistry of bimetallic surfaces, since these adatoms can change the electronic structure of the surface in a prescribed manner. We have explored the influence of oxygen adatoms on the bonding of nitric oxide to Pt(111) [8,9].

Recent investigations have focussed on bimetallic Ni surfaces. In addition to describing the chemical properties of these surfaces, these studies allow us to determine the relative importance of geometric and electronic effects in alkali promotion and sulfur poisoning of nickel and also to provide benchmark data on ensemble sizes required for chemical reactions on nickel surfaces.

Our future plans are to extend TPD and HREELS measurements of the influence of potassium on the bonding mode and chemisorption bond strength of hydrocarbons adsorbed on platinum and nickel surfaces. Particular attention will be given to the interaction of coadsorbed potassium with acetylene on Pt(111), and to the interaction of coadsorbed potassium and ethylene on Ni(100). An important goal is also to determine the influence of potassium on the decomposition kinetics of acetylene and ethylene and on the nature and stability of the hydrocarbon fragments formed. We plan to carry out surface chemistry studies of model HDS and HDN catalysts formed by vapor-depositing cobalt, palladium, or nickel on molybdenum single crystal surfaces. The composition and structure of these bimetallic surfaces can be controlled and varied in a planned manner to reveal the relative importance of the several factors that control the chemistry and catalysis of these surfaces. Particular attention will be given to hydrocarbon adsorption, especially heteroatom containing molecules, and to the role of sulfur in modifying the structure and chemistry of these surfaces.

REFERENCES

1. Koel, B. E., and Windham, R. G., in Proceed. Industry-University Advanced Materials Conference, Denver, CO, February 1987, J. G. Morse (Ed.), (The Metallurgical Society, Inc., Warrendale, PA, 1987), p. 77.
2. Windham, R. G., Bartram, M. E., and Koel, B. E., J. Vac. Sci. Technol., A 5, 457 (1987).
3. Windham, R. G., Bartram, M. E., and Koel, B. E., J. Phys. Chem., 92, 2862 (1988).
4. Windham, R. G., and Koel, B. E., J. Phys. Chem., in press.
5. Windham, R. G., Koel, B. E., and Paffett, M. T., Langmuir, 4, 1113 (1988).
6. Paffett, M. T., Campbell, C. T., Windham, R. G., and Koel, B. E., Surface Sci., 207, 274 (1989).
7. Gebhard, S. C., Paffett, M. T., Windham, R. G., and Koel, B. E., Surface Sci., 223, 449 (1989)
8. Parker, D. H., Bartram, M. E., and Koel, B. E., Surface Sci., 217, 489 (1989).
9. Bartram, M. E., Windham, R. G., Koel, B.E., and Carter, E. A., Surface Sci., in press.

PUBLICATIONS FROM THE LAST TWO YEARS RESULTING FROM THIS WORK

1. Chemical Modification of Surface Properties.
   B. E. Koel and R. G. Windham, in *Proceed. Industry-University Advanced Materials Conference*, Denver, CO, February 1987, J. G. Morse (Ed.), (The Metallurgical Society, Inc., Warrendale, PA, 1987), pp. 77-87.

2. The Influence of Potassium on Ethylene Adsorption and Decomposition on Pt(111).
   R. G. Windham, M. E. Bartram, and B. E. Koel, *J. Vac. Sci. Technol.*, **A 5**, 457-458 (1987).

3. A Model Study of Alkali Promotion of Water-Gas Shift Catalysts: Cs/Cu(111).
   C. T. Campbell and B. E. Koel, *Surface Sci.*, **186**, 393-411 (1987).

4. Surface Chemistry of Thin Palladium Films.
   D. L. Neiman and B. E. Koel, in *Physical and Chemical Properties of Thin Metal Overlayers and Alloy Surfaces*, D. M. Zehner and D. W. Goodman (Eds.),(Materials Research Society, Pittsburgh, PA, 1988), p. 143-153.

5. The Coadsorption of Ethylene and Potassium on Pt(111). 1. Formation of a π-bonded Ethylene Species.
   R. G. Windham, M. E. Bartram, and B. E. Koel, *J. Phys. Chem.*, **92**, 2862-2870 (1988).

6. Studies of the Ensemble Size Requirements for Ethylene Adsorption and Decomposition on Pt(111): Ethylene and Bismuth Coadsorption.
   R. G. Windham, B. E. Koel, and M. T. Paffett, *Langmuir*, **4**, 1113-1118 (1988).

7. A Multitechnique Surface Analysis Study of the Adsorption of H_2, CO, and O_2 on Bi-Dosed Pt(111) Surfaces.
   M. T. Paffett, C. T. Campbell, R. G. Windham, and B. E. Koel, *Surface Sci.*, **207**, 274-296 (1989).

8. Study of High Coverage States of Atomic Oxygen on the Pt(111) Surface.
   D. H. Parker, M. E. Bartram, and B. E. Koel, *Surface Sci.*, **217**, 489-510 (1989).

9. Chemisorption of Ethylene on Ordered Sn/Pt(111) Surface Alloys.
   S. C. Gebhard, R. G. Windham, B. E. Koel, and M. T. Paffett, *Surface Sci.*, 223, 449-464 (1989).

Structures of Transition Metal Hydrides

Thomas F. Koetzle, Chemistry Department, Brookhaven National Laboratory,
Upton, New York 11973

In this program, structures of catalytically-important transition metal hydrides are being studied by neutron and x-ray diffraction methods. The neutron diffraction studies, which utilize the unique facilities at the Brookhaven High Flux Beam Reactor, provide precise structural data that are essential for understanding the bonding in these compounds. A long-range goal of this research is to improve our knowledge of the role of metal hydride catalysts in such industrially-important processes as hydrogenation reactions and C-H bond activation. Current work emphasizes two classes of hydrides: complexes with intact dihydrogen ligands, and heterometallic systems with M-H-M' bridge bonds.

In work on metal dihydrogen complexes, recently completed low-temperature neutron diffraction studies of two Fe(II)(H_2) systems have provided detailed information on the hydrogen-metal bonding in these molecules. The compounds are of great importance as models for the oxidative addition of H_2 to a metal center, the primary reaction path for the activation of dihydrogen by metal-based catalyst systems. Complexes trans-$[Fe(H_2)(H)(dppe)_2]^+[BPh_4]^-$ (1, dppe = bisdiphenylphosphinoethane, studied with R.H. Morris, J.S. Ricci and co-workers) and cis,mer-$Fe(H_2)(H)_2(PEtPh_2)_3$ (2, studied with K.G. Caulton and co-workers) are octahedral, and both compounds have ordered η^2-dihydrogen ligands with H-H distances of 0.82(1)Å, or 0.08Å longer than in H_2 itself. Compound 2 is unique among dihydrogen complexes studied to date in having the H-H bond in a staggered orientation with respect to the cis Fe-P and Fe-H bonds. This conformation is believed to be stabilized by overlap between the filled Fe-H σ orbital and the empty σ^*(H-H). Such nascent H/H_2 bond formation is proposed to facilitate fluxionality among dihydrogen and hydride ligands.

The neutron diffraction studies of compounds 1 and 2 provide the first precise structural results reported for metal-dihydrogen systems and serve to test H-H distances estimated from NMR T_1 relaxation-time measurements in solution. Based on such T_1 measurements, and/or observations of large J_{H-H} couplings, quite a number of metal hydride structures recently have been reassessed and suggested to be "non-classical", i.e., to contain dihydrogen or to have short H···H contacts between terminal hydrides. One such compound investigated by us within the past year, $[IrH_3(Cp)(PMe_3)]^+[BF_4]^-$ (3, studied with D.M. Heinekey, K.W. Zilm and co-workers), originally had been postulated to contain a coordinated $[H_3]^+$ ligand. In fact, as shown by neutron diffraction, the cation in 3 has a "classical" terminal hydride structure, with normal H···H contacts in the range 1.6-1.7Å. The unusually large temperature-dependent J_{H-H} couplings observed in this and a series of related phosphine, arsine and stilbene complexes have been reinvestigated by Zilm, Heinekey et al. and can be explained in terms of a novel quantum mechanical exchange coupling between the hydrogen nuclei (Zilm, K.W.; Heinekey, D.M.; Millar, J.M.; Payne, N.G.; Neshyba, S.P.; Duchamp, J.C.; Szczyrba, J. J. Am. Chem. Soc., in press).

Our interest in heterometallic hydrides stems from the fact that a number of systems of this type show promising catalytic activity, and, in principle, this activity can be fine-tuned to improve selectivity by adjusting the metal centers. In recent work in this area, the structure of $Re(CO)_5(\mu\text{-}H)Mn_2(CO)_9$, 4, which had been isolated during the course of investigations by R.M. Bullock and co-workers of the reactivity of $HMn(CO)_5$ with cyclopropylstyrene (Bullock, R.M.; Rappoli, B.J.; Samsel, E.G.; Rheingold, A.L. J. Chem. Soc., Chem. Commun., 1989, 261-263), was analyzed by x-ray diffraction. Compound 4 (structure studied with A. Albinati) has an L-shaped metal skeleton; the coordination about each metal center is distorted octahedral with a Mn-H-Re bridge of dimensions: Mn-H 1.88(10)Å, Re-H 1.66(9)Å, and Mn-H-Re 142(1)°. The precision of the x-ray results is not sufficient to permit conclusions about any asymmetry which may be present in the bridge; definitive information on this point is expected to come from a planned neutron diffraction study of 4. Substantial asymmetry of the M-H-M' bridges was found in the two heterometallic systems studied previously by neutron diffraction: $[(PEt_3)_2Pt(\mu\text{-}H)_2IrH_2(PEt_3)_2]^+[BPh_4]^-$ (Albinati, A.; Emge, T.J.; Koetzle, T.F.; Meille, S.V.; Musco, A.; Venanzi, L.M. Inorg. Chem. 1986, 25, 4821-4827) and $(PEt_3)_2(C_6Cl_5)Pt(\mu\text{-}H)Ag(H_2O)(CF_3SO_3)$.

Future research under this program will continue to emphasize the study of heterometallic hydrides, and of dihydrogen complexes and related "non-classical" metal hydride systems. In the latter area, studies will be targeted at compounds with dihydrogen ligands in a variety of coordination environments, to investigate the variation in H-H distance, orientation of the dihydrogen relative to other ligands, mean square amplitudes of vibration of the hydrogen atoms, etc. The crystallographic work on heterometallic complexes will be extended, to utilize the x-ray diffraction facilities at the National Synchrotron Light Source in carrying out anomalous scattering studies. Here the tunable wavelength of the synchrotron source will be exploited to distinguish neighboring metals in the periodic table by making measurements near the elements' x-ray absorption edges.

Acknowledgements

I would like to thank my many collaborators in this research, who include A. Albinati, R. Bau, R.M. Bullock, K.G. Caulton, T.J. Emge, D.M. Heinekey, R.H. Morris, N.G. Payne, R.C. Stevens, L.S. Van Der Sluys, L.M. Venanzi, P.J. Vergamini and K.W. Zilm. The technical assistance of J.H. Guthy and D.A. Rathjen is gratefully acknowledged. The work is supported by the Division of Chemical Sciences under Contract No. DE-AC02-76CH00016.

Publications, 1988-1989

Bau, R.; Stevens, R.C.; McLean, M.; Koetzle, T.F. Neutron Diffraction Analysis of $HRh[P(C_6H_5)_3]_4$. Materials Science Forum, 1988, 27/28, 77-80.

Heinekey, D.M.; Millar, J.M.; Koetzle, T.F.; Payne, N.G.; Zilm, K.W. Structural and Spectroscopic Characterization of Iridium Trihydride Complexes: Evidence for Proton-Proton Exchange Coupling. J. Am. Chem. Soc., in press.

Publications, 1988-1989, ctd.

Ricci, J.S.; Koetzle, T.F.; Bautista, M.T.; Hofstede, T.; Morris, R.H.; Sawyer, J.F. Single-Crystal X-ray and Neutron Diffraction Studies of an η^2-Dihydrogen Transition-Metal Complex: trans-$[\mathrm{Fe}(\eta^2\text{-}\mathrm{H}_2)(\mathrm{H})(\mathrm{PPh}_2\mathrm{CH}_2\mathrm{CH}_2\mathrm{PPh}_2)_2]$-$\mathrm{BPh}_4$. J. Am. Chem. Soc. **1989**, 111, 8823-8827.

Stevens, R.C.; McLean, M.R.; Bau, R.; Koetzle, T.F. Neutron Diffraction Structure Analysis of a Hexanuclear Copper Hydrido Complex, $\mathrm{H}_6\mathrm{Cu}_6[\mathrm{P}(p\text{-tolyl})_3]_6$: An Unexpected Finding. J. Am. Chem. Soc. **1989**, 111, 3472-3473.

Stevens, R.C.; McLean, M.R.; Wen, T.; Carpenter, J.D.; Bau, R.; Koetzle, T.F. An X-ray and Neutron Diffraction Structure Analysis of a Triply-bridged Binuclear Iridium Complex, $[(\mathrm{C}_5(\mathrm{CH}_3)_5\mathrm{Ir})_2(\mu\text{-}\mathrm{H})_3]^+[\mathrm{ClO}_4]^-\cdot 2\mathrm{C}_6\mathrm{H}_6$. Inorg. Chim. Acta, 1989, 161, 223-231.

Van Der Sluys, L.S.; Eckert, J.; Eisenstein, O.; Hall, J.H.; Huffman, J.C.; Jackson, S.A.; Koetzle, T.F.; Kubas, G.J.; Vergamini, P.J.; Caulton, K.G. An Attractive "Cis-Effect" of Hydride on Neighbor Ligands: Experimental and Theoretical Studies on the Structure and Intramolecular Rearrangements of $\mathrm{Fe}(\mathrm{H})_2(\eta^2\text{-}\mathrm{H}_2)(\mathrm{PEtPh}_2)_3$. J. Am. Chem. Soc., in press.

SOLID STATE, SURFACE AND CATALYTIC STUDIES OF OXIDES

Harold H. Kung

Department of Chemical Engineering, and Ipatieff Laboratory
Northwestern University, Evanston, Illinois 60208

Objective

High activity and selectivity are often the deciding factors in determining the economic attractiveness of a catalytic process. In catalytic selective oxidation, surface lattice oxygen ions of an oxide catalyst commonly participate directly in the reaction cycle as a reactant. Thus the catalytic activity and selectivity of an oxide depend on its surface properties, such as surface atomic structure, and rates and extents of reduction and reoxidation, which in turn depend on the corresponding bulk properties. The objectives of this project are to elucidate and understand the interrelationship among surface, bulk and catalytic properties of an oxide.

Summary of Progress

This research program consists of two projects: selective oxidation of alkanes, and catalytic decomposition of methanol on single crystal ZnO surfaces.

Selective Oxidation of Light Alkanes:

It was previously observed that magnesium-vanadium oxides were quite active and selective in the oxidative dehydrogenation of butane. The active and selective catalysts contained 19-54 wt.% of V_2O_5 in MgO. The active phase in these catalysts was identified as magnesium orthovanadate after studying the catalysts with various spectroscopies, which included x-ray diffraction, infrared, laser Raman, Auger electron spectroscopy, and scanning electron microscopy.

Other orthovanadates were also studied, including Ba, Sm, Nd, and Eu to investigate the effect of the nature of the cations to which the lattice oxygen was bonded on the catalytic bahavior of the oxide in the oxidative dehydrogenation reaction. Mg, Sm, and Nd orthovanadates were found to be quite selective, but Eu orthovanadate was less selective but much more active than the other orthovanadates. Ba orthovanadate was found to deactivate due to the formation of barium carbonate.

Temperature programmed reduction and reoxidation of Mg, Nd, and Eu orthovanadates showed that the rates of reduction of these vanadates followed the order Mg > Eu > Nd, whereas the order was reversed for the rates of reoxidation. A model was formulated which assumed that the steady state of a catalyst is determined by its relative rates of reduction and reoxidation, which in turn determines the catalytic behavior, to explain the observations.

Alkenes were found to be the principal initial products in the oxidative dehydrogenation reaction. Dienes and other unsaturated hydrocarbons were secondary products, and carbon oxides were secondary or tertiary products. The reaction rate was found to be the slowest for ethane, intermediate for propane and butane, and the fastest for 2-methylpropane. This trend was inversely related to the C-H bond energies in these molecules. Thus the first step of the reaction was believed to be C-H bond breaking in the alkane molecule to form an alkyl species.

We have also shown that under some reaction conditions, free radical species desorbed from the vanadate surface during the oxidation of propane. The desorbed radical species initiated chain reactions in the gas phase downstream from the catalyst and resulted in higher conversions of propane than in the absence of such desorbed species. By modelling the gaseous reactions in the region immediately after the catalyst bed with oxidative pyrolysis reactions of propane, it was determined that the desorbed species was not ethyl or methyl radicals. The model did not distinguish OH or propyl radicals as possibilities, but the latter was the more likely candidate based on chemical arguments.

Methanol Decomposition on Single Crystal ZnO Surfaces:

In this project, the possible different catalytic properties of various ZnO surfaces of different atomic structures were being elucidated using the decomposition of methanol as the probe reaction. It was previously observed that the Zn-polar, the stepped nonpolar, and the O-polar surfaces of ZnO showed different rates and product distributions in the temperature programmed decomposition of methanol. It became interesting to find out if the same differences could be observed under catalytic conditions.

Reaction rates under catalytic conditions were successfully measured on Zn-polar, stepped nonpolar and O-polar surfaces at 250 to about 400°C and at two very different pressures of about 10^{-5} torr and about 10 torr. It was found that in the zeroth order regime, the turnover rates and the activation energies determined at the two different pressures were similar, and similar to the published data on powder samples. The Zn-polar surface was always much more active than the O-polar surface, and the nonpolar surface was marginally more active than the O-polar surface at low pressures, but became almost as active as the Zn-polar surface at high pressures. The results clearly demonstrated that methanol decomposition on ZnO is a structure sensitive reaction. Possible explanations for the different activities of the different surfaces were formulated. Interestingly, the major product at low pressures was formaldehyde, whereas the major product at high pressures was CO. At this point, we regard this project completed and have no further plans to continue.

Future Work

Future work will be to continue the study on the selective oxidation of alkanes. The emphasis will be on further elucidation of the relation between the structure and composition of an oxide and its activity and selectivity in the reaction. The aim is to develop sufficient understandings that would lead to the discovery of better catalysts for this reaction. Three areas of research are being planned:

1) Catalysis on highly dispersed V-Mg-O catalysts:

It was observed that the mixed oxide V-Mg-O which contained a mixture of MgO and $Mg_3(VO_4)_2$ was a more selective catalyst than $Mg_3(VO_4)_2$. The difference was probably due to the difference between highly dispersed and crystalline $Mg_3(VO_4)_2$. We propose to attempt to prepare and study the catalytic properties of a highly dispersed V-Mg-O on SiO_2 catalyst, and highly dispersed $Mg_3(VO_4)_2$ on TiO_2 and Al_2O_3.

2) Catalytic oxidative carbon-carbon bond cleavage reaction:

The oxidative dehydrogenation reaction proceeds first by the formation of alkenes. Degradation reactions of alkenes limit the selectivity that can be obtained, and they involve carbon-carbon bond cleavage. There is little work published that relates the acidic and basic properties, the reduction and reoxidation behavior, the structure, and the activity and selectivity of an oxide in oxidative carbon-carbon bond cleavage. We propose to conduct a systematic study of this reaction.

3) Reduction and reoxidation model for selective oxidation catalysis:

In the course of this study, we formulated a model that relates the rates of reduction and reoxidation of an oxide to its activity and selectivity in oxidative dehydrogenation of alkanes. In principle, the model applies to other oxidation reactions and we propose to do so. However, since the model was formulated based on data with four catalysts, it would be important to further test its validity with some more vanadates before applying it to other reactions.

Recent publications related to this project:

1) "Selective Oxidative Dehydrogenation of Butane over V-Mg-O Catalysts", M.A. Chaar, D. Patel, M.C. Kung, and H.H. Kung, J. Catal., 105, 483 (1987).
2) "Selective Oxidative Dehydrogenation of Propane over V-Mg-O Catalysts," M.A. Chaar, D. Patel, and H.H. Kung, J. Catal., **109**, 463 (1988).
3) "Catalytic Decomposition of 2-Propanol on ZnO (0001) and $(000\bar{1})$ Surfaces," M. Vest, P.J. Berlowitz, and H.H. Kung, Studies in Surface Science and Catalysis, vol. 38, J. Ward, ed., 1988, p.577.
4) "Selective Oxidative Dehydrogenation of Alkanes over Mg Vanadates," D. Patel, M.C. Kung, and H.H. Kung, Proc. 9th Intern. Congr. Catal., **4**, 1554 (1988).
5) "Oxidative Dehydrogenation of Alkanes to Unsaturated Hydrocarbons," H. Kung, and M. A. Chaar, US Patent 4,777,319 (1988).
6) "Catalytic Decomposition of Methanol on ZnO Single-Crystal Surfaces at Low and Near-Atmospheric Pressures," M. A. Vest, K. Lui, and H. Kung, J. Catal., **120**, 231 (1989).
7) "Selective Oxidative Dehydrogenation of Light ALkanes over Vanadate Catalysts," M. Kung, K. Nguyen, D. Patel, and H. Kung, in Catalysis of Organic Reactions, ed. Blackburn, 1989, p.289.
8) "Generation of Gaseous Radicals by a V-Mg-O Catalyst During Oxidative Dehydrogenation of Propane," K. Nguyen, and H. Kung, J. Catal., accepted.
9) "Oxidative Dehydrogeantion of Butane over Orthovanadates," D. Patel, P. J. Andersen, and H. Kung, J. Catal., submitted.

CHEMICAL ACTIVATION OF MOLECULES BY METALS: EXPERIMENTAL STUDIES OF ELECTRON DISTRIBUTIONS AND BONDING

Principal Investigator, Dennis L. Lichtenberger
Department of Chemistry, University of Arizona, 85721

The purpose of this research program is to obtain detailed experimental information on the different fundamental ways metals bond and activate small organic molecules. Information contributing to the development of models for the chemical and physical behavior of molecules bound to metals must come from many sources. Our research is itself a multi-faceted approach. Synthesis and preparations are important for providing specific molecules that are capable of yielding the key spectroscopic information. Theoretical calculations help clarify the developing models in terms of the fundamental principles of electronic structure and bonding, and help guide the directions of the research toward those areas where experimental information is most needed. Our contributions to developing the methods and principles of various electron spectroscopies for the study of transition metal complexes, as discussed below, represent many of the most significant and unique accomplishments of this research. The most direct relationships of this project are clearly with organometallic chemistry, surface science and catalysis. The program particularly complements many of the current synthetic studies related to homogeneous catalysis, and our methods of gas phase and surface electron spectroscopy have many features in common with studies of surface chemistry. For selected reviews see publications 48, 49, 52 and 57 (all references refer to the list of publication from the last two years).

Chemical Systems. Organometallic complexes containing the appropriate metal-molecule unit offer an intermediate system between the free organic molecule and the molecule adsorbed on the metal surface. The organometallic complexes have a major advantage in that the structures can be accurately known by standard techniques. These complexes can be studied in high-resolution in the gas phase, and the electronic environment of the metal can be perturbed in a variety of ways to map out the sensitivity of the interactions to different electronic situations. Thus the organometallic complex can be used to gain detailed knowledge of how the ionizations of small molecules are perturbed when attached in different ways to a variety of different metal systems.

We give particular attention to those molecules which are models of intermediates in important catalytic processes. The chemical systems being investigated may be classified in terms of

- the number of carbons in the hydrocarbon chain.
- the number of bonds between the hydrocarbon and the metal, such as alkyls vs methylenes.
- the kinds of bonds between the hydrocarbon and the metal, such as alkylidynes vs carbynes or metallacycles vs π donor/acceptor bonding.
- the metal and its formal d electron count.
- the ligand environment, such as sandwich complexes vs alkoxides.
- the electron environment, such as electron-rich vs electron-poor.
- the number of metal atoms bonding to the hydrocarbon, such as mononuclear vs metal dimer.
- the chemical reaction the species is related to, such as carbon-hydrogen bond activation vs carbon-carbon bond activation or metathesis vs polymerization.

The most important feature to appreciate about these chemical systems is their relationship to basic processes involving carbon-carbon and carbon-hydrogen bonds. In some cases the molecules we study are in fact active in synthetic or catalytic reactions. These systems involve examples of alkene and alkyne metathesis, carbon-hydrogen bond activation, and electron transfer processes. For example, alkyne metathesis has been shown to be facilitated with alkylidyne complexes. Possible mechanisms are through a metallacyclobutadiene or through a metallatetrahedrane (η^3-cyclopropenium). We are investigating alkylidynes, carbynes, metallacycles, acetylene coordination, and metal-cyclopropenyls in relation to this process.

Methods. Photoelectron spectroscopy is certainly one of the most direct experimental tools for revealing electronic structure and bonding features of solids, liquids, and gases. The majority of our studies have emphasized high-resolution He I/He II ultraviolet photoelectron spectroscopy (UPS) and high precision core X-ray photoelectron spectroscopy (XPS) investigations of transition metal species in the gas phase. We have developed specialized sample ionization chambers, excitation sources, and data collection hardware and software built for these purposes around a high resolution/sensitivity 36 cm radius hemispherical analyzer. Unique accomplishments with this instrumentation have been the ability to resolve metal-carbon and metal-metal vibrational fine-structure in valence ionization bands, the ability to measure highly precise core ionization energies of gas-phase transition metal complexes, and the ability to obtain high quality photoelectron data of complexes with low volatility or stability. More recent studies have included gas phase Auger experiments, electron spectroscopy of organometallic thin films in ultra-high vacuum, and scanning tunneling microscopy (STM) of inorganic complexes deposited on graphite and MoS_2.

Progress and Current Directions. We have been proceeding toward the collection of a "library" of the complete valence and core ionizations of different small molecules and fragments attached to a variety of mononuclear, binuclear, and cluster metal atom arrangements. As this library has gradually developed in our laboratory, we have observed many relationships which are having an important impact on the understanding of the electronic factors that control the physical and chemical properties of small molecules with metals. Examples are the principle of additivity of ligand electronic effects and the correlation of valence and core ionization shifts. These principles allow:

- separation of σ interactions, π interactions, and the effects of charge redistribution,
- prediction, assignment, and interpretation of the spectra of new metal complexes, and,
- extension of the information from the ionizations to complexes or environments that are not amenable to similar experimentation.

Perhaps the most exciting result of this growing library is our recent discoveries of close relationships between the ionization energies and the thermodynamic stabilities of the metal-molecule species.[63] These relationships have become apparent from correlating the ionizations of systems such as metal-methylenes with metal-ethylenes (coupling of methylenes),[48] metal-ethylene hydrides with metal alkyls (β-hydride elimination),[54] metal-alkynes with metal-vinylidenes (oligomerization), and metal-alkylidynes with metal-alkynes or metal-cyclopropenium (metathesis, in progress).

Accompanying our gas phase studies is our parallel investigations of organometallics on surfaces.[47] The surface experiments are generally useful for situations in which high signal-to-noise is desired but extremely high resolution is not a necessity. In particular, information can be obtained from samples with insufficient volatility or stability for the gas phase studies. Another point of the surface experiments is that they add the effects of intermolecular interactions to the ionization characteristics of the complexes. Of course, intermolecular interactions are the first step in chemical reactions by associative pathways. Most exciting is our recent demonstration of the ability of STM to show the molecular orientations and packing arrangements of thin films of inorganic complexes.[67]

44. R.R. Rye, J.A. Kelber, G.E. Kellogg, K.W. Nebesny, and D.L. Lichtenberger, "Localization Effects in the Auger Spectra of Ring Nitrogen Systems: Pyridine, Poly(2-vinyl)pyridine, Borazine, and Boron Nitride," R.R. Rye, J. Chem. Phys., **86**, 4375 (1987).

45. M.H. Chisholm, D.L. Clark, J.C. Huffman, W.G. Van Der Sluys, E.M. Kober, D.L. Lichtenberger and B.E. Brusten, "The Tungsten-Tungsten Triple Bond. 13. Bisalkyl Tetracarboxylates of Dimolybdenum and Ditungsten. Triple Bonds Between Metal Atoms With the Valence Molecular Orbital Description $\pi^4\delta^2$," J. Am. Chem. Soc., **109**, 6796 (1987).

46. M.H. Chisholm, J.A. Heppert, E.M. Kober and D.L. Lichtenberger, "1,3-Ditungstacyclobutadienes. 2.[1] The Synthesis of Alkoxide Derivatives of $W_2(\mu\text{-CSiMe}_3)_2(CH_2SiMe_3)4$ and Investigations of the Electronic Structures of the $M_2(\mu\text{-CSiMe}_3)_2$ Core as a Function of the d^n-d^n Interactions (n = O, M = Ta; n = 1, M = W; n = 2, M = Re)," Organometallics, **6**, 1065 (1987).

47. D.L. Lichtenberger and J.G. Kristofzski, "Intermolecular Influences on M-M Multiple Bonds From Thin Film UPS Studies of Group VI M_2 $(O_2(CH_3)_4$ Complexes," J. Am. Chem. Soc., **109**, 3458 (1987).

48. D.L. Lichtenberger and G.E. Kellogg, "Experimental Quantum Chemistry: The Photoelectron Spectroscopy of Organotransition Metal Complexes,"* Accounts of Chem. Res., Vol. **20**, 379, (1987).

49. D.L. Lichtenberger, G.E. Kellogg, and L.S.K. Pang, "Photoelectron Spectroscopy: Experimental Characterization of the Electronic Structure and Bonding in Organometallic Molecules",* in *New Developments in the Synthesis, Manipulation, and Characterization of Organometallic Compounds*, Wayda, A.L. and Darensbourg, M.Y., Eds. A. C. S. Symposium Series, 357 (1987).

50. M.T. Ashby, J.H. Enemark, and D.L. Lichtenberger, "Destabilizing dπ-pπ Orbital Interactions and the Alkylation Reactions of Iron(II)-Thiolate Complexes," Inorg. Chem., **27**, 191 (1988).

51. D.L. Lichtenberger, J.G. Kristofzski, and M.L. Bruck,"A New Tetraamidodimolybdenum Complex With a Quadrupole M-M Bond," Acta Cryst., Section C, **44**, 1523-1526 (1988).

52. D.L. Lichtenberger and G.E. Kellogg, "Characterization of Complex Metal Positive Ions in the Gas Phase by Photoelectron Spectroscopy,"* Modern Inorganic Chemistry, John P. Fackler, Jr., Series Ed., 1987.

53. D.L. Lichtenberger, A.S. Copenhaver, H.B. Gray, J.L. Marshall, and M.D. Hopkins, "Valence Electronic Structure of Bis(pyrazolyl)-Bridged Iridium Dicarbonyl Dimers. Electronic Effects of 3,5-Dimethylpyrazolyl Substitution on Metal-Metal Interactions," Inorg. Chem., **27**, 4488 (1988).

54. D.L. Lichtenberger, G.P. Darsey, G.E. Kellogg, R.D. Sanner, V.G. Young and J.R. Clark, "Relative Strengths of Early Transition Metal M-H and M-C Bonds in Substituted Niobocenes and Tantalocenes. Thermodynamic Trends and Electronic Factors of Olefin Insertion Into a Metal-Hydride Bond," J. Am. Chem. Soc., **111**, 5019 (1989).

55. D.L. Lichtenberger, A. Rai-Chaudhuri, "Electronic Structure Factors of Si-H Bond Activation by Transition Metals. The Valence Photoelectron Spectrum of $(\eta^5\text{-}C_5H_5)Mn(CO)_2HSiCl_3$," J. Am. Chem. Soc., **111**, 3583-3591, (1989).

56. D.L. Lichtenberger and A.S. Copenhaver, "Experimental Measures of the Electron Distribution and Bonding in bis(η^5-Cyclopentadienyl)Osmium from He(I) and He(II) Valence Photoelectron Spectroscopy," J. Chem. Phy., 91, 663-673 (1989).

57. D.L. Lichtenberger and R.L. Johnston, "Experimental Measures of Metal-Metal Sigma, Pi, and Delta Bonding from Photoelectron Spectroscopy," Metal-Metal Bonds and Clusters in Chemistry and Catalysis, J.P. Fackler, Jr., Ed. Plenum, 1989.

58. D.L. Lichtenberger and A. Rai-Chaudhuri, "Electronic Structure Control of Si-H Bond Activation by Transition Metals. The Valence Photoelectron Spectra of (η^5-$C_5H_4CH_3$)Mn$(CO)_2$HSiPh_3, (η^5-$C_5H_4CH_3$)Mn$(CO)_2$HSiHPh_2 and (η^5-$C_5H_4CH_3$)Mn$(CO)_2$HSiFPh_2 (Ph = C_6H_5)," J. Am. Chem. Soc., in press.

59. D.L. Lichtenberger and A. Rai-Chaudhuri, "Electronic Structure Factors of Si-H Bond Activation by Transition Metals. The Valence Photoelectron Spectra of (η^5-$C_5H_4CH_3$)Mn(CO)(PMe_3)HSiCl_3 and (η^5-$C_5H_4CH_3$)Mn(CO)(PMe_3)HSiHPh_2 (Me is CH_3, Ph is C_6H_5)", Inorg. Chem., in press.

60. D.L. Lichtenberger, R.L. Johnston, K. Hinkelmann, T. Suzuki and F. Wudl, "The Relative Electron Donor Strengths of TTF Derivatives: Effects of Chemical Substitutions and the Molecular Environment from a Combined Photoelectron and Electrochemical Study, J. Am. Chem. Soc., submitted August 1989.

61. D.L. Lichtenberger and A.S. Copenhaver, "Ionization Band Profile Analysis in Valence Photoelectron Spectroscopy," J. Elec. Spec. Rel. Phen., submitted August 1989.

62. D.L. Lichtenberger, R.H. Hogan, M.D. Healy and A.R. Barron, "Electronic Structure and Bonding in Four-Coordinate Organometallic Complexes of Aluminum. The Valence Photoelectron Spectra of BHT-H, $Me_3Al(PMe_3)$ and Me_2(BHT)Al(PMe_3) (BHT=2,6-di-tert-butyl-4-methylphenoxide)," J. Am. Chem. Soc., in press.

63. D.L. Lichtenberger and A.S. Copenhaver, "Ionization Energy-Bond Energy Relationships in Organometallic Chemistry," *ACS Symposium Series*, submitted October 1989.

64. D.L. Lichtenberger, A.S. Copenhaver and J.L. Hubbard, "The Electronic Structure of Nitrosyl and Carbonyl Supported Metal-Metal Interactions. The Photoelectron Spectra of [η^5-(C_5H_5)Fe(μ-NO)$]_2$, [η^5-($C_5(CH_3)_5$)Fe(μ-NO)$]_2$, [η^5-(C_5H_5)Ru(μ-NO)$]_2$ and [η^5-($C_5(CH_3)_5$)Co(μ-CO)$]_2$," Polyhedron, submitted November 1989.

65. C.S.J. Chang, A. Rai-Chaudhuri, D.L. Lichtenberger, and J.H. Enemark, "He I Valence Photoelectron Spectra of Oxomolybdenum(V) Complexes Containing Diolato or Alkoxide Ligands," Polyhedron, submitted November 1989.

66. D.L. Lichtenberger and A. Rai-Chaudhuri, "Cyclopentadienyl Ring Methylation and Its Effect on Si-H Bond Activation in (η^5-$C_5H_{5-n}(CH_3)_n$)Mn$(CO)_2$HSiH$(C_6H_5)_2$ (n = 0,1,5) Complexes," Organometallics, submitted November 1989.

67. Y.C. Lee, D. Sarid, D.L. Lichtenberger, M.A. Bruck, R.H. Hogan, R.L. Johnston and K.W. Nebesny, "Scanning Tunneling Microscopy and Molecular Modeling of this Film $Mo_2(O_2CCH_3)_4$ on Single Crystal Graphite," Inorg. Chem., submitted December 1989.

68. D.L. Lichtenberger and A. Rai-Chaudhuri, "Electronic Structure Factors of Ge-H Bond Activation by Transition Metals. Photoelectron Spectra of (η^5-C_5H_5)Mn$(CO)_2$HGePh_3, (η^5-$C_5H_4CH_3$)Mn$(CO)_2$HGePh_3 and (η^5-$C_5(CH_3)_5$)Mn$(CO)_2$HGePh_3 (Ph is C_6H_5)," J. Chem. Soc. Dalton Trans., submitted December 1989.

A STUDY OF CATALYSTS AND MECHANISMS IN SYNTHESIS REACTION

Jack H. Lunsford
Department of Chemistry, Texas A&M University
College Station, Texas 77843

OBJECTIVES: Surface-generated gas-phase radicals give rise to a phenomenon which is commonly known as heterogeneous-homogeneous catalysis. The objectives of the current research are to determine the factors which influence the formation of hydrocarbon radicals at surfaces, as well as their subsequent reactions on the surface and in the gas phase.

INTRODUCTION

The role of surface-generated gas-phase radicals is best illustrated in the catalytic oxidative dimerization of methane to ethane. We previously demonstrated that methyl radicals, formed on the surface of lithium-promoted magnesium oxide (Li^+/MgO) and sodium-promoted calcium oxide (Na^+/CaO) emanate into the gas phase where they couple to form ethane, which in turn is dehydrogenated to ethylene (1-3). Since the radicals collide many times with a surface before they react in the gas phase, it is important that these secondary reactions not result in undesirable side products. The reactions of radicals with metal oxide surfaces constitute a largely unexplored area of surface chemistry, therefore it was of interest to determine first the relative activities of metal oxides with methyl radicals and ultimately the specific activities of selected oxides. Moreover, it was found that a very reactive surface could be modified by the addition of an alkali metal carbonate, and that such modifications caused a profound effect on the catalytic properties of the oxide. With the addition of Na_2CO_3 it is possible, for example, to transform CeO_2 from a very active, but nonselective CH_4 oxidation catalyst to a moderately active and selective oxidative dimerization catalyst. Other systems, such as $NaMnO_4/MgO$ have been examined to determine whether the coupling even occurs in the gas phase.

As a complementary technique to the matrix-isolation electron spin resonance (MIESR) system that was developed in our laboratory, a laser-induced fluorescence (LIF) spectrometer is being employed to study OH• radicals that are formed during the oxidation of CH_4. In addition to coupling, the surface-generated CH_3• radicals become involved in chain-branching reactions which yield OH• radicals. An extended goal of the project is to determine the vibrational and rotational temperatures of the radicals relative to the temperature of the surface.

SECONDARY REACTIONS OF METHYL RADICALS WITH LANTHANIDE OXIDES AND TRANSITION METAL OXIDES

The lanthanide oxides offer an excellent opportunity to study the relationship between methyl radical formation activity, secondary reactions of methyl radicals with an oxide, and overall catalytic properties because members of the series vary greatly with respect-to each of these factors. A study has been completed on the radical forming ability of selected members of the series and the secondary reactions which occur among these oxides (4). Except for Yb_2O_3 there is an inverse relationship between radical formation ability and the efficiency for reaction with the radicals. The oxides fall into three categories with respect to radical formation/reaction: (i) the more basic sesquioxides are good radical formers, but they do not react extensively with the radicals; (ii) those oxides which exhibit multiple cationic oxidation states react extensively with the oxides; and (iii) Yb_2O_3 is neither a very good radical former nor a good radical scavenger.

Generally, in the pure form only the basic sesquioxides are good oxidative dimerization catalysts (5,6), which is consistent with their ability to produce but not react with $CH_3\cdot$ radicals. But it is also known that certain of the oxides with multiple cationic oxidation states can be transformed into selective catalysts by the addition of Na_2CO_3. Using CeO_2 as an example we have shown (Fig. 1) that the addition of Na_2CO_3 decreases the $CH_3\cdot$ reaction efficiency, increases the rate of $CH_3\cdot$ radical formation and increases the C_2 selectivity. Thus, the catalyst was transformed from being totally nonselective to one which gave 60% C_2 selectivity.

More recently we have become interested in the state of the catalysts modified with Na_2CO_3 and have chosen to study three examples of the classes noted above: La_2O_3, CeO_2 and Yb_2O_3. It was found using ion scattering spectroscopy (ISS) that the surface of the CeO_2 catalyst promoted with Na_2CO_3 was completely covered with sodium-containing compounds, which suggests that sodium oxide (e.g. Na_2O_2) was responsible for the oxidative dimerization activity, rather than a new oxide phase involving Na and Ce. The catalysts Na^+/CeO_2, Na^+/La_2O_3, Na^+/Yb_2O_3, and even Na_2CO_3 all have approximately the same specific activity for CH_4 conversion, and all have similar C_2 selectivities. Moreover, there is a good correlation between the activity for CH_4 conversion and the rate of $CH_3\cdot$ formation. Thus, the lanthanide oxides essentially function as supports for the sodium carbonate/oxide phase, and in some cases supply oxygen to this phase when molecular oxygen is not available (7).

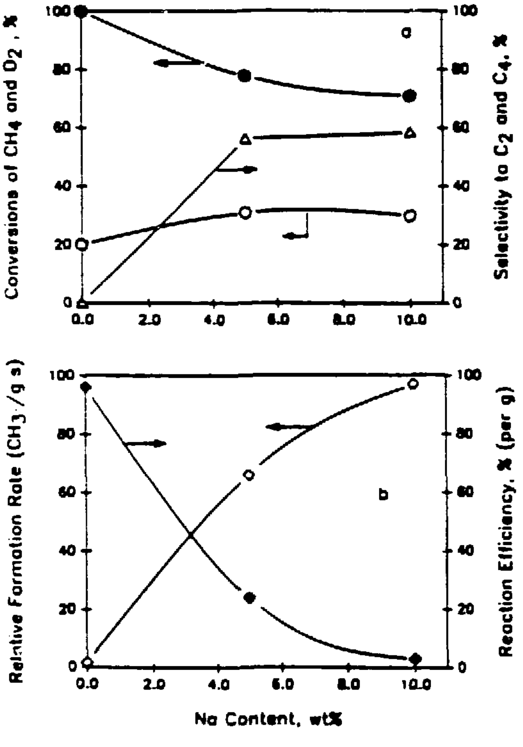

Figure 1. Effect of Na_2CO_3 addition to CeO_2 on (a) the catalytic oxidation of CH_4 and (b) the production of $CH_3\cdot$ radicals and their reaction with the catalyst: ○, CH_4 conversion; ●, O_2 conversion; △, combined C_2 and C_4 selectivity; ◇, relative formation rate of $CH_3\cdot$ radicals; ◆, reaction efficiency of $CH_3\cdot$ radicals with the catalysts. The catalytic reaction was carried out at 770°C, 1 atm, and a flow rate of 34 mL min^{-1}. The partial pressures of CH_4 and O_2 were 180 and 67 Torr, respectively. The $CH_3\cdot$ formation rates and the reaction efficiencies were determined with the catalysts at 760 and 470°C, respectively. The gas pressures were 1 and 1.5 Torr for the two cases.

A number of other transition metal oxides have been investigated as methyl radical scavengers, and all of them are quite reactive. Those metal ions having multiple oxidation states are believed to react according to

$$M^{(n+1)+}O^{2-} + CH_3\bullet \rightarrow M^{n+}(OCH_3)^- \qquad (1)$$

where the methoxide ion would be an intermediate in the formation of CO_2. The high reactivity of zirconium oxide is surprising as Zr^{4+} is difficult to reduce to the metal and does not have other easily accessible oxidation states. Sodium-promoted ZrO_2 is unique among the methane oxidation catalysts in that it yields large amounts of propane and propylene (8). Perhaps it does this by adsorbing $CH_3\bullet$ through a nonoxidative reaction.

In contrast to the numerous systems that appear to involve a heterogeneous-homogeneous reaction scheme it has been argued by Hatano and Otsuka (9) that the mechanism on the monophasic $LiNiO_2$ catalyst is primarily a surface phenomenon. That is, $CH_3\bullet$ radicals are adsorbed and couple on the surface. Under the typical conditions of the MIESR experiment, which involve very low partial pressures of O_2 so as to minimize the formation of $CH_3O_2\bullet$ radicals in the cooler regions of the system, we indeed observed that the gas phase $CH_3\bullet$ radical concentrations from $LiNiO_2$ and $NaMnO_4/MgO$ (an ARCO catalyst) were remarkably less than those observed with La_2O_3 or Li^+/MgO as the catalyst. The MIESR system was modified, however, so that the leak into the high vacuum region was in the center of a catalyst bed, operating under conventional catalytic conditions. The results depicted in Figure 2 show that the (C_2^+ yield)$^{1/2}$ is related in a linear manner with respect to the $CH_3\bullet$ radical concentration, and that the absolute values of both parameters are approximately the same for the $LiNiO_2$, $NaMnO_4/MgO$ and Li^+/MgO catalysts. These results demonstrate that in the presence of sufficient amounts of O_2 the oxidative coupling of CH_4 occurs via gas phase $CH_3\bullet$ radicals over the transition metal oxide catalysts $LiNiO_2$ and $NaMnO_4/MgO$, just as was observed previously for Li^+/MgO.

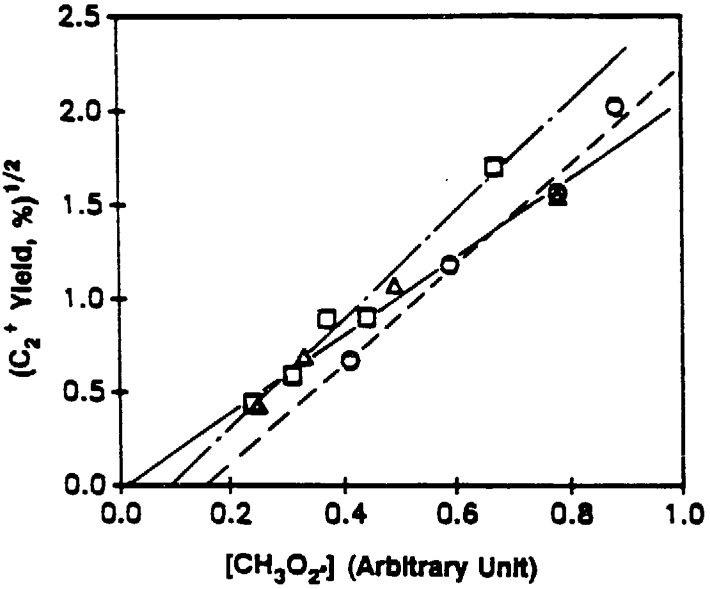

Figure 2. Relationship between the yield of C_2 products and the formation of $CH_3\bullet$ radicals (observed as $CH_3O_2\bullet$ radicals): Δ, $NaMnO_4/MgO$; □, Li^+/MgO; ○, $LiNiO_2$. The reactions were carried out at atmospheric pressure over a range of temperatures and O_2 flow rates.

DETECTION OF HYDROXYL RADICALS USING THE LASER INDUCED FLUORESCENCE SYSTEM

The laser-induced fluorescence system used in our lab consists of a Quantel dye laser pumped by a YAG laser, a Stanford Research gated photon counter with a fast preamplifier, and a lab computer used for data acquisition and instrument control. UV generation is supplied by a frequency doubling crystal with typical output energy of 10 mJ per pulse. Fluorescence is focused onto a photomultiplier tube with appropriate filters. Our initial experiments are designed for the detection of OH• radicals near a catalytically active surface using single photon excitation. Preliminary results indicate resonance fluorescence of OH (0,0) at 308 nm near a heated quartz disk with 7% Li^+/MgO on the surface in a CH_4/O_2 gas flow. Using similar techniques CH, CH_2 or other radicals might also be detected.

REFERENCES

1. Driscoll, D.J.; Martir, W.; Wang, J.-X.; Lunsford, J.H. J. Am. Chem. Soc., 1985 107, 58.
2. Campbell, K.D.; Morales, E.; Lunsford, J.H. J. Am. Chem. Soc., 1987, 109, 7900.
3. Campbell, K.D.; Lunsford, J.H. J. Phys. Chem., 1988, 92, 5792.
4. Tong, Y.; Rosynek, M.P.; Lunsford, J.H. J. Phys. Chem., 1989, 93, 2896.
5. Otsuka, K.; Jinno, K.; Morikawa, A. J. Catal., 1986, 100, 353.
6. Lin, C.-H.; Campbell, K.D.; Wang, J.-X.; Lunsford, J.H. J. Phys. Chem., 1986, 90, 534.
7. Gaffney, A.M.; Jones, C.A.; Leonard, J.J.; Sofranko, J.A. J. Catal., 1988, 114, 422.
8. Matsuhashi, H.; Sakurai, K.; Arata, K. Chem. Lett., 1989, 585.
9. Hatano, M.; Otsuka, K. J. Chem. Soc., Faraday Trans. 1, 1988, 85, 199.

PAPERS PUBLISHED

1. "Formation of Gas-Phase Methylallyl Radicals during the Oxidation of 1-Butene and Isobutylene over Bismuth Oxide," Driscoll, D.J.; Martir, W.; Lunsford, J.H. J. Phys. Chem., 1987, 91, 3585.

2. "Surface-Generated Gas-Phase Radicals: Formation Detection and Role in Catalysis," Driscoll, D.J.; Campbell, K.D.; Lunsford, J.H. Adv. Catal., 1987, 35, 139.

3. "Methane Activation by the Lanthanide Oxides," Campbell, K.D.; Lunsford, J.H. J. Phys. Chem., 1988, 92, 750.

4. "The Contributions of Gas-Phase Radical Coupling in the Catalytic Oxidation of Methane," Campbell, K.D.; Lunsford, J.H. J. Phys. Chem., 1988, 92, 5792.

5. "Secondary Reactions of Methyl Radicals with Lanthanide Oxides: Their Role in the Selective Oxidation of Methane," Tong, Y.; Rosynek, M.P.; Lunsford, J.H. J. Phys. Chem., 1989, 93, 2896.

6. "The Role of Surface-Generated Gas-Phase Radicals in Catalysis," Lunsford, J.H. Langmuir, 1989, 5, 12. [Presented as the Langmuir Lecture at the Division of Colloid and Surface Chemistry, Los Angeles ACS Meeting, Sept. 1988.]

Structure and Reactivity of Model Thin Film Catalysts

Theodore E. Madey
Rutgers, The State University of New Jersey
Department of Physics and
Laboratory for Surface Modification
Piscataway, New Jersey 08855-0849

I. Introduction

The purpose of this project is to characterize the structure and reactivity of model bimetallic catalysts, e.g., ultrathin films of Pt and other metals deposited on single crystal surfaces of tungsten. Recent studies have focused on comparisons between the atomically smooth W(110) surface and the atomically rough W(111) surface using several ultrahigh vacuum surface science methods (low energy electron diffraction, LEED, Auger electron spectroscopy, AES, and thermal desorption spectroscopy, TDS). In addition, we have used scanning tunneling microscopy (STM) to provide a microscopic view of Pt induced surface structures with Angstrom level resolutions.

Whereas a monolayer of Pt on close-packed W(110) is thermally stable to ~2000 K, we have found a surprising result for Pt on W(111). When W(111) is covered by $> 1 \times 10^{15}$ Pt atoms/cm^2 and heated in the range 800-1600 K, the surface undergoes a massive restructuring to form *microscopic facets*. At 1200 K, the average facet dimensions are >100 Å, and the dominant facet orientation is W(211). The faceting appears to be driven by a Pt-enhanced anisotropy in the surface free energy. To the best of our knowledge, the only other reports of faceting induced by a single monolayer of metal on a metal surface are based on field emission microscopy.

The Principal Investigator joined Rutgers in Fall 1988, and initiated this project shortly afterwards. It is an outgrowth of work performed by the PI and his colleagues at the National Institute of Standards and Technology (formerly NBS).

II. Recent Results

A. Pt on W(110)

Pt grows in a layer-by-layer mode on W(110) at 300K, starting with a pseudomorphic monolayer. Heating multiple layers of platinum on W(110) causes all but the first layer to agglomerate into three-dimensional clusters on the surface of the tungsten. The first layer remains dispersed in a single atomic layer with the crystal structure of the underlying tungsten, and requires a higher temperature for evaporation than does the excess platinum.

Platinum-covered W(110) exhibits unusual surface chemistry in the presence of reactive gases such as carbon monoxide and oxygen. For example, a platinum monolayer on W(110) adsorbs carbon monoxide more weakly than either bulk platinum or the tungsten substrate. Oxygen facilitates clustering of Pt on W(110), even for fractional monolayers of Pt. The unique nature of the platinum monolayer is reinforced by the results of valence-level photoelectron spectroscopy experiments performed using synchrotron radiation. The layer of Pt yields a valence spectrum that is different from those of subsequent layers; i.e., the intensity 1-2eV below the Fermi level is greatly reduced, suggesting the electronic structure of a noble metal.

B. Pt on W(111)

The behavior of Pt on W(111) is very different from that on W(110). The Pt-covered W(111) surface is unstable upon heating, and reconstructs to form facets. Evidence for facet formation is based on a combination of LEED and STM studies.

When Pt is deposited onto W(111) at 300K, no distinct new features are seen in LEED. When the surface is covered with $>1.1 \times 10^{15}$ Pt atoms/cm^2 and heated in the range 800 to 1600K, the LEED observations are very different: LEED beams appear which can be identified with the formation of microscopic W(211) facets with average facet dimensions >100 Å.

An STM image of the faceted W(111) surface is shown in Figure 1. For this experiment, the clean W(111) surface was dosed with several monolayers of Pt and heated under uhv conditions to 1200K. The Figure shows a number of pyramidal facets having average dimensions >100 Å.

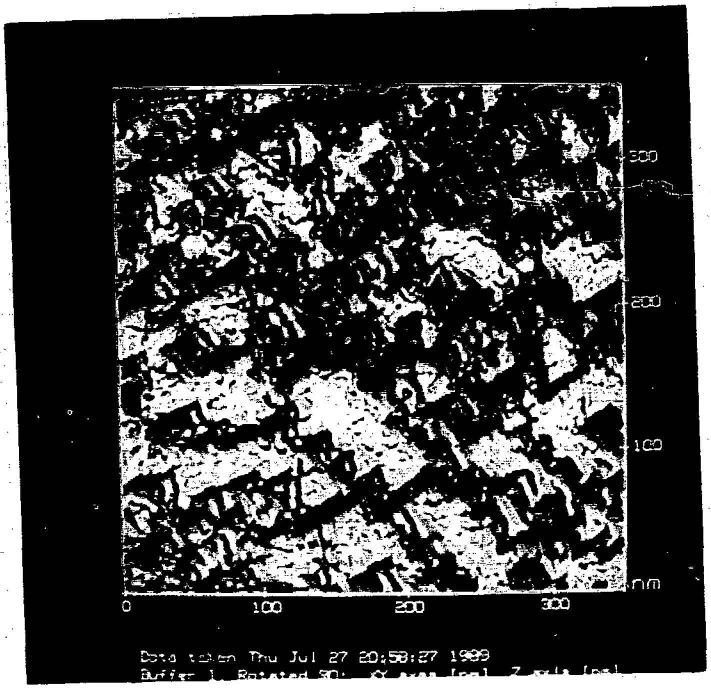

Figure 1. Scanning Tunneling Micrograph of Pt-induced facets on W(111). Top view of 3500 Å square area.

Scans over different regions of the surface show that the surface is completely covered by such pyramidal facets. In contrast, the back side of the crystal that was <u>not</u> dosed with Pt remains planar: there is no massive reconstruction of W(111) upon heating in the absence of Pt.

We are presently conducting detailed LEED and STM studies of Pt on W(111), including the kinetics of facet formation and the influence of temperature and Pt coverage on the facet morphology. We have also initiated studies of other metal films, and have found evidence that a monolayer of Au will also induce faceting of W(111).

We believe that the observation of Pt-induced faceting on W(111) may have far-reaching implications for structural effects in bimetallic catalysts. Until the present, most studies of metals-on-metals have been for atomic close-packed substrates (bcc (110), fcc (111), (100)) which do not exhibit faceting. However small catalyst particles with high defect concentration may well undergo structural rearrangements to new shapes which are different for particles coated with other metals than for "clean" metallic particles.

III. Future Plans

We will continue to study and characterize the relation between microscopic surface structure and chemical reactivity for model bimetallic catalysts, i.e., ultrathin films of metals-on-metals. We will focus on atomically rough "unstable" single crystal surfaces that may undergo massive reconstruction and faceting when coated with ultrathin metal films (~ monolayer thick), upon annealing to elevated temperatures. Such surfaces include the body-centered-cubic (111) and the face-centered-cubic (210) surfaces. The general issues we will address are:

- To identify the conditions for facet formation on atomically rough metal crystal surfaces (W, Ni, Mo, Re) covered with ultrathin metal films, (i.e., what are the effects of surface crystal orientation, nature of metal substrate, nature of metal overlayer, presence of impurity gas atoms, temperature, etc.).
- To compare the surface chemistry and catalytic activity of ultrathin films on both planar (before faceting) and faceted surfaces; i.e., to relate surface structure to reactivity. Both chemisorption (CO, O_2, H_2, C_2H_6) and catalytic activity (hydrogenolysis reactions) will be studied.

We want to know how and why facets form on bimetallic catalysts, and to what extent faceting is a factor in determining chemisorption properties and steady state catalytic reaction rates over such surfaces.

IV. Recent Publications

(1) "Characterization of Ultrathin Platinum Overlayers Deposited on a W(110) Surface", S. M. Shivaprasad, R. A. Demmin and T. E. Madey, Thin Solid Films 163, 393 (1988).
(2) "Adsorption Properties of Pt Films on W(110)", R. A. Demmin, S. M. Shivaprasad and T. E. Madey, Langmuir 4, 1104 (1988).
(3) "Photoemission Studies of Pt Overlayers on W(110)", R. A. Demmin, R. L. Kurtz, R. Stockbauer, T. E. Madey, D. L. Mueller and A. Shih, submitted.
(4) "The Interaction of Oxygen and Platinum on Tungsten (110)", R. A. Demmin and T. E. Madey, J. Vac. Sci. Technol. A7, 1954 (1989).
(5) "Faceting Induced by an Ultrathin Film: Pt on W(111)", K.-J. Song, R. A. Demmin, C. Z. Dong, E. Garfunkel, T. E. Madey, Surface Science Letters, in press (1990).

The Dynamics of Non-Dissociative and Dissociative Adsorption on Pt(111)

Robert J. Madix, Chris R. Arumainayagam, Mark C. McMaster and Greg R. Schoofs
Departments of Chemistry and Chemical Engineering, Stanford University, Stanford, CA 94305

Grant Title: Molecular Beam Studies of the Dynamics and Kinetics of Heterogeneous Reactions on Single-Crystal Surfaces

Part I: Trapping Dynamics

The first step in most heterogeneously catalyzed reactions is the adsorption of reactant gases on the surface. Hence a fundamental understanding of catalysis requires the examination of the critical parameters which govern the adsorption process. Such factors include the effects of the incident velocity, angle of incidence, surface temperature, surface coverage, binding energy, shape of the gas-surface interaction potential and changes in internal degrees of freedom. To elucidate such factors, we have investigated several non-dissociative, weakly interacting gas-surface systems. Such systems provide relatively simple cases to understand fundamental aspects of adsorption phenomena, including physical adsorption which is an important aspect of catalyst characterization.

The trapping dynamics of weakly interacting gas-surface systems can also provide insight into precursor mediated dissociation. Although direct collisional activation may occur with high probability, only a negligible fraction of a Maxwell-Boltzmann gas at room temperature possesses sufficient energy to overcome the barrier for direct dissociation. In contrast the barrier to precursor mediated dissociation may be significantly lower. Moreover, due to the statistical preponderance of molecules possessing low enough energies to trap, precursor mediated dissociation may be an important route to dissociative chemisorption.

Previously, adsorption probabilities of weakly interacting non-dissociative, gas-surface systems were measured using indirect methods such as deconvoluting angular distributions, which required making several assumptions. In addition, a majority of these studies utilized effusive molecular beam sources. In contrast, we have used *supersonic* molecular beams and a *direct* technique (Fig. 1) to probe the adsorption dynamics of weakly interacting gas-surface systems at surface temperatures sufficiently low that competitive desorption is minimal and at translational energies significantly below the threshold for direct collisional activation. We have also extended this technique to study desorption kinetics in addition to adsorption dynamics.

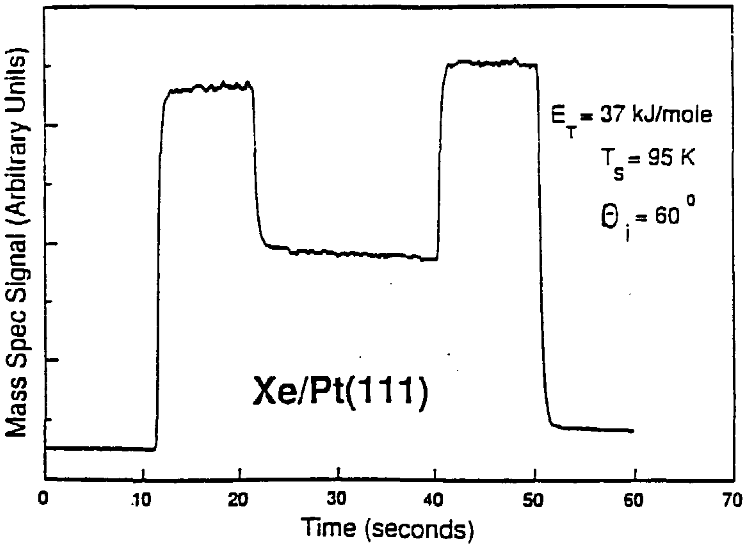

Fig. 1 Representative results obtained in a direct trapping probability experiment involving a 37 kJ/mole Xe beam incident at an angle of 60° on a Pt(111) surface held at 95 K are shown above. The trace is a plot of the Xe partial pressure in the UHV chamber as a function of time. Initially the base line pressure was recorded with no beam entering the chamber. Approximately 12 seconds later the beam was admitted into the chamber by opening the shutter, causing the Xe partial

pressure to rise. The flag in the UHV chamber prevented the beam from striking the crystal. After the Xe partial pressure had risen to its steady state value, the flag was removed causing the Xe partial pressure to drop as the Pt(111) crystal adsorbed a fraction of the incident beam. The initial trapping probability equals the ratio of the Xe partial pressure drop when the flag was removed to the Xe partial pressure rise when the shutter was opened.

We have investigated the trapping dynamics of CH_4, C_2H_6, C_3H_8, CO_2 and Xe on Pt(111). In each case the initial trapping probability decreases with increasing incident translational energy at a fixed angle of incidence (Fig. 2). This trend is readily understood since a fast atom or molecule is less likely to lose sufficient translational energy in order to be trapped than a slow atom or molecule. We have extended a one-dimensional model based on classical mechanics to include trapping and have found semi-quantitative agreement with experimental results for the dependence on translational energy. At a fixed translational energy, the initial trapping probability increases with increasing incident angle (Fig. 2) demonstrating the lesser importance of parallel momentum exchange as compared to normal momentum exchange in the trapping process. Such behavior is expected from simple one-dimensional theories. However, the angular dependence of the initial trapping probability shows the participation of parallel momentum in the trapping process. For example, the initial trapping probability of Xe on Pt(111) scales with $E_T \cos \theta_i$ rather than with $E_T \cos^2 \theta_i$ ("normal energy scaling"), in contradiction to one-dimensional theories.

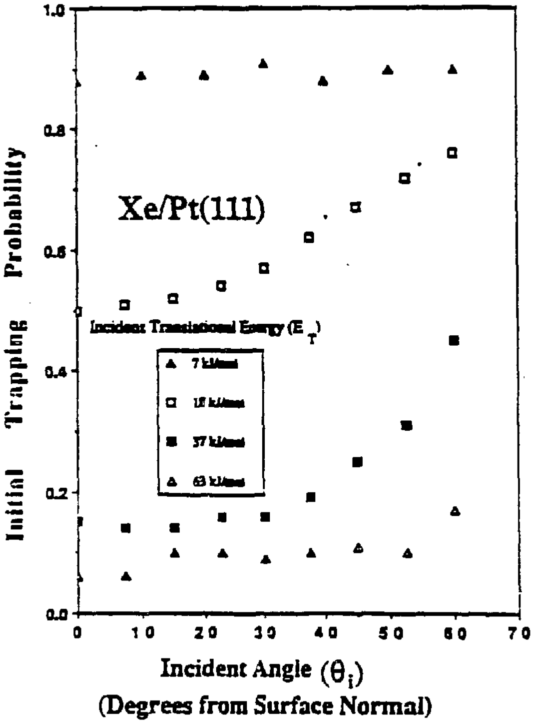

Fig 2 The initial trapping probability of Xe on Pt(111) as a function of incident angle and translational energy. The surface temperature for these experiments was 95 K.

Failure of the flat-surface models to correctly reproduce our experimental trends prompted us to collaborate with Dr. John Tully at AT&T Bell Labs to simulate our Xe/Pt(111) data for the dependence on translational energy and incident angle using three-dimensional stochastic trajectory calculations. It was necessary to employ a Morse potential instead of a Lennard-Jones potential to represent the Xe-Pt interaction in order to vary the steepness of the repulsive wall of the gas-surface potential independent of its corrugation. The calculations reproduced our experimental results employing realistic interaction parameters.

We have also partially quantified the dependence of the trapping probability on surface temperature and surface coverage. Our experimental results based on the angular distribution of CH_4 scattered from the Pt(111) surface at temperatures of 160 K and 500 K suggest that the trapping probability is not a sensitive function of surface temperature. In contrast to the sticking probability of strongly interacting gas-surface systems, the trapping probability of ethane increases with surface coverage indicating that molecules trap better onto adsorbates than onto a clean surface due to more efficient energy transfer. We are extending these measurements in order to better quantify the phenomena and to determine the dynamics of trapping into the second layer.

Our measurements of the initial trapping probability as a function of normal translational energy and previous mean translational energy measurements for molecules desorbing from Pt(111) at the surface normal agree with each other in accordance with the principle of detailed balance (microscopic reversibility).

Currently, we are investigating the trapping dynamics of more complex molecules in order to understand the role of internal degrees of freedom. We plan to study trapping on overlayers to investigate the energy exchange between incident molecules and adsorbates. In addition to providing insight into precursor kinetics, these studies can provide a basis for understanding phenomena at high pressures when the surface may be covered with adsorbed intermediates. Our experimental and theoretical studies are uncovering some general principles underlying the adsorption process, a key step in most heterogeneously catalyzed reactions.

Part II : Dynamics of Alkane Activation

Since alkanes constitute an abundant natural resource, their catalytic activation offers promise for conversion to useful chemicals. Using supersonic molecular beam and standard UHV techniques, we have delineated the role of translational energy, incident angle, surface temperature and surface corrugation in the activated chemisorption of methane on Pt(111). The nozzle temperature and stagnation pressure were both fixed so that the incident internal energy was kept constant. The initial dissociative sticking probability increases exponentially ($0.01 < S_0 < 0.19$) with incident normal translational energy (68 kJ/mole $< E_n <$ 95 kJ/mole) and is independent of surface temperature (500 K $< T_s <$ 1250 K) demonstrating that dissociation occurs *via* direct collisional activation rather than *via* trapping processes at these translational energies.

The exponential dependence of the initial dissociative sticking probability on incident normal translational energy can be fit with a model for dissociative methane adsorption proposed previously by others that involves quantum mechanical tunnelling of a hydrogen atom through a one-dimensional, parabolic barrier of height 121 kJ/mole with a thickness at half height of 0.13 Å. Differences in the initial dissociative sticking probabilities observed on Pt(111) versus Ni(111) and W(110) in studies from different laboratories can be reconciled on the basis of the different vibrational energies employed, but this explanation does not account for the high reactivity on Ir(110)-(1x2). Work is planned to determine the temperature coefficient of the reaction on Pt(111) over a wider range of translational energies to determine if differences in vibrational energies do indeed account predominantly for the different reactivities. For the results obtained to date, activation barrier heights for methane dissociation show semi-quantitative agreement with the barrier heights estimated from the bond order conservation theory.

We have performed similar experiments to study ethane activation on Pt(111). In these experiments we have varied the nozzle temperature to probe the influence of incident vibrational energy on the direct collisional activation of ethane. Our results indicate that the effect of vibrational energy on reactivity is secondary to that of translational energy in the range of energies studied.

INTERACTION OF CARBON AND SULFUR ON METAL CATALYSTS

J. J. Vajo*, G. T. Tong, B. J. Wood and B. J. Wood and J. G. McCarty
Materials Research Laboratory, SRI International, Menlo Park, CA 94025

PROJECT SUMMARY

During the past two years an investigation of the influence of sulfur chemisorption on the segregation thermodynamics of carbon on Ni(100) was completed. The effect of uniformly sulfur poisoning on Fischer-Tropsch synthesis by iron catalysts and the formation and nature of carbon deposits on ruthenium steam reforming catalysts were also investigated.

Thermodynamics of Carbon Coadsorbed with Sulfur on Ni(100)

The thermodynamics of the segregation of dissolved carbon to a Ni(100) surface containing adsorbed sulfur has been studied by stimulated desorption using a low current pulsed Ar^+ beam at 2 keV, followed by laser ionization at 193 nm of the desorbed neutral species and reflecting time-of-flight mass spectrometry of the resulting C^+ ions. Equilibrium surface carbon coverages were measured for fractional sulfur coverages of 0, 0.1, 0.16, and 0.26 monolayers (ML) over a temperature range between 700 and 1100 K. Absolute carbon and sulfur coverages were calibrated by Auger electron spectroscopy of saturated ordered overlayer structures.

Identical carbon segregation coverages were obtained for both increasing and decreasing temperature profiles indicating that the measured carbon coverages represented equilibrium values. For fractional carbon coverages > 0.15 ML, the heat of formation of adsorbed carbon on Ni(100) was -18 ± 7 kJ/mol using the Langmuir-McLean model to describe the segregation. This value is slightly lower than the results of Blakely et al.[1,2] The heat of formation of adsorbed carbon appears to be coverage dependent and increases with increasing carbon coverage. Coadsorbed sulfur does not affect the heat of formation of adsorbed carbon for sulfur coverages ≤ 0.16 ML (Figure 1), in contrast to an earlier study.[3] For a sulfur coverage of 0.26 ML the heat of formation of adsorbed carbon increases only 17 kJ/mol to -11 ± 4 kJ/mol. Coadsorbed sulfur reduces the maximum coverage of segregated carbon on Ni(100) from 0.5 ML for Ni(100) with no coadsorbed sulfur to 0.24 ML for a sulfur coverage of 0.26 ML. Therefore, the effect of chemisorbed sulfur on carbon segregation is mostly geometric with no evidence of a long-range electronic influence.

Effect of Sulfur Poisoning on Fischer-Tropsch Synthesis by Iron

In work partially supported by DOE (PETC), substantial changes in selectivity of fused iron catalysts were found following treatment to uniformly chemisorb submonolayer quantities of sulfur.[4] After reduction and passivation by accumulation of a surface layer of carbon and chemisorbed CO, approximately 40% of saturated coverage of sulfur was slowly adsorbed at 473 K on the fused iron catalyst. The passivating layer was removed and the sulfur locally dispersed by heating to 1000 K in hydrogen. Low-level (20% saturation sulfur coverage) and medium-level (about 50% saturation sulfur coverage) sulfur treated catalysts were prepared in this way.

---

* Currently at Hughes Aircraft Company Research Center, Malibu, CA

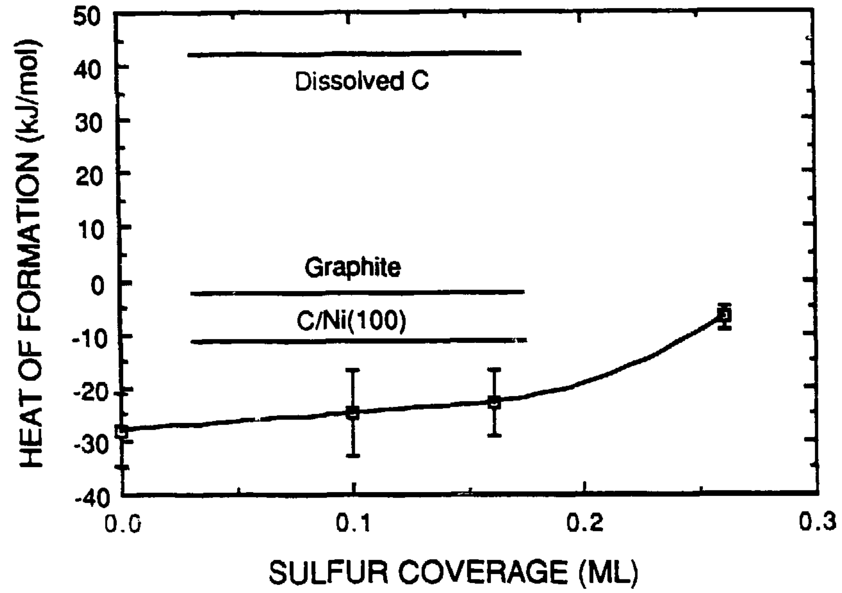

Figure 1. Heat formation for carbon segregation to the Ni(100) surface as a function of sulfur coverage.

The treated catalysts had as much as 65% reduction in methane selectivity relative to the untreated reduced fused iron in 2:1 H_2:CO syngas at 573 K and 100 kPa (Figure 2). The olefin selectivity (Figure 3) at low pressure 1-atm) approached 100% ($C_2H_4/C_2H_6 > 20$). The sulfur treatment decreased the C_{2+} production rate at 573 K to only about half the rate of the untreated catalyst per unit area and was comparable to the stationary-state activity of clean fused iron at 523 K.

The Role of Sulfur in Carbon Deposition on Steam Reforming Catalysts

In experiments supported in part by a commercial sponsor, the deposition of carbon on 2 wt% ruthenium and 15 wt% nickel alumina-supported catalysts during steam reforming of naphtha were examined as a function of sulfur coverage up to saturation.[5] The steam reforming catalysts were pretreated, as described for the iron FTS catalysts, in a recirculation apparatus with low levels of H_2S in H_2 to obtain uniform submonolayer coverages that were predictable from known equilibrium constants for chemisorption.[6] These catalysts samples were then used in 24-h steam reforming runs in a microreactor at 763 K and 25 atm with a sulfur-free naphtha feedstock containing various amounts of steam and added hydrogen. On-line mass spectrometry and gas chromatography were used to monitor the activity of the catalyst during the urn. Subsequent sequential *in situ* temperature programmed reaction (TPR) experiments in 10-atm H_2 and in dilute O_2 revealed the existence and quantity of carbon in states with characteristic reactivities.

Carbon deposits form on catalysts under a broad range of feedstock compositions, but not all deposits lead to continuous coking (Figure 4). On clean catalysts and those with low-level sulfur coverages, the deposited carbon is in states that are gasified by reaction with H_2 and steam. Such carbon can accumulate only to a limited steady-state level, hence, continuous coking does not occur at this temperature (490°C). On catalysts with sulfur coverage greater than half-saturation, carbon

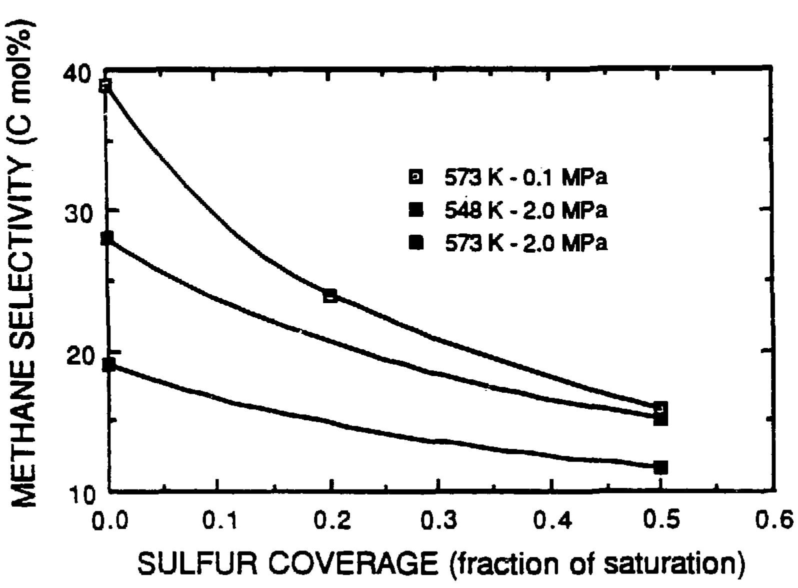

Figure 2. The effect of fractional sulfur poisoning on methane selectivity as a function of temperature and pressure for the Fischer-Tropsch synthesis by fused iron catalysts with $H_2/CO = 1$.

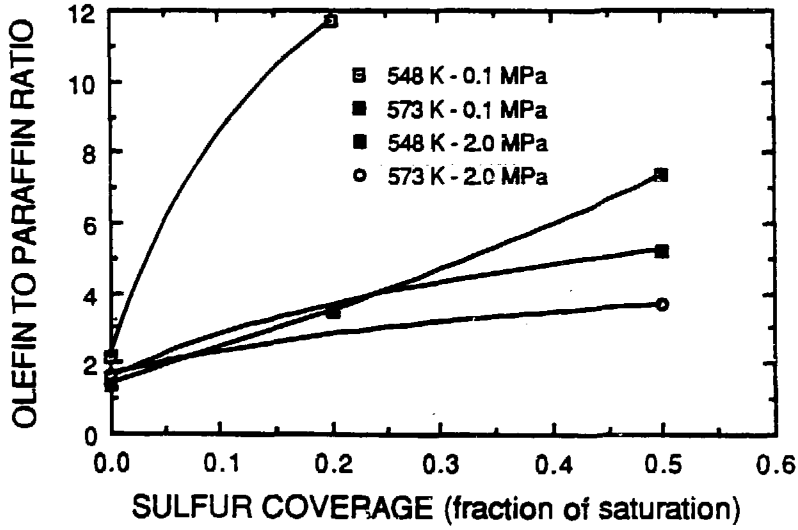

Figure 3. The effect of fractional sulfur poisoning on the olefins/paraffins ratio (C_2-C_6) as a function of temperature and pressure for the Fischer-Tropsch synthesis by fused iron catalysts with $H_2/CO = 1$.

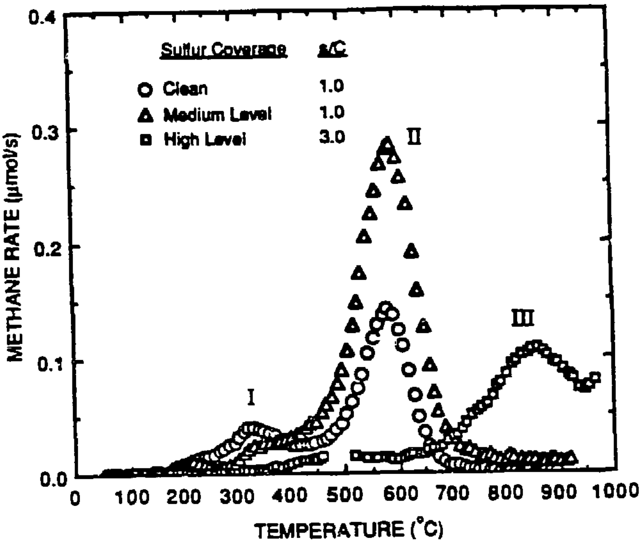

Figure 4. The effect of sulfur coverage and feedstock steam-to-carbon ratio (s/C) on the reactivity of carbon deposited on Ru/Al_2O_3 catalysts during steam reforming of light naphtha at 490 °C and 25-atm. Temperature programmed reaction with 10-atm H_2 at 0.5 K/s produces maxima in the methane formation rate at 320 °C for adsorbed hydrocarbons (I), at 580 °C for catalyst carbon (II), and at 830 °C for low reactivity carbon (III) deposited on sulfur poisoned catalysts.

deposits in non-reactive states. The amount of carbon in these states grows continuously and leads ultimately to fouling of the catalyst by coking. We have used TPR to define the boundaries for deposition of such low reactivity carbon in terms of critical steam/carbon and hydrogen/carbon ratios in the steam reforming feedstock.

FUTURE WORK

The effort of uniform sulfur poisoning on carbon deposits a Pt/Al_2O_3 catalysts will be completed before the end of 1990. Unpublished work for carbon and sulfur interaction and for , sulfur diffusion on Ni(100) and Ni(111),sulfur chemisorption on supported copper, and the effect of sulfur poisoning on FTS by fused iron will be submitted for publication.

REFERENCES

1. L. C. Isett and J. M. Blakely, Surface Sci. **47**, 645 (1975).
2. L. C. Isett and J. M. Blakely, Surface Sci. **58**, 397 (1976).
3. R. Ramanathan, M. A. Quinlan, and H. Wise, Chem. Phys. Lett. **106**, 87 (1984).
4. G. T. Tong, B. J. Wood, and J. G. McCarty, "The role of sulfur poisoning on Fischer-Tropsch selectivity by fused iron catalysts," presentation at the 10th North American Meeting of the Catalysis Society, San Diego (1987), (to be published).
5. G. T. Tong, B. J. Wood, J. G. McCarty, O. Okada, M. Masuda, and T. Tabata, "The Role of Sulfur in the Deposition of Carbon on Steam Reforming Catalysts," presentation at the 11th North American Meeting of the Catalysis Society, Detroit (1989), (to be published).
6. J. G. McCarty and H. Wise, J. Chem. Phys. **72**, 6332 (1980).

Catalytic Chemistry in Supercritical Media

J. W. Rathke, R. J. Klingler, and M. J. Chen

Chemical Technology Division
Argonne National Laboratory

Research Scope and Objectives. This research is designed to determine reaction mechanisms and to explore new catalytic chemistry associated with molecular energy resources. An array of real-time high-pressure kinetic and spectroscopic techniques is used to determine the chemistry of small molecules derived from coal, natural gas, and petroleum. Maximal concentrations of reactive gases are achieved by making use of their complete miscibilities with supercritical fluids. Thus, we have recently determined the potential energy profile for activation of hydrogen by the commercial Oxo catalyst in supercritical carbon dioxide solution using high-pressure NMR spectroscopy. In other research, solution-phase oxide catalyzed hydrogenation and water-gas shift processes that seem to parallel metal oxide surface chemistry are explored. Also investigated is the organometallic chemistry of extremely robust metallophthalocyanines designed to achieve stereoselective homogeneous hydrogenation and oxidation catalyses at unusually high temperatures.

Recent Results. Due to their complete miscibilities with these gases, supercritical fluids appear to be nearly ideal media for conducting homogeneous catalytic reactions that involve H_2, CO, and CO_2. For example, the concentration of H_2 at 25°C and a partial pressure of 300 atm in supercritical CO_2 is 12 M, while in typical liquid media such as water and n-heptane the hydrogen concentrations under these conditions are only 0.23 and 1.8 M, respectively. In addition, since there exists no liquid/gas interface in the supercritical system, stirring to achieve gas dissolution is unnecessary, and laborious measurements of gas/liquid partition coefficients are not required to produce meaningful thermodynamic and kinetic results. Because catalyst and substrate solubilities vary sharply with density of the supercritical medium, which in turn is controlled by pressure, catalyst or substrate concentrations and recovery could, in principle, be controlled solely by facile pressure alterations.

In order to begin exploration of the potential of supercritical media for homogeneous catalysis, we have recently initiated a high-pressure NMR study of reactions of the Oxo catalyst, $Co_2(CO)_8$, in supercritical CO_2 solution. The fundamental processes shown in Eqs. 1–3,

$$Co_2(CO)_8 + H_2 \rightleftharpoons 2HCo(CO)_4 \qquad (1)$$

$$Co_2(CO)_8 \rightleftharpoons Co_2(CO)_7 + CO \qquad (2)$$

$$HCo(CO)_4 \rightleftharpoons HCo(CO)_3 + CO \qquad (3)$$

were investigated at a CO_2 density near 0.5 g/ml using ^{59}Co, ^{17}O, ^{13}C, and ^{1}H NMR signals. Preliminary measurements of the equilibrium constants for the hydrogen addition reaction in Eq. 1 at total pressures near 250 atm and temperatures in the range, 80°C–140°C, yielded ΔH° and ΔS° values of 2.8 ± 1.0 kcal/mol and 1 ± 3 cal/mol·K, respectively. Second order rate constants in accord with the rate law, $-d[Co_2(CO)_8]dt = k[Co_2(CO)_8][H_2]$, for the reaction were also measured at 80°C and 100°C, yielding an approximate activation energy of 26 kcal/mol. Since CO dissociation from $Co_2(CO)_8$ in Eq. 2 is rate-determining in the hydrogen addition reaction, the step in Eq. 2 also proceeds with an activation energy near 26 kcal/mol. Independent confirmation of rate-determining CO loss was achieved using dynamic NMR measurements of CO exchange at temperatures between 80°C and 145°C resulting in a similar activation energy value of 24 kcal/mol. Carbon monoxide dissociation from the hydride in Eq. 3, measured from the CO exchange rates, was found to be rapid on the NMR time scale even in liquid CO_2, below its critical temperature of 32°C. No evidence for CO_2 coordination or exchange with either $Co_2(CO)_8$ or $HCo(CO)_4$ was detected by NMR means at 145°C. The results indicate that, at least in terms of energetics of the required hydride formation and CO dissociation steps, supercritical CO_2 may be a suitable medium for conducting a variety of reactions catalyzed by $Co_2(CO)_8$. These include hydroformylations, arene hydrogenations, alcohol homologations, and methanol synthesis, each of which may benefit from the ability to control catalyst or substrate solubilities and recoveries in supercritical media by facile pressure alterations.

The high-pressure NMR experiments described here were performed with use of a unique high-pressure NMR probe and toroid detector that allows optimum sensitivity at an extreme combination of temperature and pressure conditions not previously achieved in high resolution NMR spectroscopy. Although glass or ceramic capillary cells have been developed for use in high-field NMR magnets at high pressures, research with the insensitive nuclides commonly encountered with organometallic systems at their natural abundances is more or less exclusively the domain of metal probes. The superior mechanical properties of metal alloys, *e.g.*, Be-Cu, are required to accommodate the larger sample sizes used for these nuclei. Compared with commercial ambient pressure probes, the metal probes are extremely cumbersome and relatively insensitive. None has heretofore been developed for use in the smaller size magnets available at 300 MHz and above. In attempts to surmount these problems, we have recently conceived the idea of using a new NMR detector, an elongated toroid, which, because of its confined magnetic flux, can be operated close to the interior walls of a metal pressure vessel without suffering losses due to magnetic coupling with the vessel. Using toroids, we have designed and tested an extremely compact, variable-temperature multinuclear pressure probe. For 75.6 MHz ^{13}C measurements on the ASTM test solution, similar sample sizes (1.5–1.6 ml) result in S/N ratios near 475 for the toroid probe compared with 340 for a commercial ambient pressure 10 mm probe without sample spinning. Although this comparison may not seem remarkable, we note that pressure probe designs in the recent literature give S/N values of only 30–55 for the ASTM sample. The signal-to-noise differences stem from greater torus coil efficiency and lower magnetic coupling with the pressure vessel when compared with conventional Helmholtz and solenoid detectors. Toroid probe resolution is comparable to that achieved with other metal pressure probes and we have measured line widths of 0.5–1.0 Hz for the ^2H resonance of C_6D_6 using several toroid coil and cavity designs. Because of the radial dependence of the B_1 field strength in toroids, B_1 homogeneity is intrinsically poorer for toroids when compared with other detector types. However, this feature can be minimized by design, and we have obtained reasonably useful π-nulls for toroids having an outer radius ≤ 1.5 times the inner radius.

The combination of pressure and temperature conditions required for homogeneous catalytic C_1 chemistry studies is particularly problematic for multinuclear NMR spectroscopy. For example, in earlier work using autoclaves, we had determined all of the kinetic orders and activation parameters for the $HCo(CO)_4$ catalyzed hydrogenation of carbon monoxide at temperature/pressure combinations near 200°C and 300 atm. Although this pressure is fairly modest for NMR probes, the combination of high-pressure and high-temperature conditions presents severe heating and cooling problems for bulky metal probe systems. The new probe achieves these conditions by combining the compact pressure vessel allowed by use of a toroid detector with an efficient direct electrical resistance heater that replaces forced fluid heaters commonly used in NMR probes.

Future Research. We plan to use the new probe in combination with other spectroscopic techniques to investigate "nonclassical" molecular hydrogen adducts of transition metals that retain H-H bonding upon coordination. The high hydrogen concentrations achievable in supercritical media may allow observation of unusual trihydride and polyhydride structures appearing in recent theoretical calculations by Burdett and others. We also plan NMR investigations of homogeneous catalytic carbon monoxide hydrogenation processes that occur with cobalt and rhodium carbonyl systems, and some C-H activation processes occurring with early and late transition metal complexes.

Publications

1. Toroid Detectors in Pressure Probes

   J. W. Rathke

   J. Magn. Reson., **85**, 150–155 (1989)

2. Comparative Energy Barriers for Hydrogen Activation by Homogeneous and Heterogeneous Metal Oxide Catalysts

   R. J. Klingler, T. R. Krause, and J. W. Rathke

   Catal. Lett., **3**, 347–358 (1989)

3. Regiospecific Ortho-Lithiation of Phthalocyanines: A Route for One-Step Synthesis of Highly Soluble Trimethylsilyl Substituted Phthalocyanines

   M. J. Chen, C. M. Fendrick, R. A. Watson, K. S. Kinter, and J. W. Rathke

   J. Chem. Soc., Perkin Trans. 1, **5**, 1071-1073 (1989)

4. Homologation of Methanol Catalyzed by Manganese Carbonyl in Tertiary Amine-Methanol Solutions

   M. J. Chen and J. W. Rathke

   Organometallics, **8**, 515–520 (1989)

5. Silane-Silanol Dehydrocondensation. The Microscopic Reverse of Hydrogen Activation by an Organometallic Oxide Complex

   R. J. Klingler, T. R. Krause, and J. W. Rathke

   J. Organomet. Chem., **352**, 81–94 (1988)

THE CHEMISTRY AND PHYSICS OF TRANSITION METAL CLUSTERS

Eric K. Parks, Julius Jellinek, Mark B. Knickelbein, and Stephen J. Riley

Chemistry Division, Argonne National Laboratory, Argonne, IL 60439

Research Scope and Objective

This program is involved in the study of fundamental properties of transition metal clusters, including experimental studies of the chemistry of and on clusters and of cluster photophysics, and theoretical studies of cluster dynamics. Chemical studies include determination of reaction kinetics and mechanism, product composition, and adsorbate thermodynamics. Chemical probes of cluster geometrical structure and ionization potentials have also been developed. Studies of physical properties include threshold photoionization measurements to determine more accurate cluster ionization potentials. Theoretical effort focuses on dynamical simulations of clusters, including investigation of the effects of rotation on cluster centrifugal distortions, isomerizations, phase transitions, and fragmentation. A major component of the theoretical program is aimed at detailed studies of the dynamics and structure of transition metal clusters.

Description of Research Effort

In the experimental program, clusters are generated by pulsed laser vaporization of a target located in a continuous flow reactor. In the chemistry studies, reactant gas is introduced into the reactor at a point downstream of the target where cluster growth has terminated. In the physics studies, the downstream portion of the flow tube is cooled to liquid nitrogen temperature to enhance cluster intensity. At the end of the channel clusters expand into vacuum and are formed into a molecular beam and transported to a laser ionization time-of-flight mass spectrometer. The chemistry experiments essentially consist of monitoring changes in the mass spectrum, i.e., changes in the relative amounts of the various products, with changes in reactor conditions such as reagent pressure, temperature, and reaction time. In the physics experiments mass spectra are recorded as a function of ionizing laser wavelength.

Recent chemistry studies have focused on the reactions of clusters of iron, cobalt, nickel, and platinum with such simple molecules as hydrogen, water, ammonia, and ethylene. In one series of studies, adsorbate decomposition has been characterized for the reactions of iron clusters with water, of nickel clusters with ammonia, and of platinum clusters with ethylene. For each reaction, the decomposition is accompanied by loss of hydrogen from the clusters, but our studies suggest that the detailed mechanisms are quite different in each case.

An extensive series of studies of reactions of nickel and cobalt clusters, both bare and hydrogenated, with ammonia and with water have provided information about cluster geometrical structure. We find incontrovertible evidence that nickel and cobalt clusters in the 50- to 150-atom size range are icosahedral in structure, whether or not they are saturated with hydrogen. While Ni_{19} also appears to be icosahedral, Co_{19} seems to be octahedral. These studies are providing for the first time the sort of structural information that will be invaluable for an understanding of structure-reactivity relationships, as well as for future theoretical studies of metal cluster chemistry.

We have developed a technique for estimating cluster ionization potentials (IPs) based on the observation that the adsorption of ammonia on metal clusters lowers their IPs. IPs have been determined for iron, cobalt and nickel clusters having from 4 to 100 atoms. While the precision is not as high as for IPs determined from threshold photoionization (see below), the procedure is relatively easy to apply and does provide higher precision than simple bracketing experiments. We find that, unlike alkali metal clusters, the dependence of IP on cluster size for transition metals is not explained by the so-called spherical drop model.

Studies of the equilibrium reactions of nickel and cobalt clusters with ammonia have also been expanded by measuring at various temperatures and ammonia pressures the equilibrium constants for the adsorption reactions. From the slopes and intercepts of van't Hoff plots ($\ln K_{eq}$ vs. $1/T$) the standard enthalpy changes ΔH^o and the entropy changes ΔS^o for the reactions can be obtained. Typical values for ΔH^o and ΔS^o for near saturation coverages of ammonia are found to be -16 kcal/mol and -20 e.u., respectively.

In our second cluster apparatus, dedicated to measuring physical properties, threshold photoionization studies have been done on clusters of nickel, niobium, iron, cobalt, and scandium using a tunable ultraviolet laser system. A newly developed cryogenic cluster source produces very cold clusters and has enabled us to confidently assign IPs without having to account for the effects of residual thermal energy on the ionization threshold.

As in the ammonia adsorption studies, we find that iron, cobalt, and nickel clusters have IPs significantly lower than those predicted by the spherical drop model. One interpretation is that the "Fermi level" for transition metal clusters is still evolving over the size range studied (up to 90 atoms), and has not yet reached the bulk value. Sudden jumps in IP observed for iron and cobalt indicate the possibility that structural changes take place over a narrow range of cluster sizes. We speculate that the evolution of cluster IP toward the corresponding bulk work function may occur discontinuously in transition metals.

The new theoretical program in the cluster group has focused on carrying out detailed numerical simulation studies of cluster dynamics and structure, with particular emphasis on transition metal clusters. This has included the development, for the first time, of a procedure for separating the overall rotational and vibrational energy of any N-body system, however floppy. This partitioning leads to an effective potential governing the vibrational motion in rotating systems. We have formulated a novel quenching technique which allows us to completely "freeze out" the vibrational motion in the system, preserving its total angular momentum. This has allowed us to find the equilibrium structures of rotating clusters, and to characterize the structural effects of rotation both qualitatively and quantitatively using the ideas of centrifugal distortion, isomerization, and fragmentation. We have also formulated a new normal mode analysis scheme which automatically and exactly incorporates the effects of overall rotation on normal mode frequencies. Using this scheme in numerical simulation studies we have described and analyzed for the first time the subtle and intricate effects of rotation on the dynamical and structural properties of clusters.

Complementing the experimental work in the group we have carried out simulation studies on nickel clusters. Both the so-called embedded-atom technique and a new size-dependent approach have been used to calculate the forces between the nickel atoms in a given cluster. Structural and dynamical properties have been investigated for Ni_{13}, Ni_{19}, and Ni_{55}. A search for minimum energy structures indicates that Ni_{55} is most stable in an icosahedral geometry, in agreement with experimental conclusions. The theory also agrees with experiment that the most stable structure for Ni_{19} is the double icosahedron. The patterns of phase change transitions in nickel clusters are both similar and different from those of noble gas (Lennard-Jones) clusters. For example, Ni_{13} and Ni_{19} "melt" in a continuous fashion without passing through the coexistence stage found for Ar_{13} and Ar_{19}. On the other hand, Ni_{55} exhibits coexistence of different forms, as does Ar_{55}.

Future Research

Chemistry studies will continue to probe the structure and chemistry of clusters of the first transition series metals. Adsorbate decomposition studies will concentrate on ethylene decomposition on nickel clusters, and water decomposition on iron clusters. Two-reagent studies will be pursued to investigate actual bimolecular chemical transformations on metal cluster surfaces. Photophysical studies will concentrate on measuring the effect of adsorption of small molecules such as H_2, NH_3, and NO on the ionization potentials of transition metal clusters, as functions of both adsorbate coverage and cluster size. Such studies will be valuable in providing information on the flow of electron density accompanying the cluster-adsorbate interaction and can provide a model of chemisorption which can be directly compared to bulk surface studies. Theoretical effort will continue to include both conceptual developments and numerical simulation studies. Investigations will be carried out that aim to describe the complex rovibrational dynamics of floppy systems beyond the harmonic approximation. The search for ways to introduce potentials adequate for transition metal clusters will continue to be one of the major efforts. The numerical simulation studies will be extended to include reactive dynamics of transition metal clusters.

Publications

1. *The Kinetics of Reactions of Nickel Clusters with Hydrogen and Deuterium*, W. F. Hoffman III, E. K. Parks, G. C. Nieman, L. G. Pobo, and S. J. Riley, Z. Phys. D 7, 83 (1987).
2. *Chemistry of Isolated Transition Metal Clusters*, S. J. Riley, J. Metals **40**, 52 (1988).
3. *Chemical Probes of Metal Cluster Structure: Reactions of Iron Clusters with Hydrogen, Ammonia, and Water*, E. K. Parks, B. H. Weiller, P. S. Bechthold, W. F. Hoffman, G. C. Nieman, L. G. Pobo, and S. J. Riley, J. Chem. Phys. **88**, 1622 (1988).
4. *The Reaction of Iron Clusters with Ammonia. I. Compositions of the Ammoniated Products and their Implications for Cluster Structure*, E. K. Parks, G. C. Nieman, L. G. Pobo, and S. J. Riley, J. Chem. Phys. **88**, 6260 (1988).
5. *Metastable Decay of Photoionized Niobium Clusters: Clusters within a Cluster?* S. K. Cole and K. Liu, J. Chem. Phys. **89**, 780 (1988).
6. *Solid-Liquid Phase Behavior in Microclusters*, R. S. Berry, T. L. Beck, H. L. Davis, and J. Jellinek, in Evolution of Size Effects in Chemical Dynamics, Part 2, edited by I. Prigogine and S. A. Rice, Advances in Chemical Physics, Vol. 70 (John Wiley & Sons, New York, 1988) p. 75.
7. *Dynamics for Nonconservative Systems: Ergodicity Beyond the Microcanonical Ensemble*, J. Jellinek, J. Phys. Chem. **92**, 3163 (1988).
8. *Generalization of Nose's Isothermal Molecular Dynamics*, J. Jellinek and R. S. Berry, Phys. Rev. A38, 3069 (1988).
9. *Dynamical Effects in the "Phase Change" Behavior of Small Clusters*, J. Jellinek and P. G. Jasien, in The Structure of Small Molecules and Ions, edited by R. Naaman and Z. Vager (Plenum, New York, 1988) p. 39.
10. *Separation of the Energy of Overall Rotation in Any N-Body System*, J. Jellinek and D. H. Li, Phys. Rev. Lett. **62**, 241 (1989).
11. *The Shapes of First-Stage Sinters*, F. Amar, J. Bernholc, R. S. Berry, J. Jellinek, and P. Salamon, J. Appl. Phys. **65**, 3219 (1989).
12. *Two-Reagent Reactions of Iron Clusters with Ammonia and Deuterium: Saturated Compositions and the Kinetics of Reactions of Deuterium with Ammoniated Clusters*, W. F. Hoffman III, E. K. Parks, and S. J. Riley, J. Chem. Phys. **90**, 1526 (1989).
13. *Rotating Clusters: Centrifugal Distortion, Isomerization, Fragmentation*, D. H. Li and J. Jellinek, Z. Phys. D. 12, 177 (1989).
14. *Reactivity of Free Clusters*, S. J. Riley, Z. Phys. D **12**, 537 (1989).
15. *The Reactions of Iron Clusters with Water*, B. H. Weiller, P. S. Bechthold, E. K. Parks, L. G. Pobo, and S. J. Riley, J. Chem. Phys. **91**, 4714 (1989).

Project Summary; Contract: DE-FG02-3654

Chemical Interactions in Multimetal/Zeolite Catalysts

Principal Investigator: Wolfgang M.H. Sachtler, Northwestern University

I. Introduction

Results of our research under this DOE grant confirm the validity of two basic hypotheses motivating this work; in addition, new concepts have emerged of relevance to the following topics:

1. Formation of isolated Pt and Pd atoms in sodalite cages [3,20].
2. Formation of palladium carbonyl clusters in supercages [13,17,26].
3. Formation of mono- or bimetal particles in zeolites by reductive decomposition of volatile metal complexes [5,10,15].
4. Cation-cation interaction as a cause of enhanced reducibility [18,27].
5. Control by calcination conditions of particle formation mechanism, i.e. either via ion reduction in channels or via isolated atoms [2,12].
6. Rejuvenation of Pd/NaY and Pd/HY catalysts by oxidative redispersion [17].
7. Enhanced catalytic activity of metal particle-proton complexes [28].
8. Effect of constraints of particles in cages on selectivity [8,9].
9. Modification by Fe ions of zeolite encaged metal clusters [3,30].

In view of the steric constraints of this Project Summary, we will only discuss the above points (3), (4), and (9); the reader is referred to the published papers for the other topics; in the publication list we have therefore included the titles of the papers.

II. Formation of bimetal particles in zeolites from volatile complexes.

Cation exchange into a zeolite is impossible for elements such as Re which tend to form anions in aqueous solution and the pH range compatible with zeolite stability. Zerovalent metals can, however, be deposited inside a zeolite by decomposing ligated clusters [33,34]. We have examined the temperature programmed decomposition of $Re_2(CO)_{10}$ on NaY and NaHY in flowing H_2, and we studied the effect of Pt in supercages on this [5,15]. Temperature Programmed Reductive Decomposition with in situ mass spectrometric analysis was used to monitor hydrogen consumption and evolution of CO and CH_4. Decomposition of $Re_2(CO)_{10}$ on NaHY was found to occur in two steps: formation of $Re(CO)_x$ subcarbonyls ($x \approx 3$), which strongly interact with Brønsted protons, is followed by Re aggregation. With NaY decomposition of the carbonyl results in the formation of rhenium particles via a Re hydride-carbonyl intermediate. The presence of Pt in the supercages of NaY has a profound effect on this decomposition process: no hydrido-carbonyl is formed, but subcarbonyls are trapped by Pt particles and mixed PtRe particles are formed with high yield. This follows from the kinetics of CO release and CH_4 formation and from the catalytic signature of these catalysts in the conversion of methylcyclopentane or of n-heptane [19]. Formation of PtRe clusters in zeolites is, however, much lower when a THF solution of the mixed carbonyl cluster $PtRe_2(CO)_{12}$ is used as the precursor.

III. Cation-cation interaction as a cause of enhanced reducibility.

During calcination, ions of Ni or Co in faujasites tend to migrate into hexagonal prisms where they are all but irreducible; e.g. for Co/NaY no reduction below 750oC is detected by TPR. For PtNi/NaY[4] and non-zeolite systems such as PtRe/Al_2O_3 [35,36] we had found that reducibility can be enhanced by addition of a noble metal, but close proximity (e.g. of rhenium precursor and platinum) is necessary for enhanced reduction. The same conclusion emerges from our recent study of (PdCo)/NaY [18]. When the Pd ions are retained in the supercages, while the Co ions are positioned in smaller zeolite cages, only 15% of the Co is reduced below 750°C. However, when Pd ions are forced to migrate to the sodalite cages by applying a calcination temperature of 500oC, 75% of the Co is reduced alongside with 100% of the Pd. Most remarkably, reduction sets in at lower temperature for (PdCo)/NaY than for Pd/NaY. This suggests to us that a cation-cation bond is formed between Pd and Co, when both ions are in each other's proximity; dissociative chemisorption of hydrogen might be easier on this ion pair than on an isolated ion; moreover, the formation of atom pairs will be favored thermodynamically over the formation of isolated atoms, as the metal-metal bond energy is very strong. We will try to exploit this finding for the preparation of RhFe/NaY catalysts which are known to have intriguiging selectivities in CO hydrogenation to oxygenates.

IV. Modification by Fe ions of zeolite encaged metal clusters.

In bimetallic samples, e.g. (PtFe)/NaY or (PdFe)/NaY, the presence of the noble metal strongly enhances the reduction of Fe^{3+} to Fe^{2+}, but reduction to Fe^{0} is not detected by TPR. Mössbauer data collected by the group of professor Dumesic indicate that in both systems the Fe^{2+} ions are interacting with the noble metal particles inside the zeolite. For (PtFe)/NaY hydrogen adsorption shows that the Fe^{2+} ions act as chemical anchors; for (PdFe)/NaY EXAFS data indicate that the coordination number of Pd is lower in the bimetallic than the monometallic samples, which might also be due to anchoring. The presence of Fe^{2+} ions also modifies the adsorption characteristics of the metal particles. Less hydrogen is adsorbed per Pd atom, although the EXAFS results indicate a higher dispersion. FTIR of CO adsorbed on these samples confirms that Fe^{2+} ions decorate the surface of Pd particles. After reduction at 200oC the bands characteristic of the Pd carbonyl cluster are found, but an additional band at 1988 cm^{-1} is unique for the bimetallic system. The effects of Fe^{2+} on the FTIR spectrum of CO is more dramatic after reduction at 500oC. The peak of the linear CO has shifted and new bands, including the 1988 cm^{-1} band just mentioned, appear. It is concluded that Pd particles which carry Fe^{2+} ions on their surface are modified, similar to the well known SMSI catalysts which carry Ti^{n+} ions on the surface of reduced Rh particles. The effect of this modification on the catalytic performance of zeolite encaged Pd has to be studied.

Publications 1988-1989 DOE sponsored project "Multimetal Zeolite Systems"

P.I.: W.M.H. Sachtler

1. **"Dispersion and Catalysis of Platinum in Bimetal/Zeolite Catalysts"**, H.J. Jiang, M.S. Tzou, W.M.H. Sachtler, Applied Catalysis 1988 39, 255-65
2. **"Genesis and Characterization of Transition Metal Clusters in Y Zeolites"**, M. S. Tzou, H.J. Jiang, W.M.H. Sachtler, Solid State Ionics 26 1988, 71
3. **"Formation of Pt Particles in Y Type Zeolites; The Influence of Co-Exchanged Metal Cations"** M. S. Tzou, B. K. Teo, W.M.H. Sachtler, J. Catal. 113, 220-235 (1988)
4. **"Hydrogen Release from Ni/Faujasite Catalysts"** H.J. Jiang, M.S. Tzou, W.M.H. Sachtler, Catalysis Letters 1988 1, 99-107
5. **"Synthesis and Characterization of Bimetallic $PtRe_x$ Clusters Prepared by Sublimation of $Re_2(CO)_{10}$ onto Pt/NaY"** C. M. Tsang, S. M. Augustine, J.B. Butt and W.M.H. Sachtler, Applied Catalysis 46, (1989) 45
6. **"Elementary Steps in the Formation of Highly Dispersed Palladium in NaY; Part I: Pd Ion Coordination and Migration"** S.T. Homeyer and W.M. H. Sachtler, J. Catalysis 117 (1989) 91-101
7. **"Mössbauer Spectroscopy Studies of PtFe/NaY Zeolite"** Vijay R. Balse, W.M.H. Sachtler, J.A. Dumesic, Catalysis Letters 1 (1988) 275-82.
8. **"Characterization and Catalysis of Pt-Cu Clusters in NaY"** Giuliano Moretti, W.M.H. Sachtler, J. Catalysis 115, (1989) 205-16
9. **"Geometric Causes of the Methylcyclopentane Selectivity over Pt/NaY Catalysts"** G. Moretti, W.M.H. Sachtler. J. Catal. 116, (1989) 350-360
10. **"Mechanismβ of Particle Formation in Decomposing $Re_2(CO)_{10}$ on NaY and Pt/NaY"** C. Dossi, J. Schaefer, and W.M. H. Sachtler, Abstracts 11th North American Meeting of the Catalysis Society, Dearborn, May 1989.
11. **"Mechanism of Pd Particle Formation and Oxidation in NaY"** S.T. Homeyer, W.M.H. Sachtler, Abstracts 11th North American Meeting of the Catalysis Society, Dearborn, May 1989
12. **"Design of Metals in NaY Zeolite"** S.T. Homeyer and W.M.H. Sachtler in Zeolites: Facts, Figures, Future, P.A. Jacobs, and R.A. van Santen Eds., Elsevier, Amsterdam, 1989, p. 975-84
13. **"Ship-in-a-Bottle Formation of $Pd_{13}(CO)_x$ Clusters in Zeolite NaY"** L.L. Sheu, H. Knözinger and W.M.H. Sachtler, Catalysis Letters 1989 2 129-138
14. **"Elementary Steps in the Formation of Highly Dispersed Palladium in NaY; Part II: Particle Formation and Growth"** S.T. Homeyer and W.M.H. Sachtler J. Catal. 1989 118 266-274
15. **"Mechanism of Particle Formation on Decomposing $Re_2(CO)_{10}$ on NaY and NaHY Zeolites: Effect of Prereduced Pt Clusters in the Supercages"** C. Dossi, J. Schaefer and W. M.H. Sachtler, J. Molecular Catalysis 52 1989, 193-209
16. **"Palladium Carbonyl Clusters Entrapped in NaY Zeolite Cages; Ligand Dissociation and Cluster-Wall Interactions"** L.-L. Sheu, H. Knözinger and W.M.H. Sachtler, J.Am. Chem. Soc. 1989 111 8125-8131
17. **"Formation of Oxide Particles and Oxidative Redispersion of Pd in NaY; An Application of High Precision TPR"** S. T. Homeyer and W.M.H. Sachtler, Applied Catalysis 1989 54 189-202
18. **"Proximity Requirement for Pd Enhanced Reducibilty of Co^{2+} in NaY"** Z. Zhang, W.M.H. Sachtler, S. Suib, Catalysis Letters 1989 2, 395-402
19. **"Reforming Type Catalysis with Zeolite Supported PtRe"** C. Dossi, C.M. Tsang, W.M.H. Sachtler, R. Psaro, R. Ugo; Energy and Fuels 1989 3 468-74
20. **"Transition Metal Clusters and Isolated Atoms in Zeolite Cages"** W.M.H.Sachtler, Proceedings International Summer Institute on Surface

Science, Milwaukee, Aug.21-24, 1989, Springer Verlag Berlin (in press)

21. **"Characterization and Catalysis of Pd particles and Pd_{13} Clusters in NaY"** S.T. Homeyer, L.L. Sheu, H. Knözinger and W.M.H. Sachtler, Preprints AIChE symposium "Zeolite Catalysis - Kinetics and Characterization", San Francisco, Nov. 5-10, 1989
22. **"Characterization of Zeolite Supported Metal Clusters"** C. Dossi, S. T. Homeyer, L.L. Sheu, Z. Zhang, W. M.H. Sachtler, FACSS XVI, Chicago,1989
23. **"Chemisorption and Catalysis of Zeolite Entrapped Palladium"** S. T. Homeyer, Z. Karpiński, W.M.H. Sachtler, Recl. Trav. Chim. Pays-Bas (J. Roy. Neth. Chem Soc.) 1989 108 (in press)
24. **"Enhancement of Ni Reducibility and Dispersion in Y Zeolites by Metal Additives"** H.J. Jiang; M.S. Tzou; W.M.H. Sachtler; Zeolites for the Nineties, Recent Res. Rep. 8th Interntl. Zeolite Conference Amsterdam, July 10-14, 1989, J.C. Jansen, L. Moscou M.F.M. Post Eds., p.357-8
25. **"Zeolite Supported Bimetal Catalysts"** S. T. Homeyer, L.L. Sheu, W.M.H. Sachtler, preprint AIChE Symposium "Characterization and Kinetic Studies of Multimetallic Catalysts" San Francisco November 5-10, 1989
26. **"Characterization by CO/FTIR Spectroscopy of Palladium Supported on NaY Zeolites"** L. L. Sheu, H. Knözinger, and W. M. H. Sachtler, J. Molecular Catalysis (in press)
27. **"Location, Ligancy and Reducibility of Metal Ions in Zeolite Cages: Co and Pd in NaY"** Z. Zhang and W.M.H. Sachtler, Transactions of the Faraday Division of the Royal Society of Chemistry (in press)
28. **"Effect of Zeolitic Protons on Palladium Catalyzed Hydrocarbon Reactions"** S.T. Homeyer, Z. Karpinski, W.M.H. Sachtler; J. Catalysis (in press)
29. **"Palladium Enhanced Reducibility of Ni in NaY"** J. Schaefer, W. M.H. Sachtler ZEOLITES (submitted)
30. **"Chemical Interaction of Pd Particles with Fe ions in NaY"** S. T. Homeyer, L. L. Sheu, Z. Zhang, W.M.H. Sachtler, V. R. Balse, and J. A. Dumesic,; Applied Catalysis (to be submitted)
31. **"Identification by Diffuse Reflectance and EXAFS of the Changes in Coordination of NaY entrapped $Pd(NH_3)_x^{2+}$ Ions During Calcination"** Z. Zhang, H. Chen and W. M. H. Sachtler, Zeolites (submitted)
32. **"Promoting Efffects of Alkaline Cations on the Palladium/Zeolite Catalyzed Methylcyclopentane Conversion"** X. Bai, W. M. H. Sachtler, Catalysis Letters (submitted)

Other Literature References

33. T. Bein, S.J. Mc.Lain, G.D. Stucky, G. Woolery, D.E. Sayers, K. Moller; J. de Physique 47 1986 , Colloque C8; 277-80
34. Gallezot, P., Coudurier, G., Primet, M., Imelik, B. in Molecular Sieves II, ACS. Symp. Series 40 J.R. Katzer Ed. (1977) 144
35. Augustine, S.M., and Sachtler, W.M.H.; J. Catalysis 1987 106 417-27
36. Augustine, S.M., and Sachtler, W.M.H., J. Catal. 1989 116, 184-194

HOMOGENEOUS-HETEROGENEOUS COMBUSTION: THERMAL AND CHEMICAL COUPLING

Lanny D. Schmidt
Department of Chemical Engineering and Materials Science
University of Minnesota
Minneapolis, MN 55455

Overall Summary

The objectives of this program are to characterize homogeneous-heterogeneous reaction systems in catalytic combustors and chemicals synthesis and to determine how the coupling between homogeneous and heterogeneous reactions controls the rates and selectivities. Four PhD graduate students are working full time on this research and four manuscripts have recently been submitted. All projects involve aspects of homogeneous-heterogeneous reactions on and near metal surfaces in situations from ultrahigh vacuum studies of molecular processes to atmospheric pressure reactor behavior. The program incorporates a variety of experimental approaches to characterize these systems and extensive modeling to simulate processes and to determine the effects of various types of coupling.

Ignition and Extinction in Homogeneous-Heterogeneous Reactions

The first project we began was the characterization of ignition and quenching of homogeneous-heterogeneous reactions in several oxidation reactions over a Pt foil at atmospheric pressure. These are the conditions and geometries of industrial processes, and this information should therefore be a starting point for more detailed investigations. We examined oxidation reactions of CH_4, C_3H_8, NH_3 and a mixture of NH_3 and CH_4. Products controlling selectivities are CO and CO_2 in the hydrocarbon reactions, NO and N_2 in NH_3 reactions, and HCN, N_2, and CO in NH_3+CH_4 reactions. The hydrocarbon reactions are prototypes of catalytic combustors, while NH_3 reactions are used in synthesis of HNO_3 and HCN respectively.

The experiment is very simple, consisting of flowing heated gases over a heated Pt foil in a glass tube and determining the surface temperatures where reaction ignites and extinguishes, both catalytically and homogeneously, as functions of gas composition, flow velocity, and gas preheat.

The figure below summarizes these results for C_3H_8 and for CH_4 oxidation. Both reactions have qualitatively similar behavior with a wide composition for catalytic reaction, a range of autothermal reaction (no electrical power necessary to sustain reaction), a region of extinction near surface combustion limits, and a high temperature regime where homogeneous reaction occurs. Note, however, that the systems have quite different shapes. CH_4 ignites only at ~600K while C_3H_8 ignites at ~200K. C_3H_8 exhibits a large autothermal composition while CH_4 reacts autothermally only over a very narrow composition range. Homogeneous reaction also occurs at a much lower temperature for C_3H_8.

NH_3 behaves similar to C_3H_8, but NH_3+CH_4 exhibits very interesting and complex behavior. There are three stable autothermal states for some compositions and rate oscillations also occur. This system is used commercially in the synthesis of HCN, a Nylon intermediate, and these results have direct relevance to these processes.

Modeling Homogeneous-Heterogeneous Reactions

All of these systems involve the coupling of heat and chemical reactions between surface and the boundary layer above it. Reaction ignites at the surface because its activation energy is lower, and the heat generated heats the gas to ignite homogeneous reaction. Chemical coupling occurs because reactants are consumed in the boundary layer because of the surface reaction, and this retards homogeneous ignition.

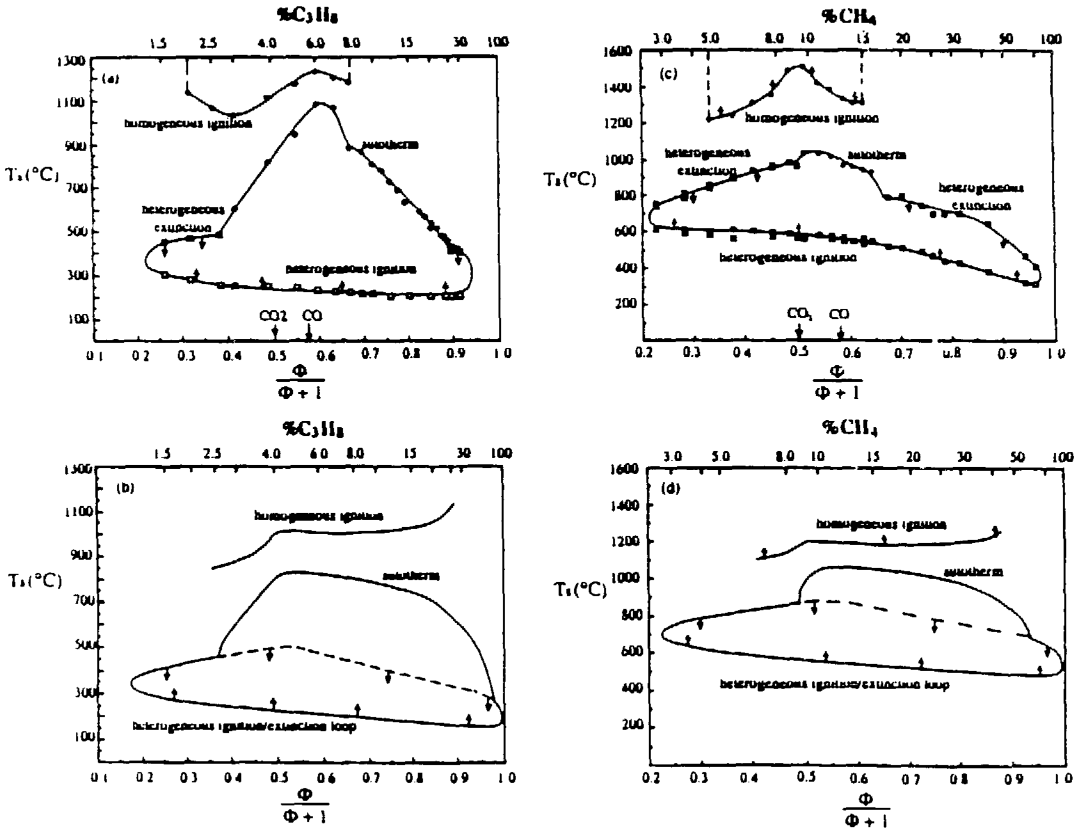

Modeling of these processes requires solution of momentum, energy, and species mass balances. This involves solution of at least four simultaneous partial differential equations which are high nonlinear because of the Arrhenius temperature dependences of surface and homogeneous reactions. We have developed a shooting method to solve these problems which is very efficient compared to finite element methods and which can incorporate realistic parameters into the system. Each simulation above required only ~10 minutes of Cray II time.

The figure shows a simulation of the experiments described in the previous section. Rate parameters are taken from experimental data for both catalytic reactions and homogeneous reactions. It is seen that the fits are quite close in most aspects of ignition and quenching. The model thus seems to be capable of predicting the behavior of these systems, and we are now using it to examine influences of system parameters on these and other homogeneous-heterogeneous reaction systems.

Radical Desorption in Surface Reactions

The model described above considers thermal coupling and the depletion of reactants consumed heterogeneous reaction. Another mechanism of coupling is generation and quenching of free radicals which are necessary to propagate chain reactions in homogeneous combustion. Important species in these systems should be OH, CH, NH, and CN. All of these species are easily detectable by laser induced fluorescence (LIF), and we are using this technique to measure concentrations of these species in the gas phase above catalytic surfaces using a tunable dye laser in a low pressure flow reactor.

We are currently examining OH desorption from a heated Pt foil at ~0.1 Torr in the oxidation reactions of H_2, CH_4, C_3H_8, and NH_3. Our interest is to compare OH from the four reaction systems, both the OH yield and its dependence on gas composition. We find that H_2 produces the largest OH but that its maximum occurs in a large O_2 excess. CH_4 yields a large OH signal and it occurs at all compositions out to a 1:1 mixture. C_3H_8 and NH_3 yield less OH and only for small fuel concentrations. All activation energies of OH production are ~40 kcal/mole, which suggests that OH is produced through the common path of $O+H \rightarrow OH$ and $OH+H \rightarrow H_2O$ in all four reactions.

We are beginning experiments on CN in CH_4+NH_3 oxidation and on OH at higher pressures where homogeneous reaction initiates. Clearly, these systems are crucial in determining the coupling in all homogeneous-heterogeneous reaction systems.

Reactions in Monoliths

These experiments involve reactions over flat surfaces. Another important geometry is the monolith which consists of channels with reactive walls. We are using ceramic monoliths (Cordierite) as catalysts in NH_3 oxidation and in CH_4 + NH_3 oxidation and are comparing these systems with Pt gauze catalysts which are now used industrially. We are using a gas chromatograph system to monitor the selectivity for different flow, gas composition, and catalyst situations. We are also determining conditions where homogeneous ignition occurs and are planning to connect this system to the LIF apparatus to detect radical species from the monolith directly.

We are also setting up a system for laser ionization mass spectrometric detection of reaction intermediates and products using a time of flight mass spectrometer. We are assembling a single photon ionization system using a tripled YAG laser by passing the beam through a rare gas cell to triple again to obtain ~10 eV photons which will ionize intermediates with uniform sensitivities without ionizing parent species.

Students Supported by this Grant

Cheinan Marks	Delaware	1985-	LIF of OH
Bill Williams	WPI	1987-	Ignition and Quenching
Max Song	Beijing	1986-	Modelling
Matt Stenzel	UM undergrad		Catalytic Combustion
Dan Hickman (NSF fellow)	Iowa State	1988-	TOF of Reaction Products

Recent Publications from this Research

X. Song, W. R. Williams, L. D. Schmidt, and R. Aris, "Ignition and Extinction of Homogeneous-Heterogeneous Combustion: CH_4 and C_3H_8 on Pt", submitted to International Combustion Institute.

W. R. Williams, X. Song, M. V. Stenzel, and L. D. Schmidt, "Bifurcation Behavior in Homogeneous-Heterogeneous Combustion: I. Experiments on Pt Foils", submitted to Combustion and Flame.

X. Song, W. R. Williams, L. D. Schmidt, and R. Aris, "Bifurcation Behavior in Homogeneous-Heterogeneous Combustion: II. Computations in Stagnation Point flow", submitted to Combustion and Flame.

D. Hickman and L. D. Schmidt, "Modeling Catalytic Gauze Reactors: Ammonia Oxidation", submitted.

KINETIC AND SPECTROSCOPIC CHARACTERIZATION OF METAL OXIDE AND SULFIDE CATALYSTS

Professor Glenn L. Schrader

Ames Laboratory-U.S.D.O.E. and
Department of Chemical Engineering
Iowa State University
Ames, Iowa 50011

Scope

Hydrodesulfurization (HDS) and selective oxidation are large scale catalytic processes which predominantly rely on the use of metal oxide and sulfide catalysts. Almost all petroleum used by the United States as well as future sources of liquid fuels from coal must undergo HDS processing to reduce sulfur emissions and to prevent sulfur poisoning of other catalysts used to process hydrocarbon feedstocks. Selective oxidation catalysts are also used by industry to produce a wide array of valuable chemical intermediates. In recent years, significant advances in developing new catalytic routes using paraffins have been achieved. These include n-butane conversion to maleic anhydride and methane oxidative coupling.

Despite the commercial importance of metal oxide and sulfide catalysts, there is a lack of fundamental understanding of the catalytic properties of these materials and the mechanisms of the associated catalytic reactions. In our research a comprehensive approach is used to study the catalytic behavior of these materials including: the development of new catalyst preparation techniques; adsorption experiments to examine the nature of adsorbed species and active sites; and continuous flow/pulse reactor studies to determine kinetic data for mechanistic investigations. Special emphasis is placed in our research program on developing in situ spectroscopic techniques which are capable of examining catalysts under actual operating conditions (such as the elevated temperatures and pressures associated with industrial use). Laser Raman spectroscopy, Fourier transform infrared spectroscopy and NMR spectroscopy are particularly powerful method for examining catalysts under these conditions.

Recent Results

Our most significant recent progress has included: 1) the development of a new experimental approach called isotopic reactive-site mapping (IR-SM) for investigating the incorporation of oxygen into hydrocarbons during selective oxidation catalysts; 2) a fundamental advance in understanding the nature of the active state of V-P-O catalysts using NMR spectroscopy; 3) new information related to phase composition and surface reduction for rare earth oxides used for methane oxidative coupling; 4) investigation of adsorption on Chevrel phase HDS catalysts using probe molecules to determine the number and nature of the active sites.

In the past few years, we have demonstrated that fundamental new insights into the mechanisms of selective oxidation reactions can be obtained using a new technique which we refer to as isotopic reactive-site mapping (IR-SM). The principles of this technique are: 1) Incorporation of ^{18}O or ^{17}O into specific lattice sites of a metal oxide catalyst. We have successfully used solid state preparative techniques but surface-reduction approaches also are valid. 2) Rigorous identification of the location of the label using spectroscopic techniques such as laser Raman spectroscopy, Fourier transform infrared spectroscopy, or NMR spectroscopy. 3) Reaction of the labeled catalyst with the hydrocarbon feed (and proposed intermediate compounds) in a pulse reactor/mass spectrometer system to determine the incorporation of the label into specific products (such as partially oxidized hydrocarbons vs. combustion products, CO_2 and H_2O. The IR-SM technique has been demonstrated to be a powerful method for determining the reactivity of specific sites for oxygen incorporation--thus, a "mapping" of the reaction pathway can be determined.

The IR-SM technique has been recently applied to the study of two important catalysts for n-butane conversion to maleic anhydride; β-$VOPO_4$ (reported last year) and $(VO)_2P_2O_7$. An example of the approach using the latter catalyst (used extensively by industry) is described as follows. An ^{18}O labeled $(VO)_2P_2O_7$ phase was prepared from β-$VOPO_{7/2}{}^{18}O_{1/2}$ by a solid state reduction technique. Laser Raman spectroscopy and Fourier transform infrared spectroscopic characterization located the ^{18}O label at specific sites, primarily in P-O-V and P-O-P bonding sites. The labeled catalyst was then reacted with n-butane and several possible reaction intermediates (1-butene, 1,3-butadiene, furan, γ-butyrlactone) to determine the ^{18}O incorporation. Based on these results it was shown that combustion reactions occur mainly at V=0 sites, particularly if olefin or C_1-C_3 hydrocarbon intermediates are produced. In contrast, P-O-V sites are capable of inserting oxygen into strongly adsorbed, dehydrogenated surface species to form furan and maleic anhydride.

Related work on V-P-O catalysts has dealt with the use of NMR spectroscopy to characterize the oxidation state of catalysts after exposure to reactive conditions.[5] A fundamental question about maleic anhydride catalysts such as β-$VOPO_4$ (V^{+5}), $(VO)_2P_2O_7$ (V^{+4}), and more complex industrial formulations (usually involving various P-to-V ratios) has been whether these materials reduce in the presence of the hydrocarbon feeds. By using spin echo mapping[5] of ^{31}P, we have determined that the active industrial catalysts contain both V^{+5} and V^{+4} (and possibly V^{+3}). Furthermore, the NMR data are consistent that these oxidation states are <u>in microscopic proximity</u> to each other in the industrial catalysts, rather than bulk mixtures of separate β-$VOPO_4$ and $(VO)_2P_2O_7$ phases. Identification of neighboring redox pairs such as V^{+5}-V^{+4} is essential for understanding the mechanism of selective oxidation catalysis, and this work represents a fundamental new advance in active-site identification for metal oxides.

Progress has also been made in the area of methane oxidative coupling. We have chosen to focus our research on the catalytic chemistry of rare earth oxides, particularly emphasizing the identification of active phases and the role of lattice-, surface-, or adsorbed-oxygen species in the activation/coupling/combustion of CH_4. In particular we have shown for La catalysts, exposure to CO_2 and H_2O (always present in selective oxidation reactors) leads to the formation of other phases at the high temperatures involved in CH_4 oxidation (650-800°C). Rigorous preparative techniques and extensive catalyst characterization by X-ray diffraction, laser Raman spectroscopy, Fourier transform infrared spectroscopy, and thermogravimetric analysis has been performed. Reactor studies have indicated that the conversion of CH_4 and the yield of C_2H_6 and C_2H_4 decrease in the order: II-$La_2O_2CO_3$ > La_2CO_3 > $La(OH)_3$ > A-La_2O_3. This result has important implications in understanding the nature of the oxygen species involved in CH_4 oxidation since addition of CO_2 to feed streams has been shown to improve catalyst performance.

We are also continuing our work in HDS dealing with a newly discovered series of reduced molybdenum sulfides. A series of lead-lutetium Chevrel phases has been compared to model MoS_2-based hydrodesulfurization catalysts for their oxygen and nitric oxide adsorption capacities, as well as their thiophene HDS activities. Although a linear correlation between oxygen chemisorption and thiophene HDS activity was not observed, it is possible to estimate oxygen adsorption cross sectional areas from the oxygen uptake and BET surface area data. For the unsupported MoS_2 catalyst, a value of 8.15 nm^2/O_2 molecule was calculated. Previously reported values for oxygen adsorption areas on MoS_2 range from 0.61 nm^2/O_2 to 9.8 nm^2/O_2. It is assumed that differences in pretreatment and preparation contribute to the wide variation in O_2 adsorption area on MoS_2. Comparison of the oxygen adsorption area of 8.15 nm^2/O_2 molecule to the area of 0.146 nm^2/molecule for physisorbed oxygen leads to the conclusion that only about 2% of the surface is covered by oxygen at saturation. This supports the concept of selective adsorption on edge or corner sites, where the molybdenum exists in reduced molybdenum oxidation states, relative to the +4 oxidation state found in the bulk of MoS_2. For the Chevrel phases studied, a mean value for the oxygen adsorption area of 0.556 nm^2/O_2 molecule was determined. In comparison to the actual oxygen surface area of 0.146 nm^2/molecule, this indicates that approximately 26% of the surface is covered by oxygen. In general, the Chevrel phases, with their reduced Mo oxidation states, were more active for thiophene HDS and adsorbed more oxygen. Also, the pre-adsorption of oxygen did not lower the thiophene HDS activity. Results for the adsorption of nitric oxide were similar.

Future Plans

Specific objectives in HDS catalysis and selective oxidation include: 1) spectroscopic characterization of active sites and adsorbed species on HDS catalysts using oriented crystallites and thin films of MoS_2 and Chevrel phases; 2) extension of the mechanistic models for thiophene HDS based on pulse reactor studies and ^1H NMR of reaction intermediates; 3) transient isotopic studies of CH_4 oxidative coupling emphasizing the reactivity of adsorbed, surface and lattice oxygen in rare earth oxide catalysts; 4) in situ Raman and infrared spectroscopy of functioning CH_4 oxidative coupling catalysts such as La and Sm oxides.

Publications (1987-1989)

K. F. McCarty and G. L. Schrader. Deuterodesulfurization of Thiophene: An Investigation of the Reaction Mechanism. J. Catal., 103, 261 (1987).

T. P. Moser and G. L. Schrader. Stability of Model V-P-O Catalysts for Maleic Anhydride Synthesis. J. Catal., 104, 99 (1987).

T. P. Moser, R. W. Wenig and G. L. Schrader. Maleic Anhydride Conversion by V-P-O Catalysis. *Appld. Catal.*, *34*, 39 (1987).

R. W. Wenig and G. L. Schrader. *In Situ* FTIR Spectroscopy of 1-Butene and 1,3-Butadiene Selective Oxidation to Maleic Anhydride on V-P-O Catalysts. *J. Phys. Chem.*, *91*, 1911 (1987).

R. W. Wenig and G. L. Schrader. *In Situ* FTIR Study of Crotyl Alcohol, Maleic Acid, Crotonic Acid, and Maleic Acid Oxidation on a V-P-O Industrial Catalyst. *J. Phys. Chem.*, *91*, 5674 (1987).

S. C. Huckett, R. J. Angelici, M. J. Ekman, and G. L. Schrader. Deuterium Exchange of Benzo[b]thiophene: Model Complex and Heterogeneous Reactor Studies. *J. Catal.*, *113*, 36 (1988).

R. L. McCormick and G. L. Schrader. A Study of the Activity and Selectivity of Molybdenum Crystallographic Shear Compounds in the Oxidation of C_4 Hydrocarbons. *J. Catal.*, *113*, 529 (1988).

G. L. Schrader, T. P. Moser, and M. E. Lashier. Oxygen-Labeled V-P-O Catalysts for n-Butane Conversion to Maleic Anhydride. *Proceedings of the 9th International Congress on Catalysis*, The Chemical Institute of Canada, Ottawa, *4*, 1624 (1988).

E. J. Markel, G. L. Schrader, N. N. Sauer and R. J. Angelici. Thiophene, 2,3- and 2,5-Dihydrothiophene, and Tetrahydrothiophene Hydrodesulfurization on Mo and Re/γ-Al_2O_3 Catalysts. *J. Catal.*, *116*, 11 (1989).

M. E. Ekman, J. W. Anderegg, and G. L. Schrader. An Investigation of the Role of Reduced Molybdenum Formal Oxidation States in Hydrodesulfurization Catalysis with Chevrel Phase Compounds. *J. Catal.*, *117*, 246 (1989).

M. E. Lashier, T. P. Moser and G. L. Schrader. Investigation of Active and Selective Oxygen in V-P-O Catalysts. *New Developments in Selective Oxidation*, (F. Trifiro and G. Centi, eds.), Elsevier, 1989.

N. N. Sauer, E. J. Markel, G. L. Schrader, and R. J. Angelici. Studies of the Mechanism of Thiophene Hydrodesulfurization: Conversion of 2,3- and 2,5-Dihydrothiophene and Model Organometallic Compounds. *J. Catal.*, *117*, 295 (1989).

G. L. Schrader and M. E. Ekman. Chevrel Phase HDS Catalysts: Structural and Compositional Relationships to Catalytic Activity. *Advances in Hydrotreating Catalysts*, (M. L. Occelli and R. G. Anthony, eds.), Elsevier-Amsterdam, 1989, pp. 41-66.

S. J. Finke and G. L. Schrader. Infrared Reflection-Absorbance Spectroscopy using Semiconductor Thin Film Structures, *Spectrochimica Acta* (in press, 1989).

J. K. Schoer, R. S. Houk, R. J. Conzemius, and G. L. Schrader. Ion Association by Time-of-Flight Mass Spectrometry: A Study of V-P-O Catalysts. *J. Amer. Soc. Mass Spectrom.* (in press, 1989).

THE EFFECT OF CATALYST PREPARATION ON CATALYTIC ACTIVITY

J.A. Schwarz
Department of Chemical Engineering and Materials Science
Syracuse University, Syracuse NY 13244.

RESEARCH SCOPE AND OBJECTIVES

Supported metal catalysts are commonly prepared by depositing catalytic precursors from aqueous electrolytes onto high surface area oxides. This impregnation step has been the focus of a number of recent studies from our laboratory which seek to relate the effect of formulation procedures on the catalytic properties of supported metal catalyst systems (1-18). Although the relationship between preparation variables and catalyst performance may in many cases be obscure, it is the goal of our studies to provide a basis for understanding the first of a series of stages in catalyst preparation: the adsorption process of metallic precursors onto the support surface. Presented here are the summaries of results of studies of three catalyst systems obtained during the period December 1986 to July 1989 under support from DOE Grant DE-FG02-87ER13650. The systems studied were (i) Ru/Al_2O_3 (ii) Ni/Al_2O_3 (iii) Al_2O_3 and TiO_2 supported Pt, Ir and Pt-Ir catalysts.

DESCRIPTION OF RESEARCH EFFORT

Ru/Al_2O_3:

The effect of preparation method and choice of metallic precursor on the performance of a series of Ru/Al_2O_3 catalysts were studied [1]. Wet impregnation and incipient wetness were the methods employed; ruthenium nitrosylnitrate and ruthenium trichloride were the reagents. In the latter case, either Ru(III)/Ru(IV) chlorospecies or mixtures of Ru(III) hydrazine complexes were the catalytic precursors. A series of Ru/Al_2O_3 catalysts, with metal loadings from 0.7 - 5 % by weight , were subjected to a battery of performance tests: CO temperature-programmed reaction (TPR), steady state CO hydrogenation and temperature-programmed surface reaction (TPSR).

The methanation activity and carbon deposited during steady state reaction varied systematically with the dispersion of Ru on alumina. High rates of methane production were found on catalysts containing a large reservoir of carbon containing reaction intermediates.

The performance of these catalysts depended on the precursor used in their preparation. The effects of weight loading, method of preparation, and variations in the impregnant pH were small within a group prepared from a common precursor.

The impact of residual chloride on the properties and performance of this series of Ru/Al_2O_3 catalysts has also been studied [2]. This work departs from previous studies in that it examines the poisoning and promoting effects of this electronegative element in CO hydrogenation as a function of the dispersion of the catalyst. The dispersion and the structure of the particles are regulated by the choice of the precursor used during preparation and the impregnation conditions. We find that, in general, chloride residues poison catalysts with a high dispersion but provide a promotional effect for catalysts with a poor dispersion.

The effects of alumina dissolution and metal ion buffering on the dispersion of alumina supported nickel and ruthenium catalysts were also studied [3]. At low initial pH values of each impregnant, more free aluminum is released into the aqueous phase in ruthenium electrolytes than in nickel electrolytes. The effect persists for longer times thus generating more adsorption sites for the ruthenium catalytic ion precursor.

The dispersions of Ni/Al_2O_3 catalysts vary dramatically with weight loading and initial impregnant pH. On the other hand, Ru/Al_2O_3 catalysts have comparable dispersions for more than a factor of five increase in weight loading. These results are consistent with the proposal that alumina dissolution facilitates continuous generation of adsorption sites which allows higher concentrations of metal salt precursor to be accommodated on the support during impregnation.

Ni/Al_2O_3:

The reducibility of a series of alumina-supported nickel catalysts was studied subsequent to various thermal treatments carried out within a temperature-programmed reduction (TPRd) apparatus [18]. After thermal treatment at 773K under Ar, the reduced and passivated catalyst showed no reduction profile during TPRd. On the other hand, normal reducibility does occur if a TPRd procedure is conducted either immediately after room temperature exposure of the reduced catalyst to oxygen or after thermal treatment at 393K under Ar. A model to account for these behaviors considers the dynamic nature of the catalyst structure during temperature cycling.

Preliminary results have been obtained for a series of Ni/Al_2O_3 catalysts. They were characterized by temperature-programmed reduction and their activity was measured using ethane hydrogenolysis as a test reaction. Care has been taken to ensure that all conditions during characterization and performance studies were identical; the only variable in this system has been the source of the Al_2O_3 support material.

The catalysts were prepared from $Ni(NO_3)_2$ at sufficient concentration to mount 6% by weight of metal. Incipient wetness procedures were used, but in some instances excess electrolyte was used. TPRd profiles of the dried precursors and hydrogenolysis rates are strongly dependent on the type of alumina support used. A comprehensive examination of the properties of the supports used in this study revealed that the crystallinity (determined by XRD) varied considerably from one alumina to the other. The greater the crystallinity, the less the alumina dissolution, the smaller the H/M value determined by TPRd, and the smaller the Ni uptake during wet impregnation.

Al_2O_3 and TiO_2 supported Pt, Ir and Pt-Ir catalysts:

The structure and activity of composite oxide (Al_2O_3 on TiO_2 and TiO_2 on Al_2O_3) supported monometal (Pt, Ir) and bimetal (Pt-Ir) catalysts have also been studied. A series of composite oxides were prepared by varying the amount of dopant in the composite oxide. The surface charge behavior of the composite oxides was characterized in terms of their point of zero charge (pzc). A model has been developed to determine the dopant surface area [5,6]. Catalyst precursors were prepared from H_2PtCl_6 and H_2IrCl_6. The adsorption rates on different supports were determined. The calcined precursors prepared by dry impregnation were characterized by TPR and TPD and by a structure sensitive reaction, the hydrogenolysis of ethane. The dried precursors were characterized by TPR and TPD and by studying the thermal decomposition gravimetrically. The metal weight loading was adjusted to 3% for monometal catalysts and 3% each for the bimetal catalysts. The pure oxide supported monometal catalysts were used as standards to compare the behavior of composite oxide supported catalysts. Bimetal formation was observed on all supports. Varying degrees of H_2 chemisorption occurred on composite oxide supported catalysts. The effect of the SMSI carrier (TiO_2) on H_2 chemisorption suppression is dependent on the composition of the composite oxide.

CURRENT AND FUTURE WORK

Catalysis is considered to be a "black art" because of our lack of understanding of the causal chain of steps usually designated as catalyst preparation. Over the past several years there have emerged from our laboratory numerous reports that approach the subject of catalyst preparation systematically. In our work we have extended well established principles of colloid chemistry to catalytic systems with the objective of establishing a scientific basis for the preparation of metal supported catalysts. Our work has demonstrated the decisive importance of pH during adsorption/impregnation.

Our future work will involve the formulation of a model for the effect of pH on divalent metal ion adsorption on amphoteric surfaces. The elements of any comprehensive model requires a quantitative description of how the surface charge density changes with the pH and how the ionized forms of the solute adsorb. The end result of such a formulation should provide direct information on the strength of interaction of catalytic precursors with oxide supports. Characterization and performance studies of the catalysts derived from adsorption/impregnation should be consistent with the parameters derived from the model. Our overall objective is to provide a basis for design of catalyst systems which includes the intrinsic properties of the supports and electrolytes used in the preparation of supported metal catalysts.

REFERENCES (PUBLISHED UNDER DOE GRANT DE-FG02-87ER13650)

1. Mieth, J.A. and Schwarz, J.A., "The Effect of Catalyst Preparation on the Performance of Alumina Supported Ruthenium Catalysts I. The Impact of Catalytic Precursor on Particle Size and Catalytic Activity", J. Catal. (in press).
2. Mieth J.A. and Schwarz J.A., "The Effect of Catalyst Preparation

on the Performance of Alumina Supported Ruthenium Catalysts, II. The Impact of Residual Chloride", J. Catal. (in press).

3. Mieth, J.A. and Schwarz, J.A., "The Effects of Alumina Dissolution and Metal Ion Buffering on the Dispersion of Alumina Supported Nickel and Ruthenium Catalysts", Appl. Catal. (submitted).
4. Mieth, J.A., Huang, Y.-J. and Schwarz, J.A., J. Coll. Int. Sci. 123 (1988) 366.
5. Subramanian, S., Noh, J.S., and Schwarz, J.A., J. Catal. 114 (1988) 433.
6. Subramanian, S., Schwarz, J.A. and Hejase, Z., "The Temperature Dependence of the Point of Zero Charge of Al_2O_3, TiO_2, and Physical Mixtures." J. Catal. (in press).
7. Huang, Y.J., Barrett, B.T., and Schwarz, J.A., Appl. Catal. 24 (1986) 241.
8. Huang, Y.-J, and Schwarz, J.A., Appl. Catal. 30 (1987) 239.
9. Huang, Y.-J. and Schwarz, J.A., Appl. Catal. 30 (1987) 225.
10. Huang, Y.-J, and Schwarz, J.A., Appl. Catal. 32 (1987) 45.
11. Huang, Y.-J., and Schwarz, J.A., Appl. Catal. 32 (1987) 59.
12. Huang,Y.-J., Schwarz, J.A., Diehl, J.R., and Baltrus, J.P., Appl. Catal. 36 (1988) 163.
13. Huang, Y.-J., and Schwarz, J.A., Appl. Catal. 36 (1988) 177.
14. Huang, Y.-J., Schwarz, J.A., Diehl, J.R., and Baltrus, J.P., Appl. Catal. 37 (1988) 229.
15. Huang, Y.-J., and Schwarz, J.A., I&E.C. Process Research & Development 26 (1987) 379.
16. Mieth, J.A., Schwarz, J.A., Huang, Y.-J. and Fung, S.C., "The Effect of Chloride on the Point of Zero Charge of Gamma-Alumina", J. Catal., (submitted).
17. Schwarz, J.A., and Heise, M.S., "Preparation of Metal Distributions Within Catalysts Supports, IV. Multicomponent Effects", J. Coll. Int. Sci., (submitted).
18. Hu, J., Huang Y.-J., and Schwarz, J.A., "The Effects of Thermal Treatment on the Reducibility of Alumina Supported Nickel Catalysts", Appl. Catal. (submitted).

ADDITIONAL LIST OF PUBLICATIONS UNDER DOE GRANT DE-FG02-87ER13650

19. Schwarz, J.A., "Segregation in Real Catalysts" to appear in Surface Segregation and Related Phenomena, Dowben, P.A. and Miller, A. Eds.
20. Huang, Y.-J., Xue, J., and Schwarz, J.A., J. Catal., 109 (1988) 396.
21. Huang, Y.-J., Xue, J., and Schwarz, J.A., J. Catal., 111 (1988) 59.
22. Heise, M.S., and Schwarz J.A., J. Coll. Int. Sci., 123 (1988) 51.
23. Xue, J., Huang, Y.-J., and Schwarz, J.A., Appl. Catal., 42 (1988) 61.
24. Brumberger, H., Farnsworth, S., Phillips, M.G. Ramaya, R. and Schwarz, J.A., J. Coll. Int. Sci., 124 (1988) 379.
25. Conner, W.C., and Schwarz, J.A., Chem. Eng. Commun., 55 (1987) 129.

Nuclear Magnetic Resonance in Solids

Charles P. Slichter
Department of Physics, Chemistry and, Materials Research Laboratory
University of Illinois at Urbana-Champaign

Summary of Total Project

The interests of this group are in fundamental studies of solids and surfaces, principally by magnetic resonance. Included are many-body problems, superconductivity, phase transitions, magnetism, solids which possess unusual properties (such as charge density waves), and electronic, structural, and dynamic aspects of surface atoms and adsorbed molecules. In conjunction with Dr. John Sinfelt of the Exxon Research Laboratories, we are studying surface phenomena of an important class of catalysts, small particles of Pt or other Group VIII transition metals (in which 5% to 75% the metal atoms are on the surface of the particles) supported on alumina. We employ the ^{195}Pt NMR to study how the electronic structure of the surface Pt atoms depends on what atoms (if any) are adsorbed on the surface. By ^{13}C, ^{1}H, $^{2}H_2$ or ^{17}O NMR, we investigate the bonding and structure of adsorbed molecules such as CO, C_2H_2 or C_2H_4. We utilize this knowledge to follow the time dependence of chemical reactions, including the dependence of the rate on temperature. We make extensive use of special methods such as observing the resonance of one species of nucleus while exciting a second resonance, to enable us to see resonances otherwise too weak to observe, or to show which nuclei are bonded to each other, measure bond lengths, and determine the structure of molecules. We did some of the first work which confirmed the pairing concept of the Bardeen-Cooper-Schrieffer (BCS) theory of superconductivity. Currently, we are studying high temperature superconductors in both normal and superconducting states. The power of NMR is its ability to pick out specific atoms (e.g. Cu, O, Y) or specific sites (e.g. Cu planes or chains).

Recent Work on Catalysis

Our NMR studies of catalysis, all done in collaboration with Dr. John Sinfelt of Exxon Research and Engineering Laboratories, continue to yield novel results in the physics and chemistry of bonding to surfaces, in determination of the structure of adsorbed molecules, in the study of the motion of atoms or molecules on the surfaces of the metal particles, in the study of ordered arrangements of atoms on surfaces, in the structure of bimetallic clusters, and in the study of chemical reactions on surfaces. We have underway studies involving six of the nine Group VIII metals (Ru, Rh, Pd, Os, Ir, Pt) supported on Al_2O_3. We cannot work with the other three, Fe, Co, and Ni, owing to their magnetism which would unduly broaden the NMR lines. We have some studies utilizing silica as a support, and some studies involving unsupported catalysts (platinum black).

Three years ago we reported the bond length of CO on Pd, the diffusion rate of CO on Pd, on the mixing of CO orbitals with the Pd conduction band, on the use of NMR to study order arrays of CO on Pt, on initial results on Pt-Rh bimetallic catalysts, and on the observation of quantum size effects. Two years ago we reported on use of deuterium NMR to confirm that C_2H_4 converts to CCH_3 at room temperature on Pt, to study the temperature at which the conversion takes place, and to observe H-D exchange between CCH_3 and D adsorbed on the surface. We also reported studies of Pt-Rh bimetallic catalysts, and further results on the quantum size effect. Last year we completed detailed studies of the conversion of C_2H_4 to CCH_3 and of H-D exchange. We developed and solved the appropriate rate equations which then enabled us to define and evaluate frequency factors and energy barriers for these two reactions. We extended our studies of the quantum size effect to fill in data for the temperature range between 4.2 K and 77 K. We reported evidence that when CO diffuses on Pt metal, there are two distinct diffusion rates originating probably in their being two types of CO bonding sites (e.g. linear and bridge bonded). We also initiated studies of alkali metal atom promoters in the system of Na adsorbed on Pt metal together with CO.

Current Work

We are studying aspects of C-C scission of acetylene or Pt and Ir, extending our earlier annealing studies in which we used ^{13}C NMR and ^{13}C-^{1}H spin echo double resonance (SEDOR) at 77 K to observe the results of annealing acetylene to progressively higher temperatures. We discovered strong evidence that acetylene had lost 1 or 2 H atoms before C-C bond scission took place. We are now directly observing ^{13}C-^{1}H SEDOR at the elevated temperature to monitor the H population. One important goal is to learn whether or not loss of hydrogen from an adsorbed molecule is reversible. We are also using ^{2}H (deuterium) NMR to study the reaction $H + CCH_2 \rightarrow CCH_3$ which may play an important role as one pathway for CCH_2 C-C scission. We have further extended our observations of the quantum size effect. We have instituted a new NMR technique to study surface diffusion, and are applying it to CO on Pd and Pt.

Our promoter studies are progressing. We are studying the sytem of Na on supported Pt particles with and without adsorbed CO. We have observed the ^{23}Na NMR and ^{13}CO NMR and ^{23}Na-^{13}CO SEDOR. The ^{13}CO NMR characteristics prove that the CO is on the Pt. Thus, the existence of a ^{23}Na-^{13}CO double resonance proves that the ^{23}Na signal is from Na on the Pt. The absence of a Na Knight shift shows that the Na is fully ionized (Na^+).

<u>List of publications, last two years</u>

J.-Ph. Ansermet, P.-K. Wang, C. P. Slichter, and J. H. Sinfelt
NMR study of electronic properties of the chemisorption of CO on supported Pt catalysts
Phys. Rev. B. **37**, 1417-1428 (1988).

J.-Ph. Ansermet, C. P. Slichter, and J. H. Sinfelt
An NMR study of the geometry of a CO layer chemisorbed on Pt particles
J. Chem. Phys. **88**, 5963-5971 (1988)

C. P. Slichter
A reflection on the character of magnetic resonance and of one of its practitioners
Rev. Roum. Phys. **33**, Nos. 4-6, 934-940 (1988)

C. H. Pennington, D. J. Durand, D. B. Zax, C. P. Slichter, J. P. Rice, and D. M. Ginsberg
Cu NMR of aligned single crystals of $YBa_2Cu_3O_{7-\delta}$
Phys. Rev. B **37**, 7944-7947 (1988)

J. S. Waugh and C. P. Slichter
Mechanism of nuclear spin-lattice relaxation in insulators at very low temperatures
Phys. Rev. B **37**, 4337-4339 (1988)

Z. Wang, J.-Ph. Ansermet, C. P. Slichter, and J. H. Sinfelt
Nuclear magnetic resonance study of Pt-Rh bimetallic clusters
J. Chem. Soc., Faraday Trans. 1, 1988, **84**(11), 3785-3802

C. H. Pennington, D. J. Durand, C. P. Slichter, J. P. Rice, E. D. Bukowski, and D. M. Ginsberg
Static and dynamic Cu NMR tensors of $YBa_2Cu_3O_{7-\delta}$
Phys. Rev. B **39**, (Rapid Commun.) 2902-2905 (1989).

C. P. Slichter
Nuclear magnetic resonance studies of simple molecules on metal surfaces, <u>AIP Conference 180</u>, <u>Proc. Int. Sym. Frontiers in Science</u>, (University of Illinois, Urbana, 1987), S. S. Chan, P. G. Debrunner, eds. (AIP, NY, 1988), pp. 25-38.

C. H. Pennington, D. J. Durand, D. B. Zax, C. P. Slichter, J. P. Rice, E. D. Bukowski, and D. M. Ginsberg
Single crystal nuclear magnetic resonance studies of high-temperature superconductors
<u>Advances in Magnetic Resonance</u>, Vol. 13, <u>Proc. Waugh Sym</u>., MIT, Cambridge, MA, January 1989 , ed. W. S. Warren, (Academic Press, NY, 1989), pp. 1-15.

C. H. Pennington, D. J. Durand, C. P. Slichter, J. P. Rice, E. D. Bukowski, and D. M. Ginsberg
NMR measurement of the exchange coupling between Cu(2) atoms in $YBa_2Cu_3O_{7-\delta}$(T_c=90K)
Phys. Rev. B **39**, 274-277 (1989).

D. B. Zax, C. A. Klug, C. P. Slichter, and J. H. Sinfelt
Reaction kinetics of ethylene conversion and hydrogen exchange on Pt by ^2H NMR
J. Phys. Chem. **93**, 5009-5012 (1989).

J. S. Waugh and C. P. Slichter
Reply to "Comment on 'Mechanism of nuclear spin-lattice relaxation in insulators at very low temperatures'"
Phys. Rev. B **40**, 4203 (1989) II.

D. J. Durand, S. E. Barrett. C. H. Pennington, C. P. Slichter, E. D. Bukowski,
T. A. Friedmann, J. P. Rice, and D. M. Ginsberg
NMR studies of $YBa_2Cu_3O_{7-d}$(T_c=90K)
Proc. IBM Japan Int. Sym. on Strong Correlation and Superconductivity, 21-25 May 1989 (Springer, to be published 1989).

P.-K. Wang, C. P. Slichter, and J. H. Sinfelt
The similarities and differences in the C-C bond scission of ethylene and acetylene on supported Ir and Pt clusters
J. Phys. Chem (Drickamer's Special Issue "Festschrift"), accepted for publication.

J. H. Ross, Jr., Z. Wang, and C, P. Slichter
NMR studies of $NbSe_3$: Electronic structures, static charge density wave measurements and observations of the moving CDW
Phys. Rev. B (accepted for publication).

S. E. Barrett, D. J. Durand, C. H. Pennington, C. P. Slichter, T. A. Friedmann,
J. P. Rice, and D. M. Ginsberg
^{63}Cu Knight shifts in the superconducting state of $YBa_2Cu_3O_{7-d}$(T_c=90K)
Phys. Rev. B. (accepted for publication).

H. Monien, D. Pines, and C. P. Slichter
Spin and charge excitations in $YBa_2Cu_3O_7$: Constraints from spin relaxation rates in the normal state
Phys. Rev. B (accepted for publication).

C. P. Slichter
Principles of Magnetic Resonance, Third Ed. (Springer, NY, 1989), 655 pp.

C. H. Pennington and C. P. Slichter
Nuclear magnetic resonance studies of $YBa_2Cu_3O_{7-\delta}$
Physical Properties of High Temperature Superconductors II, D. M. Ginsberg, ed. (World Scientific, NJ, 1990)

MOLECULAR SURFACE SCIENCE AND ITS APPLICATION TO HETEROGENEOUS CATALYSIS AND COATINGS.

G.A. Somorjai

Center for Advanced Materials, Materials and Chemicals Sciences Division
Lawrence Berkeley Laboratory, and Department of Chemistry
University of California, Berkeley, California 94720.

There are two major aims of our studies of surfaces. 1) To determine the atomic surface structure and chemical bonding of metals, adsorbed organic monolayers, oxides and sulfides; 2) To apply this knowledge to understand, on the molecular level, important macroscopic surface phenomena, heterogeneous catalysis and the formation of hard coatings. The experimental techniques most frequently used in these studies include low energy electron diffraction, various electron spectroscopies, the scanning tunneling electron microscope, low pressure plasmas, mass spectroscopy and gas chromatography. We utilize single crystal surfaces in our studies whenever possible.

I. STUDIES OF THE SURFACE STRUCTURES OF METALS, ORGANIC MONOLAYERS, OXIDES AND SULFIDES. THE SURFACE CHEMICAL BOND.

The purpose of these investigations is to determine the structure of single crystal surfaces and of adsorbed molecules (e.g. benzene on a (111) or stepped crystal face of platinum) by three independent techniques. Low energy electron diffraction permits the study of the ordered structure of the top 3-5 atomic layers at the surface. These studies are carried out in ultra high vacuum ($<10^{-8}$ torr) or in the presence of high purity vapors. The surface structures are determined, in part, from the diffraction pattern. The diffraction beam intensities are then measured and matched to those obtained by computer calculations using a program in which the atomic positions are the only adjustable parameters. High resolution electron energy loss spectroscopy is utilized to obtain the vibrational spectra of adsorbed atoms or molecules. This way the surface structures of both ordered and disordered monolayers can be studied. Scanning Tunneling Microscopy yields the image of the surface structure with atomic resolution and is uniquely suited to investigate defects (steps) and disorder at surfaces.

At present, the structure of organic monolayers (acetylene, benzene, etc.) adsorbed on platinum, rhodium, palladium and molybdenum crystal surfaces are studied. The effects of coadsorption of electron donors (K, Na) or electron acceptors (O, Cl, S) on the bonding of adsorbed molecules on Pt and Rh are investigated. Scanning tunneling electron microscopy studies also explore the metal-oxide interface (Rh-TiO_2, Fe-Al_2O_3).

II. STUDIES OF CATALYTIC REACTIONS USING CRYSTAL SURFACES.

The purpose of our research in heterogeneous catalysis is to elucidate the relationship between the atomic structure of surfaces, their composition and valency, and their reactivity. The surface structure is determined by low energy electron diffraction and electron loss spectroscopy, the surface composition by Auger electron and photoelectron spectroscopies. The product composition is monitored by a mass spectrometer at low pressures ($<10^{-4}$ torr) or a gas chromatograph at high pressures ($>10^3$ torr).

The reactions under investigation include a) the conversion of hydrocarbons (hydrogenation, dehydrogenation, hydrodesulfurization and dehydrocyclization) on platinum, molybdenum and rhenium surfaces; b) the hydrogenation of CO and CO_2 over copper to produce methanol and c) isomerization and de-alkylation over alumina-silicate sputtered thin films.

Transition metal oxides are grown as ordered thin films on metal single crystals by vapor deposition and are used in these studies. The metal catalyst surfaces are modified by the deposition of oxide islands, other metals, electron donors (potassium) or acceptors (chlorine) and their effects on the reaction rates and product distributions are explored.

III. SCANNING TUNNELING AND ATOMIC FORCE MICROSCOPY STUDIES OF SURFACES (STM AND AFM).

The atomic surface structures of metals, adsorbed monolayers of sulfur, of oxides and of organic molecules are studied by STM and AFM. The AFM is also utilized to measure the forces perpendicular and parallel to the surface that are necessary to break bonds or to slide. The structure and orientation of molecules sandwiched between two solid surfaces are explored.

This research is supported by the Director, Office of Energy Research, Basic Energy Sciences, Materials Science Division of the U.S. Department of Energy.

References 1988-89

1. The Effects of Potassium on the Ammonia Synthesis Over Iron Single crystal Surfaces (with D.R. Strongin), J. of Catal. 109, 51-60 (1988), LBL-23403.
2. Vibrational and Electronic Spectroscopy of Pyridine and Benzene Adsorbed on the Rh(111) Crystal Surface (with C.M. Mate, H.W.K. Tom, X.D. Zhu and Y.R. Shen), J. of Chem. Phys. 88, 441(1988), LBL-23628.
3. Alumina and Titania Overlayers on Rhodium: A Comparison of the Chemisorption and Catalytic Properties (with M.E. Levin, K.J. Williams, M. Salmeron and A.T. Bell), Surf. Sci. 195, 341-351 (1988), LBL-23052.
4. The Characterization of Ti and Al Oxide Overlayers on Rhodium and Gold by XPS (with M.E. Levin, M. Salmeron and A.T. Bell), Surf. Sci. 195, 429-442 (1988), LBL-23562.
5. Organic Monolayers on Transition Metal Surfaces. The Catalytically Important Sites (with M.A. Van Hove and B. Bent), J. Phys. Chem. 92, No.4, 973-978(1988), LBL-23627.
6. On the Rate Enhancement of Ammonia Synthesis Over Iron Single Crystals by Coadsorption of Alumina Oxide with Potassium (with D.R. Strongin) Catalysis Letters 1, 61-66(1988), LBL-24633.
7. The Surface Structure and Thermal Decomposition of Acetylene on the Rh(111) Single Crystal Surface and the Effect of Coadsorbed Carbon Monoxide (with C.M. Mate, C.-T. Kao and B.E. Bent), Surf. Sci. 197, 183-207 (1988), LBL-23736.
8. Thiophene Hydrodesulfurization over Transition Metal Surfaces: Structure Insensitive over Molybdenum and Structure Sensitive over Rhenium (with M.E. Bussell and A.J. Gellman), J. of Cat. 110, 423-426(1988), LBL-23953.
9. Atomic Arrangement of Sulfur Adatoms on Mo(001) at Atmospheric Pressure: A Scanning Tunneling Microscopy Study (with B. Marchon, P. Bernhardt, M.E. Bussell, M. Salmeron and W. Siekhaus), Phys. Rev. Letters 60, 12, 1166-1169(1988), LBL-24237.
10. A HREELS Study of CO_2 Adsorbed on Re(0001) (with M. Asscher and C.-T. Kao, J. of Phys. Chem. 92, 2711-2714(1988), LBL-24981.

11. An ISS and AES Study of Alkali Metal Induced Sintering of an Iron Oxide Monolayer Adsorbed on Pt(111) (with G.H. Vurens, D.R. Strongin and M. Salmeron), Surf. Sci. 199(1988) L387-L393, LBL-24332.
12. An XPS Study of the Oxidation and Reduction of the Rhenium-Platinum System Under Atmospheric Conditions (W.T. Tysoe and F. Zaera), Surf. Sci. 200, 1-14 (1988), LBL-23032.
13. Molecular Structure of Benzene Coadsorbed with CO on Pd(111); A Dynamical LEED Analysis (with H. Ohtani and M.A. Van Hove), J. of Phys. Chem. 92, 3974 (1988), LBL-24011.
14. Structure, Composition and Chemisorption Studies of Thin Ordered Iron Oxide Films on Platinum(111) (with G.H. Vurens and M. Salmeron), Surf. Sci. 201, 129-144 (1988), LBL-24328.
15. Ethanol Reactivity on Model Vanadium Oxide Catalysts (with Ted S. Oyama), Proc. 9th Int. Cong. Catal. Soc., Calgary, 1988, 4, 1489, M.J. Phillips and M. Ternan, Eds., Chemical Institute of Canada, Ottawa, 1988.
16. Molecular Ethylene Adsorption on Rh(111) and Rh(100): Estimation of the C-C Stretching Force Constant From the Surface Vibrational Frequencies (with B.E. Bent, C.M. Mate, C.-T. Kao and A.L. Slavin), J. Phys. Chem. 92, 4720 (1988), LBL-24240.
17. The Preparation and Characterization of Rhenium Modified Pt(111) and Pt(100) Modified Re(0001) Single Crystal Surfaces (with D.J. Godbey), Surf. Sci. 202, (1988) 204-226, LBL-23058.
18. Structure Determination with HREELS and LEED: The Molecular Structure of Chemisorbed Benzene on Pd(111) (with H. Ohtani, B.E. Bent, C.M. Mate and M.A. Van Hove), Presented at the 4th ICSFS, Hamamatsu, Japan, August 23-27, 1987, Applied Surface Science 33/34, (1988) 254-260, LBL-23881.
19. The Role of Adsorbate Overlayers in Thiophene Hydrodesulfurization over Molybdenum and Rhenium Single Crystals (with M.E. Bussell and A.J. Gellman) Catalysis Letters 1, (1988) 195-202 , LBL-25304.
20. The Formation of Ethylidyne on the Rh(100) Single Surface by the Co-adsorption of Ethylene and Carbon Monoxide, (with A.J. Slavin, B.E. Bent and C.-T. Kao), Surf. Sci. 202, (1988) 388-404, LBL-24510.
21. The Adsorption and Co-Adsorption of Sulfur and Carbon Monoxide on Rhenium Single Crystal Surfaces (with D.G. Kelly, A.J. Gellman, M. Salmeron, V. Maurice, M. Huber and J. Oudar), Surf. Sci. 204, (1988) 1-25, LBL-24414.
22. The Adsorption and Desorption of Hydrogen and Carbon Monoxide on Bimetallic Re-Pt(111) Surfaces (with David J. Godbey) Surf. Sci. 204, (1988) 301-318, LBL-24960.
23. Molecular Surface Science of Organic Monolayers presented at the 6th International Conference on Surface and Colloid Science, June 5-10, 1988, Hakone, Japan, Pure & Appl. Chem. 60, 10(1988), 1499-1516.
24. An ISS, AES and CO Chemisorption Study of Titania Overlayers on Rh(111) (with K.J. Williams, M. Salmeron and A.T. Bell), Surf. Sci. 204, 3(1988), L745, LBL-25345.
25. Ethylene Hydrogenation and Ethane Hydrogenolysis on a Rh Foil with Titania Overlayers (with K.J. Williams, M.E. Levin, M. Salmeron, A.T. Bell), Cat. Letts. 1, 10(1988) 331-338, LBL-25856.
26. Homogeneous, Heterogeneous and Enzymatic Catalysis (with S. Ted Oyama), J. Chem Education 65, 765 (1988), LBL-23107.
27. The Structures of CO, NO and Benzene on Various Transition Metal Surfaces: Overview of LEED and HREELS Results (with H. Ohtani and M.A. Van Hove), ICSOS Proc. (1987), Applied Surf. Sci. 33-4, 254-260 (1988), LBL-23537.
28. Thermal Fragmentation of Ethylene on the Rh(100) Single Crystal Surface in the Temperature Range of 200 - 800 K (with A.J. Slavin, B.E. Bent and C.-T. Kao) Surf. Sci. 206, 124-144 (1988), LBL-24757.

29. Carbon Monoxide Induced ordering of Adsorbates on the Rh(111) Crystal Surface: Importance of Surface Dipole Moments (with C.M. Mate and C.-T. Kao) Surf. Sci. 206, 145-168 (1988), LBL-25085.
30. Mix of Molecular Adsorption Sites Detected for Disordered CO on Pt(111) by Diffuse Low-Energy Electron Diffraction (with G.S. Blackman, M.-L. Xu, D.F. Ogletree and M.A. Van Hove), Phys. Rev. Lett. 61, 20(1988) 2352-2355, LBL-25123.
31. LEED and HREELS Studies of the Coadsorbed CO + Ethylidyne and NO + Ethylidyne Systems on the Rh(111) Crystal Surface (with G.S. Blackman, C.-T. Kao, B.E. Bent, C.M. Mate and M.A. Van Hove) Surf. Sci. 207, 66-88(1988), LBL-25128.
32. The Synthesis of Butyronitrile from n-Butanol and Ammonia over Rhodium (111) and (331) Single Crystal Catalysts (with B.M. Naasz, I. Böszörmenyi) J. of Cat. 115, 2(1988) 399-409, LBL-22563.
33. Concepts in Surface Science and Heterogeneous Catalysis (with Roger M. Nix) Jortner/Pullman "Perspectives in Quantum Chem." (1988), LBL-25554.
34. The Effect of Argon During the Plasma-Assisted Chemical Vapor Deposition of Tin (with M.R. Hilton, M. Salmeron) Thin Solid Films 167, L31-34(1988), LBL-25697.
35. Photoelectron Spectroscopy Studies of Thiophene Chemisorption and Decomposition on the Mo(100) Surface (with A.J. Gellman and W.T. Tysoe), Surface Science to be published (1989), LBL-24241.
36. Benzene Adsorption and Acetylene-to-Benzene Conversion on Pd(111), Rh(111) and Ru(0001) Surfaces (with I.E. Idrissi-Rachidi, C. Minot and M.A. Van Hove), submitted to Surf. Sci. (1988), LBL-25177.
37. Thiophene Hydrodesulfurization over Rhenium Surfaces: The Effects of Structure and Adsorbates (C and S) (with M.E. Bussell), J. of Phys. Chem. 93, 2009-2016(1989), LBL-25218.
38. The Surface Chemical Bond of Adsorbed Organic Monolayers and Adsorbate-Induced Restructuring of Surfaces (with Ted S. Oyama) Proceedings of the Solvay Conference on Surface Science, University of Texas at Austin Dec. 14-18, 1987, Springer Series in Surf. Sci. 14, 120-128 (1988), LBL-25272.
39. The Hydrogenolysis of Ethane Over Re-Pt(111) and Pt-Re(0001) Bimetallic Crystal Surfaces (with David J. Godbey and Francois Garin) J. of Cat. 117, 144-154(1989), LBL-25695.
40. Bonding and Chemistry of Hydrocarbon Monolayers on Metal Surfaces (with Brian Bent) (review paper) J. of Advances in Colloid and Interface Science 29, 223-275 (1989), LBL-25627.
41. STM Study of the Structure of the Sulfur (1x2) Overlayer on Molybdenum (001) in Air: Ordered Domains, Phase Boundaries and Defects (with B. Marchon, D.F. Ogletree, M.E. Bussell, M. Salmeron and W. Siekhaus) Proc. of the 3rd Int'l Conf. on Scanning Tunneling Microscopy, Oxford, Great Britian, July 4-9, 1988, in press J. of Microscopy, LBL-25736.
42. Surface Restructuring as a Mechanism for Bond Breaking and Catalytic Reactions at Metal Surfaces (with M.A. Van Hove), Cat. Letts. 1, 12(1988) 433-437, LBL-26272.
43. Ammonia Pretreatment Induced Restructuring of Iron Single Crystal Surfaces: Its Effects on Ammonia Synthesis and on Coadsorbed Aluminium Oxide and Potassium (with D.R. Strongin), J. of Cat. in press (1988), LBL-26338.
44. Adsorbate-Induced Restructuring of Surfaces (with M.A. Van Hove) Progress in Surface Science 30, 201-231 (1989), LBL-26299.

Structural and Electronic Properties of Iron and Cobalt Molecular Sieve Catalysts

Steven L. Suib
Departments of Chemistry and Chemical Engineering
University of Connecticut
November 20, 1989

The structure sensitivity of iron and cobalt zeolite catalysts in cyclopropane ring opening, hydrogenation, hydrogenolysis and oligomerization reactions has been the focus of our research program. Small cobalt particles (< 5 angstroms) trapped in NaX zeolite catalyze ring opening reactions, larger (8 - 10 angstrom) particles catalyze hydrogenation reactions and even larger (> 10 angstrom) particles catalyze hydrogenolysis reactions.[1,2] The smallest particles are 100% dispersed and have been characterized by a variety of methods including chemisorption, ferromagnetic resonance and spin echo nuclear magnetic resonance (SENMR) methods. The unique aspects of this research include the preparation of extremely small particles via microwave discharge decomposition of organometallic precursors and the characterization of such particles with several complementary techniques, the most promising of which is SENMR.[3]

The SENMR method is carried out in zero external magnetic field on ferromagnetic and superparamagnetic materials like Co and Fe. The advantage of this method is that the structure of the particles can be determined as well as a relative particle size, especially in the 5 angstrom regime. The size and shape of such small particles trapped in zeolites are difficult to characterize with more classical methods such as transmission electron microscopy due to the low contrast between the particles and the matrix[4] or by characterization with chemisorption due to the extremely high dispersion.[1,2] SENMR can also be used to study alloys in zeolites and it may be useful in further characterization studies of catalysts.[4]

SENMR data for a variety of cobalt complexes are given in Table I.

Table I. SENMR Data for Cobalt Complexes

sample	treatment	SENMR,[a] frequency
1. Co, bulk metal, fcc[b]	*d*	217.2
2. Co, bulk metal, hcp[c]	*d*	228
3. $Co_2(CO)_8$	*d*	*e*
4. $Co_2(CO)_8$, NaX	sublimed	*e*
5. $Co_2(CO)_8$, NaX	sublimed, Ar plasma, 3 W	*e*
6. $Co_2(CO)_8$, NaX	sublimed, Ar plasma, 3 W, 120 °C	*e*
7. $Co_2(CO)_8$, NaX	sublimed, Ar plasma, 3 W, >160 °C	219 ± 1
8. $Co_2(CO)_8$, NaX	sublimed, 120 °C	219 ± 1
9. $Co_2(CO)_8$, NaX	sublimed, Ar plasma, 10 W	219 ± 1
10. $(C_5H_5)_2Fe$, $Co_2(CO)_8$, NaX	sublimed, Ar plasma, 3 W	228 ± 3
11. $CoFe_9$	*d*	275 ± 3

[a] Collected at 4.2K, values in MHz. [b] fcc = face-centered cubic. [c] hcp = hexagonal close-packed. [d] No treatment. [e] No signal observed.

Entries 1 and 2 serve as standards for face centered cubic (fcc) and hexagonal closest packed (hcp) bulk cobalt metal. No SENMR signal is observed for samples 3-4 since $Co_2(CO)_8$ as a solid or in the pores of NaX is an isolated species. No SENMR signal is observed for sample 5, although this material shows a ferromagnetic resonance which indicates that the Co particles are superparamagnetic. These single domain particles when heated to 120°C also show no SENMR signal as shown for sample 6. Samples 5-6 show chemisorption indicative of 100% dispersion. The absence of an SENMR signal for these samples that are known to be superparamagnetic from FMR experiments indicate that the particles are smaller than about 5 angstroms.

Sample 7 of Table I is $Co_2(CO)_8$ sublimed into NaX zeolite that has been heated to 160°C. The signal near 219 MHz indicates that particles have aggregated into fcc cobalt and this observation suggests that the superparamagnetic precursors [plasma treated then $T < 160^{\circ}C$)] may be pseudocubic in shape. Thermal treatment of $Co_2(CO)_8$ in NaX at 120°C without exposure to the plasma also leads to fcc cobalt particles. Notice that the size of the particles remains small with the plasma treated sample when heated to 120°C (sample 6) whereas thermal treatment itself (no plasma) produces large fcc particles. These data suggest that the plasma decomposition process leads to smaller particles than thermal treatment and that even after plasma preparation of small cobalt particles that these materials are more stable to higher temperatures than nonplasma treated samples.

As the power of the microwave plasma decomposition is increased to 10 watts from 3 watts fcc particles are observed in the NaX zeolite sample as shown for sample 9. This indicates that at high powers larger particles are being formed.

When $(C_5H_5)_2Fe$ is codeposited with $Co_2(CO)_8$ in NaX and subjected to an Ar plasma, hcp cobalt particles are observed as shown for sample 10. These data suggest that codeposition procedures can be used to control the structure of the cobalt particles.

Finally, if $Fe_2(CO)_9$ is codeposited with $Co_2(CO)_8$ in NaX followed by plasma decomposition, a Co(5 % Fe) alloy can be prepared as indicated by the observation of a new SENMR signal at 250 MHz. Such an alloy cannot be prepared by either first depositing the iron precursor or by first depositing the cobalt precursor. Thermal methods do not lead to such alloys.

To fully understand the distribution of particle sizes and shapes it is important to characterize the particles with SENMR, chemisorption, TEM and ferromagnetic resonance. Theoretical simulations of ferromagnetic resonance data have led to excellent fits of FMR data and to the information concerning magnetic anisotropies as well as particle sizes.[5] Ferromagnetic resonance data need to be collected over a wide range of temperature (-160°C to 160°C) to obtain such information. By comparing data from FMR, SENMR and other methods it is possible to obtain a firm understanding of particle size distributions in these metal zeolite systems. Our studies suggest that the smallest particles are produced by the plasma decomposition route and that such particles are about 5 angstroms in size, and homogeneously distributed in the zeolite pores.

The surface and bulk concentrations of iron and cobalt in NaY zeolite have been determined by Rutherford backscattering methods.[6] These data show that it is possible to distinguish large concentrations of metal at the surface of a zeolite from large concentrations of metal inside the pores of a zeolite. Theoretical depth profiles were generated that clearly show the difference between these two cases. While RBS cannot readily distinguish elements close to each other in atomic number, (i.e., Si, Al), the total concentration of such elements is very accurate.

Other supports that have been used for trapping small metal particles include aluminophosphates.[7] The surface properties of $ALPO_4$-5 and $ALPO_4$-11 have been compared and their degradation by mineral acids, EDTA, $SiCl_4$ and other chemicals has been reported.[7a,b] Small cobalt particles have also been prepared in $ALPO_4$-5 supports.[7c]

The use of luminescence methods to probe molecular sieve catalysts is the subject of our recent review paper.[8] Luminescence methods have been used to monitor the decomposition process[8] occuring during microwave discharge treatment of cobalt carbonyl in NaX zeolite. The enhancement of luminescence of a variety of emitting molecules has been accomplished by trapping small silver clusters (< 10 angstroms) in zeolites.[9] This surface enhanced luminescence is related to surface enhanced Raman scattering and has allowed us to detect extremely low concentrations (ppm) of luminescent molecules near the small silver clusters in zeolites.

Finally, metal particles are known to poison fluid cracking zeolite catalysts. We have been studying the poisoning of fluid cracking catalysts (FCC) by vanadium with electron paramagnetic resonance, luminescence, Mössbauer spectroscopy, X-ray photoelectron spectroscopy and secondary ion mass spectrometry. Model catalysts[10] and real commercial catalysts[11] have been analyzed and the effects of the metal seem to be very similar in both cases. In general, vanadium poisons destroy the structure of the zeolite component of the FCC by producing vanadia and rare earth vanadates. A review of the model FCC materials has been assembled.[12]

Our most recent research has involved transient studies of cyclopropane and hydrogen in zeolites. We have found that molecular hydrogen is trapped in the sodalite cages of zeolite NaX. The location of the hydrogen has been probed by using a variety of ion-exchanged zeolites that are known to have specific ions in specific crystallographic sites. Diffusivities of the trapped hydrogen have also been measured. Similar studies with cyclopropane have shown that it sorbs in NaX zeolite. In some cases the cyclopropane ring opens to propylene , especially when ions like Eu^{3+} are present due to the Brönsted acid groups introduced during the exchange of the lanthanide ions.

Publications Acknowledging DOE Support

1. S. L. Suib, Z. Zhang, Structure Sensitive Reactions of Cyclopropane with Cobalt and Iron Zeolite Catalysts, in Perspectives in Molecular Sieves, ACS Symposium Series, 368, Washington, DC, W. H. Flank, T. E. Whyte, 569-578.

2. A. Efsthasiou, Z. Zhang, C. O. Bennett, S. L. Suib, J. Catal., submitted, 1989.

3. Z. Zhang, S. L. Suib, Y. D. Zhang, W. A. Hines, J. I. Budnick, Spin Echo NMR of Cobalt Zeolite Catalysts: Control of Particle Size and Structure, J. Am. Chem. Soc., 110, 5569- 5571, 1988.

4. S. L. Suib, Z. Zhang, E. V. R. Borgstedt, C. O. Bennett, Abstracts of 11th North American Meeting of the Catalysis Society, May 1989, Detroit, A40.

5. S. S. Nam, L. E. Iton, S. L. Suib, Z. Zhang, Chem. Materials, 1989, 1, 529-534.

6. S. A. Baumann, M. D. Strathman, S. L. Suib, Nondestructive Depth Profiling of Rare-Earth and Actinide Zeolites via Rutherford Backscattering Methods, Anal. Chem., 60, 1046-1051, 1988.

7. (a) A. M. Winiecki, S.L. Suib, Chemical Stability of Aluminophosphate Molecular Sieves, Langmuir, 1989, 5, 333-338.
   (b) A. M. Winiecki, Ph.D. Thesis, University of Connecticut, 1988.
   (c) Z. Zhang, Ph. D. Thesis, University of Connecticut, 1988.

8. S. L. Suib, Photochemical Probes in Molecular Sieves, Focus on Photochemistry and Photophysics, CRC Press, in press, 1989.

9. (a) J. F. Tanguay, Proceedings of the Fifth International Symposium on Inclusion Phenomenon and Molecular Recognition, Surface Enhanced Luminescence with Silver Zeolites, 1988, in press.
   (b) J. F. Tanguay, Ph.D. Thesis, University of Connecticut, 1988.

10. C. A. Altomare, G. S. Koermer, E. Martins, P. F. Schubert, S. L. Suib, W. S. Willis, Vanadium Interactions with treated Silica Aluminas, Applied Catalysis, 45, 291-306, 1988.

11. P. F. Schubert, C. A. Altomare, G. S. Koermer, W. S. Willis, S. L. Suib, Metal Poisoning of High Zeolite Cracking Catalysts, Chem. of Materials, 1989, 1, 459-463.

12. S. L. Suib, M. W. Anderson, M. L. Occelli, Tin Passivation of Vanadium Contaminants in Model Fluid Cracking Catalysts (FCC): Spectroscopic Studies, ACS Symposium Series 411, Washington, DC, 1989, 40-45.

PROJECT SUMMARY

Enhancement of Activity and Selectivity By Metal-support Interactions

M. Albert Vannice
Department of Chemical Engineering
The Pennsylvania State University
University Park, PA 16802

Scope

This research is focused on two general topics: 1) the utilization of metal-support interactions (MSI) to enhance activity and alter selectivity in hydrogenation reactions involving molecules with both carbonyl bonds and unsaturated C=C bonds, and 2) a better understanding of the chemical state of the support, its influence on the electronic properties of small metal particles, and the nature of the catalytic sites that are present.

The first topic addresses the problem of selective intramolecular hydrogenation in more complicated molecules and it impacts directly on the area of specialty chemicals and various commercial processes. It also builds on the results we have obtained in our past DOE program in which we have shown that the rates of hydrogenation of carbonyl bonds can be enhanced 100-fold to 1000-fold by a judicious choice of the appropriate support, while rate enhancements up to 10-fold can be obtained for BTX's (benzene, toluene, xylenes).

The second topic will utilize HREELS, angle-resolved XPS, and AES to characterize: a) TiO_x species deposited on Pt, b) Pt dispersed on TiO_2 single crystals, and c) CO and acetone adsorbed on these surfaces after different pretreatments and reaction in a high-pressure chamber attached to the UHV system. In addition, IR spectroscopy (including DRIFTS) will also be used for in situ studies of the hydrogenation of acetone and benzene.

Recent Results

In an earlier part of this program, we showed that the turnover frequency (TOF) in CO hydrogenation was increased by two orders of magnitude or more over Pt and Pd (1,2). A model invoking special sites at the metal-titania interface was proposed (3), and it was tested by examining the hydrogenation of acetone (4). An even greater enhancement in acetone TOF was obtained over high-temperature reduced (HTR) Pt/TiO_2 catalysts, as shown in Figure 1. Kinetic studies and theoretical calculations both showed that the addition of the second hydrogen to acetone was the rate determining step (4). A more demanding test of this model was then used -- crotonaldehyde hydrogenation -- to determine if MSI could alter the selectivity of the intramolecular hydrogenation of carbonyl versus C=C double bonds (5). As shown in

Table 1, hydrogenation of the carbonyl bond can be enhanced to increase selectivities to crotyl alcohol from zero over Pt/SiO_2 and Pt/Al_2O_3 to above 35% over (HTR) Pt/TiO_2 catalysts.

Finally, we have found that turnover frequencies for the hydrogenation of benzene, toluene, and xylenes over Pd can be increased by the appropriate pretreatment of acidic SiO_2-Al_2O_3 and TiO_2 supports (6, 7). However, the effect decreases as methyl groups are added to the benzene ring, as shown in Figure 2 (7).

Future Plans

There is still debate regarding the reason for the higher activity of carbonyl bond hydrogenation over Pt/TiO_2. We plan to test our explanation that special active sites in the metal-support interfacial region are responsible for this rate increase by trying to identify variations in the adsorbed state of CO and acetone on model Pt/TiO_2 systems. A very sensitive technique is required, thus we will utilize HREELS to try and obtain evidence for the presence of unique adsorption sites created after different pretreatments in the attached high-pressure chamber. Additional surface characterization by angle-resolved XPS and AES will identify the valence states of Ti and the Ti/O ratios. In addition, the CO and acetone hydrogenation reactions will be run in this chamber, then quenched and the catalyst will be rapidly transferred to the UHV system for surface analysis. As mentioned, TiO_x species on a Pt foil as well as Pt dispersed on a TiO_2 single crystal will be examined in this fashion.

These studies will be augmented by the application of both diffuse reflectance and dispersive IR spectroscopy in two separate IR/reactor systems to obtain information about the species present during acetone and benzene hydrogenation.

References

1. Wang, S.-Y., Moon, S. H., and Vannice, M. A., J. Catal. 71, 167 (1981).
2. Vannice, M. A. and Twu, C. C., J. Catal. 82, 213 (1983).
3. Vannice, M. A. and Sudhakar, C., J. Phys. Chem. 88, 2429 (1984).
4. Sen, B. and Vannice, M. A., J. Catal. 113, 52 (1988).
5. Vannice, M. A. and Sen, B., J. Catal. 115, 65 (1989).
6. Chou, P. and Vannice, M. A., J. Catal. 107, 129, 140 (1987).
7. Rahaman, M., M. S. Thesis, Pennsylvania State University, 1989.

Figure 1

Initial Activity and Selectivity of Supported Platinum Catalysts during Crotonaldehyde Hydrogenation
(P = 1 atm; H_2/CROALD = 22.7)

Catalyst	Pre-treatment[a]	Conversion (%)	T (K)	Initial activity (μmol CROALD/s · g Pt)	TOF[b] (s^{-1})	Selectivity (mol%)[c]		
						BUTALD	CROALC	BUTNOL
0.7% Pt/SiO_2	A	7	308	158.7	0.056	100	0	0
5% Pt/SiO_2	A	20	319	63.4	0.044	100	0	0
0.6% Pt/SiO_2	A	17	319	30.7	0.046	100	0	0
2.1% Pt/η-Al_2O_3	A	10	317	70.3	0.047	100	0	0
2.1% Pt/η-Al_2O_3	A	—	318	10.5	0.007	100	0	0
0.2% Pt/TiO_2 (LTR)	B	30	318	324.5	0.063	69.7	13.7	16.6
0.4% Pt/TiO_2 (LTR)	B	15	308	74.2	0.021	84.3	6.2	9.5
0.4% Pt/TiO_2 (LTR) + Cl	B	57	318	340	—	100	0	0
1.9% Pt/TiO_2 (LTR)	B	19	317	112.4	0.029	79.0	12.6	8.4
4.6% Pt/TiO_2 (LTR)	B	30	319	60.9	0.024	85.8	14.2	0
0.2% Pt/TiO_2 (HTR)	C	14	307	147.0	0.74	70.9	19.9	9.2
0.4% Pt/TiO_2 (HTR)	C	7	307	29.0	0.29	83.4	3.8	12.8
0.4% Pt/TiO_2 (HTR) + Cl	C	16	317	93.0	—	100	0	0
1.9% Pt/TiO_2 (HTR)	C	12	318	70.5	1.68	62.8	37.2	0
4.6% Pt/TiO_2 (HTR)	C	53	319	108.9	8.34	52.5	0	47.5
Pt powder	C	88	318	0.57	0.143	92.2	0	7.8
Pt powder	C	32	328	0.22	0.052	100	0	0
Pt powder + TiO_2	C	20	314	0.39	0.102	100	0	0

[a] See text.

[b] Molecule C_4H_6O (CROALD) reacted · s^{-1} · Pt_s^{-1}.

[c] Butyraldehyde (BUTALD), crotyl alcohol (CROALC), butanol (BUTNOL).

Table 1

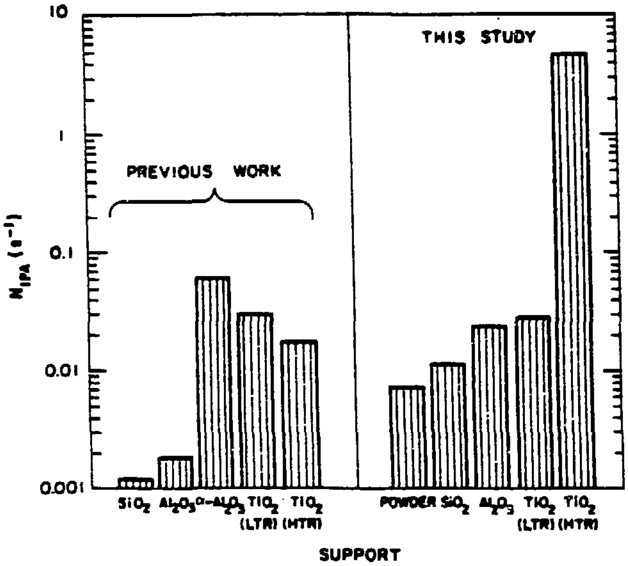

FIG. 3. Comparison of turnover frequencies at 303 K for the formation of IPA from acetone over supported Pt (P = 0.1 MPa, P_{H_2}/P_A = 3.06). Previous work includes Refs. (*39, 44, 54*); results from this study are average values obtained from Table 2.

Table 2

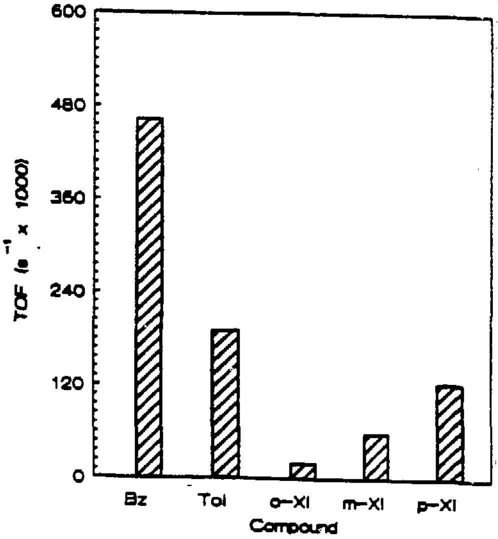

Figure A.5 Turnover Frequencies for the Hydrogenatio Various Aromatic Hydrocarbons over Pd/TiO_2 (448K) at 413 Torr Aromatic Compound, and 680 Torr Hydrogen.
Benzene, Bz ; Toluene, Tl ; o-Xylene, o-Xl;
m-Xylene, m-Xl; p-Xylene, p-Xl.

PUBLICATIONS FROM DOE-BES PROGRAM

Vannice, M. A., "Strong Metal-Support Interactions," In Closed-Cycle, Frequency-Stable CO2 Laser Technology, C. E. Batten et al. Eds., NASA Conf. Pub. 2456, p. 121, 1987.

Chou, P. and Vannice, M. A., "Benzene Hydrogenation over Supported and Unsupported Pd. I. Kinetic Behavior," J. Catal., 107, 129 (1987).

Chou, P. and Vannice, M. A., "Ibid. II. Reaction Model," J. Catal., 107, 140 (1987).

Vannice, M. A., "The H_2-D_2 Exchange Reaction on Pd," J. Catal., 107, 589 (1987).

Sen, B., and Vannice, M. A., "Metal-Support Effects on Acetone Hydrogenation over Pt Catalysts," J. Catal., 113, 52 (1988).

Vannice, M. A. and Sen, B., "Metal-Support Effects on the Intramolecular Selectivity of Crotonaldehyde Hydrogenation over Pt.," J.Catal., 115, 65 (1989).

Chen, A. A., Benesi, A. J., and Vannice, M. A., "NMR Characterization of the Hydrogen and Deuterium Phases Present in Pd/SiO_2 Catalyst," J. Catal., 119, 14 (1989).

Vannice, M. A., "The Use of "MSI" (Metal-Support Interactions) to Selectivity Activate Carbonyl Bonds, J. Molec. Catal., In Press.

W. HENRY WEINBERG
DEPARTMENT OF CHEMICAL AND NUCLEAR ENGINEERING
UNIVERSITY OF CALIFORNIA
SANTA BARBARA, CA 93106

RECENT RESULTS

We have made very good progress in a number of areas with the support of this grant for the past six months. We have quantified both the trapping-mediated and the direct dissociative chemisorption of ethane on the Ir(110)–(1x2) surface, as well as the trapping-mediated dissociative chemisorption of both methane and ethane on the Pt(110)–(1x2) surface. We have also simulated the surface segregation of two reactants into separate islands of the reactants due solely to chemical reaction between the two species (in the absence of any adsorbate-adsorbate interactions), while allowing for variable surface mobilities of the two reactants.

Experimental measurements of the initial probability of adsorption of ethane on Ir(110)–(1x2) have been made which probe the dynamics of the interaction. The data were obtained from supersonic molecular beam measurements with an incident kinetic energy E_i ranging between 1.2 and 24 kcal/mol, surface temperatures T_s between 77 and 550 K, and incident angle θ_i between 0° and 45°. Experimentally determined values of the initial trapping probability ζ_0 of ethane into a physically adsorbed state at T_s=77 K as function of E_i and θ_i and experimentally determined values of the initial probability of dissociative P_r as a function of E_i, θ_i and T_s were evaluated. The value of ζ_0 was found to decrease with increasing E_i, consistent with the fact that an increasingly larger fraction of the incident kinetic energy must be dissipated in order for the molecule to adsorb physically. The initial probability has a relatively weak dependence on θ_i, and the value of ζ_0 was found empirically to scale as $E_i\cos^{0.5}\theta_i$. Two distinct mechanisms of dissociative chemisorption on the bare surface are revealed. At low E_i a temperature-dependent trapping-mediated chemisorption mechanism dominates, while at relatively high E_i a temperature-independent direct mechanism dominates. For E_i less than 13.4 kcal/mol, the value of P_r decreases rapidly with increasing T_s, consistent with a trapping-mediated mechanism. For a surface temperature of 150 K, P_r decreases with increasing E_i for $1.2 \leq E_i \leq 13.4$ kcal/mol, in a manner similar to that for the molecular trapping probability. The data in the low E_i regime also support quantitatively a kinetic model consistent with a trapping-mediated chemisorption mechanism. The difference in the activation energies for desorption and chemisorption from the physically adsorbed, trapped state E_d–E_r is 2.2 ± 0.2 kcal/mol. In the trapping-mediated chemisorption regime, the value of P_r was found to be rather insensitive to incident angle, scaling with $E_i\cos^{0.5}\theta_i$ just for trapping of molecular ethane into a physically adsorbed state. For a normal energy $E_i\cos^{0.5}\theta_i$ greater than 8 kcal/mol, chemisorption via a direct mechanism becomes significant and increases with increasing E_i. Values of P_r in the direct chemisorption regime scale with normal energy and are independent of T_s over the range from 350 to 1350 K.

The initial probability of dissociative chemisorption P_r of methane and ethane on the highly corrugated, reconstructed Pt(110)–(1x2) surface has been measured in a microreactor by counting the number of carbon atoms on the surface following the reaction of methane and ethane on the surface which was held at various constant temperatures between 450 and 900 K during the reaction. Methane chemisorbs dissociatively on the Pt(110)–(1x2) surface with an apparent activation energy of 14.4 kcal/mol and an apparent preexponential factor of 0.6. Ethane chemisorbs dissociatively with an apparent activation energy of 2.8 kcal/mol and an apparent preexponential factor of 4.7×10^{-3}. Kinetic isotope effects were observed for both reactions. The fact that P_r is a strong function of surface temperature implies that the dissociation reactions proceed via a trapping-mediated mechanism. A model based on a trapping-mediated mechanism has been used to explain the observed kinetic behavior. Kinetic parameters for C-H bond dissociation of the thermally accommodated methane and ethane have been extracted from the model. The preexponential factor and activation energy (with respect to the bottom of the physically adsorbed well) are approximately $6x10^{12}s^{-1}$ and 18.9 kcal/mol for methane activation, and approximately $5x10^{10}s^{-1}$ and 10.8 kcal/mol for ethane activation.

Monte-Carlo simulations have been performed for a Langmuir-Hinshelwood reaction between two species *A* and *B* adsorbed on a square lattice. Adsorption of each species occurs when a gas-phase molecule, either *A* or *B*, impinges upon a vacant lattice site. The probability that a molecule impinges upon and adsorbs successfully into a vacant lattice site per unit time is $p_a/2$ for both species. Desorption is not allowed and the surface reaction is allowed to occur only between nearest-neighbor *AB* pairs. For each nearest-neighbor *AB* pair, the probability of reaction per unit time is p_r. Particles of both species are allowed to migrate by hopping to vacant nearest-neighbor sites, where the probability of a hop per unit time is p_m. In all these simulations p_m was set equal to unity, and p_r was varied from 0.01 to unity. The value of p_a was set equal to $p_r/5$ for all the simulations in order to maintain moderately low fractional surface coverages. 'Islanding' of each type of particle occurs even for the lowest value of p_r. For the range of values of p_r used, the 'islands' grow to a finite steady-state size; and the 'islands' that are formed are not fractal. It is possible to define quantities describing the process of 'islanding' which are analogous to the order parameter and the temperature in thermal phase transitions. The exponent for the order parameter in this model is a mean-field exponent.

PLANS FOR 1990

We shall continue the research of the past six months that is aimed at understanding the reactivity of the Ir(110)–(1x2) and Pt(110)–(1x2) surfaces for C-H bond activation in alkanes. In particular, we shall *quantify* the trapping-mediated C-H bond activation in methane and propane on Ir(110)–(1x2), and in propane, n-butane and iso-butane on Pt(110)–(1x2). We shall use selectively and fully deuterated propane, n-butane and isobutane to address the issue of steric vs. electronic effects in C-H bond cleavage via the formation of primary, secondary or tertiary alkyes on the surface. In this work, the measurements will be carried out in both a molecular beam scattering machine and in a catalytic microreactor.

Furthermore, we shall quantify the mechanism and the rates of the elementary reactions that occur in the dehydrogenation (decomposition) of the ethyl group that is produced on the Ir(110)–(1x2) surface following the dissociative adsorption of ethane at 130 K. This work will be executed using high-resolution electron energy loss spectroscopy.

PUBLICATIONS

1. "Kinetics of Dissociative Chemisorption of Methane and Ethane on Pt(110)–(1x2)", Y.-K. Sun and W. H. Weinberg, J. Vac. Sci. Technol. A (in press).
2. "Dynamics of the Interaction of Ethane with Ir(110)–(1x2)", C. B. Mullins and W. H. Weinberg, J. Vac. Sci. Technol. A (in press).
3. "Trapping-Mediated Dissociative Chemisorption of Ethane on Ir(110)–(1x2)", C. B. Mullins and W. H. Weinberg, J. Chem. Phys. (submitted).
4. "Reactant Segregation in a Langmuir-Hinshelwood Surface Reaction. I", H. C. Kong, M. W. Deem and W. H. Weinberg, J. Chem. Phys. (submitted).

Morphological Aspects of Surface Reactions

DE-FG05-86ER13626

John M. White, Principal Investigator
Department of Chemistry
University of Texas at Austin
Austin, Texas 78712
(512)471-3704

Overview.

This program involves the preparation and characterization, both structural and kinetic, of a variety of metal-based catalysts and adsorbates thereon. Both model and technically attractive adsorbate-substrate systems are being investigated using the tools of catalytic and surface chemical science. The substrates include rhodium and silver as well as combinations of the two. Single crystal, thin film, oxide-bound molecular metal species and oxide-supported particles are included in an integrated program. Oxides of silicon, aluminum and titanium are used to support particles and thin metal films. The morphology and electronic structure of the metals are being characterized by tunneling microscopy and tunneling spectroscopy. Adsorbates include carbon oxides, halogenated hydrocarbons, benzene, and alkalis. Particular attention is being given to the synthesis of hydrocarbon fragments, for example, methyl, ethyl, and propyl, by photochemical and electron-induced methods, at temperatures low enough to accumulate and preserve the fragments for subsequent structural, kinetic, and reactivity characterization. The short-range goal of this research is to develop detailed structural and kinetic parameters for well-characterized adsorbate-substrate systems by controlling and elucidating the substrate preparation chemistry, the adsorbate-substrate chemistry, and the product evolution chemistry. Throughout, even-handed attention is given to structure and kinetics. The long-range goal of the research is to develop relevant kinetic and structural parameters for technically important systems based on model laboratory catalytic systems.

Recent Progress.

We have examined the behavior of thin (< 10 monolayer) Fe films on W(100) with regard to their kinetic interactions with H_2, N_2 and NH_3. Generally, for Fe coverages < 2 monolayer, the substrate does not behave towards these adsorbates as a superposition of Fe and W; rather, unique substrate properties appear. In particular, for 1 monolayer of Fe, there is an increase in both the adsorption bond strength and the N_2 sticking probability compared to bulk Fe. There is also a high temperature desorption state for H_2, attributed to the adsorption of H at the metal-metal interface between Fe and W.

In a series of studies, we have examined the detailed surface science of K on Ag(111), the reaction of water with K/Ag(111), and formation of carbonate in $CO_2/H_2O/K/Ag(111)$ systems. The results, which qualitatively follow expectations based on other K-metal systems and inorganic chemistries, provide a detailed set of well-characterized systems for future kinetic study. These include: (1) KOH/Ag(111) and CO_3^{2-}/K/Ag(111), whose decomposition kinetics can be examined in detail and compared to bulk decomposition characteristics, (2) thermal reactions with adsorbates including CO, CO_2 and C_2H_4, and (3) photochemical kinetics involving, for example, CH_3Cl.

On Ag(111) the three methyl halides, Cl, Br. and I, readily adsorb at 100 K, but only the iodide undergoes thermal decomposition. The absence of thermal decomposition of the chloride and bromide open the way for establishing unequivocally the presence of photo- and electron-induced chemistry. It is of tremendous interest to us that surface-bound methyl groups, formed by the decomposition of the C-I bond in methyl iodide, do not undergo any C-H bond cleavage during TPD. The only desorbing products are ethane and, at high temperatures, atomic iodine. The absence of C-H bond cleavage extends to ethyl iodide, which thermally decomposes on Ag(111) to give adsorbed ethyl groups that recombine to form butane with no C-H or C-C bond cleavage.

In conjunction with these studies, we have examined the behavior of adsorbed H and D on Ag(111), in the presence and absence of Cl. Atomic hydrogen, prepared by dissociation of gas phase dihydrogen, adsorbs readily on Ag(111) with or without Cl. In the presence of Cl, atomic hydrogen is stabilized, but the saturation coverage is significantly less.

We have studied reactions of silica-bound Rh complexes formed by the covalent bonding of $Rh(C_3H_5)_3$ to OH groups on silica. These complexes are very interesting because they are reactive with CO, NO and H_2 in controlled cyclic fashion, i.e., once the µ-oxo carbonyl is formed by exposure to CO, an oxide can be formed by reaction with NO. The carbonyl can be reformed by redosing with CO, or an aggregate (not a Rh metal crystallite) can be formed by exposure to H_2. The latter can be converted back to the µ-oxo species by treatment with CO. Thus, reactions can be run without sintering the Rh up to 473 K. Controlled conversion to Rh particles is realized by thermal treatments at 873 K.

Present/Future Work.

We have constructed a UHV scanning tunneling microscope for the investigation of metal particles and films on model oxide materials. This instrument allows the sample to be moved from the tunneling position to positions for thermal desorption, Auger, low energy electron diffraction, and dosing. Thus, we are able to perform STM (both topology and barrier height modes), move the sample to a metal doser position, then to Auger position, and finally back to STM position.

To date we have successfully imaged Si(111), imaged the surface oxide formed in situ, and imaged 1 ML of Rh deposited at 300 K. We intend to examine, by standard surface science methods and by tunneling methods, these as-deposited and thermally processed Rh/SiO_2 surfaces.

We have also successfully carried out a broad-based study of the photochemistry of ethyl chloride (C_2H_5Cl), methyl bromide (CH_3Br), and methyl iodide (CH_3I) adsorbed on Ag(111) at 100 K. We used ultrahigh vacuum conditions with temperature programmed desorption (TPD), X-ray and ultraviolet photoelectron spectroscopies (XPS, UPS) and work-function change measurements ($\Delta\Phi$). All of these molecules adsorb molecularly on Ag(111) at 100 K. Photodissociation of these adsorbed molecules occurs upon irradiation with UV photons from a high pressure Hg arc lamp. Photodissociation involves only carbon-halogen bond cleavage. During irradiation, the photodissociation products are Cl(a), C_2H_5(a), and C_2H_5(g) for C_2H_5Cl; Br(a), CH_3(a), and CH_3(g) for CH_3Br; and I(a), CH_3(a), and CH_3(g) for CH_3I. In the post-irradiation TPD, Cl(a) and Br(a) desorb as AgCl and AgBr, respectively, while I(a) desorbs atomically. The surface hydrocarbon fragments, R(a), undergo only recombination to form R_2(g). They do not decompose to form hydrogen, carbon, or any other products.

Compared to the gas phase, the photochemistry of these molecules adsorbed on Ag(111) is strongly perturbed. For chemisorbed C_2H_5Cl, CH_3Br and CH_3I, the red shift is 2.2, 1.5, and 1.0 eV respectively. While the photodissociation of C_2H_5Cl and CH_3Br is enhanced significantly, that of CH_3I is quenched slightly. The photodissociation of physisorbed CH_2H_5Cl and CH_3Br is also red-shifted by 1.4 and 0.75 eV, respectively, and enhanced significantly, but that of physisorbed CH_3I is not noticeably red-shifted. The red shift and the surface photodissociation processes can be discussed on the basis of both direct adsorbate excitation and substrate excitation.

We intend to examine the detailed characteristics of these photochemical processes on Ag(110), Rh(111), Rh(100), and Ag films on Rh substrates. High resolution electron energy loss measurements, work at 193 nm, and desorption dynamics measurements are planned, in addition to the spectroscopic measurements outlined above.

Publications for the Past Two Years

1. "Adsorption of H_2, N_2, NH_3 and PF_3 on Ultra-thin Fe Films on W(100)," X.-L. Zhou, C. Yoon and J. M. White, Surface Sci. 203(1988)53.

2. "Interaction between D_2 and N_2 on (100) Oriented W Foil," X.-L. Zhou and J. M. White, Appl. Surf. Sci. 35 (1988-89) 435.

3. "Properties of Monolayer and Multilayer Ni Films on the Ru(0001) Surface," Paul J. Berlowitz, J. E. Houston, J. M. White, and D. Wayne Goodman, Surface Sci. 205 (1988) 1.

4. "Interactions of CO and Surface K: Negligible CO Adsorption on K/Ag(111)," B. Roop, P. M. Blass, X.-L. Zhou and J. M. White, J. Chem. Phys. 90 (1989) 608.

5. "Electron Spectroscopy and Temperature Programmed Desorption of Potassium on Ag(111)," P.M. Blass, X.-L. Zhou and J.M. White, Surface Sci. 215 (1989) 74.

6. "Coadsorption and Reaction of Water and Potassium on Ag(111)," P. M. Blass and J. M. White, J. Phys. Chem. (in press).

7. "Carbonate Formation and Decomposition on KOH/Ag(111)," P.M. Blass, X.-L. Zhou, and J.M. White, J. Vac. Sci. Technol. A7 (1989) 2009.

8. "Vibrational Study of CO_2^- on K-promoted Pt(111)," Z. M. Liu, Y. Zhou, F. Solymosi, and J. M. White, J. Phys. Chem. 93 (1989) 4383.

9. "Adsorption and Decomposition of Methyl Halides (Cl, Br and I) on (100) Oriented Polycrystalline W," X.-L. Zhou, C. Yoon and J. M. White, Surface Sci. 206 (1988) 379.

10. "Interactions of Methyl Halides (Cl, Br and I) with Ag(111)," X.-L. Zhou, F. Solymosi, P. M. Blass, K. C. Cannon, and J. M. White, Surface Sci. 219 (1989) 294.

11. "Thermal Decomposition of C_2H_5I on Ag(111)," X.-L. Zhou and J. M. White," Catal. Lett. 2 (1989) 375.

12. "Chemisorption of Atomic Hydrogen on Clean and Cl-covered Ag(111)," X.-L. Zhou, J. M. White, and B. E. Koel, Surface Sci. 218 (1989) 201.

13. "The Reaction of Nitric Oxide and Silica-Attached Rhodium Carbonyl Complexes," K.C. Cannon, S.K. Jo, and J.M. White, J. Amer. Chem. Soc. 111 (1989) 5064.

14. "Reaction of Hydrogen Atoms with Oxygen Adsorbed on Cu(110)," M. Nakashima, Y. Zhou, and J. M. White, Surface Sci. 206 (1988) 395.

15. "The Surface Chemistry of Isolated and Aggregated Silica-bound Rhodium Complexes," K. C. Cannon and J. M. White, J. Catal. (in press).

16. "SIMS of Coadsorbed Layers Involving Potassium," J. M. White, Alkali Adsorption on Metals and Semiconductors, H. P. Bonzel, A. M. Bradshaw, and G. Ertl, eds. (Elsevier, in press).

17. "Decomposition of Methyl Iodide on Ru(001)," Y. Zhou, M. A. Henderson, W. M. Feng and J. M. White, Surface Science (in press).

18. "Adsorption of H_2O and H_2S on Thin Films of Cobalt Oxide Supported on Alumina," E. Auschitzky, A. B. Boffa, J. M. White, and T. Sahin, J. Catal. (submitted).

Theoretical Studies of Chemisorption and Surface Reactions on Nickel and Silicon

Grant DE-FGO2-84ER45100.AOO7

Jerry L. Whitten

State University of New York at Stony Brook
and
North Carolina State University

Research Scope

The research is part of a theoretical program on the structure of molecules adsorbed on solid surfaces and dissociative chemisorption with emphasis on transition metal substrates and electronic materials. An embedding theory for treating chemisorption on metals is further developed and applied to the reaction of hydrocarbon fragments and hydrogen coadsorbed on nickel, the dissociation of water on nickel, and the systems H/ Ni, NH_3/Ni, and C_6H_6/Ni. The main emphasis of the work is on the energetics of adsorption as a function of surface site, the potential energy for adsorbate motion between surface sites and the energetics of surface reactions. Equilibrium geometries, vibrational frequencies and ionization potentials are also calculated. Studies of π bonding on Si(111) were also completed and work was begun on the Auger ionization of F/Si.

Description of Research Effort

The original form of the embedding theory has been extended to make use of an effective potential representation of the bulk electrons interacting with the embedded surface region. Surface sites are described by an improved basis (radial, polarization and correlation functions), and in the case of transition metals by variable d occupancy. Electronic wavefunctions are constructed by configuration interaction and the coupling of the local subspace and adsorbate to the bulk lattice electrons, $\{\varphi\}$, defined by a localization transformation, is represented by a pseudopotential (4,6).

$$\Psi = \Sigma_k \lambda_k A(\chi_1^k \chi_2^k \cdots \chi_n^k \varphi'_m \cdots \varphi'_N)$$

local region pseudopotential

The nickel surface calculations are carried out by modelling the lattice as a 26-atom, three layer cluster which is extracted from a larger cluster by the orbital localization transformation. Hydrogen atoms are found to bind strongly to the Ni(111) surface at three-fold and bridge sites (4). Calculated H binding energies are the range 2.50-2.66 eV, for optimized Ni-H bond lengths ranging from 1.81 to 1.87 Å. Vibrational frequencies are in the range 1043-1183 $cm.^{-1}$ These quantities are in excellent agreement with experiment. Work on the recombination reaction of hydrogen on nickel was also started during this period. Studies of H-H interactions show a repulsive interaction for hydrogens adsorbed in adjacent three-fold sites that share two nickel atoms compared to separated three-fold sites sharing only one nickel atom. Similar behavior was found in earlier studies of hydrogen adsorbed on Ti(0001).

The following reactions have been studied in detail on Ni(111) (9,10):

$$CH + H = CH_2 \qquad CH_2 + H = CH_3 \qquad CH_3 + H = CH_4$$

Energetics and structural information are obtained for the CH, CH_2, CH_3 and H species at the most stable sites on Ni(111) and for intermediate steps along the reaction pathway. Both CH and CH_2 species are found to bind strongly to the surface at three-fold and bridge sites. A three-fold site is the most stable for CH_3 with indistinguishable adsorption energies for filled or hollow sites. Adsorption energies are between 2.9 and 3.1 eV for CH adsorption, 2.5 and 2.9 eV for CH_2 adsorption and 1.7 eV for CH_3. Atop Ni adsorption sites are more than 1 eV higher in energy. The Ni-C bond lengths range from 2.00 to 2.04 Å for CH and CH_2 on the surface. Vibrational frequencies for HC-surface and H_2C-surface vibrations are between 400 and 600 cm^{-1} and CH stretching frequencies are around 3050 cm^{-1} in both CH and CH_2. The reaction of $CH + H = CH_2$ on the nickel surface is 1.45 eV exothermic; however a barrier exists to moving H to a three-fold site adjacent to one occupied by CH. Energy barriers exist for the approach of H toward the adsorbed fragments until distances become short enough to begin to establish C-H bonds. Experimental values for the adsorption energies of hydrocarbon fragments on nickel are inferred only indirectly; however, the reaction $CH_3 + H = CH_4$ is known to be nearly energetically neutral as is found by the calculations. Calculations on the dissociation of CH_4 on Ni(111) show that an atop Ni dissociation site is most favorable energetically, but the calculated barrier to dissociation is quite high, 23 kcal/mol (9).

During this period, studies of the adsorption of H_2O and NH_3 on Ni(111) were also completed (12,13). These lone pair electron species are found to adsorb preferentially at atop Ni sites, but energy differences between the 3-fold, bridge and atop sites are calculated to be very small, < 0.2eV. These results are in sharp contrast to those for hydrocarbon and H atom fragments for which high symmetry sites were energetically preferred. Molecular H_2O adsorbed on the Ni(111) surface is found to prefer an atop atom site with an adsorption energy of 12 kcal/mol and a Ni-O equilibrium distance of 2.06 Å. The equilibrium geometry of H_2O is calculated to lie in a plane inclined by about 25° to the normal to the surface, but tilting the plane of the molecule from 0° to 50° or rotating the molecule about the Ni-O axis changes the energy only slightly. The OH radical binds strongly to the Ni(111) surface at both three-fold and bridge sites with adsorption energies of 87 kcal/mol and Ni-O bond lengths from 2.02 to 2.08 Å. The OH axis of adsorbed OH is inclined about 10° from the surface normal at a three-fold site. Dissociation of H_2O to OH and H adsorbed at nearby three-fold sites is exothermic, and for OH and H at a large distance of separation, the reaction $H_2O(ads) = OH(ads) + H(ads)$ is 52 kcal/mol exothermic. A high energy barrier is found at the initial stage of dissociation. The work function decreases by ≈ 0.5 eV on H_2O adsorption and increases by ≈ 0.2 eV on OH adsorption.

In studies of benzene adsorption on nickel, C_6H_6 is found to be adsorbed molecularly, parallel to the surface, at a three fold site, bonding primarily through its π electron system. The equilibrium distance is 2.2 Å from the surface. The calculations show no distortion of the benzene ring other than a 2 percent expansion. C-H bonds tilt away from the surface 8.5°. The adsorption energy is calculated to be 1.2 eV. Adsorption at the three fold hollow site gives a slightly higher energy than the hcp site, but the difference may be within the uncertainty of the calculation. The energy of the bridge adsorption site is higher than that of the hcp site by 0.5 eV. The photoemission spectrum of adsorbed benzene is explained in terms of final state relaxation effects analogous to image charge formation in the metal following ionization of benzene (15).

The role of π bonding in the (2 x 1) reconstruction of Si (111) was investigated (1). The difference in total energy (ΔE) between the planar and twisted Si-Si π systems in a single π bond (Si_2H_4), a pair of π bonds (Si_4H_6) and a Si_6 chain with 3 π bonds embedded in an Si_{12} cluster show a uniform decrease in ΔE with the number of π bonds. For the largest system studied, a Si_{12} cluster model of the (111) surface, ΔE is negligibly small. These results suggest that the partial breaking of Si-Si π bonds does not energetically inhibit surface reconstruction.

Future Research

Work planned for the near future includes the investigation of Si and SiH_x adsorption and decomposition on silicon surfaces and interactions with a Si(100) stepped surface in order to better understand surface diffusion and surface layer growth. Reaction of propene with Si(100) will also be studied in order to understand mechanisms for depositing C on silicon by vapor deposition techniques. A third project will involve surface reactions on Cd, Te semiconductor systems. New directions will be explored for the reaction of methane with nickel. Previous results strongly suggest an atop atom site for the CH_4 = CH_3 + H reaction, driven by the need to accommodate the products in separated sites on Ni(111). It is important to investigate the simultaneous involvement of two electronic configurations of Ni (d^9s and d^{10}), states known to be important in single Ni atom interactions with CO and CH_4, to determine whether the interaction would lead to a lower calculated barrier for methane dissociation. Substitutional replacement of Ni by a more reactive transition metal atom will also be investigated to determine is there is sufficient retention of reactivity to induce dissociation of methane. The current theory which permits configuration interaction in the local subspace is ideally suited to address these questions. In collaborative work with P. Cremaschi, hydrogen interactions with Fe(110) will be calculated to determine vibrational excitations and dissociation probabilities on H_2 collision with a Fe wall.

References (papers published 1988-89).

1. A. Chattopadhyay, P. Madhavan, R. Fischer, I. P. Batra and J. L. Whitten, "The Effect of Pi Bonding in the (2x1) Reconstruction of Si(111)," invited paper, J. Mol. Struct. (Theochem), 163, 63 (1988).

2. P. Madhavan, F. v. Trentini and J. L. Whitten, "Electronic States of a Nickel Atom on the Ni(001) Surface," invited paper, Progress in Surface Science, 26, 201 (1988).

3. Y. Zhang, N. Sukumar, J. L. Whitten and R. N. Porter, "*Ab Initio* Evaluation of the Born Correction, Born Couplings and Higher Derivative Matrix Elements with Gaussian Lobe Orbitals," J. Chem. Phys., 88, 7662 (1988).

4. H. Yang and J. L. Whitten, "Chemisorption of Hydrogen on Ni(111)," J. Chem. Phys., 89, 5329 (1988).

5. L. Hanley, J. L. Whitten and S. L. Anderson, "Collision Induced Dissociation and *Ab Initio* Studies of Boron Cluster Ions: Determination of Structures and Stabilities," J. Phys. Chem., 92, 5803 (1988).

6. J. L. Whitten, "Chemisorption Theory For Metal Surfaces," American Chemical Society New Orleans Meeting, 1988 (invited paper).

7. J. L. Whitten and Hong Yang, "Reaction of Methane on Nickel," 62nd Colloid and Surface Science Symposium, Penn. State Univ., June 21, 1988.

8. H. Yang and J. L. Whitten, "Reaction of CH + H on Nickel," Bull. Am. Phys. Soc. (1989).

9. H. Yang and J. L. Whitten, "Reaction of CH_4 with Ni(111)," Chapter 10 in *The Challenge of d and f Electrons, Theory and Computation*, D. R. Salahub and M. C. Zerner, eds., ACS Symposium Series, 394, 140 (1989).

10. H. Yang and J. L. Whitten, "Reaction of Chemisorbed CH and H on Ni(111)," J. Chem. Phys., 91, 126 (1989).

11. C. R. Fischer and J. L. Whitten, "Dissociation of O_2 on Cu(001)," Phys. Rev. B40, 5745 (1989).

12. H. Yang and J. L. Whitten, "The Adsorption of Water and Hydroxyl on Ni(111)," Surface Science, 222, (1989).

13. H. Yang and J. L. Whitten, "The Adsorption of Ammonia on Ni(111)," J. Phys. Chem. submitted (1989).

14. H. Yang and J. L. Whitten, " Reaction of Chemisorbed CH and H on Ni(111)," J. Chem. Phys., 91, 126 (1989).

15. Z. Jing and J. L. Whitten, "The Adsorption of Benzene on Nickel," submitted (1989).

16. J. Tasi and J. L. Whitten, "Influence of Surface Impurity on Impact Response of Lattices, submitted (1989)."

VIBRATIONAL SPECTROSCOPIC STUDIES OF SURFACE CHEMICAL INTERACTIONS IN CHEMISORPTION AND CATALYSIS

John T. Yates, Jr., Surface Science Center, University of Pittsburgh

Modern methods of surface science are being applied to the study of chemisorption and catalysis on both single crystal and high area catalytic surfaces. A number of interrelated themes are being investigated, and these are listed below:

RESEARCH ACTIVITIES - ADSORPTION AND CATALYSIS

- Binding Modes of CO on Ni(111) and their Thermal Interconversion.
- Influence of Surface Defect Sites on CO Chemisorption and Catalytic Reactivity on Stepped Pt Single Crystals.
- Xe Physisorption as a Probe of Surface Defect Sites on Stepped Pt Single Crystals.

Model Single Crystal Studies

- Influence of Electronic Modification on CO Dissociation on Ni Films- Al modifier.
- Comparison of S and Se as Surface Modifiers- Effect on CO Vibrational Dynamics on Pt(111) Sites.

Model Surface Modifier Studies

- Oxide Supported Rh Catalysts- Spectroscopic Observation of Participation of -OH groups in Rh(0) → Rh(I) Conversion.
- Model Supported Catalyst Studies: Ni Films Deposited on Al_2O_3 Films and Studied by HREELS- Metal/Support Interactions.
- Isotopic Exchange between Chemisorbed CO Species on Rh/Al_2O_3 Catalysts.
- C-H Bond Activation on Rh/Al_2O_3 Catalysts.

Supported Catalyst Studies

- Spectroscopic Study of $-OCH_3$ Rotation on Al_2O_3 Surfaces.
- Development of New Techniques for Study of Chemisorption and Catalysis on Single Crystal Catalysts- Improved Digital Data Acquisition and Smoothing for HREELS Measurments.
- Development of New Techniques for Study of Chemisorption and Catalysis on High Area Catalysts- IR Cell Capable of 100 - 1500 K Range, with Rapid Temperature Programming.

New Methods for Catalysis Research

These 12 areas of research are designed to answer fundamental questions about catalytic chemistry, mixing high resolution studies on single crystals and on real catalysts. In almost all of this work, surface vibrational spectroscopy, applied in four separate ways, is the linking feature of the work.

IRAS STUDIES OF SINGLE CRYSTAL SURFACES

A new FT-IRAS system has recently become operational and is delivering information about adsorbed species on Ni(111). A diagram of the apparatus accompanied by the principle utilized to distinguish tilted from normal chemisorbed second-layer NH_3 is shown in Figure 1 and Figure 2. The adsorption of second layer substances has allowed us to probe the influence of electric fields on the underlayer (CO).

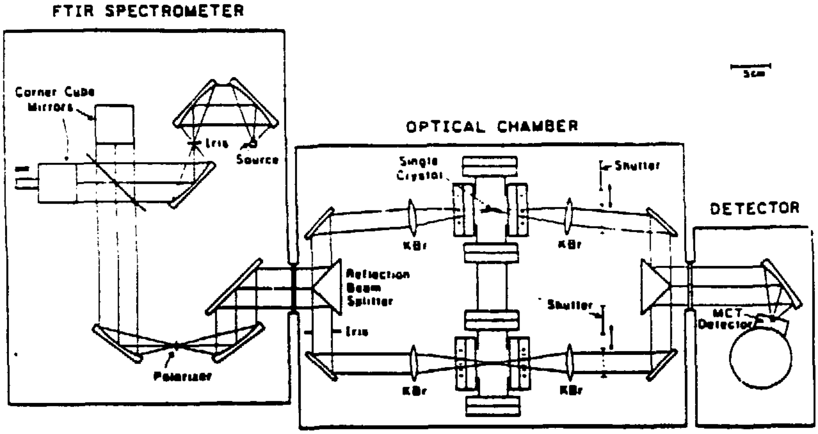

Figure 1. FT-IRAS Instrument, Featuring Rapid Background Subtraction Methods.

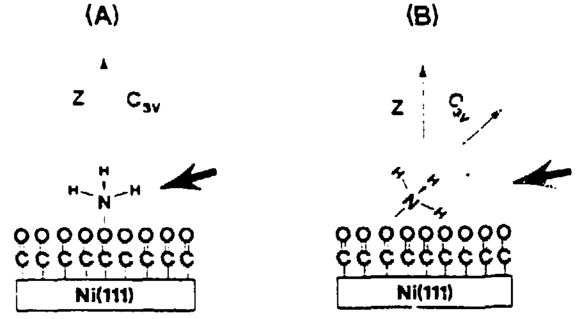

Possible Adsorption Structures for NH_3 on top of Saturated CO Layer on Ni(111)

Figure 2. Principle for Determining That Second Layer NH_3/CO is a Tilted Species.

Possible NH_3 vibrational modes which can be detected by "p" polarized infrared radiation

(A)	(B)
1. Symmetric Deformation	1. Symmetric Deformation
2. Symmetric Stretch	2. Symmetric Stretch
	3. Asymmetric Deformation
	4. Asymmetric Stretch

HREELS STUDIES OF MODEL SUPPORTED CATALYSTS

Ni films of various dispersion have been deposited on top of an Al_2O_3 film to produce a model supported Ni catalyst. CO adsorption has been studied as a function of the Ni dispersion as shown in Figure 3. It may be seen that at high dispersion, only terminal-CO is observed (2049 cm^{-1}). At higher levels of Ni deposition, bridged-CO is also observed (1935 cm^{-1}). The carbonyl spectra are superimposed on top of strong Al_2O_3 phonon modes.

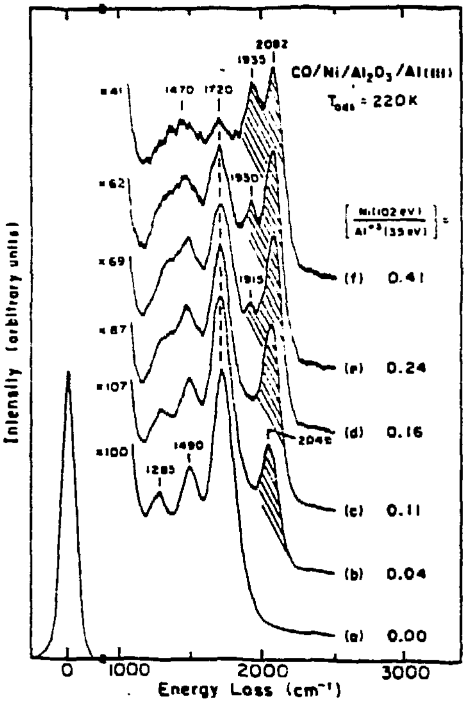

Figure 3. HREELS Measurements of CO Adsorption on Ni Films Held on Al_2O_3.

TRANSMISSION IR STUDIES- SUPPORTED Rh/Al_2O_3

Studies of the oxidation of supported Rh catalyst particles have demonstrated that surface -OH groups are consumed as the process $Rh(0) \rightarrow Rh(I)(CO)_2$ takes place. A schematic diagram of the proposed surface redox process is shown in Figure 4.

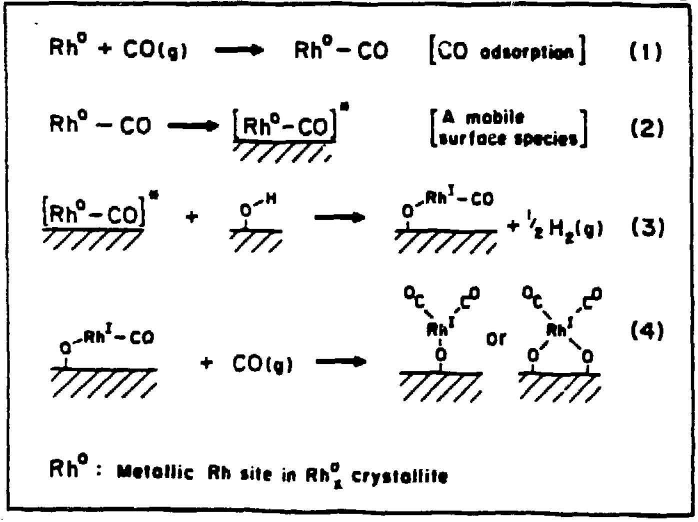

Figure 4. Postulated Mechanism for the Formation of $Rh(I)(CO)_2$ on Hydroxylated Oxide Supports.

SUMMARY OF DOE SUPPORTED PUBLICATIONS 1988-1990.

- "Rhodium - Carbon Monoxide Surface Chemistry: The Involvement of Surface Hydroxyl Groups on Al_2O_3 and SiO_2 Supports", P. Basu, D. Panayotov and J.T. Yates, Jr., J. Amer. Chem. Soc. 110 (1988) 2074.
- "Dissociative Chemisorption of CO on Ni Films Promoted by Al - Detection of a Precursor State to Dissociation by EELS", J.G. Chen, J.E. Crowell, L. Ng, P. Basu and J.T. Yates, Jr., J. Phys. Chem. 92 (1988) 2574.
- "IRAS Study of the Adsorption of CO on Ni(111): Interrelation Between Various Bonding Modes of Chemisorbed CO", L. Surnev, Z. Xu and J.T. Yates, Jr., Surface Science 201 (1988) 1.
- "Site Interconversion in Chemisorbed CO on Ni(111): IRAS and Work Function Studies," L. Surnev, Z. Xu and J.T. Yates, Jr., Surface Science 201 (1988) 14.
- "Ni Cluster Chemistry on Al_2O_3 - A Vibrational EELS Study Using Chemisorbed CO on a Model Catalyst: $Ni/Al_2O_3/Al(111)$", J.G. Chen, J.E. Crowell and J.T. Yates, Jr., Surface Science 187 (1987) 243-264.
- "The CO Isotopic Exchange Reaction Over Rh/Al_2O_3: Non-Dissociative Exchange on Metallic Rh Sites", D. Panayotov, P.Basu and J.T. Yates, Jr., J. Phys. Chem. 92 (1988) 6066.
- "A Wide Temperature Range IR Spectroscopy Cell for Studies of Adsorption and Desorption on High Area Solids", P. Basu, T.H. Ballinger and J.T. Yates, Jr., Rev. Sci. Inst. 59(8) (1988) 1321.
- "Structural Rearrangements in Chemisorbed Hydrocarbon Layers: 1,3-Butadiene on Rh/Al_2O_3", P. Basu and J.T. Yates, Jr., J. Phys. Chem. 93 (1989) 2028.
- "Summary Abstract: Subsurface Hydrogen on Ru(0001): Quantification by Cu Titration", C.H.F. Peden, D.W. Goodman, J.E. Houston and J.T. Yates, Jr., J. Vac. Sci. Tech. A(6)3 (1988) 822.
- "C-H Bond Lability in Adsorbed Hydrocarbon Layers: Butadiene-Derived Species on Rh/Al_2O_3", P. Basu and J.T. Yates, Jr., J. Phys. Chem. 93 (1989) 6110.
- "Improved Data Acquisition and Smoothing Methods in High Resolution Electron Energy Loss Spectroscopy", P.J. Chen, M.L. Colaianni and J.T. Yates, Jr., accepted, J. Vac. Sci. Tech.
- "Comparison of Sulfur and Selenium as Surface Modifiers - Effect on the CO/Pt(111) System", M.P. Kiskinova, A. Szabo and J.T. Yates, Jr., accepted, Surface Science.

- "A Dynamical Study of the Rotation of Chemisorbed Methoxy Species on an Alumina Surface", T.P. Beebe, Jr., J.E. Crowell and J.T. Yates, Jr., submitted to J. Chem. Phys.

- "The Influence of Surface Defect Sites on Chemisorption and Catalysis", J.T. Yates, Jr., A. Szabo and M.A. Henderson, Division of Petroleum Chemistry, American Chemical Society Symposium, "Structure in Heterogeneous Catalysis", Boston, MA, April 1990.

- "A Comparative Kinetic Study of Xenon Adsorption on a Flat Pt(111) and Stepped Pt(557) and Pt(112) Surfaces", H.R. Siddiqui, P.J. Chen, X. Guo and J.T. Yates, Jr., submitted to J. Chem. Phys.